Reconstructing the climate of the Western Warm Pool of the tropical Pacific using oxygen isotopes from the long-lived bivalves, *Tridacna* sp.

Kevin Welsh

Thesis submitted for the degree of
Doctor of Philosophy
University of Edinburgh
2008

For my parents

I attest that:

All material presented in this document was compiled and written by myself unless otherwise acknowledged.

Kevin Welsh

Acknowledgements

I would like to acknowledge the help of Colin Chilcott for help with stable isotopic analysis, Nic Odling for help with X-ray diffraction analysis, Nicola Cayzer for assistance with the scanning electron microscope. Thanks to Yusuke Yokoyama for radiocarbon analysis of several *Tridacna* sp. A special thanks to Mike Hall for thin section preparation of increasingly strange and difficult organisms during the course of my studies in Edinburgh. Thanks to Carrie Davidson and Philippa Lynam for micromilling of samples from T58 and T14 during their Honours projects at University of Edinburgh. Thanks for help and encouragement from Sandy Tudhope. Thanks to C. Dix for support during the AGU meeting in San Francisco, 2005. Thanks to E. Wilson for the loan of a laptop to finish this thesis on. Thanks to John Pandolfi's group, especially Dean and Merrick for help in retrieving sample T58 from 8 metres up the face of the Holocene terrace. Special thanks to John Chappell for showing us round the field area on the Huon Peninsula and for giving us the benefit of his many years of experience in this region. Thanks to the people of Hubegong for access to their land and assistance in collecting specimens. Thanks most of all to my supervisor, Mary Elliot for supervision *in extremis*.

Abstract:

The configuration of ocean basins and coupling of atmospheric and oceanic circulation in the tropical Pacific causes the build up of the West Pacific Warm Pool (WPWP) along the equator near Papua New Guinea. This is the largest body of warm water in the global ocean with average annual temperatures above 29°C. The WPWP is a region of prime importance as part of the heat engine that drives atmospheric circulation and is also central to the dynamics of the El Niño-Southern Oscillation (ENSO). The ENSO cycle is a fluctuation between unusually warm (El Niño) and unusually cool (La Niña) conditions in the tropical Pacific. There is evidence to suggest that under different boundary conditions, the variability of that system could be increased or decreased. Understanding the consequences for the long term variability of the ENSO system in a world with increased average global temperatures requires the development of accurate models that can be shown to predict its behaviour under different boundary conditions. There is therefore a requirement to accurately reconstruct the past climate history of the WPWP and ENSO with which to test these models during radically different global climates such as are seen on orbital or sub-orbital timescales. However, there are difficulties associated with such reconstructions. Firstly deep basins and low productivity in the WPWP mean that there are few high resolution marine palaeoclimate records available. Secondly, while many studies have produced annually resolved reconstructions of WPWP climate, prior to the last millennium these are predominately from stable isotope records derived from corals. Though these records are invaluable, they are complicated by species dependent kinetic effects on stable isotope values and unaltered records from prior to the Holocene are difficult to locate due high coral skeleton porosity.

In this study specimens of the relatively long-lived, reef dwelling bivalve mollusc *Tridacna* sp. were collected from the Huon Peninsula, Papua New Guinea, which is in the heart of the WPWP. Uplifted terraces there have been extensively studied and are well dated providing an unrivalled opportunity to reconstruct WPWP climate. Seasonally resolved and averaged samples of carbonate were analysed for their stable

isotopic content to reconstruct the climate of the WPWP on interannual, glacial and finally sub-orbital time scales.

To test the ability of these records to work as a proxy for climate in this region, seasonally resolved timeseries of oxygen and carbon stable isotope ratios were produced from a modern *Tridacna gigas* collected on the Huon Peninsula. $\delta^{18}O$ timeseries are shown to correlate highly with precipitation and temperature anomalies and also the Niño 3.4 box temperature anomaly record, which is often used as an index for ENSO. The bivalve $\delta^{18}O$ timeseries also shows a high degree of correlation with $\delta^{18}O$ records from two *Porites* corals for two different locations and environments on the peninsula with a constant offset of 3.9‰. This comparison shows that contrary to previous studies, given a high enough resolution, there is no attenuation of the climatic reconstruction available from *Tridacna gigas* $\delta^{18}O$. It also proves that the stable isotopic signature of ENSO has a demonstrable regional footprint at Huon Peninsula which is independent of organism.

Seasonally resolved and averaged $\delta^{18}O$ measurements from *Tridacna* sp. from early to mid Holocene and during Marine Oxygen Isotope Stage 3 (MIS3) were used to reconstruct changes in interannual variability (ENSO) and mean state of the WPWP. The results of this investigation agree with previous studies showing a suppressed ENSO variability in the early to mid Holocene. In terms of mean state however, they also indicate a greater reduction in precipitation/ increase in salinity or a more "El Niño-like" climate in the tropical Pacific for this period. This result disagrees with some studies from other areas in the larger Indo-Pacific Warm Pool, which indicates either more regionally differentiated climate at this time or a change to the $\delta^{18}O$ signature of precipitation predicted by some models. Results from MIS3 indicate a slight increase in salinity/ reduction in precipitation, agreeing with those studies that show a more "El Niño-like" configuration for the tropical Pacific during the last glacial period. Short seasonally resolved records were recovered from this time period. Though they generally agree well with other studies that indicating the ENSO cycle is suppressed in terms of the strength or number of events during the glacial period, some increased variability was seen in samples recovered from previously

unsampled terraces. Unfortunately these records are too short to be of statistical significance.

Finally, by taking advantage of the fact that the morphology of the terraces in this area is controlled largely by eustatic sea level variation and extensive prior dating of the terraces by U/Th dating of corals, *Tridacna* sp. derived $\delta^{18}O$ results were correlated with millennial scale climate variations in the North Atlantic. Whilst there remain some uncertainties associated with the timing of sea level events, these data appear to show shift towards lighter $\delta^{18}O$, probably indicating a warmer or wetter mean climate, during Northern Hemisphere stadials. This would disagree with studies that suggest super-ENSO conditions in the Pacific are related to, and potentially even cause cold conditions in the North Atlantic region, but it does appear to support suggestions that the Intertropical Convergence Zone (ITCZ), a region of high precipitation where the Northern and Southern trade winds meet, is depressed to the south during Northern Hemisphere cold events. Uncertainties regarding the extent to which earlier stages of these transgressive terraces may be buried beneath later sediments mean that further investigation of the lower sections of these terraces are required to confirm this observation.

Table of Contents

1 Introduction to ENSO on different timescales

The El Niño – Southern Oscillation (ENSO) is a complex interplay between atmospheric and oceanic processes in the tropical Pacific that dominate global interannual climate change. El Niño events have global socio-economic consequences of extreme events (Glantz, 2005; Patz *et al.*, 2005) especially through the modulation of the Asian, African and American monsoon systems which can have a profound effect on farming in areas influenced by these systems (Bouma *et al.*, 1997; Dunbar and Cole, 1999; Caviedes, 2001; Chen *et al.*, 2001; Goddard and Dilley, 2005). An apparent increase in extreme events since the 1970's (Allan and D'Arrigo, 1999; Gergis and Fowler, 2006) and the possible link with increased average global temperatures (Fedorov and Philander, 2000) has provoked an interest in prediction of the behaviour of the ENSO system on interannual and longer timescales in response to different boundary conditions (e.g. Cane *et al.*, 2006).

Two approaches enhance our understanding of ENSO: 1) climate modelling (e.g. Timmermann *et al.*, 1999) and 2) proxy data for the state of ENSO under different boundary conditions (e.g. Tudhope *et al.*, 2001; Brown *et al.*, 2001). The comparison of climate models and proxy data helps to validate models, which can then be used with confidence to predict the response of ENSO to global temperature rise predicted in the coming decades (IPCC Working Group I, 2007).

1.1 Modern ENSO

El Niño-Southern Oscillation (ENSO) results from a complex interaction of atmospheric and oceanic processes that take place in the tropical Pacific and result in a globally altered climate. ENSO is the most potent source of interannual climate variability in the modern climate system and occurs semi periodically on typically 2-7 year periods between two extremes of El Niño and La Niña. Bjerknes (1969) first

described the positive feedback mechanisms that give rise to this coupling of the ocean-atmosphere in the tropical Pacific. He observed that despite receiving the same amount of heat, the east Pacific was 4 to 10 °C cooler than the west. In the "normal" mode, trade winds pile up a large pool of some of the warmest water in the world in the west Pacific along the equator, deepening the thermocline there. In the eastern Pacific a raised thermocline and cool sea surface temperatures are associated with the upwelling of cold water off the West coast of South America. Bjerknes feedback keeps the system in this mode. During "El Niño" Kelvin waves, which are initiated by seasonal wind anomalies in the Western Pacific Warm Pool (WPWP), move warm water across the equator and disrupt the thermocline in the east Pacific causing SST anomalies, this in turn causes trade winds slacken and feedback begins to work in reverse (Figure 1-1). El Niño is a term that was used long ago by Peruvian fishermen to describe the coming of warmer waters around Christmas time. The opposite part of the cycle to El Niño is La Niña, in which trade wind strength increases; greater upwelling occurs in the east and higher precipitation is seen in the west.

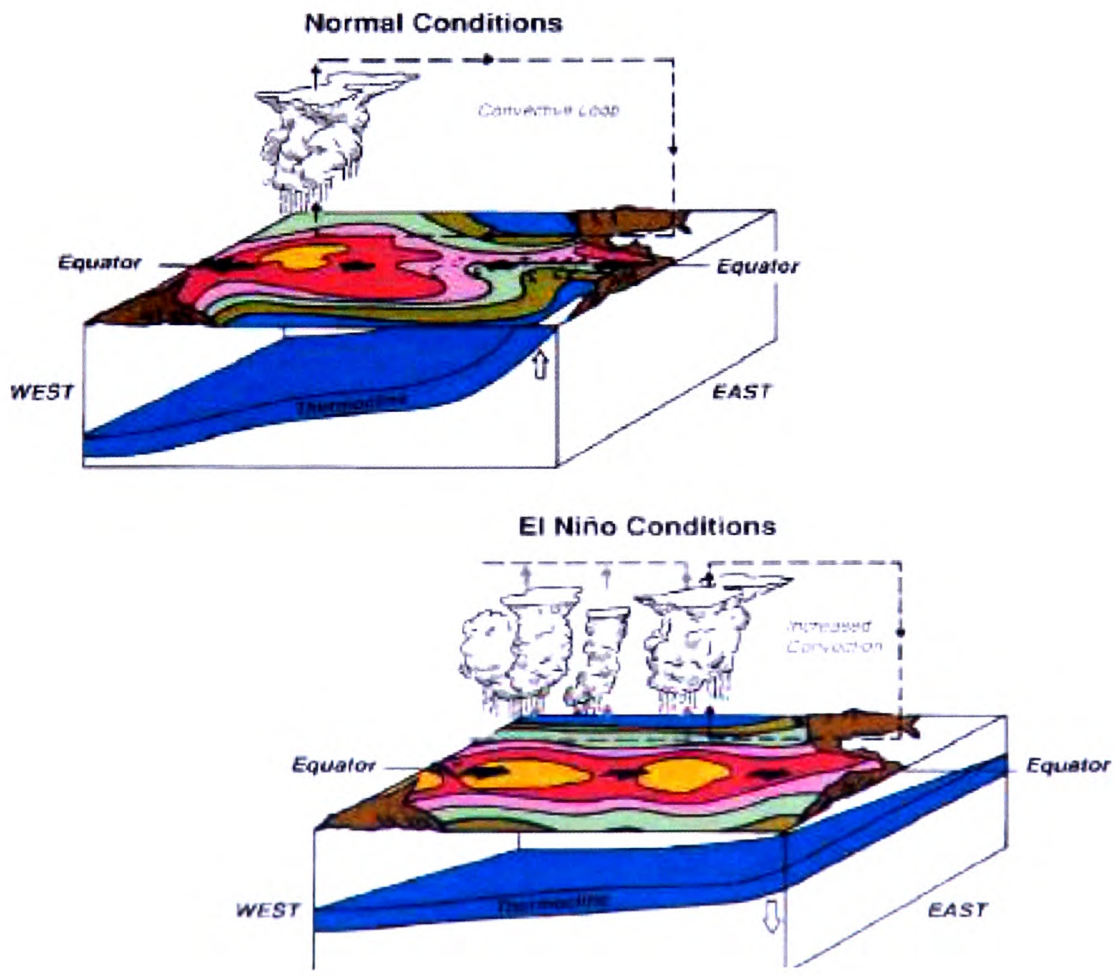

Figure 1-1 Schematic diagram showing the state of the Tropical Pacific during "Normal" and El Niño Conditions (After Cane *et al.*, 2006)

To test the predicative ability of ENSO models to reproduce the physics of the ENSO system under different boundary conditions it is necessary to reconstruct the state of ENSO and the mean state of the tropical Pacific in the past. There is good reason to think that ENSO may vary in the past, as interannual climate variation caused by ENSO is locked into the seasonal cycle. It has been suggested that "Tropical Pacific climatology must be thought of as the results of similar physics acting on different timescales" (Clement *et al.*, 1999) and therefore, the physical connections that form the ENSO system may hold together over longer periods of time and cause the mean state of the tropical Pacific to change (Cane, 1998) in addition to changes in the strength and frequency of extreme events.

1.2 Challenges in Palaeo-ENSO reconstruction

Palaeoclimate records that are used to reconstruct ENSO fall into two categories: low resolution records such as chemical and faunal proxies from deep sea cores or peat bogs which show perhaps several data points per century at best but are continuous over tens of thousands of years and through major global climate transistions (e.g. CLIMAP Members, 1976; Martinez *et al*, 1997; Stott *et al.*, 2002 Koutavas *et al.*, 2002; Haberle *et al.*, 2001 or Turney *et al.*, 2004), or alternatively records with annual resolution such as tree ring growth (e.g. D'Arrigo and Jacoby, 1991 and D'Arrigo *et al.*, 2005) or $\delta^{18}O$ timeseries from corals (e.g. Tudhope *et al.*, 1995 and 2001; McGregor and Gagan, 2004; Cobb *et al.*, 2001, Ayliffe *et al.*, 2004; Asami *et al.*, 2004 and 2005; Quinn *et al.*, 2006) may be used. These records tend to be shorter, perhaps a few decades to a few hundred years in the late Holocene and much shorter during the last glacial period. Splicing together shorter records to give annual resolution records over long periods of time has been used with respect to both tree rings (e.g. D'Arrigo *et al.*, 2005) and corals (Cobb *et al.*, 2001) in the late Holocene, however there are not sufficient numbers of well dated timeseries available at present to take the same approach with the early to mid Holocene and the last glacial period.

These limitations present a problem for reconstructing the history of a phenomenon that operates on interannual timescales but may vary on millennial to glacial

timescales. Hence most of our understanding of the history of ENSO prior to the last millennia comes from either low resolution sources which can give us an insight into the "mean state" of the tropical Pacific, or short records (usually coral $\delta^{18}O$ time series) which give short windows of information relative frequency and strength of ENSO events. However corals suffer from important drawbacks. Corals are highly porous, which makes their skeletons susceptible to diagenetic alteration from secondary aragonite in the marine environment (Enmar *et al.*, 2000) and from infiltration of water in the vadose zone (McGregor and Gagan, 2003) that may dissolve the skeleton and precipitate secondary calcite. Also corals precipitate an aragonitic skeleton that is depleted in $\delta^{18}O$ relative to the isotopic values of ambient seawater (Weber and Woodhead 1972). This offset can vary significantly between individual corals of the same species living at the same location (Guilderson and Schrag 1999; Linsley *et al.*, 1999). Therefore whilst corals are very useful in producing time series of relative changes in sea surface temperature and salinity from which information regarding variations in the number and strength of ENSO events can be determined, they have limitations in determining absolute climate conditions.

Some authors have suggested that the topics are an important driver of climate on glacial and millennial timescales as the source (Lea *et al.*, 2001, Stott *et al.*, 2002, Cane *et al.*, 1998; Peirrehumbert, 2000 and Clement *et al.*, 2001) or amplifier (Ivanochko *et al.*, 2005 and Timmermann *et al.*, 2005) of global climatic change. This question is yet to be resolved, but will not be determined with confidence without accurate records that are able to determine important aspects of tropical climate both the mean state of the tropical Pacific and more subtle changes to ENSO on glacial and millennial timescales.

1.2.1 Review of tropical Pacific climate and palaeo-ENSO reconstruction

What follows is a review of information that is available regarding the mean state of the tropical Pacific and a review of some of the information gathered from high resolution records.

Our understanding of the climate of the tropical Pacific has changed greatly in the last two decades. The Climate Long-Range Investigation, Mapping and Prediction (CLIMAP Members, 1976) investigation showed a temperature change of only 1-2°C in the tropical Pacific during the Last Glacial Maximum (LGM) using faunal analysis of foraminifera. This was at odds with many terrestrial proxies that indicated a much greater cooling in the LGM tropics (Thompson *et al.*, 1995, Stute *et al.*, 1995). Subsequent studies have identified that the cooling was in fact much greater (e.g. Lee and Sowerby, 1999). Using a General Circulation model, Yin and Battisti (2001), showed that small changes in the sea surface temperatures in the tropics (1°C) could have large effects on high latitude atmospheric temperatures. Lea *et al.*, (2000) combined Mg/ Ca and $\delta^{18}O$ measurements in planktonic foraminifera from two cores in the tropical Pacific, one from the Western Pacific Ontong Java Plateau and the other from the Eastern Pacific cold tongue near the Galápagos Islands. They show a decrease in temperatures of 2.8 ± 0.7°C at the Last Glacial Maximum (LGM), and also demonstrate that temperatures in the tropical Pacific coincide with Antarctic changes in temperature and precede ice volume changes by up to 3 ka suggesting that the tropics have a role to play in driving glacial/ interglacial climate change. Lea *et al.*, (2000) also show that the $\delta^{18}O$ of sea water in Western Pacific during the glacial indicates greater precipitation, and combined with a greater temperature gradient between East and West Pacific, indicates a more "La Niña-like" climate. Conversely, other studies have shown more "El Niño" conditions in the Pacific with higher salinity in the Western Pacific (Martinez *et al.*, 1997 and Stott *et al.*, 2002) and cooler temperatures in the east (Koutavas *et al.*, 2002). Models of the glacial Pacific using bias corrected temperatures from CLIMAP produce (Hostetler *et al.*, 2006) simulations of the tropical Pacific that are more consistent with El Niño-like climate during the LGM.

1.2.2 Orbitally induced changes in ENSO

Since the mid 1980's forecasts of ENSO have been made using simple coupled ocean-atmosphere dynamical climate models (Cane *et al.*, 1986; Zebiak and Cane, 1987). Clement *et al.*, (1999) used this model to show the timing of the boreal perihelion controls the "strength" of ENSO as the numbers and strength of El Niño events is reduced when the perihelion is in the boreal summer or winter. The predicted numbers of El Niño events in 500 year non-overlapping periods over the last 140 ka derived from the model is shown in Figure 1-2.

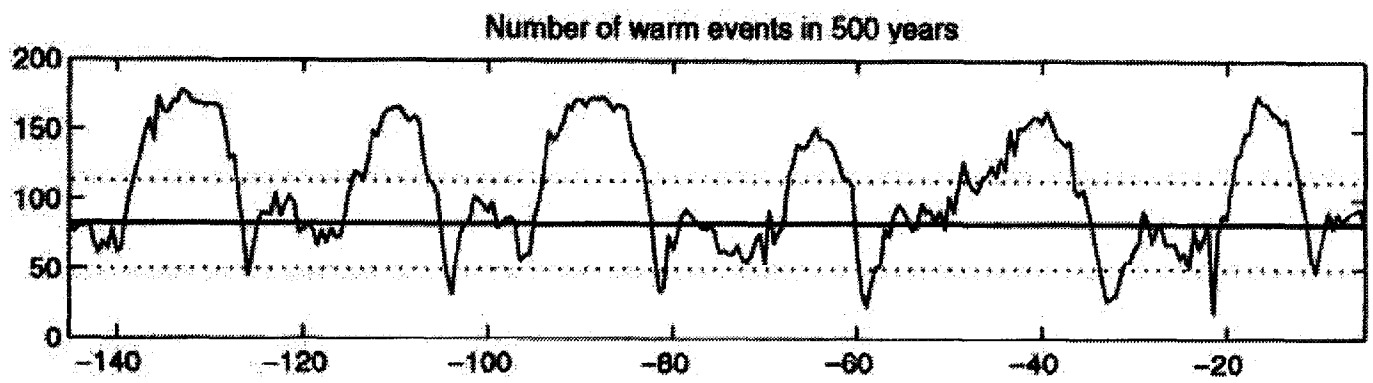

Figure 1-2 Y axis shows the number of warm events (El Niño) predicted in every 500 years from the Zebiak-Cane model forced with Milankovich solar forcing as a function of thousands of years before present (notice the time axis decreases towards the left. (After Clement *et al.*, 1999). Thick line shows mean and dashed lines show 95% confidence limits.

This model predicts an increased frequency of El Niño events during the LGM (20-18 ka) and during Marine Oxygen Isotope Stage 3 between (50-40 ka). Clement *et al.*, (2000) also show that a reduced number of El Niño events are expected during the early to mid Holocene with an increase in variability towards the modern day. Otto-Bliesner *et al.*, (2003) and Brown *et al.*, (2006) show that this reduction in ENSO during the early Holocene is also produced in General Circulation Models. Otto-Bliesner *et al.*, (2003) also make similar predictions for the LGM climate.

A $\delta^{18}O$ record from a deep sea core recovered from the Seram Trough, Eastern Indonesia (Brijker *et al.*, 2006) and charcoal and pollen records from Papua New Guinea (Haberle *et al.*, 2001) indicate warmer and wetter conditions, or a more "La-Niña like" climate in the early Holocene, whereas in the East Pacific (Sandweiss *et al.*, 1996 and Rodbell *et al.*, 1999) predict more "El Niño-like" climates.

Some studies from the western Pacific during the LGM and MIS 3 show freshening WPWP surface hydrology (De-Garidel Thoron *et al.*, 2007 and Lea *et al.*, 2000) indicating more La Niña-like climate, whilst others notably from the West of the WPWP near Indonesia, show increased salinity (Martinez *et al.*, 1997; Stott *et al.*, 2002 and Rosenthal *et al.*, 2003) more reminiscent of an El Niño-like mean climate state. In the east Koutavas *et al.*, (2002) show reduced east-west temperature gradients that indicate more "El Niño-like" climate. These conflicts in interpretation may indicate that the mean state of the climate in the Pacific may not be analogous to ENSO states at all times (De-Garidel Thoron *et al.*, 2007). For example the region of highest rainfall in the WPWP may move eastward, freshening the eastern part of the WPWP.

It may not be clear how these longer-term changes in state relate to variations in the ENSO cycle. Does a more "El Niño-like" climate infer an increase in the frequency of ENSO events or a reduction? Model studies such as Clement *et al.*, (1999) predict that changes to the state of the tropical Pacific are forced by changes to the seasonal cycle, making it more or less sensitive to ENSO variability. Seasonally resolved records are therefore also required to investigate these changes.

Increasingly, seasonally resolved data from the early to mid Holocene is showing that the reduction in ENSO variability linked to orbital forcing, and predicted by these modelling studie are correct. In particular, the seasonally resolved records from the WPWP show reduced numbers and frequency of El Niño events (Tudhope *et al.*, 2001 and McGregor *et al.*, 2004) during the early to mid Holocene.

Tudhope *et al.,* (2001) has shown that during periods of Marine Oxygen Isotope Stage 3 (50 to 35 ka), where the Clement *et al.,* (1999) model predicts a greater than present ENSO variability, coral records show a reduced ENSO variability. As yet there are no annually resolved records from the Last Glacial Maximum in the WPWP.

1.2.3 Millennial-scale climate variation and ENSO

Millennial scale climate variation (sub-orbital but greater than century-scale) has been observed in a great many records from as far afield as the North Atlantic (e.g. Dansgaard *et al.*, 1993 and Bond *et al.*, 1993), the tropical Atlantic region (e.g. Arz *et al.*, 1998), Chinese loess (Porter and An, 1995), and the Arabian Sea (e.g. Shultz *et al.*, 1998). There are good reasons to expect millennial scale variations in the climate of the tropical Pacific. Clement *et al.*, (2001) show that during certain stages of the precessional cycle (which we have seen probably exerts a control on the strength and frequency of ENSO events), ENSO can lock into the seasonal cycle and become amplified through Bjerknes feedback flipping into a mode where La Niña events are common and amplified. This should happen on millennial time scales and be visible in palaeoclimatic reconstructions of WPWP hydrology.

The key study to identify potential sub-orbital variations in WPWP hydrology is presented in Stott *et al.*, (2002). Using $\delta^{18}O$ coupled with Mg/ Ca in a core from the eastern edge of the Indonesian archipelago, (MD98-2181) Stott *et al.* (2002) show that the surface salinity of the WPWP varies by as much as 1 to 2‰ p.s.u. on timescales of a few thousand of years during the last glacial cycle which, they point out, is similar in character to variations in temperature over Greenland derived from $\delta^{18}O$ in ice core records. This study correlates higher salinities in the South China Sea record with cold Greenland stadials and freshening during warm Greenland interstadials. Since higher salinities at the modern core site are associated with El Niño events, they propose that the ENSO system is changing state from one mode to another on millennial timescales (a "Super-ENSO"). However, the correlation of millennial scale events at this timescale is problematic when dating techniques such as radiocarbon have uncertainties associated with them on the timescale of such

events that are being dated. Also it has been suggested that the site of this core is more strongly influenced by the Asian Monsoonal system than ENSO (Rosenthal and Broccoli, 2004). There is some support for this from two other studies from deep sea cores in the Indo-Pacific warm pool (Chen *et al.*, 2005 and Levi *et al.*, 2007). However another study of humification in peat from northeastern Australia (Turney *et al*, 2004) shows the opposite, with periods of increased precipitation related to Heinrich events, which occur during cold stadials in the North Atlantic.

Because of the difficulty in obtaining records that are in the WPWP, and issues relating to correlation of events at millennial timescales at the limit of the use of radiocarbon dating this issue has not yet been resolved.

1.3 Aims of this study

The intention of this study is to attempt to reconstruct the mean state of the WPWP and the state of ENSO in the same archive during periods that have been modeled and to compare with current models of climate reconstruction at these periods. It takes advantage of an area in the WPWP at Huon Peninsula on the north east coast of Papua New Guinea where fossil coral reef material is available to be studied. To allow for the investigation of both mean climate and the state of ENSO archives will be derived from the giant bivalve mollusk, *Tridacna* sp. which can be found in this region and provide the opportunity to extract proxy information for the mean state of climate from $\delta^{18}O$ values as *Tridacna* sp. which, unlike corals, are thought to calcify their shells in isotopic equilibrium with sea water. These long lived bivalves also provide the potential for extracting multi-decade $\delta^{18}O$ timeseries which can be used as archives of the relative strength and frequency of ENSO. The relationship between seasonally resolved $\delta^{18}O$ timeseries extracted from a modern *Tridacna* sp. and an index of ENSO is investigated and a comparison is made between modern *Tridacna* sp. and corals from the same region to determine whether the same methods for ENSO reconstruction can be applied to *Tridacna* sp.

A detailed chronology will be developed to for fossil *Tridacna* sp. to facilitate 1) the removal of a ice volume component from measured $\delta^{18}O$ values, 2) potentially allow the comparison of proxy information from this study with other records of millennial scale climate variation.

Finally seasonally resolved and mean values for $\delta^{18}O$ will be used to investigate the mean state and state of ENSO during the early to mid Holocene (9-7 ka), MIS3 (60-35 ka) and a major climatic event during Heinrich event 4 in the North Atlantic. These data will be compared with other climate proxies and current models to assess their fitness.

References:

Allan R, and R. D'Arrigo (1999) 'Persistent' ENSO sequences: how unusual was the 1990–1995 El Niño? *The Holocene,* **9,** 101–118.

Asami, R., Yamada, T., Iryu, Y., Meyer, C.P., Quinn, T., and G. Paulay (2004), Carbon and oxygen isotopic composition of a Guam coral and their relationships to environmental variables in the western Pacific, *Palaeogeography Palaeoclimatology Palaeoecology*, **212**, 1-22

Asami, R., Yamada, T., Iryu, Y., Meyer, C.P., Quinn, T., and G. Paulay (2005), Interdecadal variability of the western pacific sea surface condition for the years 1787-2000: Reconstruction based on stable isotope record from a Guam coral, *Journal of Geophysical Research,* **110**, C05018

Arz, H. W., Patzold, J. and G. Wefer (1998), Correlated millennial-scale changes in surface hydrography and terrigenous sediment yield inferred from last-glacial marine deposits off northeastern Brazil, *Quaternary Research,* **50,** 157-166

Ayliffe, L.A, Bird, M.I., Gagan, M.K., Isdale, P.J., Scott-Gagan, H., Parker, B., Griffin, D., Nongkas, M. and M.T. McCulloch. (2004), Geochemistry of coral from Papua New Guinea as a proxy for ENSO ocean–atmosphere interactions in the Pacific Warm Pool, *Continental Shelf Research*, **24**, 2343-2356

Bjerknes, J. (1969), Atmospheric teleconnections in the equatorial Pacific, *Monthly Review of Weather*, **97**, 163-172

Bond, G., Broecker, W., Johnsen, S., MacManus, J., Labeyrie, L., Jouzel, J. and G. Bonani, (1993), Correlations between Climate Records from North-Atlantic Sediments and Greenland Ice, *Nature*, ***365***, 143-147

Bouma, M., Kovats, R., Goubet, S., Cox, J., and A. Haines (1997), Global assessment of El Niño's disaster burden, *The Lancet,* **350**, 1435–1438

Brijker, J.M., Jung, S. J. A., Ganssen, G. M., Bickert, T. and D. Kroon (2006), ENSO related decadal scale climate variability from the Indo-Pacific Warm Pool, *Earth and Planetary Science Letter,* **253**, 67-82

Brown, J., Collins, M. and A. Tudhope (2006), Coupled model simulations of mi-Holocene and comparisons with coral oxygen isotope records, *Advances in Geosciences*, **6**, 29-33

Cane, M., Zebiak, S. E. and S. C. Dolan (1986), Experimental forecasts of El Niño, *Nature*, **321**, 872-832

Cane, M.A. (1998), A role for the Tropical Pacific, *Science*, **282**, 59-61

Cane, M.A., Braconnot, P., Clement, A., Gildor, H., Joussaume, S., Kageyama, N., Khodri, M., Paillard, D., Tett, S. and E. Zorita (2006), Progress in Paleoclimate Modelling, *Journal of Climate*, **19**, 5032-5058

Caviedes, C. (2001), El Niño in History: Storming throughout the Ages. *University Press of Florida*, Gainesville, FL.

Chen, C., McCarl, B., and R. Adams (2001), Economic implications of potential ENSO frequency and strength shifts, *Climatic Change,* **49**, 147–159

Chen, M. H., Li, Q., Zheng, F., Tan, X., Xiang, R. and Z. Jian (2005), Variations of the Last Glacial Warm Pool: Sea surface temperature contrasts between the open western Pacific and South China Sea, *Paleoceanography*, **20**, PA001057

Clement, A. C., Seager, A. and M. A. Cane (1999), Orbital controls on the El Niño/Southern Oscillation and the tropical climate, *Paleoceanography*, **14**, 441-457

Clement, A. C., Seager, A. and M. A. Cane (2000), Suppression of El Niño during the mid-Holocene by changes in the Earth's orbit, *Paleoceanography*, **15**, 731-737

Clement, A. C., Cane, M. A. and R. Seager, (2001), An orbitally driven tropical source for abrupt climate change, *Journal of Climate,* **14**, 2369-2375

CLIMAP Project Members, (1976), The surface of the Ice Age Earth, *Science*, **191**, 1131-1137

Cobb, K., Hunter, D.E. and C. D. Charles (2001), A central tropical Pacific coral demonstrates Pacific, Indian and Atlantic decadal climate connections, *Geophysical Research Letters,* **28**, 2209-2212

Dansgaard, W., Johnsen' S.J., Clausen, H.B., Dahl-Jensen, D., Gundestrup, N.S., Hammer, C.U., Hvidberg, C.S., Steffensen, J.P., Sveinbjörnsdottir, A.E., Jouzel, J. & G. Bond (1993), Evidence for General Instability of Past Climate from a 250-Kyr Ice-Core Record, *Nature*, ***364***, 218-220

D'Arrigo R., and G. Jacoby (1991), A thousand year record of northwestern New Mexico winter precipitation reconstructed from tree rings and its relation to El Niño and the Southern Oscillation, *The Holocene,* **1**, 95–101

D'Arrigo R, Cook E, Wilson R, Allan R, and M. Mann (2005), On the variability of ENSO over the past six centuries, *Geophysical Research Letters,* **32**, 1–4

De Garidel-Thoron, T., Rosenthal, Y., Beaufort, L., Bard, E., Sonzogni, C. and A.C. Mix (2007), A multiproxy assessment of the western equatorial Pacific hydrography during the last 30 kyr, *Paleoceanography*, **22**, 3204-322

Dunbar, R., and J. Cole (1999), Annual Records of Tropical Systems (ARTS); Recommendations for Research, *IGBP Science Series*, Geneva

Enmar, R., Stein, M., Bar-Matthews, M., Sass, E., Katz, A. and B. Lazar (2000), Diagenesis in live corals from the Gulf of Aqaba. I. The effect on paleo-oceanography tracers, *Geochimica et Cosmochimica Acta,* **64**, 3123-3132

Fedorov, A. and G. Philander, (2000), Is El Niño changing? *Science*, **288**, 1997-2002

Gergis J, and A. Fowler (2006) How unusual was late twentieth century El Niño–Southern Oscillation (ENSO)? Assessing evidence from tree ring, coral, ice and documentary archives, A.D. 1525–2002, *Advances in Geosciences,* **6**, 173–179

Glantz M., (2005), Usable Science 9: El Niño Early Warning for Sustainable Development in the Pacific Rim and Islands. *Report of workshop held 13–16 September 2004 in the Galapagos Islands, Ecuador*, National Center for Atmospheric Research, Boulder, Colorado, USA

Goddard, L. and M. Dilley (2005), El Niño: catastrophe or opportunity, *Journal of Climate*, **18**, 651–665

Guilderson, T.P. and D.P. Schrag (1999), Reliability of coral isotope records from the western Pacific warm pool: a comparison using age-optimized records, *Paleoceanography,* **14**, 457–464

Haberle, S. G., Hope, G. S. and S.v.d. Kaars (2001), Biomass burning in Indonesia and Papua New Guinea, natural and human induced fire events in the fossil record, *Palaeogeography, Palaeoclimatology, Palaeoecology*, **171**, 250-268

Hostetler, S., Pisias, N. and A. Mix (2006), Sensitivity of the Last Glacial Maximum Climate to uncertainties in tropical and subtropical ocean temperatures, *Quaternary Science Reviews*, **25**, 1168-1185

IPCC, 2001: *Climate Change 2001: The Scientific Basis. Contribution of Working Group I to the Third Assessment Report of the Intergovernmental Panel on Climate Change* [Houghton, J.T.,Y. Ding, D.J. Griggs, M. Noguer, P.J. van der Linden, X. Dai, K. Maskell, and C.A. Johnson (eds.)]. Cambridge University Press, Cambridge, United Kingdom and New York, NY, USA, 881pp.

Ivanochko, T. S., Ganeshram, R.S, Brummer, G.A., Ganssen, G., Jung, S.G.A., Moreton, S.G. and D. Kroon (2005), Variations in tropical convection as an amplifier of global climate change at the millennial scale, *Earth and Planetary Science Letters*, **235**, 302-314

Koutavas, A., Lynch-Stieglitz, J., Marchitto, T. M. Jr. and J. P. Sachs (2002), El Niño-like pattern in ice age tropical Pacific sea surface temperature, *Science*, **297**, 226-230

Lea, D. W., Pak, D.K. and H.J. Spero, H.J. (2000), Climate impact of late quaternary equatorial Pacific sea surface temperature variations, *Science*, **289**, 1719-1724

Lee, K. E. and N.C. Slowely (1999), Cool surface waters of the subtropical North Pacific Ocean during the last glacial, *Nature*, **397**, 512-514

Levi, C., L. Labeyrie, F. Bassinot, F. Guichard, E. Cortijo, C. Waelbroeck, N. Caillon, J. Duprat, T. de Garidel-Thoron, and H. Elderfield (2007), Low-latitude hydrological cycle and rapid climate changes during the last deglaciation, *Geochemistry Geophysics Geosystems*, **8,** 2006GC001514

Linsley, B.K., Messier, R.G., and R.B. Dunbar (1999), Assessing between colony oxygen isotope variability in the coral *Porites lobata* at Clipperton Atoll, *Coral Reefs*, **18**,13–27

Manabe, S. and R.J. Stouffer (1995) Simulation of abrupt climate change induced by freshwater input in to the North Atlantic Ocean, *Nature*, **378**, 165-167

Martinez, J. I., DeDekker, P. and A.R. Chivas (1997), New estimates for salinity changes in the Western Pacific Warm Pool during the Last Glacial Maximum: oxygen-isotope evidence, *Marine Micropaleontology*, **32**, 311-340

McGregor, H. V. and M.K. Gagan (2003), Diagenesis and geochemistry of Porites corals from Papua New Guinea: Implications for paleoclimate reconstruction, *Geochimica et Cosmochimica Acta*, **67**, 2147-2156

McGregor, H.V. and M.K. Gagan (2004), Western Pacific coral $\delta^{18}O$ records of anomalous Holocene variability in the El Niño-Southern Oscillation, *Geophysical Research Letters,* **31**, 2147-2156

Patz, J., Campbell-Lendrum, D., Holloway, T., and J. Foley, (2005), Impact of regional climate change on human health. *Nature,* **438**, 310–317

Peirrehumbert, R.T., (2000) Climate change and the tropical Pacific: the sleeping dragon awakes. *Proceedings of the National Academy of Science*, **97**, 1355-1358

Porter, S. C., and C. S. An (1995), Correlation between Climate Events in the North-Atlantic and China during Last Glaciation, *Nature*, **375**, 305–308

Otto-Bliesner, B. L., Brady, E. C., Shin, S-I., Lui, Z. and C. Shields (2003), Modelling El Niño and its tropical teleconnections during the last glacial-interglacial cycle, *Geophysical Research Letters*, **30**, 2198-2202

Quinn, T. M., Taylor, F.W. and Crowley, T. (2006), Coral-based climate variability in the Western Pacific Warm Pool since 1867, *Journal of Geophysical Research,* **111**, C110006

Rodbell, D. T., Seltzer, G.O., Anderson, D.M., Abbott, M.B., Enfeld, D.B. and J.H. Newman (1999), A ~15,000 year long record of El Niño driven alleviation in South Western Ecuador, *Science,* **283**, 516-519

Rosenthal, Y., de Garidel-Thoron, T., Oppo, D. W., Linsley, B. K., Beaufort, L., Bassinot, F. and A. Mix (2003), Late quaternary paleoclimatology of the western equatorial Pacific, *Geochimica Et Cosmochimica Acta*, **67,** 401-410

Rosenthal, Y., and A. J. Broccoli (2004), In search of paleo-ENSO, *Science*, **304**, 219-221

Sandweiss, D.H., Richardson, J.B., Reitz, E.J., Rollins, H.B. and K.A. Maasch (1996), Geoarchaeological evidence from Peru for a 5000 years B.P. onset of El Niño, *Science*, **273**, 1531-1533

Stott, L., Poulsen, C., Lund, S. and R. Thunell (2002), Super ENSO and global climate oscillations at Millennium timescales, *Science*, **297**, 222-226

Stute, M., Forster, M., Frischkorn, H., Serejo, A., Clark. J.F., Schlosser, P., Broecker, W.S. and G. Bonani (1995), Cooling of tropical Brazil (5°C) during the last glacial maximum, *Science,* **269**, 379-383

Timmermann, A., Latif, M., Bacher, A., Oberhuber, J. and E. Roeckner (1999), Increased El Niño frequency in a climate model forced by future greenhouse warming, *Nature*, **398**, 694-696

Timmermann, A., Krebs, U. Justino, F. Goosse, H. and Ivanochko, T. (2005) Mechanisms for millennial-scale global synchronization during the last glacial period, *Paleoceanography*, **20**, PA00109

Thompson, L., G, Mosley-Thompson, E.G., Davis, M.E., Lin, P.-N., Henderson, K.A., Cole-Dai, L. Bolzan, J.F. and K.B. Liu (1995) A last glacial stage and Holocene tropical ice core records from Huascaran, Peru, *Science,* **269**, 46-50

Tudhope, A.W., Shimmield, G.B. Chilcott, C.P. Jebb, M., Fallick, A.E. and A.N. Dalgleish (1995) Recent changes in climate in the far western equatorial Pacific and their relationship to the Southern Oscillation: oxygen isotope records from massive corals, Papua New Guinea, *Earth and Planetary Science Letters,* **136**, 575-590

Tudhope, A., W., Chilcott, C.P., McCulloch, M.T., Cook, E.R., Chappell, J. Ellam, R.M., Lea, D., Lough, J.M. and G.B. Shimmield (2001), Variability in the El Niño - Southern oscillation through a glacial-interglacial cycle, *Science*, **291**, 1511-1517

Turney, C.S.M., Kershaw, A.P., Clemens, S.C., Branch, N., Moss, P.T. and Fifield L.K. (2004), Millennial and orbital variations of El Niño/Southern Oscillation and high-latitude climate in the last glacial period, *Nature,* **428**, 306-310

Weber, J.N. and P.M.J Woodhead (1972), Temperature dependence of oxygen-18 concentration in reef coral carbonates, Journal of Geophysical Research **77**, 463–473

Yin, J. H. and D.S. Battisti (2001), Importance of Tropical Sea surface temperature patterns in simulations of Last Glacial Maximum Climate, *Journal of Climate*, **14**, 565-581

Zebiak, S.E. and M.A. Cane (1987), A model of El Niño-Southern Oscillation. *Monthly Weather Review*, **115**, 2262-2278

2 Study area and *Tridacna* sp.

Chapter Abstract

This study uses fossil *Tridacna* sp. recovered from the Huon Peninsula, Papua New Guinea. This chapter describes the field area at Huon Peninsula including detailed descriptions of the modern and fossil reef settings, the uplift regime along the coast, sampling of *Tridacna* sp. and sampling localities. The oceanographic setting and the position of the Huon Peninsula relative to the Western Warm Pool of the Tropical Pacific is also described.

Timeseries of modern environmental data (e.g. sea surface temperature, precipitation and salinity) are required to test proxy records, however only a few short *in situ* records are available for comparison in this area. Datasets are available comprising blended ship or gauge and satellite data that are combined in models to produce spatially resolved time series of climate variables such as sea surface temperatures, precipitation and salinity. These datasets are described and evaluated against the available *in situ* records. The variables are also used to demonstrate the strong correlation between regional climate conditions at Huon Peninsula and the El Niño-Southern Oscillation.

Finally a brief discussion of the use of bivalves as climate archives is given with descriptions of Tridacnidae general morphology, taxonomy, geographical distribution and habitat.

2.1 Huon Peninsula

The Huon Peninsula (147.5E, 6.5S), is situated on the North East Coast of Papua New Guinea (see Figure 2-1). This is just south of the Equator and is within the mean annual sea surface temperature (SST) 29°C isotherm, at the heart of the Western Pacific Warm Pool (WPWP).

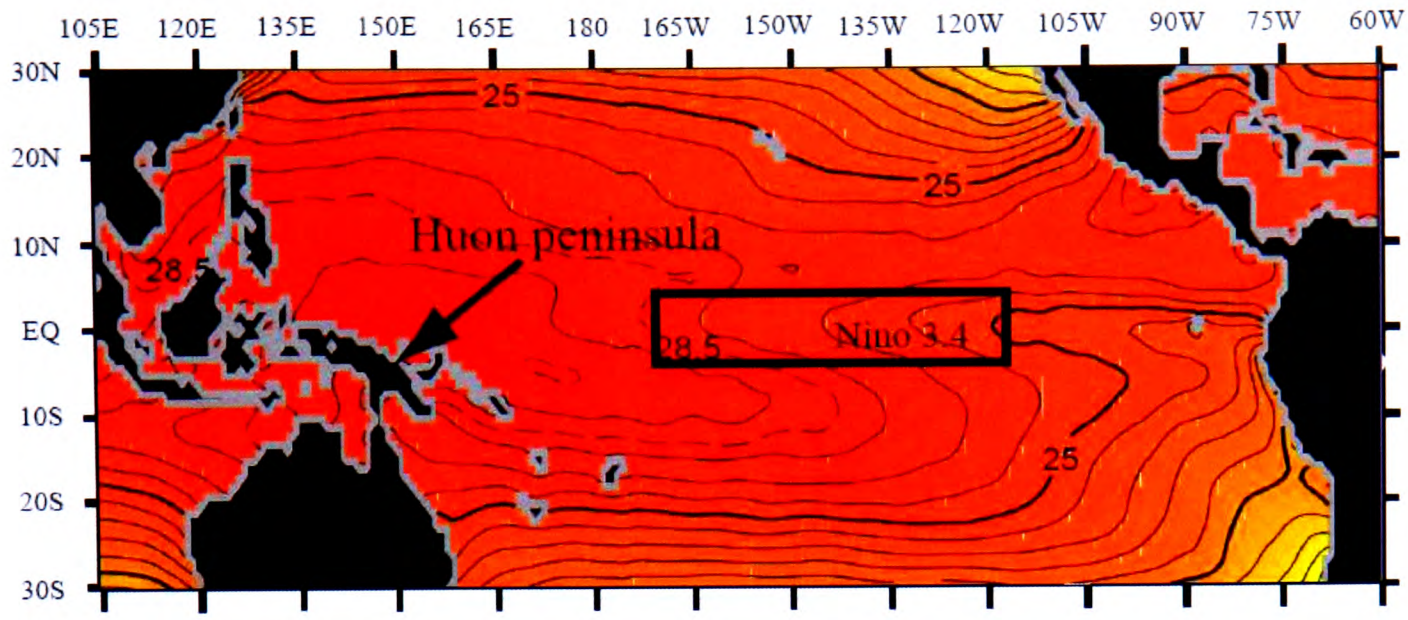

Figure 2-1 Shows the Position of the Huon Peninsula (black arrow) on the North East Coast of Papua New Guinea and the Niño 3.4 Box. Numbers show mean average sea surface temperature contours. The North coast of Papua New Guinea is in the centre of the Western Warm Pool of the Tropical Pacific (mean annual temperatures >29^{0}C). (Source: WOA 2005)

2.2 Geological setting

The collision of the West Pacific and Australian tectonic plates causes uplift along the coast of the peninsula. Pleistocene reefs form the flanks of the Finisterre mountains (see Figure 2-2) overlying Neogene carbonates, which in turn overlie a Palaeogene Volcanic Arc. The terraces ascend to over 1000m above sea level and run parallel to the coast for 80 km (Fairbridge, 1960) with the youngest reefs being closest to sea level. These reefs show repeated reef terrace development, especially during the last glacial cycle.

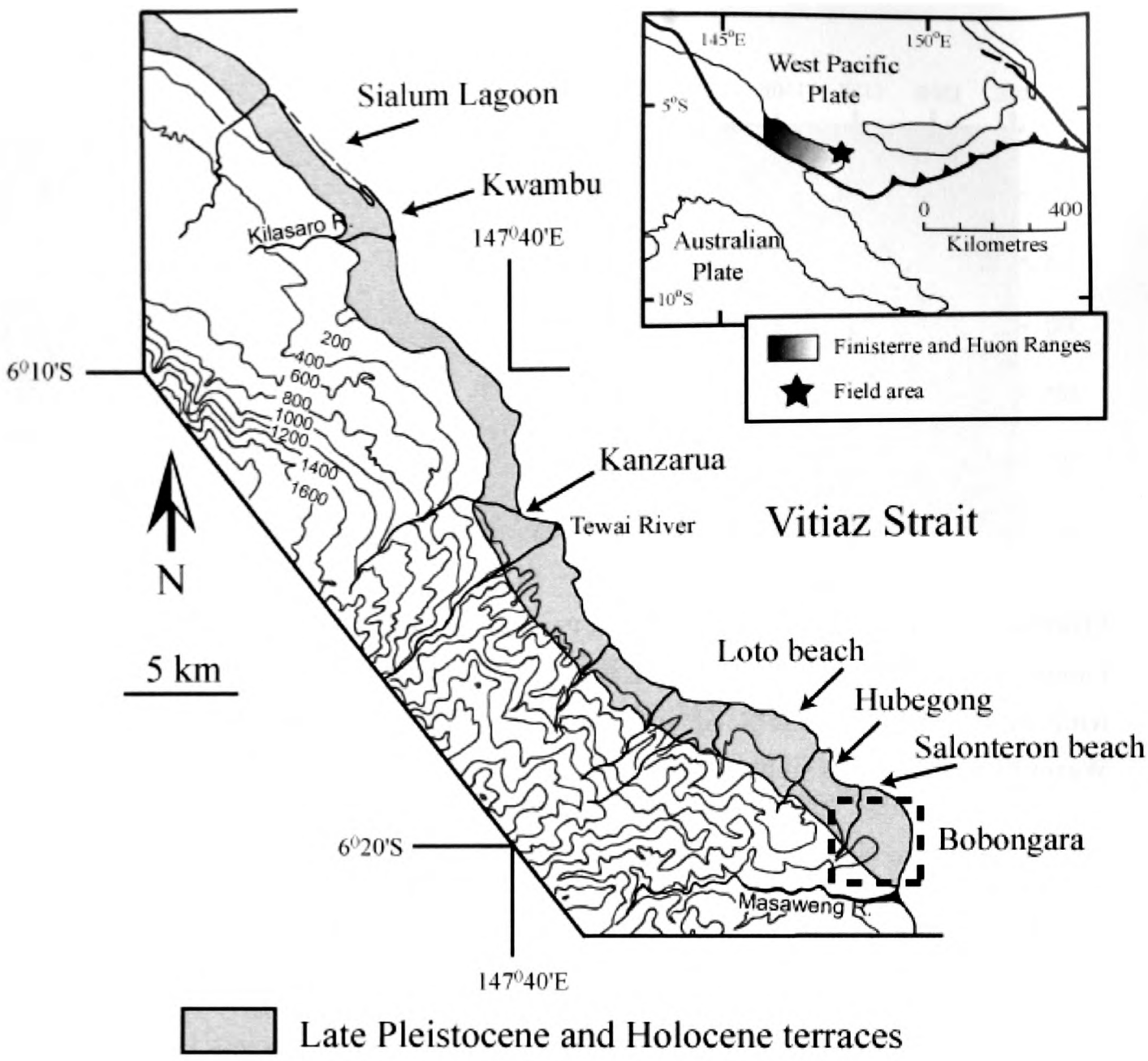

Figure 2-2 Map showing the coast line at Huon Peninsula and highlighting sampling locations of fossil *Tridacna* sp. collected for this study (modified after Ota *et al.*, (1993)). The outlined box highlights the Bobongara area where all the MIS 3 samples were collected. Modern sample Tg-MT7-il was collected from near to Kanzarua. Shaded area highlights the Pleistocene and Holocene reef terraces.

The terraces are continuous along the coast with individual terraces being traced from section to section and are named according to a numerical system presented in Chappell (1974) (see Figure 2-5).

The fossil reefs at Huon Peninsula are not thought to show major differences in taxonomy composition and species diversity in the past despite being subject to different temperature, CO_2 and global sea level (Pandolfi, 1996). The reefs do not show development of lagoons/ barrier complexes except during periods of stable sea level during the Last Interglacial (Reef VII) and the Holocene (Reef I) at Bobongara.

The fossil reefs along the Huon Coast have been extensively dated using radiometric dating of corals and molluscs providing good stratigraphic control on the age of material collected here. The magnitude and timing of Pleistocene sea level changes have been reconstructed using detailed stratigraphic analysis and topographic surveys (Veeh and Chappell, 1970; Bloom *et al.,* 1974; Chappell, 1974; Chappell, 1983; Chappell 2002; Chappell and Veeh 1978; Chappell and Shackleton, 1986; Stein *et al.,* 1992; Edwards et al., 1993; Chappell and Pandolfi, 1996a; Yokoyama *et al.*, 2000; Yokoyama et al., 2001). Rapid sea level rise is thought to be the primary factor that cause the formation of terraces dated between 65 and 30 cal ka (Chappell and Shackleton, 1986; Pandolfi and Chappell, 1994).

In this study fossil *Tridacna* sp. were collected from mid to early Holocene reefs dated between 6.5 and 10 cal ka (Chappell and Polach, 1976; Bloom *et al.*, 1974; Aharon, 1980; Ota *et al.*, 1993; Chappell *et al.,* 1996b; Edinger *et al.*, 2007) and approximately 65 and 30 cal ka (Chappell and Polach, 1976; Bloom *et al.*, 1974; Aharon, 1980; Chappell *et al.*, 1996a; Yokoyama *et al.*; 2000; Yokoyama *et al.*, 2001). The material that was deposited between 30 Ka and the Holocene reefs is either still currently submerged or covered by Holocene reefs due to rise in sea levels since the Last Glacial Maximum (≈ 20-18 cal ka).

Uplift regime at Huon Peninsula

Uplift has been shown to occur in 2-4m incremental coseismic events (Ota *et al.*, 1993; Chappell *et al.,* 1996b) and causes coral reefs that grow along the shoreline to be uplifted and subaerially exposed. Uplift is thought to occur over the last glacial cycle at a relatively constant rate. There are several pieces of evidence to suggest that the uplift rate is broadly linear over longer time periods. Firstly, the rate of uplift measured in the Holocene terrace appears to have been relatively constant (Ota *et al.*, 1993). Secondly, the rate of uplift that is calculated in several regions along the Huon coast from the subaerially exposed transgressive Holocene terrace matches closely the uplift rate calculated by dating the last interglacial terrace in the same region (Ota *et al.*, 1993). Finally, the sea level reconstructions extrapolated from

several different sections of the coast with different average uplift rates matches very closely, which would be unlikely, though not impossible, if uplift rates varied significantly (Chappell, 2002). It is important to realise that without assuming broadly linear uplift rates sea level cannot be reconstructed with any confidence.

2.2.1 Holocene reef terrace

The Holocene terrace forms prominent cliffs along the coast of the Huon Peninsula and is composed of transgressive coral reefs that grew during the post glacial sea level rise. Emergence of the Holocene terraces commences approximately 6-7 ka when post glacial sea level rise began to slow and no longer keeps up with tectonic uplift (Ota and Chappell, 1999). The terraces rises from between 8-12m above sea level at Sialum to 20-23 m near Bobongara and the width of the terrace varies from 100 to 500m. The Holocene reef is mostly composed of fringing reef and with large lagoonal environments seen only at Bobongara and Sialum (Figure 2-2). Analysis of coral and coralline algae shows that the Holocene terraces represent environments of between 2 and 6 metres water depth (Edinger *et al.*, 2007). Holocene age samples were collected between Bobongara and Kwambu approximately 30 km to the North West along the coast at locations marked on Figure 2-2. Samples were collected *in situ*, that is still attached to the fossil reef in life position with both valves together and *ex situ*, i.e. fallen from the face of the Holocene reefs or eroded on the surface of the terrace. It is possible that some of the *ex situ* fossils were merely modern samples that have been washed up on the beaches or carried there by local villagers, however all *ex situ* samples used in this report were radiocarbon dated to exclude this possibility.

2.2.2 Bobongara

Reef terraces between aged between ≈30 and 65 cal ka (equivalent of Marine Oxygen Isotope Stage 3) samples were exclusively collected from Bobongara (147.48E, 6.19S) on the south easterly end of the Peninsula (see Figure 2-2). The terraces at Bobongara are some of the highest on the Huon Peninsula, undergoing a rate of uplift of 3.2m/ ka (Chappell *et al.*, 1996a).

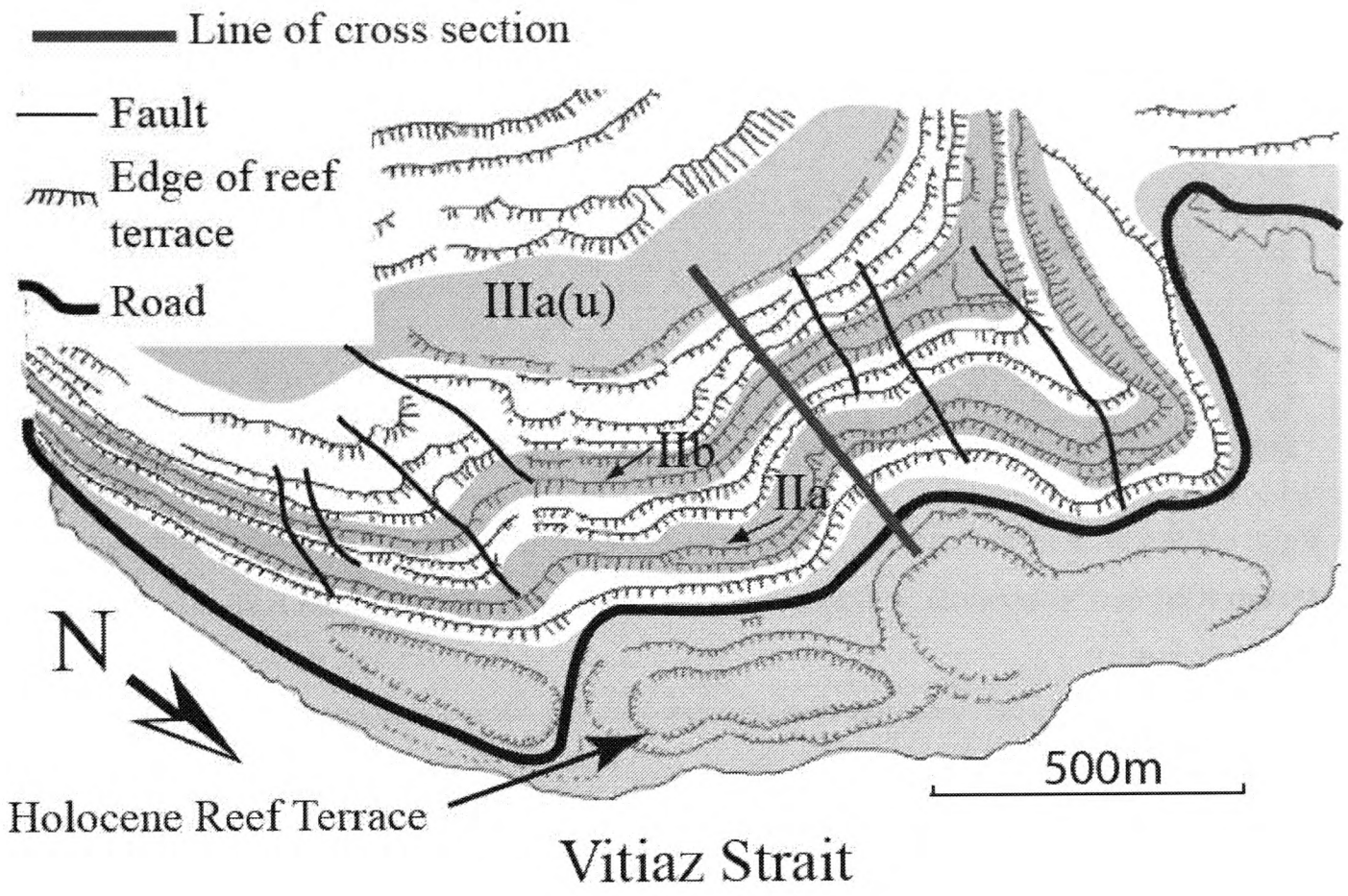

Figure 2-3 A map of Bobongara reef terraces on the Huon Peninsula, where some of the Holocene age *Tridacna* sp. and all of the *Tridacna* sp. aged 30 – 65 cal ka used in this study were collected. Terraces IIIa (u) is at approximately 130m and the Holocene reef is approximately 23m high at the seaward edge. Numbers denote where samples were collected from. Thick blue line denotes the section shown in Figure 2-5

The reef terraces have been extensively surveyed at Bobongara (Chappell 1974; Pandolfi and Chappell, 1994 and Chappell *et al.,* 1996). Pandolfi and Chappell (1994) show that all the major terraces show regular changes in facies reef slope, to reef crest to reef platform from bottom to top, showing that these reefs are growing as transgressive "catch up" or "keep up" type reefs in response to sea level rise.

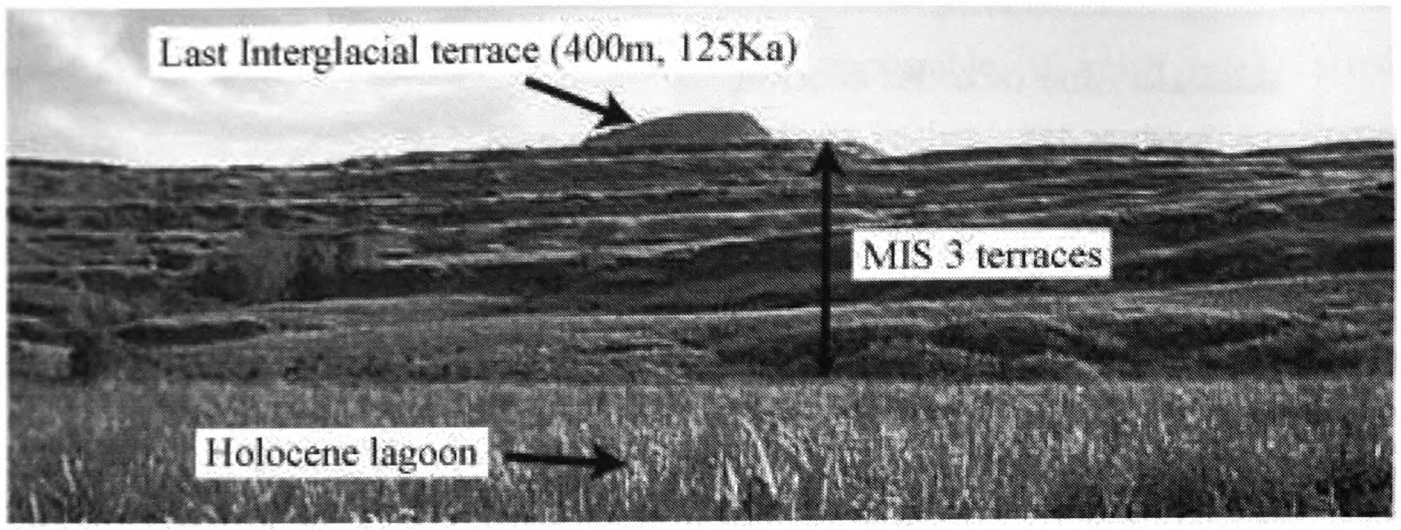

Figure 2-4 Photo of terraces at Bobongara taken from the crest Holocene reef (facing South). (From Esat and Yokoyama., 2006). A cross section through these reefs is seen in Figure 2-5

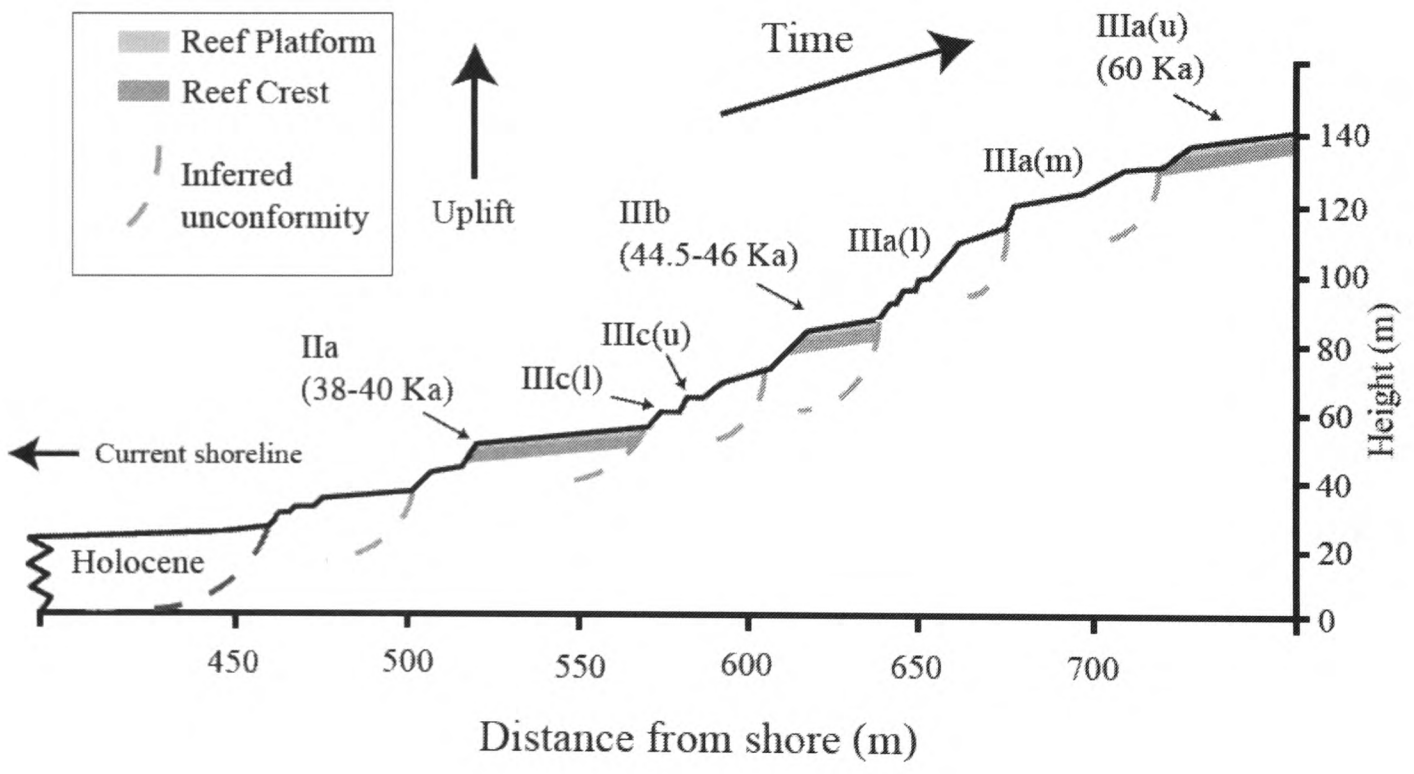

Figure 2-5 Section of Bobongara reef terrace sequence from Pandolfi and Chappell, (1994). Numerals show individual reef terraces and age marked in cal ka. Reef crest and platform facies identified in Pandolfi and Chappell (1994) are marked. Other facies are thought to be upper reef slope with small amounts of reef crest in places. Recent observations identified small amount of reef crest in other places such as IIIc(l) and IIIc(u) (Chappell, pers. comm..).

2.2.3 Sample Collection

The intention of this project was to collect several *Tridacna gigas,* the longest lived of the genus *Tridacna,* from over the growth history of each terrace so that the longest possible time series of climate proxy information could be analysed to detect subtle changes in ENSO during the period of each terrace's growth. Despite help from local villagers clearing the ground and helping to search, it was difficult to locate as many samples as were initially planned and the sampling strategy had to be modified to make use of what material was available by collecting smaller species of *Tridacna* wherever they could be found.

Tridacna sp. were located by walking across the surface and face of each reef terrace and locating samples fallen from the Holocene reefs. When i*n situ* and *ex situ* samples of *Tridacna* sp. were located, their position was noted using GPS and in the case of *in situ* samples, the distance of the *Tridacna* sp. in metres from the top of each reef terrace was noted. For the MIS3 terraces at Bobongara barometric and GPS height elevation were not sufficiently accurate to determine elevation to within ±20m, therefore elevation was later estimated using measurements of the distance from top of terraces transferred to the accurate topographic section presented in Chappell *et al.,* (1996a).

Once located, fossil *Tridacna* sp. were removed from the terraces using chisels, hammers and crow bars. Obtaining a modern sample of *Tridacna gigas* was problematic since they are listed by the International Union for the Conservation of Nature (IUCN) as "threatened" and therefore it was not felt that one could be collected live. Modern samples were provided by local villagers who collect them occasionally for food, eating the large adductor muscle, and who subsequentially use them as pig troughs. Locals informed us that the large modern sample provided had been collected live the previous year in approximately March 2003. It is not clear how reliable this information was, however it was noted that the samples collected were not significantly altered by exposure to precipitation, soil and pig faeces, therefore whilst it is possible that this sample was an heirloom the excellent

preservation of the shell makes this seem unlikely. Samples that were small enough (<40cm along long axis) were assigned a name (T*n* for fossil samples, MT*n* for modern samples). Samples that were greater than this size were trimmed using chisels and hammers to make them more manageable to carry. A total of 75 samples of fossil and modern *Tridacna* sp. were collected although not all were used in this study.

2.3 Modern oceanographic setting

2.3.1 Modern reef environment

Fringing reefs and lagoons have developed over most of the north eastern shore of the peninsula. The coral reefs that grow along the shore of the Huon coast are largely fringing reefs with a lagoon and barrier complex seen near the village of Sialum (see Figure 2-2). The topography of the sea floor varies along the coast. There is a lagoon at Sialum, but no lagoons in the sampling area. Nakamori (1994) surveyed a transect at Hubegong village (see Figure 2-2) which is close to Bobongara (one of the main sampling localities). Here the fringing reefs form on a narrow wave cut platform and slope away from the shore at an angle of 30^0. Hermatypic corals are very abundant in the shallow parts of the reef (0-5m), but become rare with depth, with no hermatypic corals at depths deeper than 30m. There are several small streams near to Bobongara, and it is approximately 3-4 km from the mouth of the larger Masaweng River. River flow can exert a control a local coastal salinities however the catchments areas of these remain small and do not exert a strong influence (Pandolfi, 1996).

The modern sample of *Tridacna gigas* (Tg-MT7) that is discussed in Chapter 3 was collected from Kanzarua (Figure 2-2). This is an area of fringing reefs again, with no lagoonal influence. However the large Tewai River flows into the Vitiaz Strait at this point, and therefore this area receives more riverine influence than at Bobongara (Pandolfi, 1996).

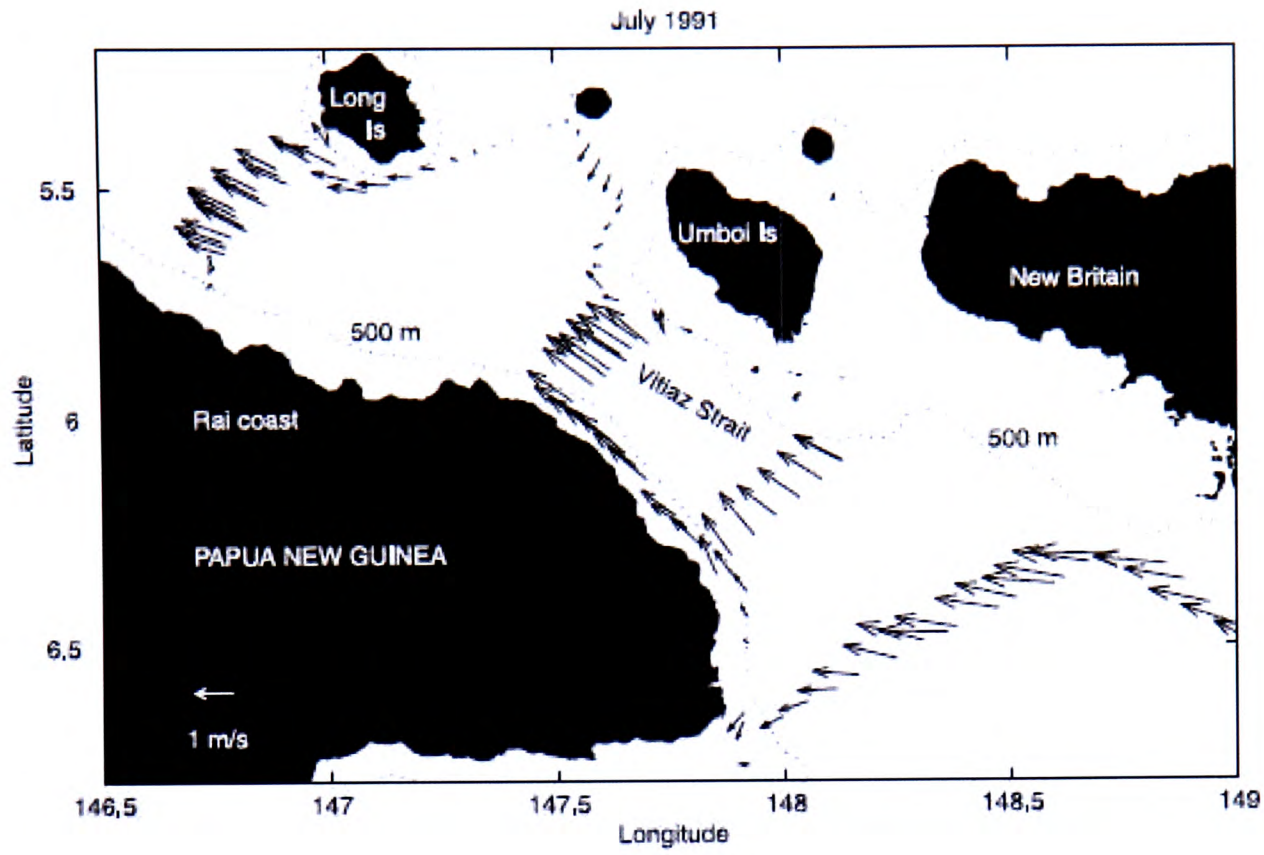

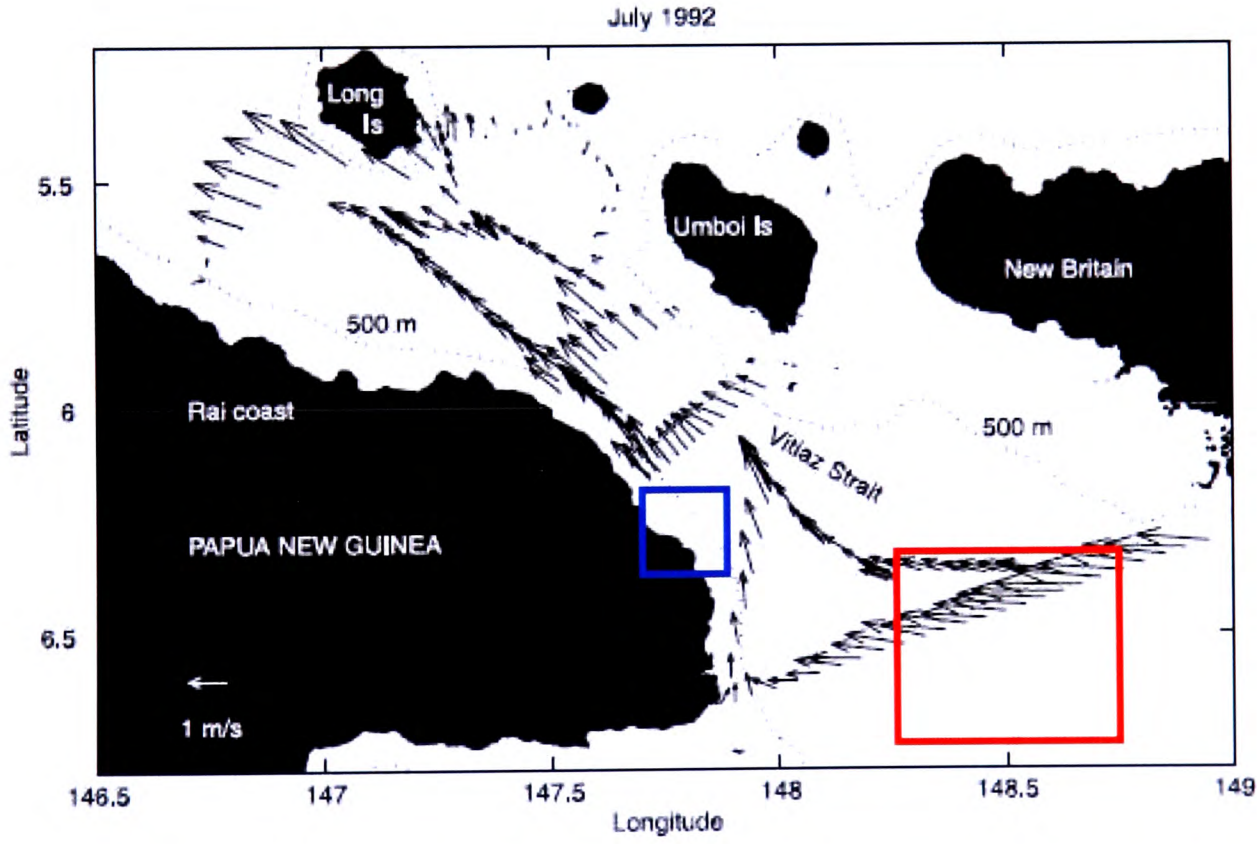

Figure 2-6 Shows the position of the Huon Peninsula on the North East Coast of Papua New Guinea, adjacent to the deep (1200m) Vitiaz Strait. Arrows show near surface current vectors measured on the ADCP (Acoustic Doppler Current Profiler) *Franklin* on voyages in July 1991 (upper) and July 1992 (lower). Blue square indicates the field area, the red square shows the position of the box from which interpolated climate records where taken. (From Cresswell, 2000)

The coastline is adjacent to the Vitiaz Strait between the Bismark Sea to the North and the Solomon Sea to the South, and lies in the heart of the Western Pacific Warm Pool (Figure 2-6). The Vitiaz Strait (see Figure 2-6) is deep (1200m at deepest) and narrow (30 km wide), and where the residence time of the water is low (Aharon and Chappell, 1986; Creswell, 2000). At the surface the New Guinea Coastal Current flows westwards at > 0.5 ms^{-1} during the SE monsoon and eastward at < 0.5 ms^{-1} during the NW monsoon (Fine *et al.*, 1994).

According to the World Ocean Atlas, (2005) surface salinity in the Vitiaz Strait is low, fluctuating between 33.2 – 34.4 ‰ p.s.u. and average annual SST is 29.1°C with small fluctuations between 28.1°C in August/ September to 29.7°C in December/ January (based upon 1° x 1° square centered on 6.5°S, 148.5°E).

Studies indicate that the oceanic mixed layer in the West Pacific is deep (approximately 30m) (Lindstrom *et al.*, 1987; Lukas and Lindstrom, 1991). This is likely to be due to salinity stratification due to high levels of precipitation and low wind speeds.

2.4 Climatological setting

Water circulation on the reefs is affected by seasonal movements of the Intertropical Convergence Zone (ITCZ). This passes over the equator twice during the year in response to changes in the South East trade winds and North West Monsoon. There is a pronounced wet and dry season coinciding with the Austral summer and winter respectively. There is a lack of *in situ* climatological data from Huon Peninsula since there are no permanent stations monitoring climate variables such as sea surface temperature or sea surface salinity, however there are available blended ship and satellite data. These integrate measurements from several sources and produce gridded square data time series of climate variables and are often used in climate models. Because these variables are not direct measurements and are averaged over substantial areas it is important to evaluate each one and compare them against shorter instrumental records where possible. This study uses records collected from

a grid square centred on 6.5S, 148.5E to extract data from. Figure 2-6 shows the position of this grid square (marked in red) relative to the Huon Peninsula field area (mark in blue).

2.4.1 Sea surface temperature (SST) records

Two datasets provide monthly SST time series; HadISST and IGOSS nmc. HadISST data set of SST and sea ice cover provided by the UK Met Office spans from 1870 to the present day and is a globally complete 1x1 degree latitude-longitude modeled data set that is corrected for ship and satellite observations (Rayner *et al,*. 2003). IGOSS nmc (Integrated Global Ocean Services System) (Reynolds *et al.*, 2002) is a very similar dataset of modeled SSTs, 1970 to present that is also corrected using the COADS (Comprehensive Ocean Atmosphere Data Set) (Slutz *et al.*, 1985).

Comparison with in situ records

Two data loggers were left in the lagoon at Sialum (see Figure 2-2) to record temperature by A. Tudhope during 1996-1998. These data are compared to HadISST and IGOSS nmc for the same period in Figure 2-7. The data logger at 2.5m depth behind the fringing reef was present from 1995 to 1997, and another placed at 8m depth near the entrance tp the lagoon collected data from 1996 to 1997. A temperature range of 25.8-30.4 °C was recorded over approximately two years. For comparison results of temperatures extracted from the HadISST data set and the IGOSS NMC data set are compared with these records.

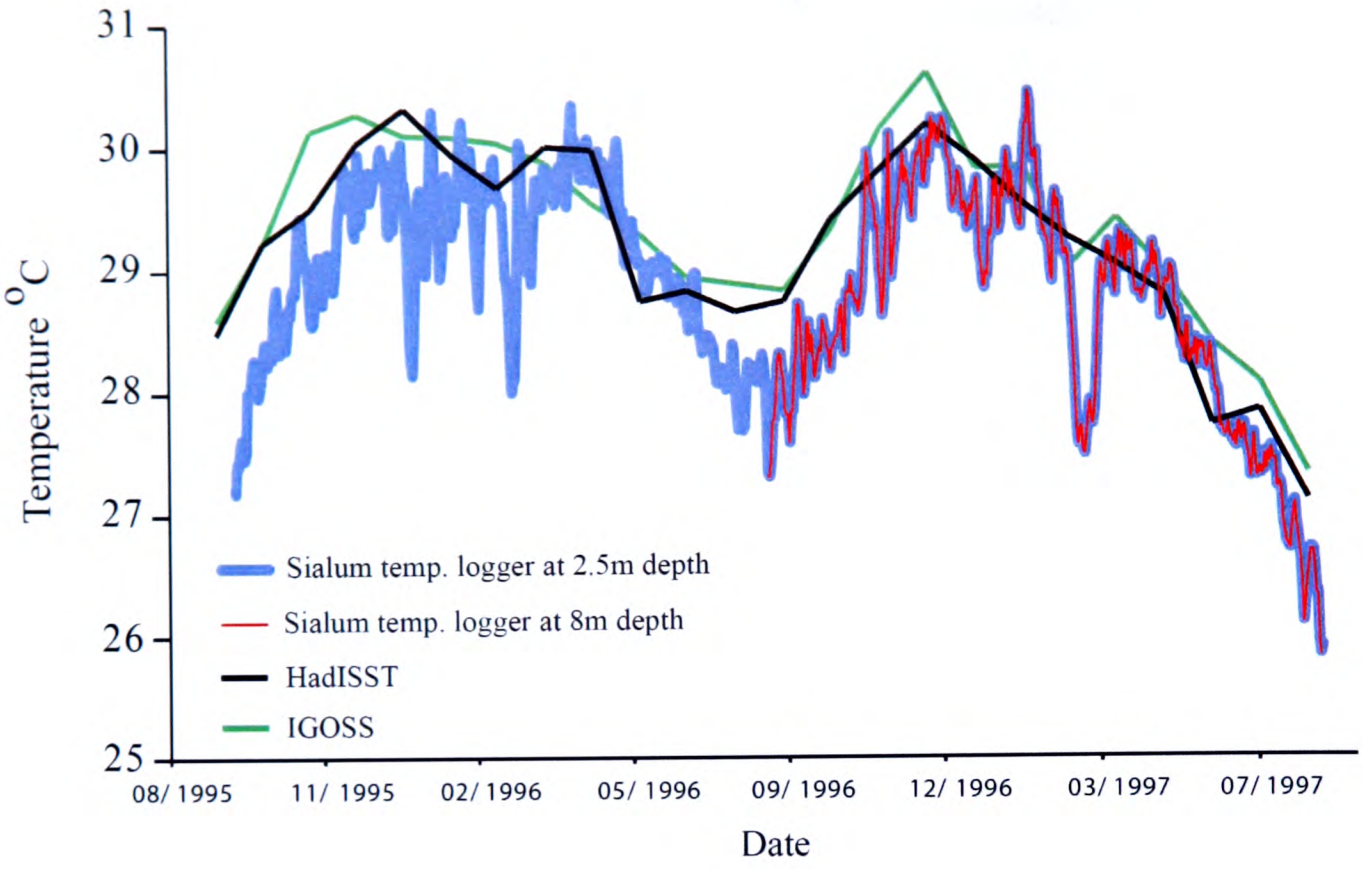

Figure 2-7 SST results of Temperature Loggers placed behind the Lagoon Barrier at 2.5m below Mean Low Water Springs (MLWS) (13/09/95-12/08/97) and at the base of the fringing reef opposite the lagoon entrance, 8m below MLWS (25/08/96-12/08/97) in Sialum Lagoon, Huon Peninsula provided by A. Tudhope pers. comm.. (unpublished data) and record derived from HadISST and IGOSS data sets for the degree square centred on 147.5E, 6.5S. Correlation coefficient between Loggers over period 25/08/96-12/08/97 is 0.97.

Comparing the IGOSS dataset with the Sialum Temperature loggers (See Figure 2-7 and Table 2-1) it can be seen that the both the HadISST dataset and the IGOSS nmc data reproduce the temperatures recorded at Huon extremely well, whilst not reproducing the full range of temperatures seen in the temperature logger record. The HadISST dataset appears to reproduce more of the extreme temperature values than the IGOSS record. The mean temperature range is slightly higher (0.4°C and 0.5°C in HadISST and IGOSS respectively).

Source of Temperature data	Mean Temperature (°C)	Standard Deviation	N=
Temperature Logger (2.5m)	28.8	0.87	697
IGOSS dataset	29.3	0.79	24
HadISST dataset	29.2	0.83	24

Table 2-1 Showing the mean temperature and standard deviation over the period August 1995 to September 1997 for in situ measurements made in Sialum Lagoon and records derived from interpolated ship and satellite datasets.

By comparing the HadISST and IGOSS records (See Figure 2-8) over the period 1981 to 2005 we can see that the HadISST record is more variable than the IGOSS record, especially showing cooler temperatures in the Austral winter, which both records seem to underestimate compared to the temperature loggers. Therefore it is assumed that the HadISST record is likely to be a better representation of the actual temperature record than IGOSS, though both are likely to underestimate the full range of variability in SST at Huon Peninsula most probably due to averaging over large areas.

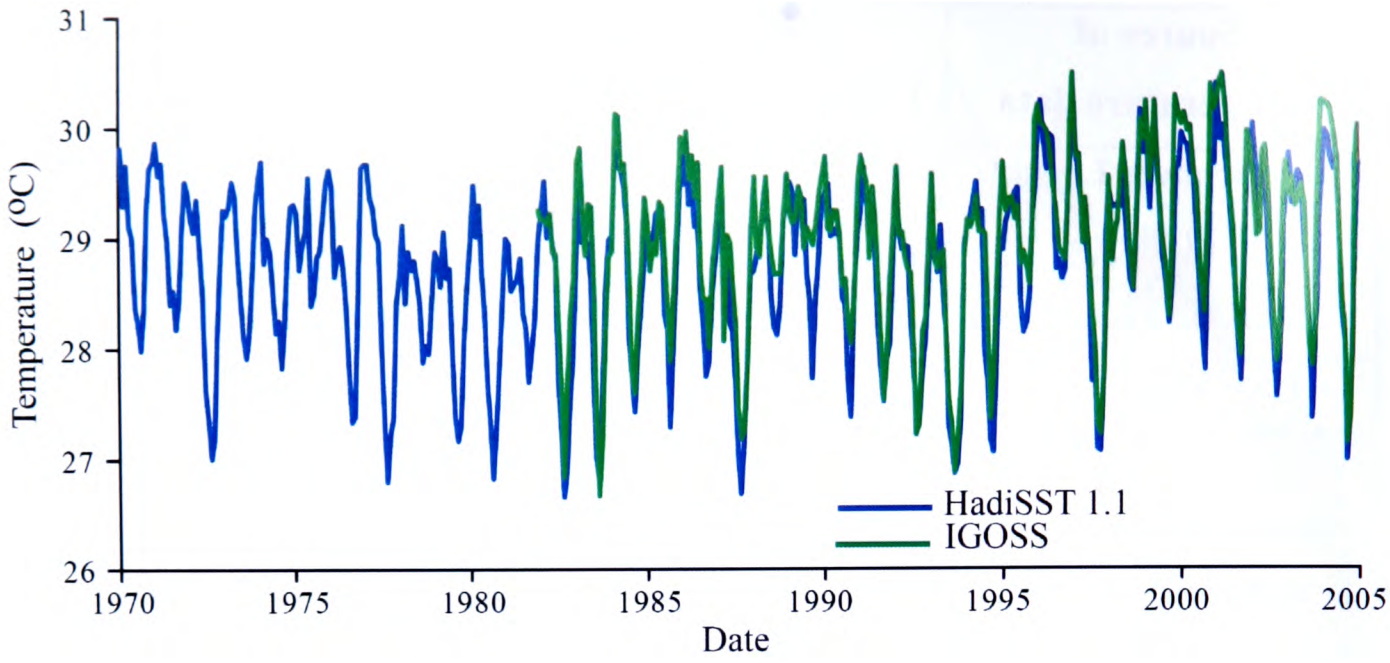

Figure 2-8 Temperature record for the Huon Peninsula area (Grid square centred on 147.5 E, 6.5 S) from the HadISST data set. HadISST dataset shows larger annual amplitude than IGOSS nmc.

SST and water depth

NODC World Ocean Atlas 2005 (Locarnini et al., 2006) data allows us to examine the likely temperature profile at depth in the Vitiaz Strait. There is very little temperature change with depth and a deep thermocline with changes of only (0.5°C in top 50m). This effect may be more pronounced nearer to the shore, and as this data is blended and averaged it is likely that this may not show the full variability. Cresswell (2000) shows that this may be greater during some years (up to 1°C in top 10m). Temperature readings from both Sialum lagoon loggers are essentially identical, which may be because lagoonal water is restricted, however the sampler that was placed at 8m was near to the entrance of the lagoon.

2.4.2 Precipitation records

There are no permanent stations measuring amount of precipitation at Huon Peninsula. The nearest weather station is at Madang to the North West of the Huon Peninsula (5.13S, 145.47E), which has some gaps in data and for which I only have a record to 1995. Therefore it becomes necessary to use blended observation and satellite data, but these records can be checked against the data available from

Madang. The data set used here is version 2 of the NASA GPCP Combined Precipitation Dataset of combined satellite and gauge measurements centered on a degree square 146.25E 6.25S.

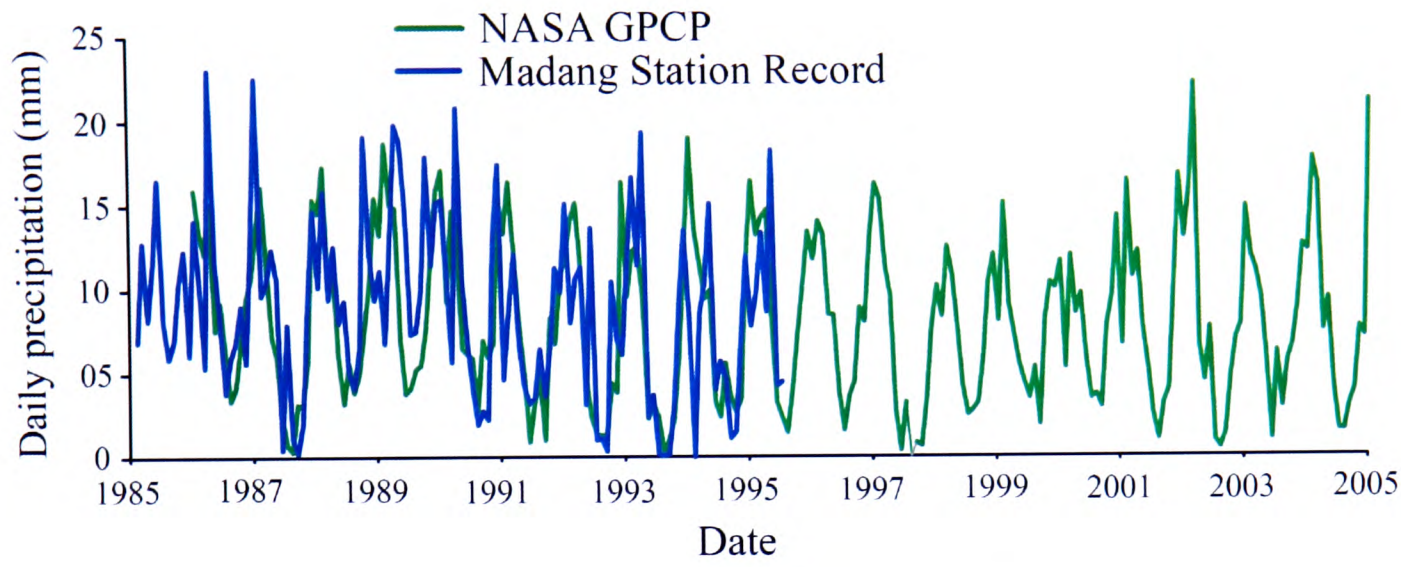

Figure 2-9 Comparison of in situ precipitation records from Madang Station and NASA GPCP combined satellite and gauge data.

Figure 2-9 shows the relationship between the NASA GPCP estimate of monthly precipitation on the Huon Peninsula and the Madang Station rainfall record. There is an extremely good correlation in terms of interannual variability between the two records. However this is likely to be caused at least in part because the Madang Station is the closest station to the Huon Peninsula and is used to calibrate satellite data.

2.4.3 Surface salinity records

The Carton-Giese SODA Version 1.4.3: UMD Simple Ocean Data Assimilation Reanalysis output was used for salinity records. No *in situ* salinity measurements were available for comparison with the salinity record at Huon Peninsula.

2.4.4 Average monthly climate at Huon Peninsula

Figure 2-10 shows the mean monthly values for SST, precipitation and salinity for the years 1985-2005 from the records quoted above. Precipitation and SST show strong anti-correlation with salinity.

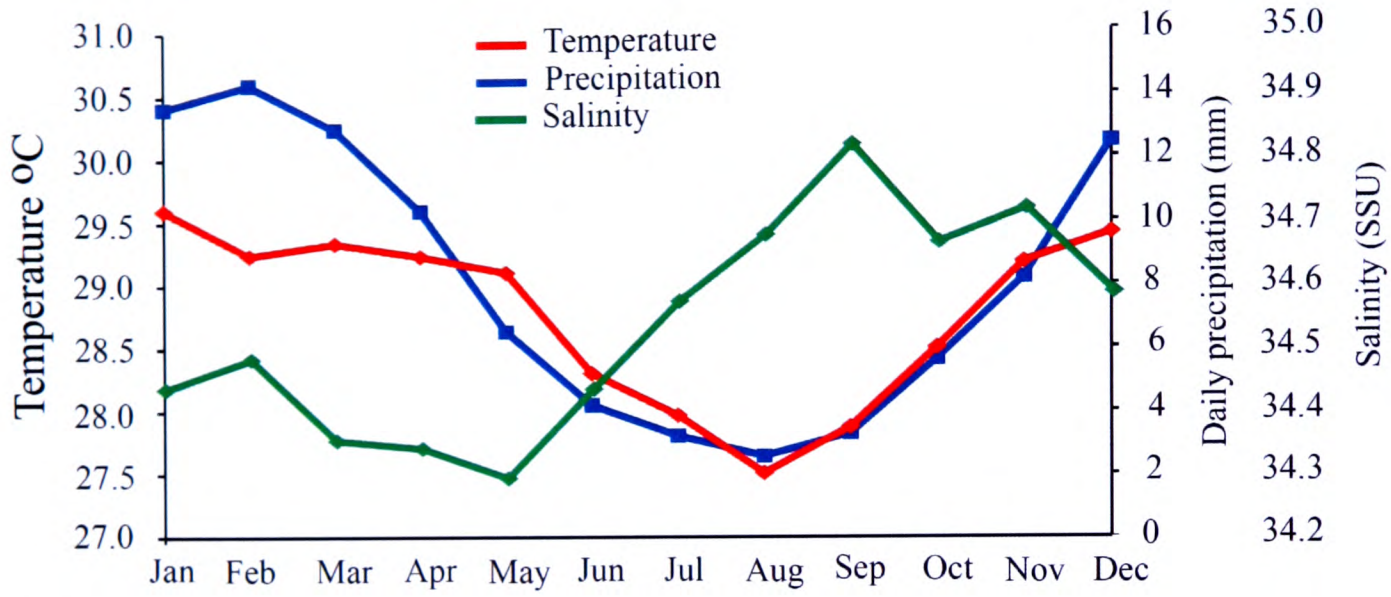

Figure 2-10 Mean monthly values for SST, precipitation and salinity for the years 1985-2005 for the grid square centred on 147.5E, 6.5S.

2.4.5 Isotopic measurements in precipitation and sea water

Based upon measurements of water from the River Tewai, precipitation at Huon Peninsula is thought to have a strongly negative $\delta^{18}O$ of –9.9‰ (Aharon and Chappell, 1986).

In situ measurements of $\delta^{18}O_w$ in sea water are rare. Measurements of the oxygen isotope ratios of seawater in the Sialum Lagoon (0.18‰ relative to SMOW, where N=9) and the Vitiaz Strait (-0.07‰ relative to SMOW where N=1) were collected during October 1977 (Aharon and Chappell, 1986). Considering the negative $\delta^{18}O$ value of precipitation it is perhaps surprising that $\delta^{18}O$ of seawater is thought to be so isotopically positive. There are several possible explanations for this. Firstly the positive $\delta^{18}O$ values from Sialum Lagoon may be as a result of its restricted water exchange with the open ocean. Secondly, as residence time of the seawater in the Vitiaz Strait is low the coastal waters may be highly mixed so that the negative

impact of precipitation on surface waters is short lived. Finally these results were all taken during the dry season (September) when there is little input from precipitation.

Some backing for the *in situ* measurements of $\delta^{18}O$ come from LeGrande and Schmidt (2006) who use a model to extrapolate average $\delta^{18}O_w$ of approximately 0.1-0.2 for seawater near Papua New Guinea. However these are regional values and as mentioned above $\delta^{18}O_w$ may vary significantly locally, especially near shore environments and seasonally. Furthermore the dataset produced by LeGrande and Schmidt (2006) incorporates these *in situ* measurements; therefore they are probably not reliable under the same criteria as the *in situ* measurements.

However, Tudhope et al., (1995) suggest since precipitation in the WPWP has a very negative oxygen isotopic signature and is effectively entering a small volume of water due to stratification (30m mixed layer depth) this is likely to have a relatively strong impact on $\delta^{18}O$ ratios in the carbonate skeletons of reef dwelling organisms.

It is possible to estimate a $\delta^{18}O_w$ of sea surface water using Fairbanks et al., (1997) relation between $\delta^{18}O_w$ and salinity for tropical seawater. An annual variation in $\delta^{18}O$ can be estimated at $\approx$ 0.02‰ for sea water at the Huon Peninsula.

2.4.6 Relation of local climate to ENSO

The climate of the Huon Peninsula is strongly affected by the ENSO system. A commonly used index of ENSO is the SST anomaly in the Niño 3.4 box (Trenberth, 1997) which is a region in the Equatorial Pacific: (5N-5S x 170W-120W) (see Figure 2-1) where the change in SST anomaly is correlated with El Niño/La Niña state in the Tropical Pacific. El Niño is identified when a 5 month anomaly from mean exceeds 0.4°C in the Niño 3.4 box (-0.4°C for La Niña) (Trenberth, 1997).

A good correlation between deviation from mean values of SST, precipitation and salinity and any index of ENSO is expected. Figure 2-11 shows 5 point smoothed

monthly anomalies for temperature and precipitation and salinity for the Huon Peninsula compared the Niño 3.4 index for the period 1985 to 2005.

A strong interannual correspondence exists between temperature and precipitation and salinity records for most of the period sampled, with very similar trend except in the years 1998-2001. It is also clear that years with El Niño events are associated with a reduced SST, reduced precipitation and increased salinity.

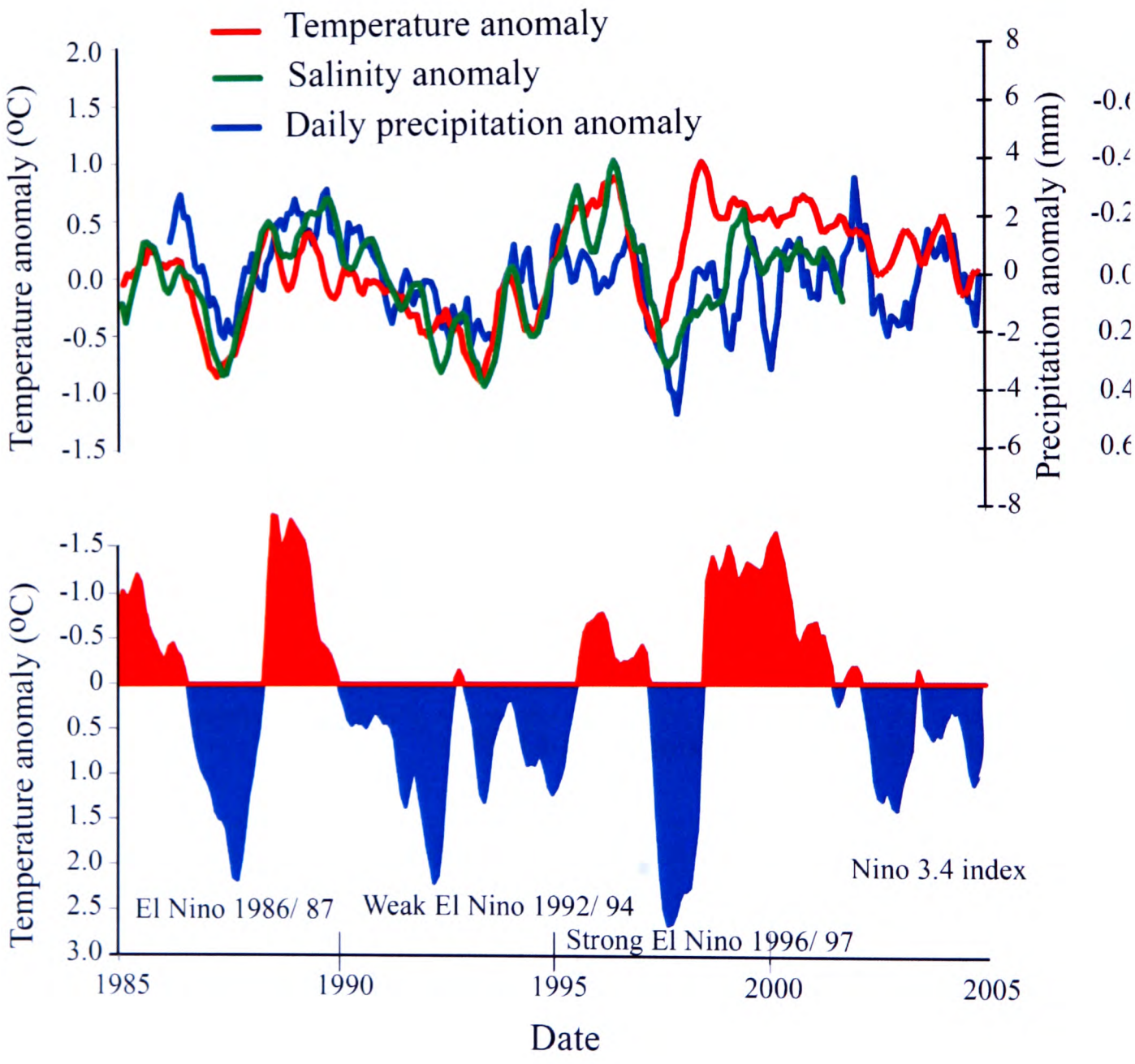

Figure 2-11 SST, precipitation and salinity anomalies (5 pt smoothed) at Huon Peninsula compared to 3 month smoothed SST anomaly in the Niño 3.4 box. Note that salinity anomaly axis and Niño 3.4 SST axis are reversed.

2.5 Bivalves as climate archives

Bivalve molluscs are commonly used as archives for annually resolved studies of past climates (e.g. Arthur *et al.*, 1983; Aharon and Chappell, 1986; Romanek *et al.*, 1987; Elliot *et al.*, 2003; Weidman and Jones, 1994; Carre *et al.*, 2005; Scourse *et al.*, 2006). The long lived reef dwelling bivalve *Tridacna* has been well studied in a variety of environments (Aharon and Chappell, 1986; Romanek *et al.*, 1987; Romanek and Grossman, 1989; Watanabe and Oba, 1999; Watanabe *et al.*, 2004 and Elliot *et al.*, (submitted)). This bivalve lives on coral reefs near the ocean surface, and some species have been shown to live for up to 60 years (Watanabe *et al.*, 2004). *Tridacna* has also been shown to precipitate its skeleton in isotopic equilibrium with sea water (Aharon and Chappell, 1986; Romanek and Grossman, 1989; Aharon, 1991; Watanabe and Oba, 1999; Elliot *et al.*, (submitted)). The shells of *Tridacna* are also very dense aragonite crystals which make them more likely to be resistant to diagenetic alteration.

2.5.1 Tridacnidae

Giant clams of the bivalve molluscan family Tridacnidae (Rosewater, 1965) are found in the Indo-Pacific region. The family appears to have existed since the Eocene (Rosewater, 1965) with six species extant today. They are highly specialized, bearing zooxanthellate algae; they are obligated to live in the photic zone of coral reefs and atolls. Depending on species they are either attached by a byssus, burrow into coral (*Tridacna crocea*) or simply remain unattached resting on the sea floor (*Tridacna gigas*). *Tridacna gigas* is the largest of the Tridacnids and the most common of the species on the modern reefs of the Huon Peninsula (Aharon and Chappell, 1986). They may be occasionally exposed by low tides, and when covered by sea water they open their valves and protrude symbiont bearing mantle lobes. The bivalves are thought to be able to "farm" food through the photosynthesizing algae that live in their mantle (Yonge, 1936).

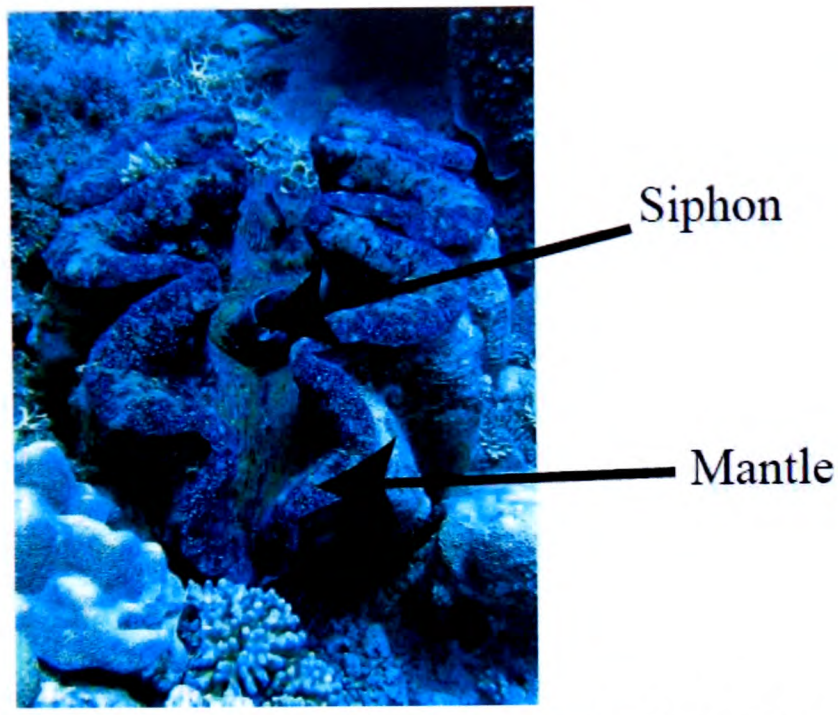

Figure 2-12 *Tridacna gigas* from the Great Barrier Reef (photographed by Jan Derk, 2002)

Morphology of the Tridacnidae

Many aspects of the Tridacnidae morphology are related to adaptations that allow them to best use their zooxanthellae which reside in lens-like structures called hyaline organs in the bivalve's mantle and provide increasing light penetration through the mantle surface. The increase in the mantle-siphon tissues that hold the zooxanthellae have caused the umbo, hinge and ligaments to be pushed antero-ventrally. The anterior teeth are lost and the posterior teeth are actually located anterior to the umbo (Figure 2-13).

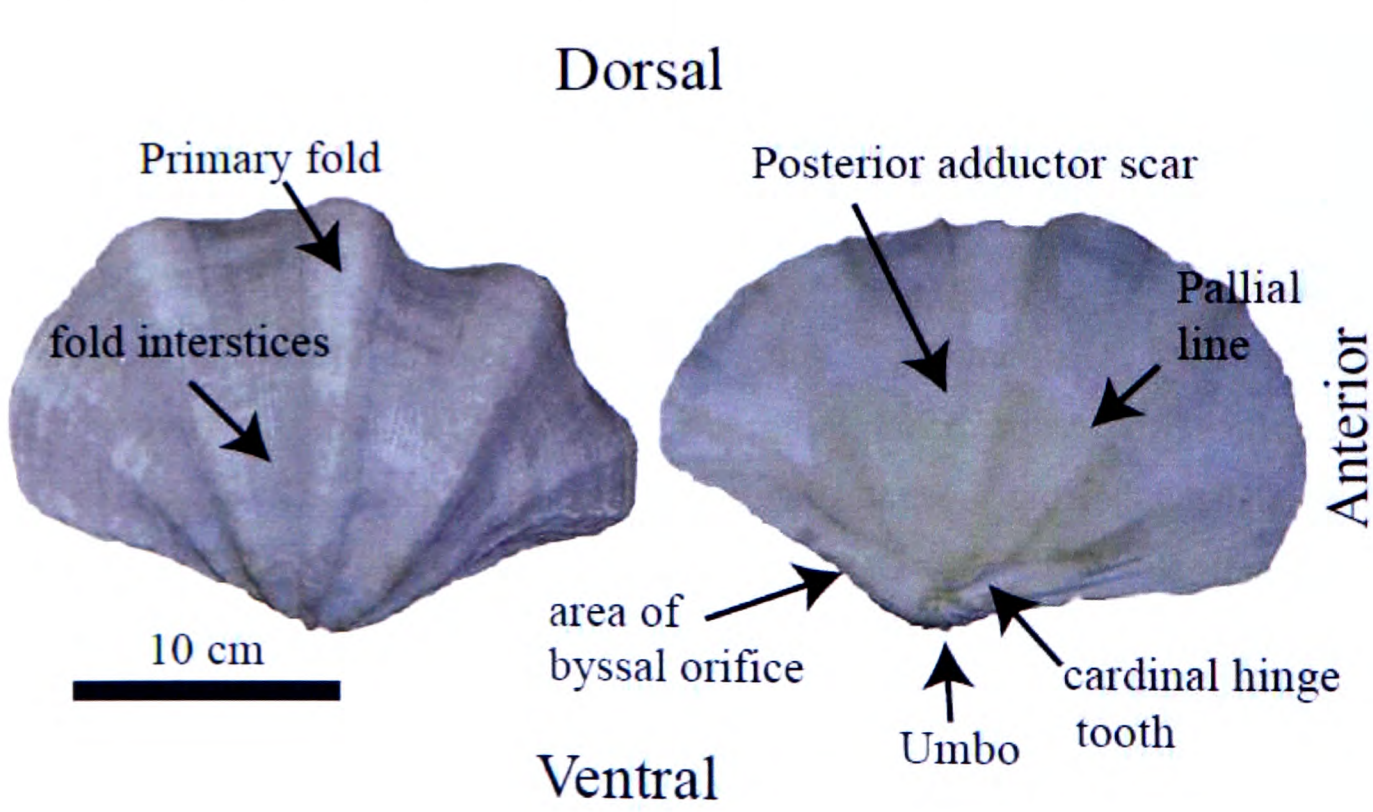

Figure 2-13 Photoraph of the anatomical features of a juvenile *Tridacna gigas* taken at the Natural History Museum, London

As the mantle-siphon material is so large and is everted over the edge of the valve when it is open the mantle retractor muscles are thick and produce prominent scars at the pallial line.

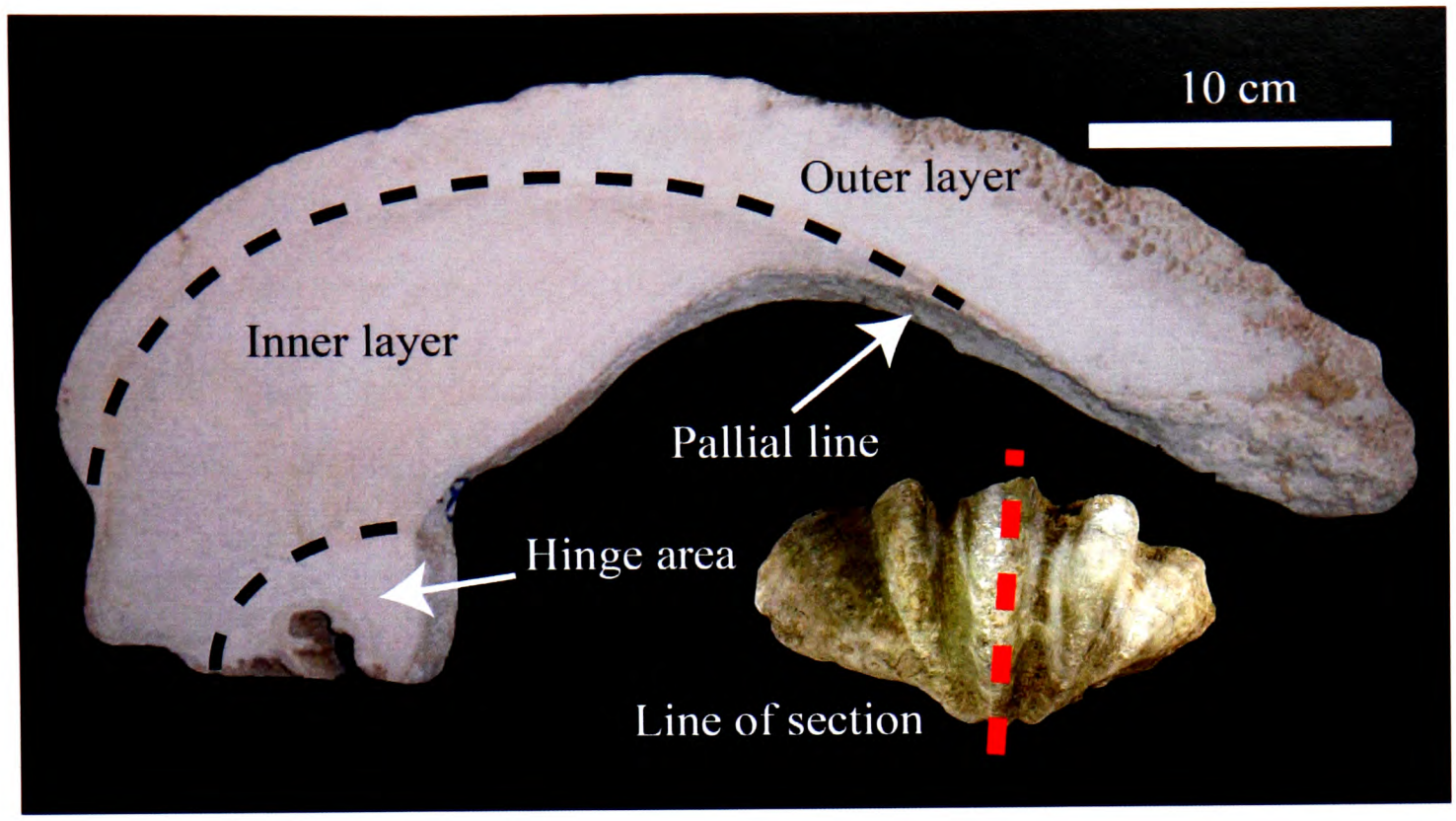

Figure 2-14 A section through a *Tridacna gigas* from the Huon Peninsula

The pallial line delimits the outer part of the shell from the inner layers. The outer part of the valves show thick growth bands of up to 2cm thick and composed of prismatic aragonite crystals (see Figure 2-14). The inner layer and hinge region are composed of smaller nacreous crystals and much finer banding.

Geographic distribution of the Tridacnidae

The larger species of Tridacnidae (*T. gigas, T. derasa* and *Hippopus hippopus*) are thought to be limited to the western Pacific and Micronesia (Rosewater, 1965). *T. crocea* is similarly restricted in its range, however *T. squamosa* is found from central Polynesia to East Africa. *T. maxima* have the greatest range being found from East Africa through to southeastern Polynesia.

Taxonomy of the Tridacnidae

The family Tridacnidae contains two genera: *Hippopus* and *Tridacna.* Both *Tridacna* and *Hippopus* seem to have arisen in the Miocene from *Byssocardium* (Stasek, 1962). *Hippopus* is separated from the other *Tridacna* as it does not posses hyaline organs, which may indicate a primitive situation (Rosewater, 1965). *Hippopus* also possesses a large byssal gape, even in adults. There are at least five species of *Tridacna* found in the waters surrounding Papua New Guinea: *T. gigas, T.*

derasa, T. squamosa, T. crocea and *T. maxima. T. gigas* is the least specialised with a very small byssal opening as adult individuals live unattached on sandy bottoms and attain a very large size (1370 mm) (Rosewater, 1965) with little or no ornamentation on the outer surface of the shell and can weigh in excess of 260 kg (Miner, 1938).

T. derasa attains the next largest size of up to 514mm (Rosewater, 1965). Because of its large size, *T. derasa* is often mistaken for *T. gigas*, however it usually has more ribs on the outer surface and the umbo is displaced towards the posterior (Rosewater, 1965). *T. squamosa* has a fairly symmetrical shape like *T. gigas*, but displays large scales on the outer surface of its valves and lives attached to coral by weak byssal strands. *T. crocea* is the smallest of the *Tridacna* (approximately 10-15 cm long), and is often found deeply imbedded in coral. *T. crocea* has a very large byssal opening and low ribs which can be ornamented with scales, though these are often lost as a result of burrowing into coral. *T. maxima* are a strongly inequilateral in shape with scales present on the outside surface of its valves. This *Tridacna* often excavates shallow depressions in coral, and is always tightly attached by byssal threads and therefore displays a large byssal gape.

Habitat

The Tridacnidae are to be found on coral reefs or sandy substrate and are generally found in the top 5m of water and not below 10m. *T. derasa* is often found on the outer edges of barrier reefs and coral atoll lagoons and is usually unattached (Rosewater, 1965). *T. gigas* often lives on coral reefs, often on sand. *T. crocea* lives fully embedded in coral reefs, whereas *T. maxima,* usually lives only partly embedded in hard substrate. *T. squamosa* lives on the surface of coral reefs, preferring sheltered localities (Stevenson *et al.*, 1931).

2.6 Concluding remarks

The coral reefs along the Huon Peninsula that grew during the early to mid Holocene (10-6.5 ka) and the between during Marine Oxygen Isotope Stage 3 (65-30 ka) are

now uplifted and sub-aerially exposed. These reefs have been extensively studied and well dated.

Whilst few *in situ* instrumental records are available, it has been shown that interpolated data sets can be used with some confidence to compare with proxy records from modern samples of *Tridacna* sp. to evaluate their fidelity.

The climatological setting of the Huon Peninsula means that sea surface temperatures, sea surface salinity and precipitation are all highly correlated and controlled by the El Niño-Southern Oscillation. The combination of all these factors makes the Huon Peninsula the ideal place to collect samples that can be used to study the state of ENSO in the past.

References:

Aharon, P., Chappell J. and Compston, W. (1980), Stable Isotope and Sea-Level Data from New-Guinea Supports Antarctic Ice-Surge Theory of Ice Ages, *Nature*, **283**, 549-651.

Aharon, P., and J. Chappell (1986), Oxygen Isotopes, Sea-Level Changes and the Temperature History of a Coral-Reef Environment in New-Guinea over the Last 105 Years, *Palaeogeography Palaeoclimatology Palaeoecology* **56**, 337-379

(WOA 2005 Salinity)
Antonov, J. Locarnini, R. A. Boyer, T.P., Mishonov, A.V. and Garcia, H.H. (2006), *World Ocean Atlas 2005, Volume 2: Salinity,* S Leavitus, Ed. NOAA Atlas, NESDIS 62. U.S. Government Printing Office, Washington D.C. 182 pp.

Arthur, M., Williams, D. F., and D.S. Jones (1983), Seasonal temperature-salinity changes and thermocline development in the mid Atlantic Bight as recorded by isotopic composition of bivalves, *Geology*, **11**, 655-659

Bloom, A. L., Broecker, W.S., Chappell, J. Matthews, R.K and K.J. Mesolla. (1974), Quaternary Sea-Level Fluctuations on a Tectonic Coast - New Th- 230-U-234 Dates from Huon-Peninsula, New-Guinea, *Quaternary Research,* **4**, 185-205

Bond, G., Broecker, W., Johnsen, S., MacManus, J., Labeyrie, L., Jouzel, J., and G. Bonani, (1993), Correlations between Climate Records from North-Atlantic Sediments and Greenland Ice, *Nature*, **365**, 143-147

Carre, M., Bentaleb, I., Blamart, D., Ogle, N., Cardenas, F., Zevallos, S., Kalin, R.M., Ortlieb, L. and M. Fontugne (2005) Stable isotopes and sclerochronology of the bivalve *Mesodesma donacium*: Potential application to Peruvian palaeoceanographic reconstructions, *Palaeogeography, Palaeoclimatology, Palaeoecology,* **228**, 4-25

Chappell, J. (1974), Geology of Coral Terraces, Huon-Peninsula, New-Guinea - Study of Quaternary Tectonic Movements and Sea-Level Changes, *Geological Society of America Bulletin*, **85**, 553-570

Chappell, J. (1983), A Revised Sea-Level Record for the Last 300,000 Years from Papua-New-Guinea, *Search*, **14**, 99-101

Chappell, J. (2002), Sea level changes forced ice breakouts in the Last Glacial cycle: new results from coral terraces, *Quaternary Science Reviews*, **21**, 1229-1240

Chappell, J., and H. A. Polach, (1976), Holocene sea level change and coral reef growth at Huon Peninsula, Papua New Guinea. *Geological Society of America Bulletin* **87**, 235-240.

Chappell, J. and H. H. Veeh, (1978), $^{230Th}/^{234}U$ age support of an interstadial sea level of ~40m at 30, 0000 yr bp. *Nature*, **276**, 602-604

Chappell, J., and N. J. Shackleton (1986), Oxygen Isotopes and Sea-Level, *Nature*, **324,** 137-140

Chappell, J. and H. Polach, (1991) Post-glacial sea level rise from a coral record at Huon Peninsula, Papua New Guinea. *Nature* **349**,147-149

Chappell, J., Omura, A., Esat, T. M., McCulloch, M. T., Pandolfi, J., Ota Y., and B. Pillans, (1996a), Reconciliation of late Quaternary sea levels derived from coral terraces at Huon Peninsula with deep sea oxygen records. *Earth and Planetary Science Letters,* **141**, 227-236.

Chappell, J. Ota, Y. and K. Berryman (1996b), Late quaternary coseismic uplift history of Huon Peninsula, Papua New Guinea, *Quaternary Science Reviews*, **15**, 7-22

Cresswell, G. R. (2000), Coastal currents of northern Papua New Guinea, and the Sepik River outflow, *Marine and Freshwater Research*, **51**, 553-564.

Edinger, E. N., Burr. G. S. Pandolfi, J.M., and J.C. Ortiz, (2007), Age accuracy and resolution of quaternary corals used as proxies for sea level. *Earth and Planetary Science Letters*, **253**, 37-49.

Edwards, R. L., Beck, J.W., Burr, G.S., Donahue, D.J., Chappell, J.M.A., Bloom, A.L., Druffell, E.R.M., and F.W. Taylor. (1993), A Large Drop in Atmospheric C-14/C-12 and reduced melting in the Younger Dryas, documented with Th-230 Ages of Corals, *Science*, **260**, 982-986

Elliot, M., DeMenocal, P., Linsley, B. and S. S. Howe (2003), Environmental controls on the stable isotopic composition of *Mercenaria mercenaria*: Potential application to palaeoenvironmental studies, *Geochemistry, Geophysics and Geosystems*, **4**, 1056 - 1072

Elliot, M., Welsh, K., Chilcott, C., McCulloch, M., Chappell, J. and Ayling, B. (submitted to *Paleoceanography*) Profiles of trace elements (Mg/ Ca, Sr/ Ca, and Ba/ Ca) derived from long-lived *Tridacna gigas* bivalves.

Esat, T. and Yokoyama, Y. (2006), Growth patterns of the last ice ages coral terraces at Huon Peninsula. *Global and Planetary Change*, **54**, 216-224

Fairbanks, R. G., Evans, M.N., Rubenstone, J.L., Broad, K., Moore, M.D. and C.D. Charles, (1997), Evaluating climate indices and their geochemical proxies measured in corals, *Coral Reefs*, **16**, 93-100 (Suppl.)

Fairbridge, R.W. (1960), The Changing level of the sea. *Scientific American*. **202**, 70-79

Fine, R. A., Lukas, R., Bingham, F. M., Warner, M. J., and Hammond, R. H. (1994), The western equatorial Pacific: a water mass crossroads. *Journal of Geophysical Research,* **99**, 25063–80

Gagan, M.K., Ayliffe, L. K., Hopley, D., Cali, J. A., Mortimer, G. E., Chappell, J., McCulloch, M. T., and M.J. Head(1998), Temperature and surface-ocean water balance of the mid-Holocene tropical western Pacific, *Science*, **279**, 1014-1016

Heinrich, H. (1988), Origin and Consequences of Cyclic Ice Rafting in the Northeast Atlantic-Ocean During the Past 130,000 Years, *Quaternary Research*, **29**, 142-152

LeGrande, A. N., and G. A. Schmidt (2006), Global gridded data set of the oxygen isotopic composition in seawater, *Geophysical Research Letters*, **33,** L12604

Lindstrom, E. Lukas, R. Fine, R. Firing, E. Godfrey, S. Meyers, G. and Tuschiya, M. (1987), The Western Pacific Ocean circulation study. *Nature*, **330**, 533-537

(WOA Temperature)
Locarnini, R. A., A. V. Mishonov, J. I. Antonov, T. P. Boyer, and H. E. Garcia, 2006. *World Ocean Atlas 2005, Volume 1: Temperature*. S. Levitus, Ed. NOAA Atlas NESDIS 61, U.S. Government Printing Office, Washington, D.C., 182 pp.

Lukas, R and Lindstrom, E. (1991), The mixed layer of the Western Equatorial Pacific Ocean. *Journal of Geophysical Research*, **96**, 3345-3357

McCulloch, M., Mortimer, G. Esat, T., Xianhua, L. Pillans, B. and J. Chappell (1996), High resolution windows into early Holocene climate: Sr/Ca coral records from the Huon Peninsula, *Earth and Planetary Science Letters*, **138**, 169-178

Miner, R.W. (1938) On the bottom of the Pearl Lagoon. *The National Geographic Magazine,* **74**, 365-382

Nakmori, T., Wallensky, E. and Campbell, C. (1994), Recent hermatypic coral assemblages at Huon Peninsula. In *Study on coral reef terraces of the Huon Peninsula, Papua New Guinea: Establishment of Quaternary Sea Level and Tectonic History* Y. Ota. Ed., pp. 119-139

Pandolfi, J. and Chappell, J. (1994), Stratigraphy and relative sea level changes at the Kanzarua and Bobongara sections, Huon Peninsula, Papua New Guinea, In *Study on coral reef terraces of the Huon Peninsula, Papua New Guinea: Establishment of Quaternary Sea Level and Tectonic History* Y. Ota. Ed., pp. 119-139

Pandolfi, J. M. (1996), Limited Membership in Pleistocene Reef Coral Assemblages from the Huon Peninsula, Papua New Guinea: Constancy During Global Change. *Paleobiology*, **22**, *152-176.*

Ota, Y., Chappell, J., Kelley, R., Yonekura, N., Matsumoto, E., Nishimura, T., Head, J., (1993), Holocene coral reef terraces and coseismic uplift of Huon Peninsula, Papua New Guinea. *Quaternary Research,* **40**, 177-188

Ota, Y. and Chappell, J. (1999), Holocene sea level rise and coral reef growth on a tectonically rising coast, Huon peninsula, Papua New Guinea. *Quaternary International,* **55,** 51-59

Rayner, N. A.; Parker, D. E.; Horton, E. B.; Folland, C. K.; Alexander, L. V.; Rowell, D. P.; Kent, E. C.; Kaplan, A. (2003), Global analyses of sea surface temperature, sea ice, and night marine air temperature since the late nineteenth century, *Journal of Geophysical Research,* **108**, 4407
(HadISST 1.1 - Global sea-Ice coverage and SST (1870-Present), (Internet). British Atmospheric Data Centre, 2006, (Accessed 06/06) Available from http://badc.nerc.ac.uk/data/hadisst/)

Romanek, C.S., Jones, D.S., Williams, D.F., Krantz, D.E. and R. Radtke, (1987) Stable isotopic investigation of physiological and environmental changes recorded in shell carbonate from the giant clam *Tridacna maxima*, *Marine Biology,* **94,** 385–393

Romanek, S. and E.L. Grossman (1989), Stable Isotope Profiles of *Tridacna maxima* as Environmental Indicators, *Palaios*, **4**, 402-413

Rosewater, J. (1965), The family Tridacnidae in the Indo-Pacific, *Indo-Pacific Mollusca*, **1,** 347-396

Reynolds, R.W., N.A. Rayner, T.M. Smith, D.C. Stokes, and W. Wang, (2002), An Improved In Situ and Satellite SST Analysis for Climate. *Journal of Climate*, **15**, 1609-1625
(http://iridl.ldeo.columbia.edu/SOURCES/.IGOSS/.nmc/.Reyn_SmithOIv2/)

Scourse, J.D., Richardson, C., Forsythe, G., Harris, I., Heinimeier, J., Fraser, N., Briffa, K. and P. Jones (2006), First cross-matched floating chronology from marine fossil record: data from growth lines of the long-lived bivalve mollusk *Arctica islandica, The Holocene,* **16**, 967-974

Slutz, R.J., S.J. Lubker, J.D. Hiscox, S.D. Woodruff, R.L. Jenne, D.H. Joseph, P.M. Steurer, and J.D. Elms, (1985), *Comprehensive Ocean-Atmosphere Data Set; Release 1.* NOAA Environmental Research Laboratories, Climate Research Program, Boulder, CO, 268 pp.

Stasek, C. R. (1962), The form, growth and evolution of the Tridacnidae (Giant Clams), *Archives de Zoologie Expérimental et Générale,* **101,** 1-40

Stein, M., Wasserberg. G.J, Aharon, P. Chen, J.H. Zhu, Z.R., Bloom, A.H. and Chappell, J. (1992), TIMS U-series dating and stable isotope from the last interglacial event in Papua New Guinea. *Geochimica et Cosmochimica Acta*, **57**, 2541-2557

Stevenson, T. A., Stephenson, A., Tandy, G., and M. Spender, (1931), The Structure and Ecology of the Low Isles and other reefs, *Scientific Reports, Great Barrier Reef Expedition*, **3**, 17-112

Tudhope. A.W., Shimmield, G.B., Chilcott, C.P., Jebb, M., Fallick, A.E. and Dalgleish, A.N. (1995), Recent changes in climate in the far western equatorial Pacific and their relationship to the Southern Oscillation; oxygen isotope records form massive corals, Papua New Guinea. *Earth and Planetary Science Letters*, **136**, 575-590

Trenberth, K. E. (1997), The definition of El Niño. *Bulletin of the American Meteorological Society*, **78**, 2771-2777

Veeh, H. H. and J., Chappell, (1970), Astronomical Theory of Climate Change: Support from New Guinea. *Science*, **167**, 862-865

Watanabe, T. and T. Ota (1999), Daily reconstruction of water temperature from oxygen isotopic ratios of a modern Tridacna shell using a freezing microtome sampling technique, *Journal of Geophysical Research*, **104**, 20,667–20,674

Watanabe, T., A. Suzuki, H. Kawahata, H. Kan and S. Ogawa. (2004), A 60-year isotopic record from a mid-Holocene fossil giant clam (Tridacna gigas) in the Ryukyu Islands: physiological and paleoclimatic implications, *Palaeogeography Palaeoclimatology Palaeoecology*, **212**, 343-354

Weidman, C.R. and G.A. Jones (1994), The long-lived mollusk *Arctica islandica*: A new paleoceanographic tool for the reconstruction of bottom temperatures for the continental shelves of the northern North Atlantic Ocean, *Journal of Geophysical Research*, **99**, 18305-18314

Yokoyama, Y., Esat, T., Lambeck, K. and K Fifield, (2000), Last ice age millennial scale climate changes recorded in Huon Peninsula corals, *Radiocarbon*, **42**, 383-401

Yokoyama, Y., Esat, T. and K. Lambeck, (2001), Coupled climate and sea level changes deduced from Huon Peninsula coral terraces of the last ice age, *Earth and Planetary Science Letters*, **193**, 579-587

Yonge, C. M. (1936), Mode of Life, Feeding, Digestion and Symbiosis with Zooxanthellae in the Tridacnidae, *Scientific Reports, Great Barrier Reef Expedition*, **1**, 283-321

3 Testing the fidelity of *Tridacna gigas* from the Huon Peninsula to record ENSO

Chapter Abstract

The climate of the Huon Peninsula Papua New Guinea, has been shown to be strongly affected by El Niño Southern Oscillation (ENSO) because of its position in the centre of the Western Warm Pool of the Tropical Pacific. $\delta^{18}O$ records from corals from the Huon Peninsula have been shown to accurately reflect changes in temperature and evaporation/ precipitation balance associated with El Niño/ La Niña and therefore used to infer changes in the state of ENSO in the past. Other carbonate secreting, reef dwelling, organisms such as long lived bivalves can also be used to reconstruct the modern record of ENSO. A 17 year long stable isotopic record was derived from the bivalved mollusc *Tridacna gigas* collected on the Huon Peninsula. The $\delta^{18}O$ time series produced correlates with a prediction of $\delta^{18}O$ derived from temperature and precipitation anomalies at Huon Peninsula and can therefore be used to reconstruct local climate. This bivalve $\delta^{18}O$ record also shows a high degree of correlation with isotopic records from two *Porites* corals from two different locations on the Huon Peninsula with a consistent offset of 3.9‰. This comparison also shows that, given sufficient resolution, there is no attenuation in annual cycle recorded by *T. gigas* growth. This comparison proves that the stable isotopic signature of ENSO has a demonstrable regional footprint here and is independent of organism.

3.1 Introduction

To be able to predict how the ENSO system will evolve when boundary conditions in the Tropical Pacific change, such as may happen due to the increase in global CO_2 levels, requires the testing of models that predict the behaviour of ENSO under these new boundary conditions. To test the fitness of these models to capture ENSO dynamics it is necessary to reconstruct ENSO under different boundary conditions so that the full range of ENSO behaviour can be determined and also to test model

ability to reproduce past states. This may be achieved by reconstructing the climate in regions that can be shown to be affected by the ENSO system using archives that are able to reproduce the climate in key areas of the tropical Pacific and preferably with the ability to produce records of interannual resolution.

There is however, a lack of sub-millennial resolution climate records of past climate in the WPWP. This is largely due to low oceanic productivity and a deep carbonate compensation depth that limits the use of deep-sea cores for high resolution investigation of climate in this region.

The Western Pacific Warm Pool contains areas of abundant coral reef growth such as the fringing reefs that grow on the Huon Peninsula, Papua New Guinea. Uplifted fossil reefs offer a semi-continuous and potentially high resolution source of material to investigate the ENSO at millennial time scales using stable isotopic ratios derived from the carbonate skeletons of reef dwelling organisms.

The oxygen isotope ratio ($^{18}O/^{16}O$) of marine biogenic carbonate is controlled by temperature and the oxygen isotope composition of the seawater from which it precipitates (McCrea, 1950; Epstein *et al.*, 1953; Grossman and Ku, 1986; Bemis *et al.*, 1998). As temperatures increase and/ or sea water becomes more depleted in ^{18}O, the ratio of $^{18}O/^{16}O$ expressed in units per mille (‰) relative to a standard reference PDB ($\delta^{18}O$) will be reduced or become more negative. At Huon Peninsula there is a coupling between decreased precipitation and lower temperatures on a seasonal basis and a very strong coupling on inter-annual basis (the El Niño/ Southern Oscillation) (See Chapter 2). Tudhope *et al.* (1995, 2001) showed that this climate signature was clearly visible in $\delta^{18}O$ of *Porites* coral from the Huon Peninsula.

Many of the reef dwelling organisms can be used to reconstruct climate, each with its own advantages and disadvantages. Corals have been shown to be excellent recorders of climate (e.g. Tudhope *et al.*, 1995, Evans *et al.*, 2000, Asami *et al.*, 2004) however they are potentially more subject to diagenetic alteration than

molluscs as they have more porous aragonite skeletal structure (Aharon *et al.*, 1980; Watanabe and Oba, 1999; McGregor and Gagan, 2003), and show isotopic disequilibrium (Weber and Woodhead, 1972; Dunbar and Wellington, 1981; McConnaughey, 1989a). Bivalves, on the other hand, have relatively compact and fine-layered shells that may be composed of aragonite or calcite. The reduced porosity of bivalve skeletons means that there is a lower chance of diagenetic alteration by the infiltration of ground water in humid tropical climates. *Tridacna* sp. valves are composed entirely from aragonite (Aharon, *et al.*, 1980, Watanabe and Oba, 1999) therefore diagenetic alteration of fossil valves, which predominantly takes place by precipitation of secondary calcite, should be relatively easy to detect.

Long lived bivalves of the genus *Tridacna* inhabit these reefs and may be used as well as corals for climatic reconstruction (Aharon *at el.*, 1980, Aharon and Chappell, 1983; Aharon and Chappell, 1986; Romanek *et al.*, 1987; Romanek and Grossman, 1989; Patzold *et al.*, 1991; Aharon, 1991; Watanabe and Oba, 1999; Watanabe *et al.*, 2004) *Tridacna gigas* (Rosewater, 1965) is the member of the *Tridacnidae* with the fastest growth, and specimens have been documented to live up to 60 years (Watanabe *et al.*, 2004).

Unlike corals, a significant number of studies have shown that bivalves precipitate their shells in isotopic equilibrium with surrounding waters over most or all of the year (Epstein *et al.*, 1953; Arthur *et al.*, 1983; Jones *et al.*, 1989; Surge *et al.*, 2001; Elliot *et al.*, 2003). Though there is evidence of kinetic effects in some bivalves (e.g. Thebault *et al.*, 2005) studies of *Tridacna* sp. indicate that these bivalves primarily precipitate their shell in equilibrium with surrounding water (Grossman and Ku, 1989; Aharon, 1991; Watanabe and Oba, 1999) with only potentially minor kinetic effects shown in some studies (Elliot *et al.*, submitted).

However, variation in growth across the shell of bivalves often varies during the lifespan of each specimen and during the seasonal cycle. The full range in seasonal temperatures and salinity may not be recorded due to changes in growth. There are several causes for this such as reproductive breaks (Hall *et al.*, 1974; Sato 1995), but

the primary candidates are extremes of temperature (Romanek and Grossman, 1989, Elliot *et al.,* 2003) and reduction in growth through ontogeny (e.g. Aharon, 1991). All these factors can cause the attenuation of environmental proxy information derived from bivalves.

In many bivalves attenuation of growth in later stages of ontogeny mean that seasonal amplitudes become reduced due to reduced width of growth bands (e.g. Romanek *et al.,* 1987, Aharon, 1991; Kennedy *et al.,* 2001) and the record may be biased towards the early stages of growth or a particular season of growth. Studies of stable isotopic profiles in giant bivalves have often suffered from the limitations of resolution offered by handheld hobby or dental drills and large amounts of powder required to produce reliable results. More recently micromilling and freezing microtome techniques have allowed much higher sampling resolution of bivalves for stable isotope studies (e.g. Watanabe and Oba, 1999). Specifically, Aharon (1991) shows stable isotope records from the *Tridacna gigas* and a *Porites* coral from the Great Barrier Reef which indicate that the growth patterns in *Tridacna gigas* cause the isotopic record to become attenuated. This may be an artefact of the resolution of sampling techniques used. Other studies have indicated that tropical bivalves are more likely to grow year round whereas bivalves growing at higher latitudes may have interrupted growth patterns (Elliot *et al.*, 2003) though some tropical specimens, such as those inhabiting restricted lagoons, may be subject to extreme summer temperatures which cause a reduction or cessation of growth during summer months (Romanek and Grossman, 1989).

Aims of this chapter

It has been shown that corals accurately reflect the ENSO system at Huon Peninsula and this is potentially the same for long lived bivalves, however variations in the growth patterns of bivalves and disequilibrium associated with changes in growth rates may reduce the reliability with which climate can be reconstructed. This chapter will:

1. investigate the stable isotopic record of *Tridacna gigas* to assess the effect of growth changes throughout ontogeny

2. assess the accuracy with which the stable isotope records derived from *Tridacna gigas* can be used to reconstruct the changes in temperature and $\delta^{18}O_w$ at Huon Peninsula
3. assess the ability of stable isotopic analysis to accurately record the state of ENSO
4. compare the $\delta^{18}O$ record obtained from *Tridacna gigas* with $\delta^{18}O$ records from *Porites* corals obtained from Huon Peninsula
5. compare the *Tridacna* record with two records derived from *Porites* corals to test the assumption that bivalves are comparable to corals in terms of reflecting climate.

At Huon Peninsula large variations in $\delta^{18}O_w$ over annual/ interannual timescales are related to variations in precipitation/ evaporation balance (Tudhope *et al.*, 1995). The results for Huon Peninsula are compared with a sample of *Tridacna gigas* from the Great Barrier Reef where $\delta^{18}O$ in the aragonite is dominated by seasonal temperature variations. This approach is used to investigate growth patterns and isotopic equilibrium in modern *T. gigas* (Elliot *et al.*, submitted). Secondly, a stable isotopic record from a *Tridacna gigas* collected at Huon Peninsula is studied to test the presence of an ENSO climate signal.

3.2 Sampling sites and sample descriptions

Stable isotopic records collected from two modern samples of *Tridacna gigas* were used in this study and compared to two isotopic records extracted from *Porites* corals collected by S. Tudhope. The locations for each of these are shown in Figure 3-1 and Figure 3-2.

Tridacna gigas samples

Modern *Tridacna gigas* sample from the Huon Peninsula (Tg-MT7) was collected from the fringing reefs adjacent to the village of Kanzarua (147.41 E, 6.13S) (see Figure 3-2). For a detailed description of the area see Chapter 2. It is not known at

what water depth the sample was collected from, however this specimen would have weighed approximately 40 kg and it could not have been recovered from any significant depth (we estimate no more than 2-5m) without specialist equipment. [1] The sample was identified as *Tridacna gigas* due to its large size (57cm in length) and the lack of external scales which differentiates this specimen from *Tridacna maxima*, and five ribs which differentiates it from *Tridacna derasa* (which has 6-7) (Rosewater, 1969).

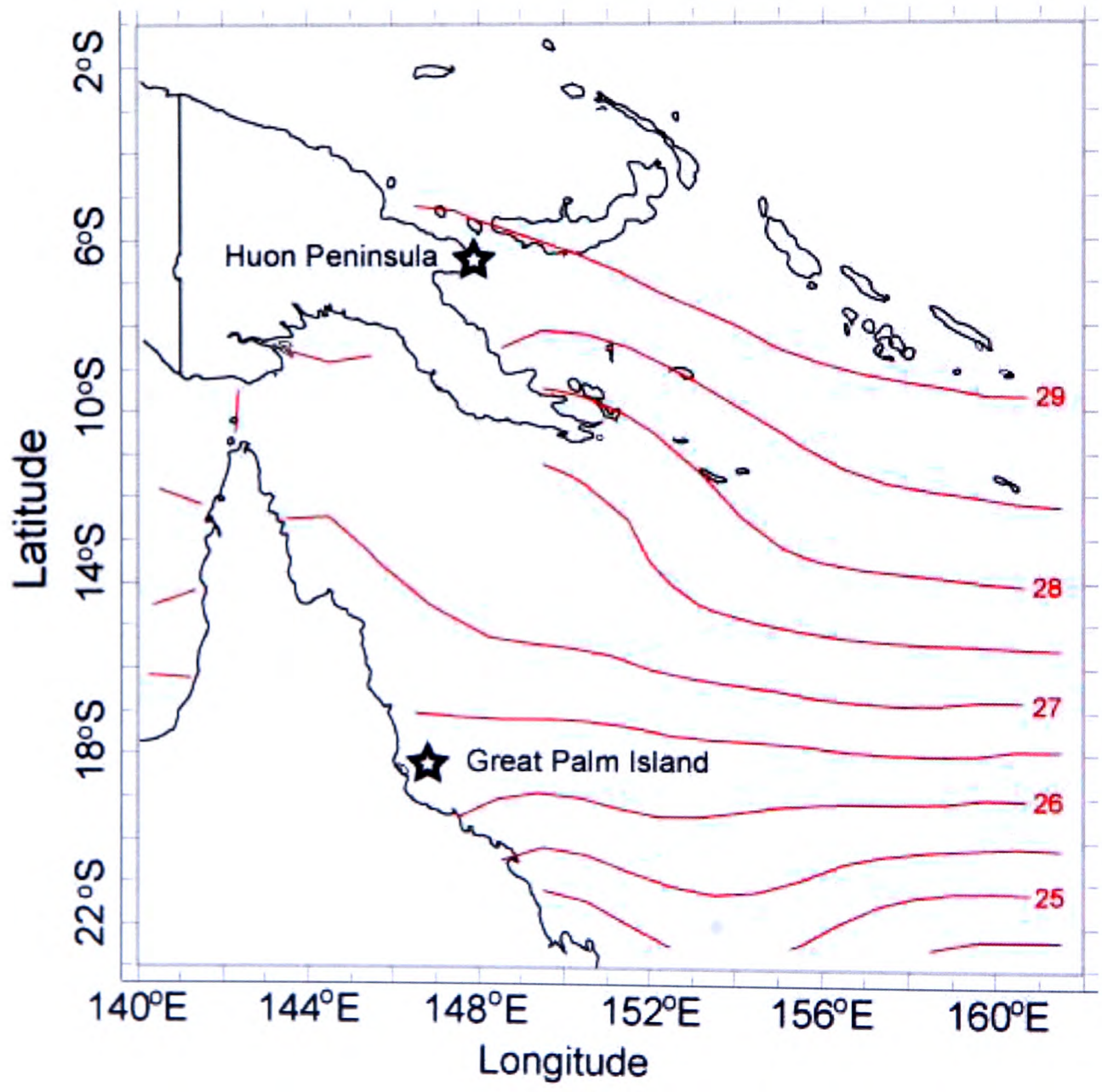

Figure 3-1 Locations used in this study shown in relation to mean annual temperatures (Red contours in) (1971-2000) **(NOAA NCEP EMC CMB GLOBAL Reyn_SmithOIv2 climatology c7100 sst)**

CHANGE if found

[1] Local villagers reported that it was collected from the reef platform by the village sometime in February/ March 2003, however stable isotope analysis indicate that the last year of growth is up to February/ March 2002

A *Tridacna gigas* was also sampled from the fringing reefs next to Great Palm Island on the Great Barrier Reef (Tg-GBR) (146.34 E, 18.31S) at 5m depth in 1980, stable isotope results are discussed in Elliot *et al.* (Submitted).

Porites samples

Both *Porites* corals were drilled from live colonies on the Huon Peninsula. H96-64 was sampled in Sialum Lagoon (147.36 E 6.05 S) in 1995, behind the barrier and relatively close to the open ocean. H01-9 was collected from the fringing reefs off Loto Beach in 2001 (147.46 E, 6.17 E) (see Figure 3-2). Both of these *Porites* corals were cored on field seasons in 1995 and 2001 by S. Tudhope. The oxygen isotopic record from coral H96-64 is published in Tudhope *et al.*, (2001).

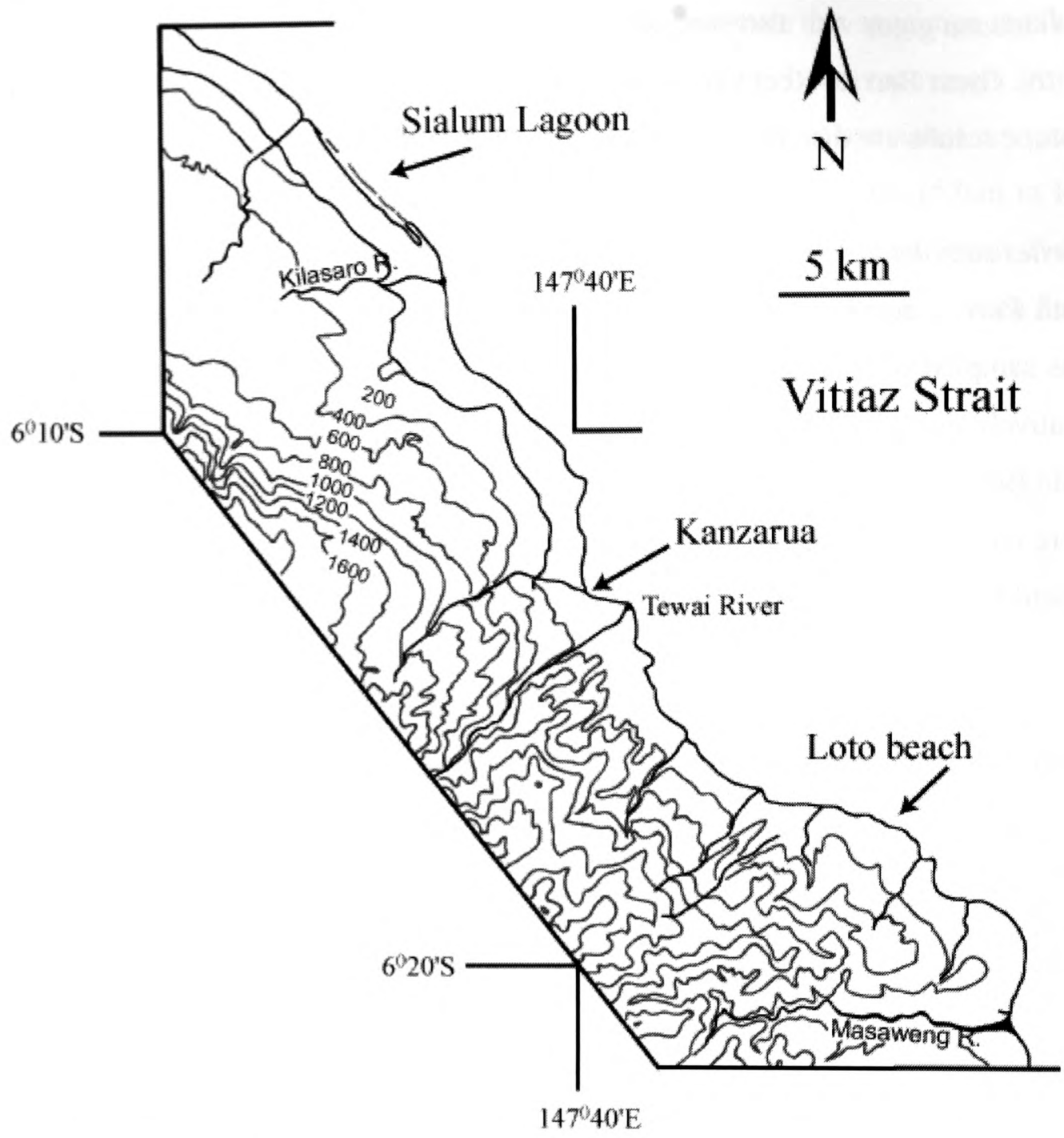

Figure 3-2 Region on Huon Peninsula showing were samples were the sample of *Tridacna gigas* MT7 (Kanzarua) and the samples of *Porites* H95-64 (Sialum Lagoon) and H01-9 (Loto Beach) were collected (redrawn from Chappell *et al.*, 1996a)

3.3 Methods

Carbonate sampling

One valve of the shell was taken and sliced along the maximum growth axis. The inner layer (carbonate secreted behind the pallial line) (see Figure 3-3) was sampled for the modern sample from Huon Peninsula (Tg-MT7) and Palm Island (Tg-GBR) specimens and the hinge area was also sampled (Figure 3-3) in Tg-GBR. These

areas were cut into overlapping 25 x 75mm slabs which were mounted onto glass slides using epoxy resin, trimmed using a rock-saw and polished down to 0.8mm thick thin sections using diamond paste. The slabs were scanned using a digital scanner and mounted onto the base plate of a Mercantek computer controlled Micromill. Lines of carbonate were drilled parallel to growth lines observed in the structure of the *Tridacna* sp. sample using reflected and transmitted light (see Figure 3-4) using a tungsten carbide drill bit with a tapered point and an effective diameter of 200 μm when drilling to a depth of 200μm. The lines drilled were approximately 10mm in length, and drilled continuously at a resolution of approximately 0.2mm. The samples were collected by sharply banging the base plate onto laboratory weighing paper which was then folded and powder transferred into 1.5ml polyethylene PCR vials.

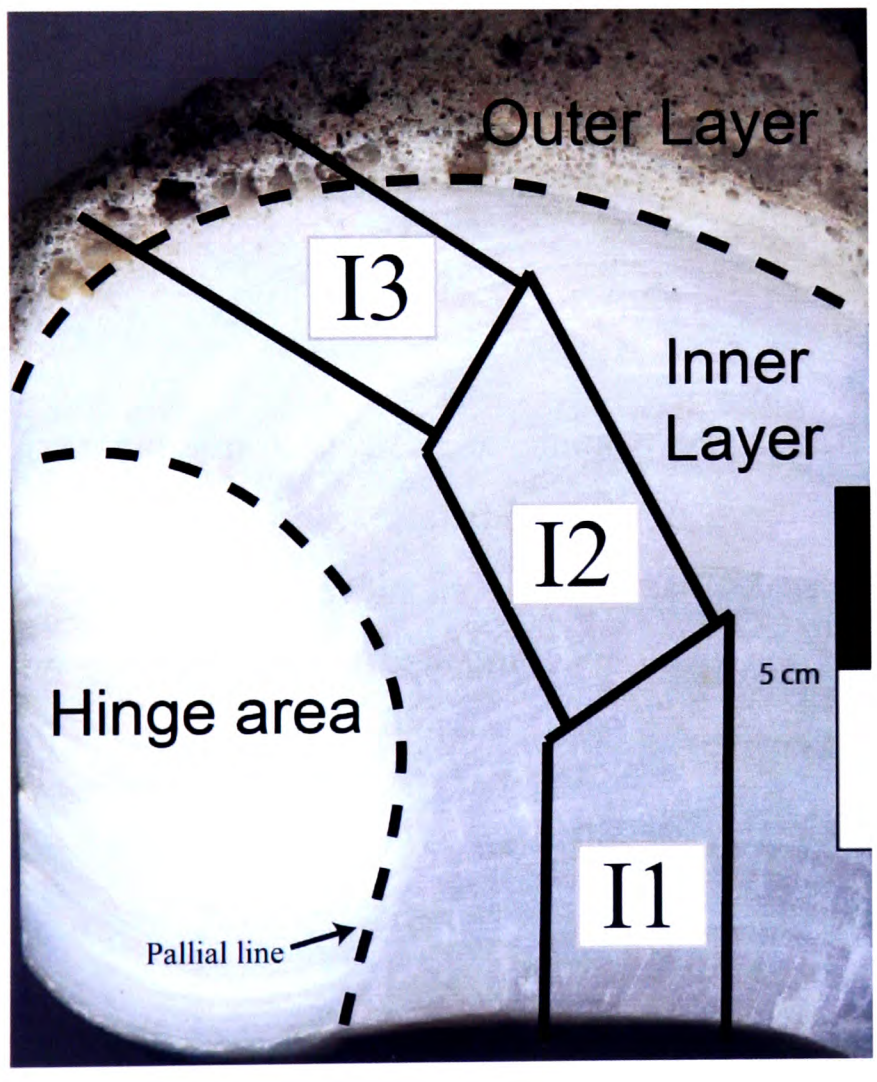

Figure 3-3 Cross section through a *Tridacna gigas* (Tg-MT7) showing the different layers associated with the pallial line (reflected light). The inner layer is the part of the shell that is deposited behind the pallial line. The outer layer and the hinge form a continuous region, though the outer layer displays variations in growth patterns in many species of Tridacnids and much smaller growth per year is observed in the hinge area. Thick black lines show the position of the slabs that were taken from the inner layer.

A section approximately 1cm thick was removed from the maximum growth axis. Sections were then cut from the inner layer and hinge area into overlapping slabs of 25mm x 60mm. The slabs were glued to a glass slide using epoxy resin and polished

using 2 μm diamond paste to a uniform thickness of 0.8mm. The slides where then scanned using Digital Scanner and mounted on the base plate of the Micromill in the Grant Institute, University of Edinburgh School of GeoSciences using melted wax. The slabs were wiped with a tissue and acetone to ensure the top surface was clean and uncontaminated.

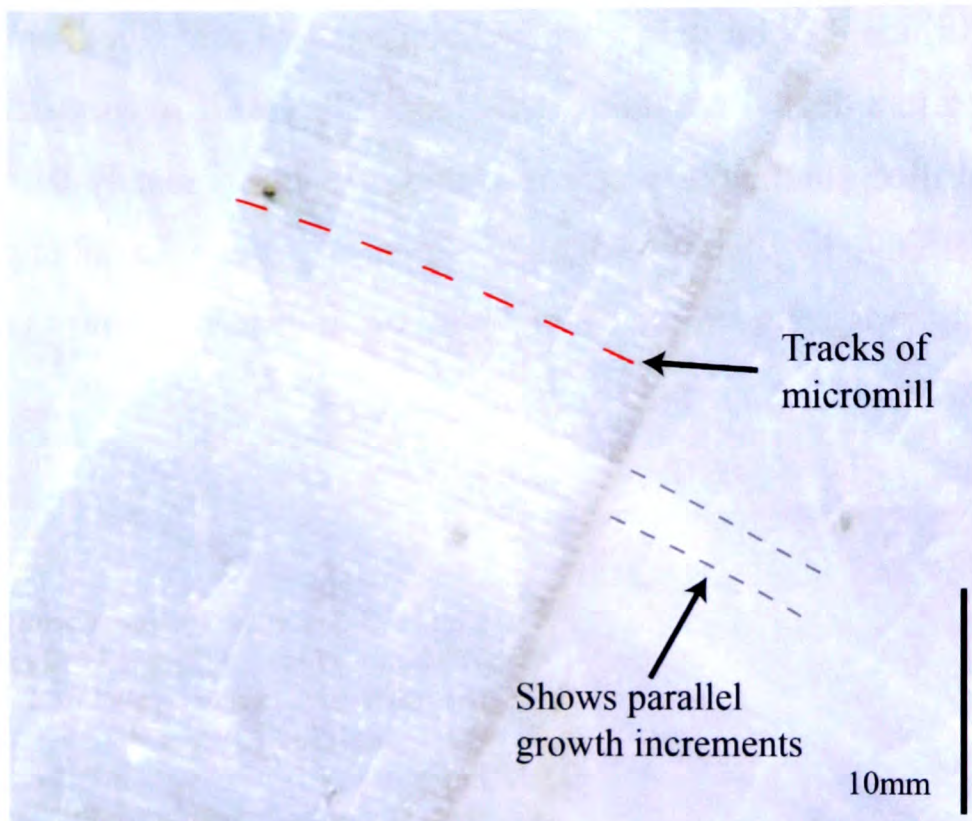

Figure 3-4 Showing a section of MT7-il 3 under reflected light that has been sampled using micromilling techniques. A single micromill track is marked in red and runs parallel to growth banding. Each track is 200 μm.

To collect sufficient material for stable isotopic analysis (0.2 micrograms) and leaving a reserve for resampling, lines of approximately 15mm in length with a drilling depth of 200 μm were drilled. The depth was achieved with 4 passes of 50 μm depth to prevent fracturing of the brittle aragonite and therefore reduce mixing between samples. Samples were taken continuously with a resolution of 200 μm.

Stable isotope mass spectrometry

Oxygen and carbon stable isotope analyses were performed on 0.1 - 0.2 mg sub-samples. Some samples near the edge of the slabs were very small, however most samples were weighed at 0.2 mg. The carbonate samples were reacted with 100% orthophosphoric acid at 75 °C in a Kiel Carbonate III preparation device and the resulting CO_2 was then analysed on a Thermo Electron Delta+ Advantage stable isotope ratio mass spectrometer. The standard deviation for a laboratory standard

marble powder (MAB2B) that has been used as a standard since the installation of the instrument in July 2005, is ± 0.09‰ for $\delta^{13}C$ and ± 0.08‰ for $\delta^{18}O$. All carbonate isotopic values are quoted relative to PDB.

Alternate samples were analysed for most of the ontogeny of the clam, changing to every sample after approximately 12 years of growth as the annual thickness produced here is approximately 2mm y^{-1} or less (See Figure 3-8). Growth bands were used to correlate between slabs in each area and overlapping samples collected to ensure that records were matched correctly. The same technique was used to sample and analyse carbonate from Tg-GBR-il (Elliot *et al.,* submitted).

3.4 Stable isotopic results

Figure 3-5 shows the stable isotopic profile from the inner layer of sample MT7 as a function of distance from the edge of the shell in mm. Average $\delta^{18}O$ for MT7-il is -1.2 ‰ (vs PDB) (*n=331*) with an overall range of -2.0 to -0.4 ‰ with a s.d. of 0.29. This gives identical results to "bulk" samples collected by drilling across all growth bands using a hand held hobby drill. (-1.2‰ *n*= 2). Overlapping section match very well with extremely similar values, which allows timeseries results from each slab to be joined very accurately. Average values of $\delta^{13}C$ are 1.9‰ with a range 1.1‰ to 2.2‰ with an s.d. of 0.17. $\delta^{13}C$. Amplitudes of $\delta^{13}C$ vary with the age of the bivalve, with small variations of 0.2‰ in the early part of life and increasing to 0.5‰ in later stages of life. $\delta^{13}C$ values also appear to exhibit a trend from heavier values (1.9‰ in the first 60mm of growth) to lighter values (1.7‰ in adult phase of growth).

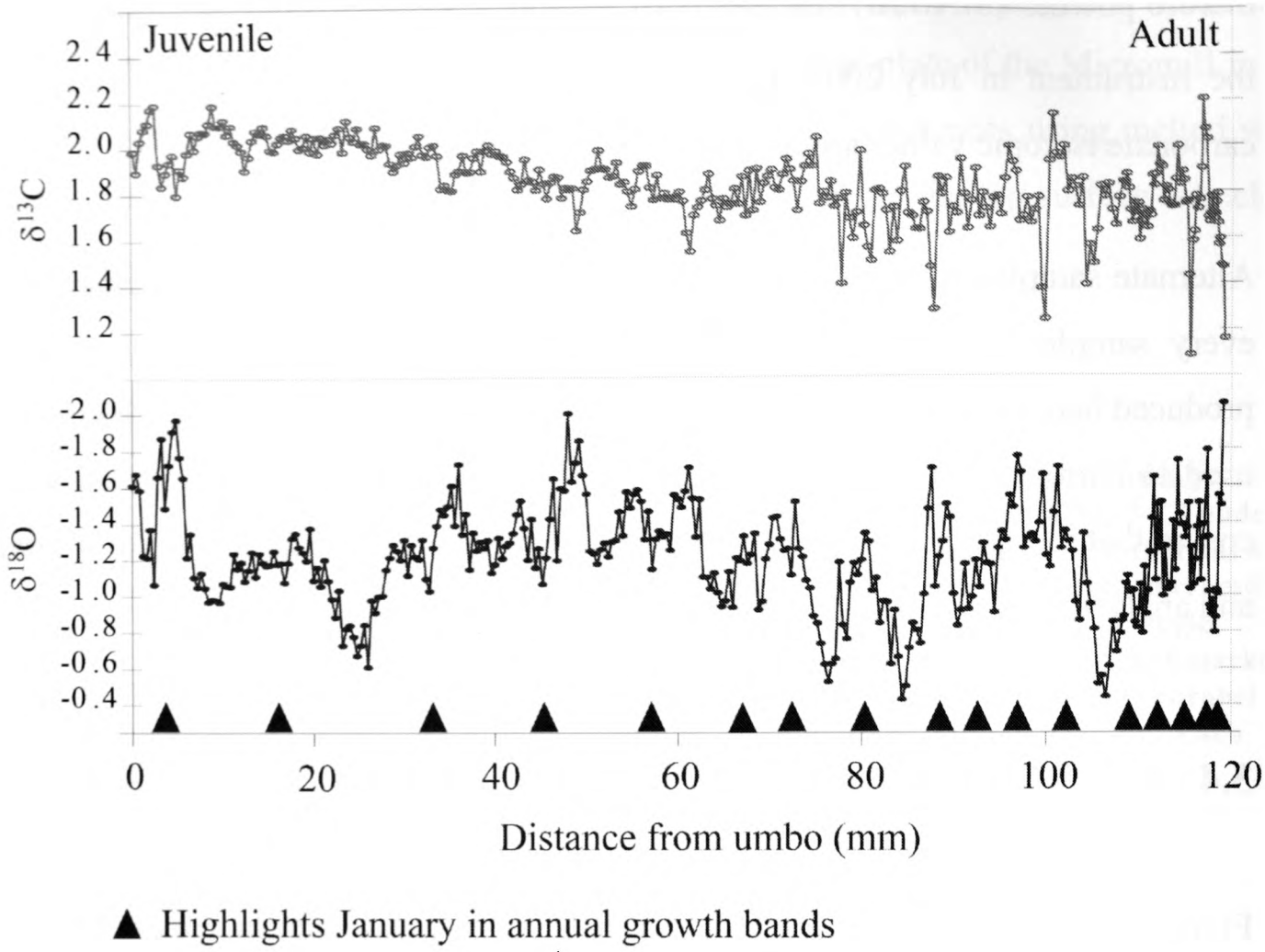

Figure 3-5 Stable isotopic record from the inner layer area modern *T. gigas* collected at Kanzarua, Huon Peninsula against distance from the edge of the shell. Growth direction is from right to left. $\delta^{18}O$ axis is inverted.

3.5 Discussion

3.5.1 Developing a chronology and investigating growth

All parts of the shell of *Tridacna* sp. show alternating dark and light bands. This banding may be the result of changes in the amount of organic matter that is incorporated into the aragonitic shell, however investigations of *Tridacna* sp. using staining agents such as Mutvei's Solution (see Schone *et al.*, 2005 for full description of this technique) do not show annual banding more clearly than transmitted light techniques, which implies very low concentrations of polysaccharides and other organic material. Investigation of these annual bands under Scanning Electron Microscope shows that these annual bands are the result of changes in the size of

aragonite crystals (as determined by average the long axis length of crystals in the inner layer) with larger crystals causing the shell to be more transparent.

The banding of *T. gigas* is thought to vary in concert with seasonal variation in temperature based upon the correlation between more transparent bands (larger crystals) and more negative $\delta^{18}O$ of shell carbonate (Pätzold *et al.*, 1991; Elliot *et al.*, (submitted)). To assign a chronology to stable isotopic results from *Tridacna* sp., couplets of dark and light bands were assumed to be annual and variation in transparency was noted as samples were collected. The centre of the lightest or most transparent part of the annual band was identified and assumed to be produced during the warmest month.

Annual bands can be picked out with relative ease in most *Tridacna* sp., especially in the outer layer and the hinge area, however it is more difficult to recognise annual banding in the samples from Huon Peninsula (See Figure 3-6). This could be due to the small annual change in sea surface temperature at this locality. Also, as variations in colour/ transparency are subtle, picking reliable beginning and end points for each year was difficult for specimen MT7-il, therefore scans were made of the slabs from which samples were collected and the contrast on these photos was enhanced.

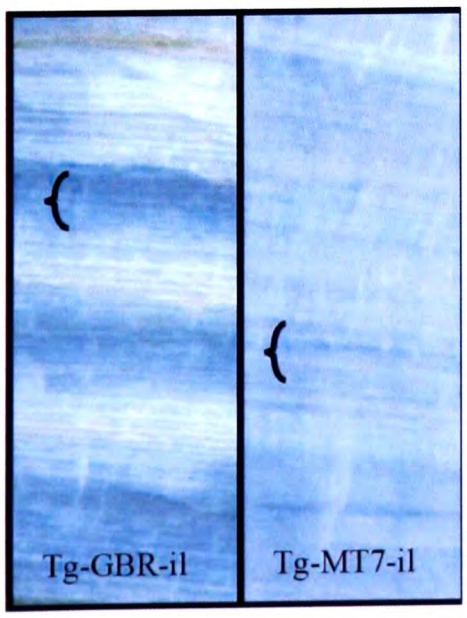

Figure 3-6 Two thin sections from the inner layers of two *Tridacna gigas* samples from two different environments (image has contrast enhanced). Tg-GBR-il is from an environment with greater seasonal variability in temperature. Annual bandings can be seen more clearly in Tg-GBR-il than in MT7-il. Annual variation in temperature at each site is 6°C and 2.5°C respectively.

Another way of assigning chronologies to stable isotope records is to identify annual variations in $\delta^{18}O$. As $\delta^{18}O$ in biogenic carbonate is largely controlled by variations in the temperature and the $\delta^{18}O$ of water in which the mollusc grew, annual banding is relatively easy to pick out in areas where there is significant annual change in temperature and limited variation in rainfall such as the Great Barrier Reef, (Elliot *et al.*, submitted). However, since there are small variations in temperature and a strong seasonal variation in precipitation with a very strong isotopic signature (see Chapter 2), the annual cycles in $\delta^{18}O$ are complex and more difficult to identify than the Tg-GBR-il sample.

Observations of the relative thicknesses of transparent/ opaque couplets in annual bands in the sample Tg-GBR-il indicate that the maximum growing season on the great barrier reef is during the summer, however there is no strong differentiation between the summer and winter observable in sample Tg-MT7il from the Huon Peninsula probably because there is little environmental difference between the summer and winter seasons.

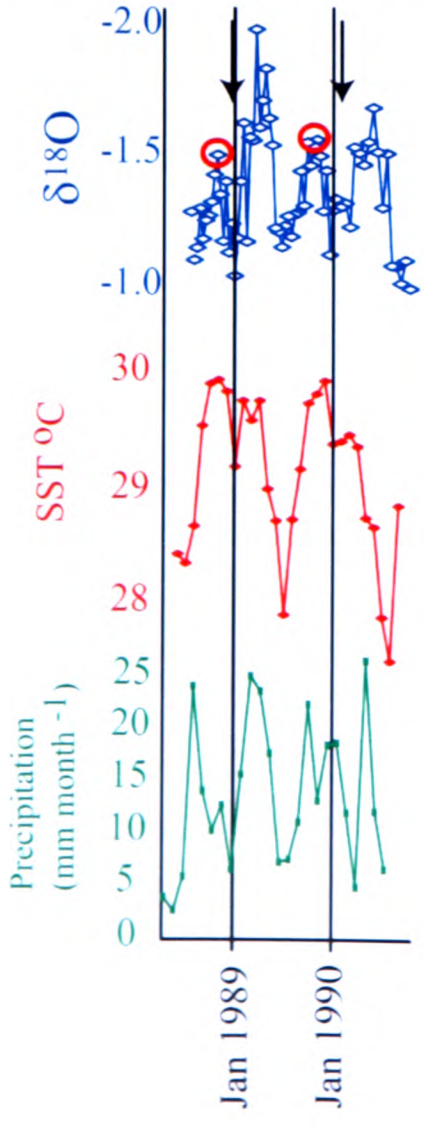

Figure 3-7 "Double peaks" seen in the annual cycle of $\delta^{18}O$ in two of the early years of growth of Tg-MT7-il compared with SST reconstruction from HadISST and the Madang precipitation record. Arrows show the position of double peaks. Red circles indicate December in the isotopic record. Note that temperatures here are gridded reconstructions based on blended satellite and ship measurements and may lack detail (see Chapter 2).

The annual $\delta^{18}O$ cycle is not always sinusoidal, but often a "double peak" is often seen around the time of the hottest part of the year (December to February) with a shift towards more positive values. A similar pattern of $\delta^{18}O$ has been reported in corals from this region (Tudhope *et al.,* 1995) and is caused by the bimodal distribution of annual precipitation in the region as the ITCZ passes overhead during December and February though this is more pronounced in some years than others.

In Tg-MT7-il double peaks in $\delta^{18}O$ were generally more observable in the earlier phase of growth where resolution is sufficient (see Figure 3-7). As datasets that are based upon blending ship and satellite data are averaged over large areas, they may smooth out details in annual climatic cycles such as the bimodal distribution of precipitation; however this can be seen more clearly in instrumental data taken from the Madang station on the Huon Peninsula. The Madang station rainfall record is incomplete and cannot be used for comparison with the whole record, however it was available for the years 1989 and 1990, and this is shown in Figure 3-7.

Therefore, whilst the alternating light and dark bands on the shell give an approximate guide chronology, it is most easily distinguishable by combining this data with the stable isotopic record. This technique was also used by Tudhope *et al.*, (2001) and Elliot *et al.* (submitted). Figure 3-8 shows the cross section through MT7 with the position of the cut slabs marked on and labelled, with short black lines marking the approximate position of the Austral Summer (January) on each shell. These were identified partially by sight, but also by cross reference with $\delta^{18}O$ profiles. This information has been used to derive an age model for the stable isotopic profiles (see Figure 3-9) and an estimate of changing growth rates through ontogeny (see Figure 3-10).

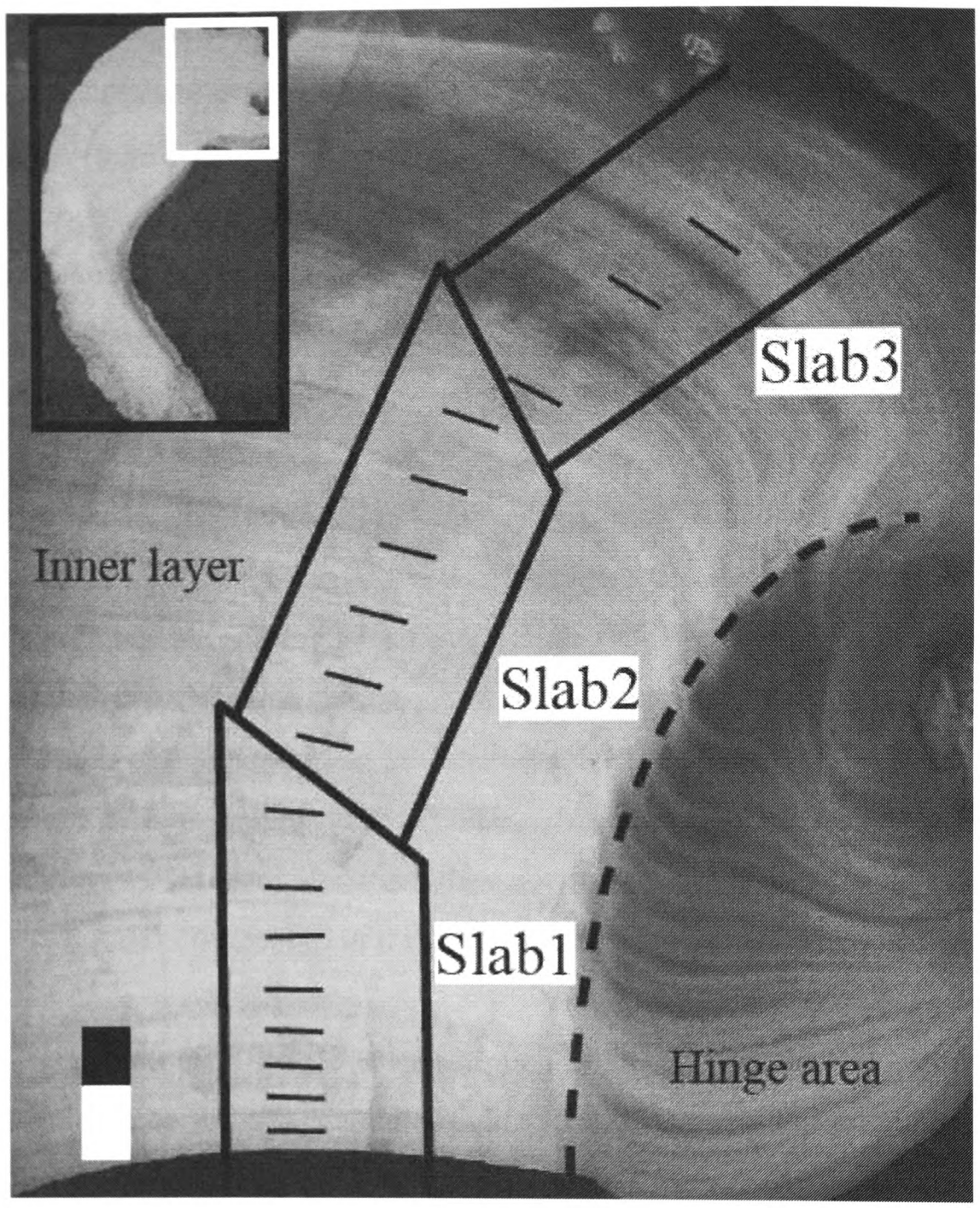

Figure 3-8 A cross section through modern *Tridacna gigas* Tg-MT7-il under transmitted light. Dark lines mark annual bands (in the approximate position of the warmest month December) by identifying the lightest/ most transparent part of the year's growth. Scale bar is 1cm. 16 full years of growth can be seen. Insert show position of slabs in the cross section of Tg-MT7-il (This is the same cross section seen in Figure 3-3).

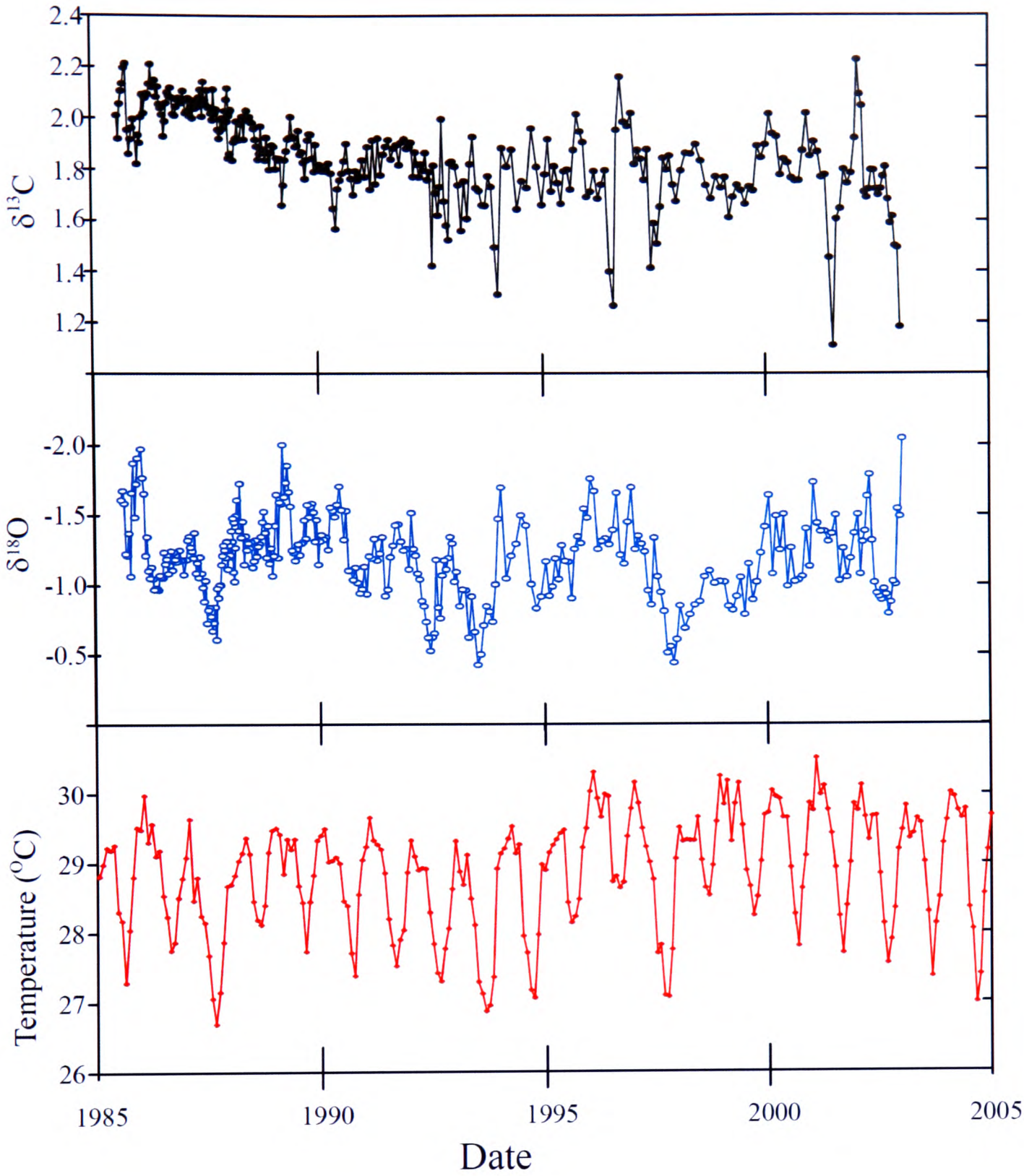

Figure 3-9 Stable isotopes ($\delta^{13}C$ (to) and $\delta^{18}O$ in (middle) VPDB) from inner layer of modern *Tridacna gigas* Tg-MT7 compared to a temperature record for Huon Peninsula 1985-2005 (bottom). Temperature record is obtained from the HadISST data set for a degree square centred on -6.5N and 147.5 E (see Chapter 2 for description of this record).

3.5.2 Growth curves in *Tridacna gigas*

Tg-MT7-il shows reduction in growth/ year throughout ontogeny as does Tg-GBR-il. Growth during the early phase of growth (between 1 and 8 years) is on average 11.2 mm yr^{-1}, and 4.0 mm yr^{-1} during the later stages.

Figure 3-10 shows the growth curve for modern *Tridacna gigas* Tg-MT7 inner layer, from the Huon Peninsula. Figure 3-11 show the growth the curve for the modern *Tridacna gigas* Tg-GBR inner layer from Palm Island, Great Barrier Reef. The length of the 16 year long record for Tg-MT7-il is 123mm and the length of the 19 year record for Tg-GBR-il is 64mm. There are several possible explanations in the marked difference in record length. It is possible that there was greater growth on the Huon Peninsula due to increased productivity or more consistently warm temperatures. The sections removed for MT7-il were cut in a curve to maximise the length of the slabs recovered and so increase potential resolution (see Figure 3-3). The growth curves are very similar despite there being substantial interannual climate variability on the Huon Peninsula.

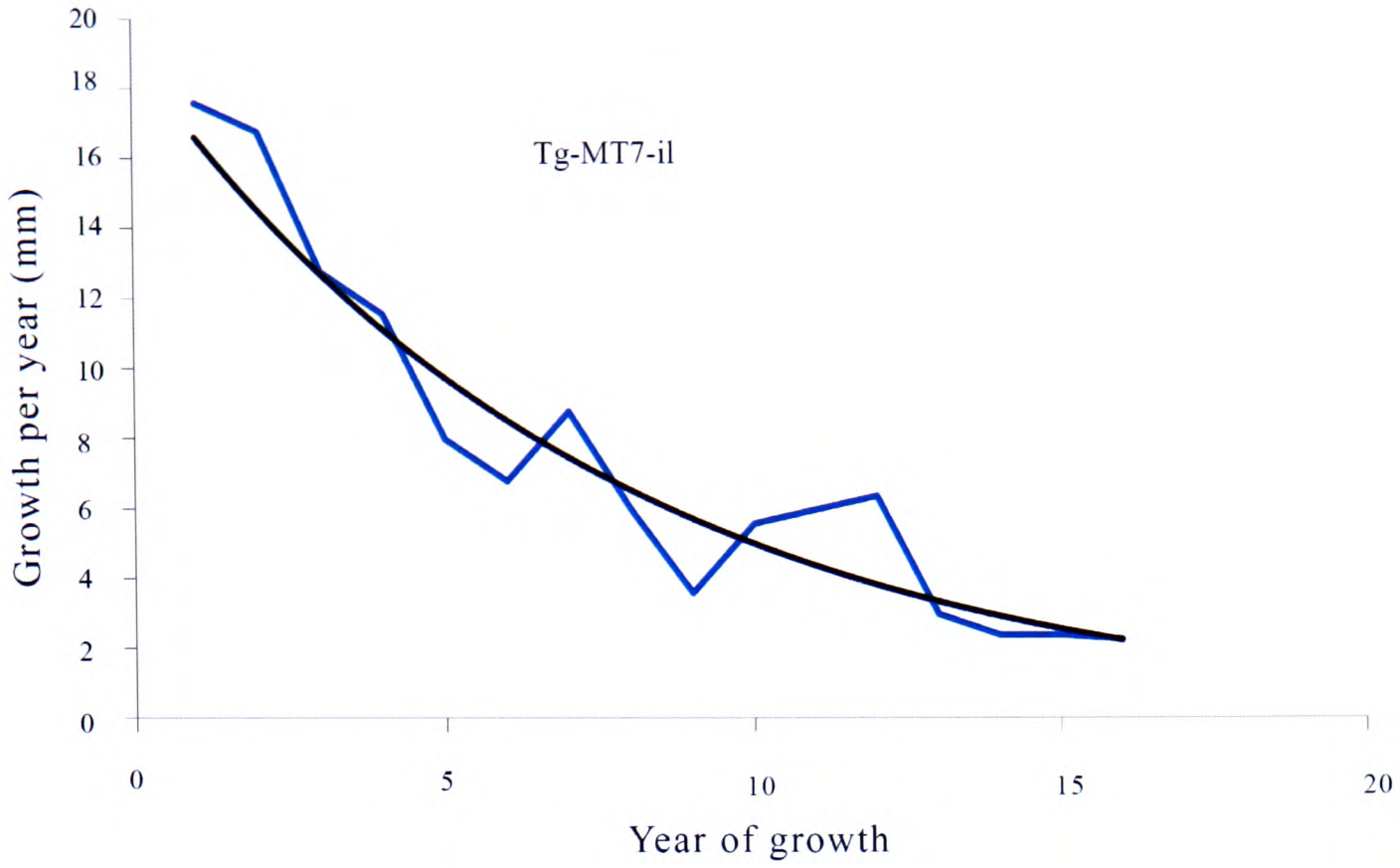

Figure 3-10 Growth curve in mm/ year for modern *Tridacna gigas* samples Tg-MT7, Huon Peninsula (black line highlights growth trend)).

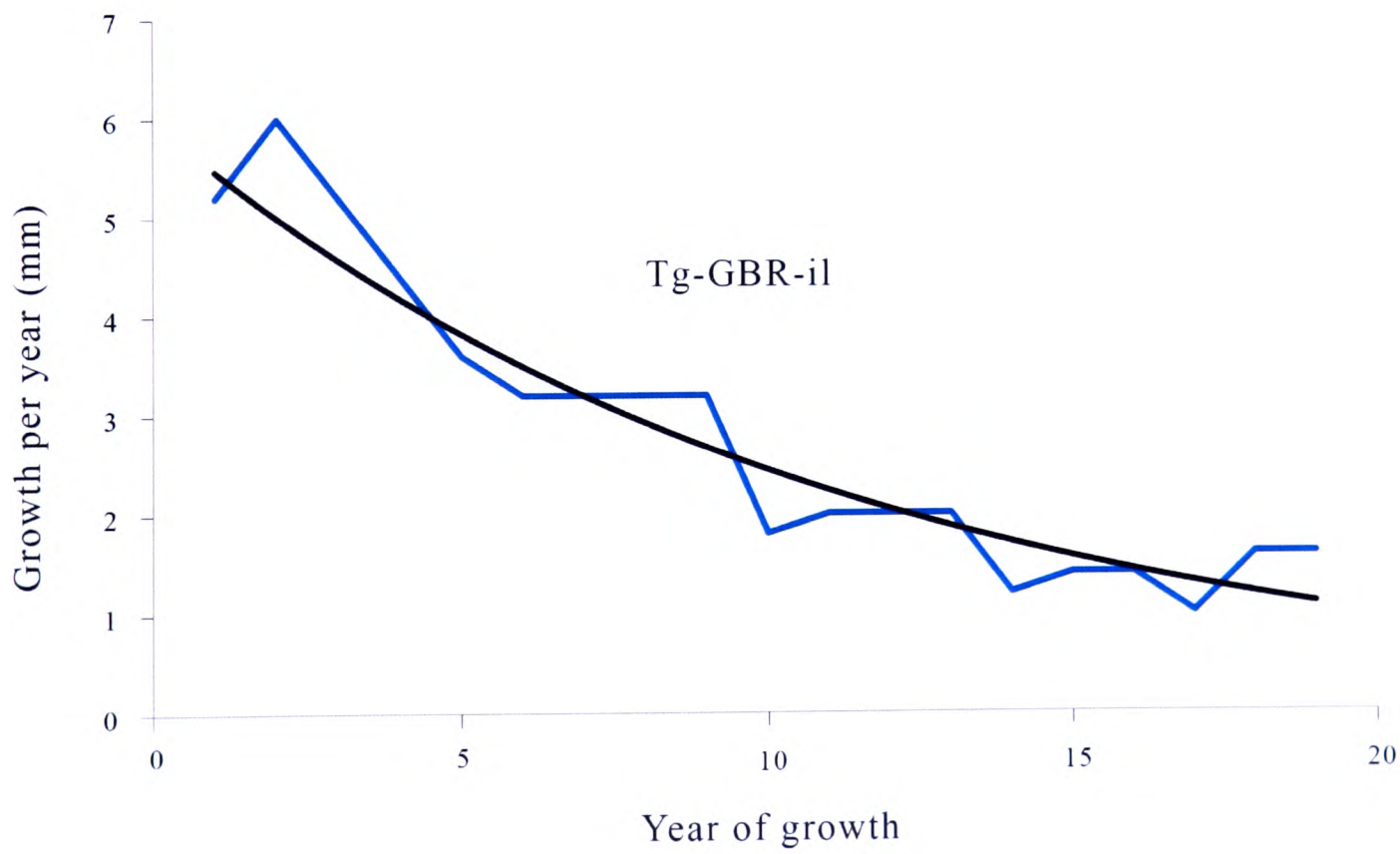

Figure 3-11 Rate of growth in mm/ year for modern *Tridacna gigas* sample Tg-GBR from Palm Island, Great Barrier Reef (black line highlights growth trend).

3.5.3 Environmental controls on carbon isotope profiles

There is no correlation between $\delta^{13}C$ and $\delta^{18}O$ seen in Tg-MT7-il, indicating that variation in $\delta^{13}C$ is not seasonal (See Figure 3-9). Other studies of *Tridacna* sp. have shown positive correlations between $\delta^{13}C$ and $\delta^{18}O$ (Jones *et al.*, 1986; Aharon and Chappell, 1980; Aharon, 1991; Watanabe and Oba, 1999 and Watanabe *et al.*, 2004). Aharon and Chappell (1980) used stable isotopic results from *Tridacna* sp. present $\delta^{18}O$ and $\delta^{13}C$ averaged over the life of each individual and collected from the Huon Peninsula, but these averaged results mask seasonal signals.

The stable isotopic profile presented in Elliot *et al.* (Submitted), which is presented at the end of this thesis, does not show a strong seasonal cycles in $\delta^{13}C$. This suggests that a number of biological factors which may be independent of seasonal environmental control also affect $\delta^{13}C$. This is confirmed by their observation that $\delta^{13}C$ is not reproducible between different areas of the shell (such as the hinge area, outer or inner layers). These areas of the shell are deposited under different conditions as the explained in Chapter 1, therefore implying a strong biological control.

3.5.4 Environmental controls on *T. gigas* $\delta^{18}O$

There have been several studies investigating the use of stable isotope profiles in *Tridacna gigas* as a climate archive (Aharon and Chappell, 1986; Aharon, 1991, Patzold *et al.*, 1991, Watanabe and Oba, 1999 and Elliot *et al.*, submitted). Aharon and Chappell (1986) and Aharon (1991) show $\delta^{18}O$ records from Huon Peninsula and Palm Island on the Great Barrier Reef respectively. Elliot *et al.*, (submitted) also show a *Tridacna gigas* isotopic record from the modern Great Barrier Reef. All of these studies show that *Tridacna gigas* precipitates its shell in equilibrium with seawater.

To investigate how well the $\delta^{18}O$ time series reflect variation in temperature and $\delta^{18}O$ of seawater at Huon Peninsula, $\delta^{18}O$ time series are compared with local records of

sea surface temperature and $\delta^{18}O$ of sea water. There are no long-term *in situ* environmental records from the Huon Peninsula, instead satellite data is used here (see Chapter 2).

The temporal resolution of the stable isotope records varies throughout the ontogeny from nearly weekly resolution in the first few years to closer to monthly in the later stages of growth. In order to compare monthly temperature and salinity records, bivalve $\delta^{18}O$ time series have been interpolated using the Analyseries Program (Paillard and Labeyrie, 1996) to twelve samples per year. Figure 3-12 compares the initial data and the monthly interpolated $\delta^{18}O$ time series. The interpolation does not attenuate the signal.

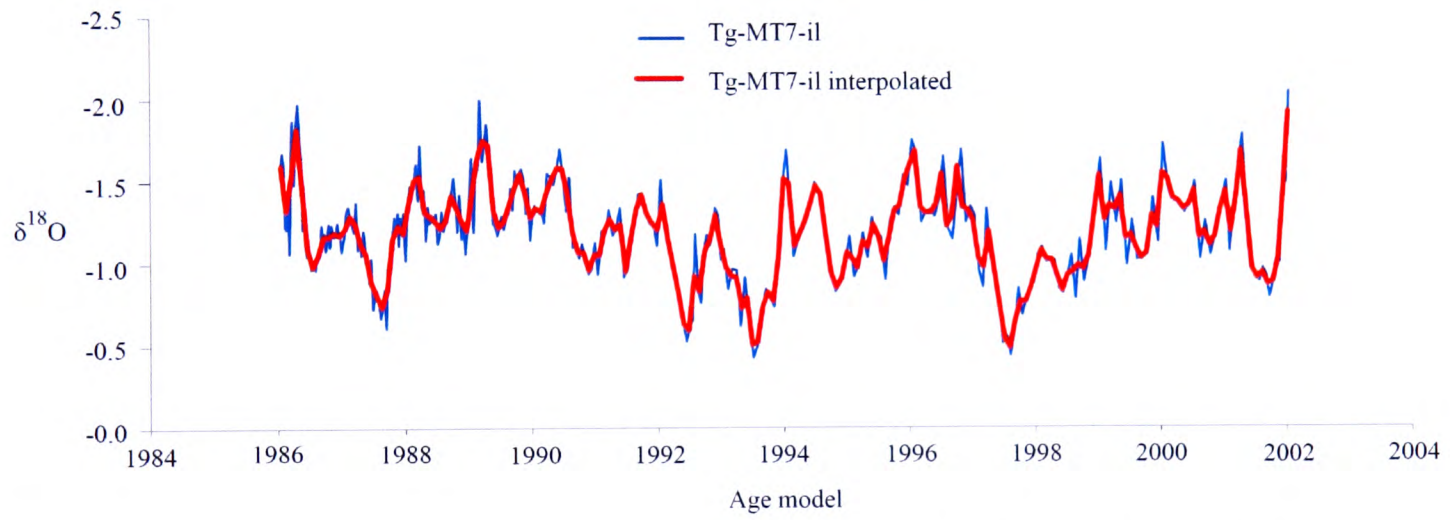

Figure 3-12 $\delta^{18}O$ record from the inner layer of modern Huon *Tridacna gigas* Tg-MT7 versus chronology explained above and same record interpolated to 12 samples per year

Given that the $\delta^{18}O$ of the *Tridacna gigas* valve is dependent upon the temperature of the water from which the carbonate is precipitated ($\delta^{18}Oc$) and the $\delta^{18}O$ of the water in which calcification occurs ($\delta^{18}O_w$), a prediction of $\delta^{18}O_c$ can be made based upon a combination of these factors. The HadISST blended ship and satellite dataset was used to provide a temperature record (see Figure 3-9). Several temperature equations are available (e.g. Aharon, 1983; Watanabe and Oba, 1999). We have decided to use the more general equation for aragonitic bivalves and foraminifera developed by Grossman and Ku (1989) which is:

Equation 1 $$T(^{o}C) = 21.8 - 4.69\ (\delta^{18}O_c - \delta^{18}O_w)$$

where $\delta^{18}O_c$ is the $\delta^{18}O$ value of the shell (vs PDB) and $\delta^{18}O_w$ is the $\delta^{18}O$ value of the sea water. $\delta^{18}O_w$ is measured against SMOW and then converted to the PDB scale by application of a correction. Different authors use different values for this correction in their equations. Grossman and Ku use a correction of +0.2‰.

Historical records are very rare for $\delta^{18}O_w$, however, since $\delta^{18}O_w$ is controlled by evaporation/ precipitation balance (Schmidt, 1999) an estimate can be obtained by using the relationship between sea surface salinity and $\delta^{18}O_w$. $\delta^{18}O$ is linearly related to sea salinity though the relationship varies from the tropics to high latitudes (Schmidt, 1999) and changes regionally. In this study the equation produced by Fairbanks *et al.*, (1997) from comparison of various sites in the Tropical Pacific is used.

Equation 2 $$\delta^{18}O_w = \text{salinity} \times 0.273 - 9.4$$

A salinity record was obtained from the interpolated data base Carton-Giese SODA salinity model, which derives salinity measurements based upon measurements and reanalysis using modelled factors such as SST and wind stress. Comparison of this salinity record with the average seasonal values available from the WOA 2005 dataset suggests that it may underestimate the full range of seasonal variability in salinity, however WOA does not provide time series data and this study must include interannual variability.

By substituting we obtain the formula:

Equation 3 $$\delta^{18}O_c = (T-21.8)/4.69+\delta^{18}O_w+C$$

where T = temperature, $\delta^{18}O_w$ has been predicted from the salinity record and C is the correction applied to convert to PDB. Comparison of predicted and measured $\delta^{18}O$ are shown in Figure 3-13.

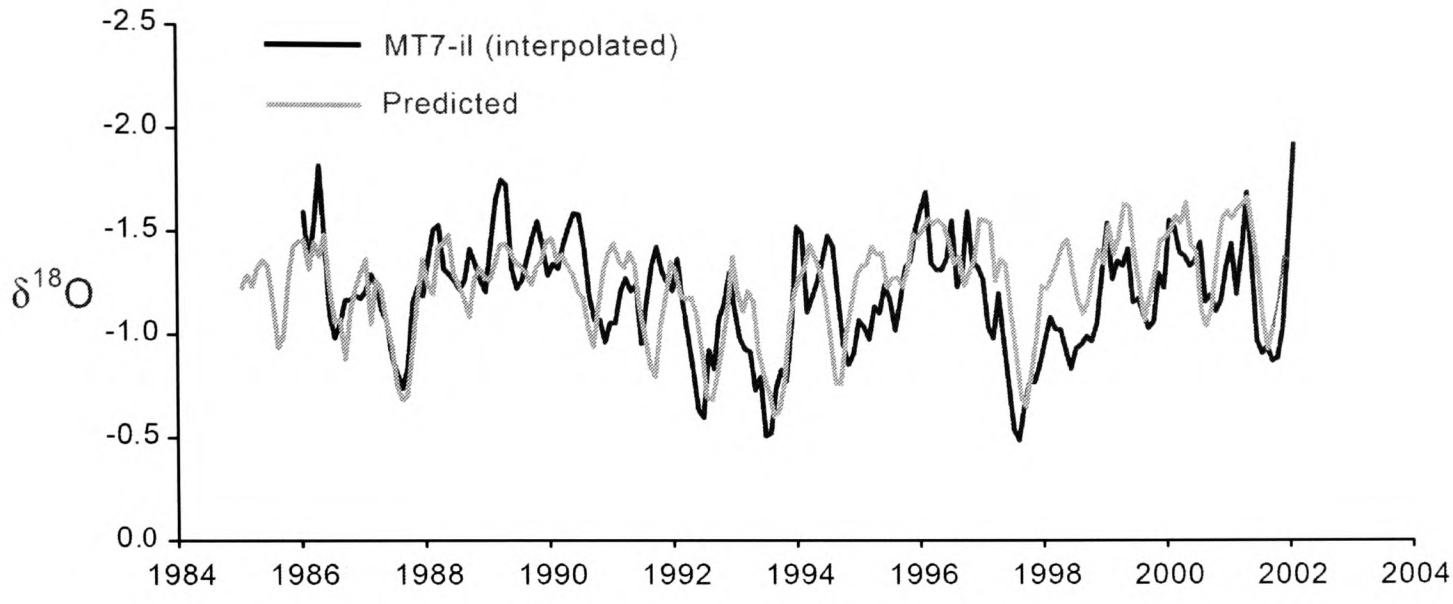

Figure 3-13 Comparison of the predicted $\delta^{18}O$ and measured $\delta^{18}O$ for Tg-MT7-il (interpolated to 12 samples/ year)

Considering the uncertainties in producing a prediction for $\delta^{18}O$ because temperature records and salinity records upon which this prediction is based are integrated across large areas, the gross fit between the two records appears very good. The correlation coefficient between the two records is very good (0.6), however this is likely to be influenced by the fact that annual variations in $\delta^{18}O$ are by necessity correlated because the $\delta^{18}O$ record from Tg-MT7 chronology is developed to fit a seasonal pattern. Comparing the average annual $\delta^{18}O$ values from each record will give a much better indication of the relationship between these two records. Performing a linear regression on these values gives an R^2 of 0.4, which indicates that there is a reasonable correlation between the two records.

Average predicted $\delta^{18}O$ is –1.3‰, which compares well with the shell average of –1.2‰ measured here[2]. The good correlation between measured and estimated $\delta^{18}O$

[2] Aharon (1983) measured an average of –1.6‰ in modern *Tridacna gigas* form Huon Peninsula that grew between approximately 1960 and 1980 whereas the results obtain here give an average of -1.2‰. Difference in temperature between the 1960-1980 and 1985-2001 periods cannot account for this as a difference of 0.4‰ would imply that it was approximately 1.5°C warmer during 1960-1980. Using the HadiSST dataset (See Chapter 2 for full description) to estimate the temperature difference yields 27.7°C mean temperature for the period 1960 to 1980 and slightly warmer 28.0°C mean temperature for the period 1985-2001. Using the same salinity record and the Fairbanks *et al.*, 1997 relationship for tropical salinity and $\delta^{18}O_w$ an average can be calculated. This produces a mean value of 0.03‰ and 0.02‰ for the periods 1960-1980 and 1980 to 2001 respectively. I conclude that there must have been systematic offset between stable isotope results measured here and those

agrees with previous studies that show that *Tridacna* sp. calcify their shells in isotopic equilibrium with sea water. More accurate environmental datasets measured *in situ* would be needed to improve this result.

3.5.5 Attenuation of $\delta^{18}O$ profiles in *Tridacna gigas*

Aharon (1991) show that the annual amplitude of $\delta^{18}O$ in *Tridacna gigas* is attenuated when compared to a $\delta^{18}O$ profile of a *Porites* coral from the same region, with a reduction in the amplitude of the annual $\delta^{18}O$ cycle toward the mature adult phase of growth (see Figure 3-14). Elliot *et al.,* (submitted) show no such attenuation in the seasonal cycle in Tg-GBR. Figure 3-15 shows the predicted $\delta^{18}O$ at Palm Island, and the measured $\delta^{18}O$ from Tg-GBR-il following a similar approach from Section 3.5.4, but on the Great Barrier Reef $\delta^{18}O_w$ was considered to be insignificant. We can clearly observe that there is no significant attenuation in the annual $\delta^{18}O$ cycle in Tg-GBR-il.

reported in Aharon, 1991. A possible explanation for this is that Aharon roasted samples at 400°C prior to stable isotope analysis to remove organic matter.

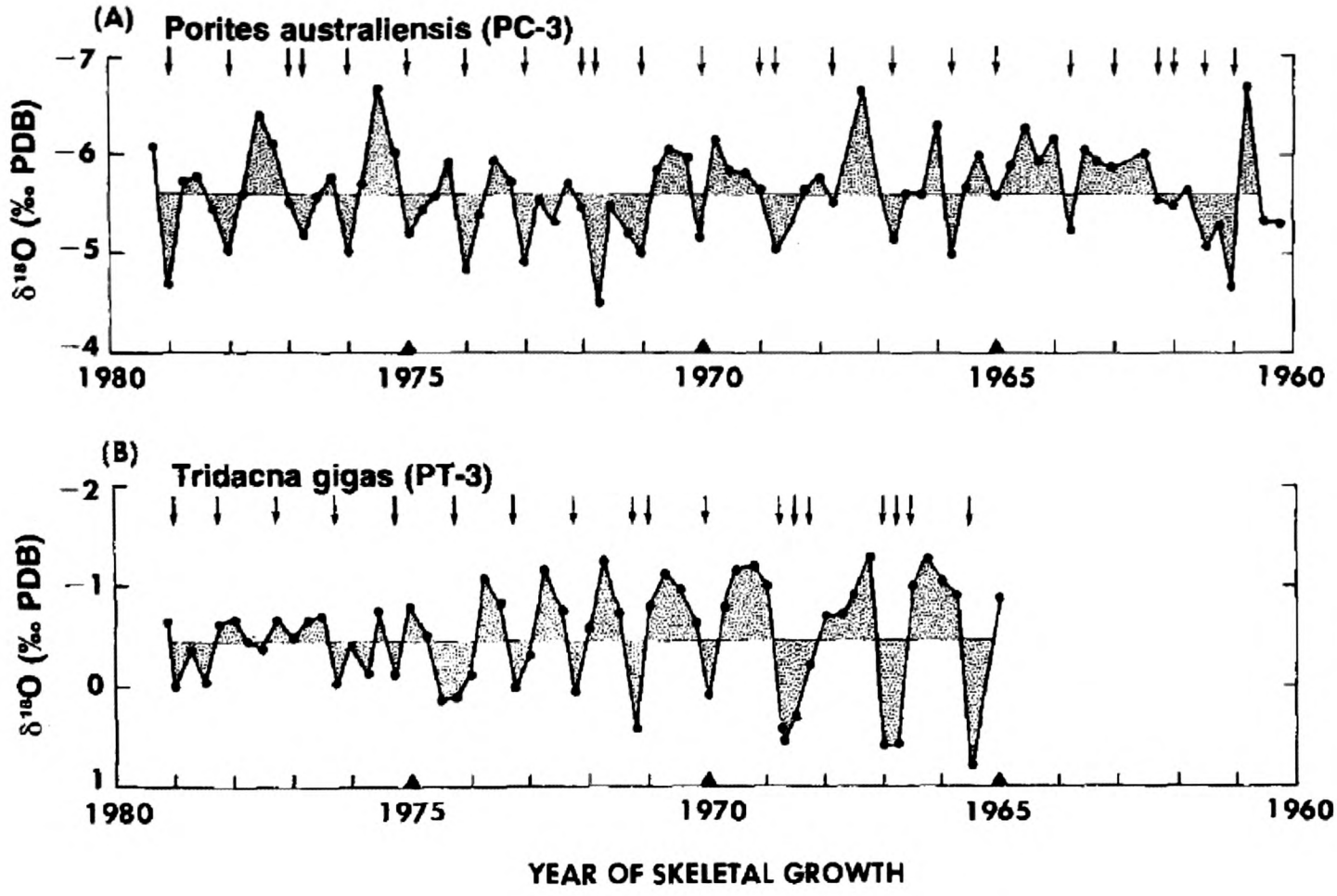

Figure 3-14 Stable isotopic results from Aharon (1991) showing relationship between $\delta^{18}O$ time series from a *Porites* coral and *Tridacna gigas* (inner layer). Aharon shows here an attenuation of the isotopic record in the later stages of life of the *Tridacna gigas*. Note here that Aharon shows an offset of approximately 5‰ and that the time axis is reversed running from right to left.

This may be explained by lower sampling resolution. The record that Aharon presents has only 2 to 4 samples per year in the final years of growth, whereas using more precise sampling techniques enables 7 samples or more per year to be obtained (this study and (Elliot *et al.,* submitted). Therefore we can conclude that though the thickness in the annual bands is reduced in the adult stages of growth, given sufficient resolution the inner layer of *Tridacna gigas* can provide a complete record of the seasonal cycle without significant attenuation.

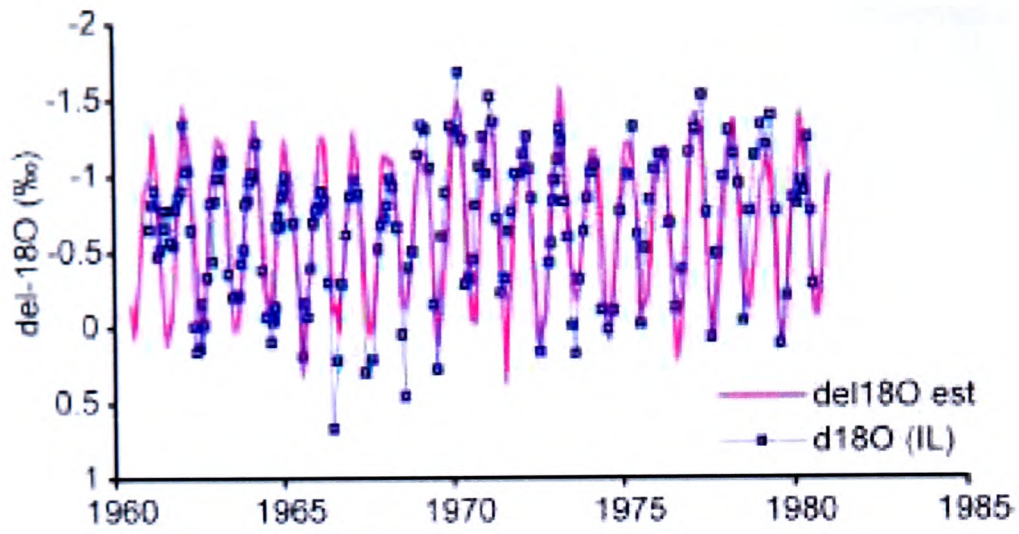

Figure 3-15 Comparison of measured and estimated $\delta^{18}O$ for Palm Island from Elliot *et al.*, (submitted). Data is plotted as a function of age from 1961 to 1980. Correlation coefficient for these two series is 0.8.

3.6 Intercomparison of $\delta^{18}O$ from *Tridacna gigas* and two *Porites* corals

Figure 3-16 shows two modern *Porites* coral $\delta^{18}O$ records from different localities on the Huon Peninsula and the $\delta^{18}O$ record from Tg-MT7-il (see Figure 3-2). The *Porites* $\delta^{18}O$ scale is offset by 3.9‰ from the *Tridacna gigas* $\delta^{18}O$ scale. Both coral records are interpolated to 12-14 samples per year. The chronology for the coral records was constructed by using the most positive $\delta^{18}O$ of the year and assigning that to the coolest/ driest part of the year (Tudhope *et al.*, 1995, 2001 and pers. comm..). The *Tridacna gigas* chronology was developed as described in Section 3.5.1. Since the chronologies for both bivalve and coral were constructed using the same approach, it is expected that there would be a good match between seasonal $\delta^{18}O$ cycles. Therefore, when assessing the closeness of fit between the bivalve and coral $\delta^{18}O$ records we should look at changes in annual $\delta^{18}O$ amplitudes and interannual $\delta^{18}O$.

Mean $\delta^{18}O$ for H95-64 and H01-09 are –5.1‰, whilst mean value for Tg-MT7-il is

-1.2‰, which is an offset between the *Porites* and *Tridacna gigas* of –3.9‰. The early part (pre-1992) of the Loto Beach record is slightly more positive (0.13‰) than the *Porites* from Sialum Lagoon. This is the equivalent of approximately 0.5°C warmer for H95-64, and may be due slightly elevated temperatures in the lagoon.

Previous studies have shown offsets between *Tridacna* sp. and *Porites* of 4.5‰ ±0.2 (Chakroborty and Romesh, 1993) for a *Tridacna maxima* and *Porites* in the Indian Ocean and 5.1‰ between *Porites* and *Tridacna gigas* at Palm Island, on the Great Barrier Reef (Aharon, 1991), on samples collected 3km apart.

Chakroborty and Ramesh's (1993) result may be explained by the comparison of maximum and minimum values using quite different resolution of sampling. A possible explanation for the slightly larger offset in Aharon's (1991) result is that the *Tridacna gigas* was collected at 0.5m and the *Porites* was collected at 4.5m. Though we lack specific information on the depth of MT7 and the corals, the thermocline is very deep (see Chapter 2), therefore the effects of different depth are likely to be very small.

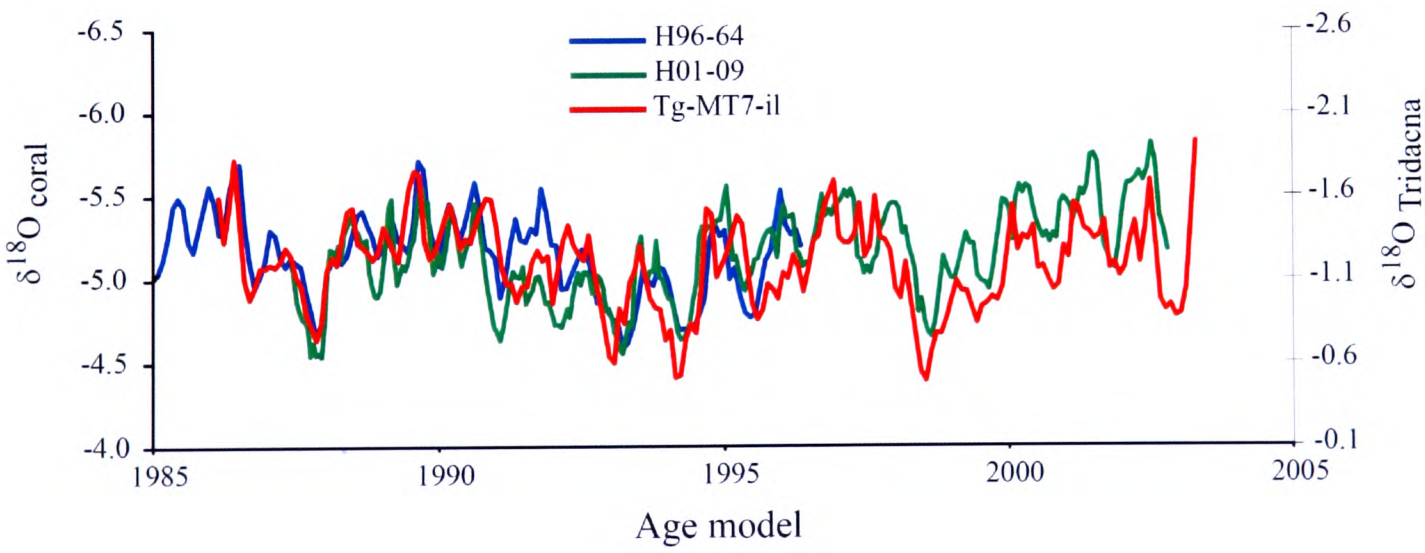

Figure 3-16 MT7-il $\delta^{18}O$ from Kanzarua plotted against coral H95-64 $\delta^{18}O$ from Sialum lagoon, see and *Porites* H01-9 from Loto Beach (note that the y axes are inverted).

3.6.1 Comparison of interannual $\delta^{18}O$ variations between coral and bivalve

The $\delta^{18}O$ profiles from the two *Porites* and Tg-MT7-il show remarkably similar variations in $\delta^{18}O$ over the 8 years that they overlap. There are two specific questions of this record that are of interest here:

1. Does the *T. gigas* record show the same interannual variability as the *Porites* records?
2. Does the $\delta^{18}O$ record from *Tridacna gigas* record the full range of seasonal variability $\delta^{18}O$ seen in *Porites*?

Comparison of mean annual $\delta^{18}O$ in T. gigas and Porites

The mean annual $\delta^{18}O$ was calculated for both *Porites* records and the *Tridacna* record. The results are shown in Figure 3-17. There is a reduced mean annual $\delta^{18}O$ during 1987, 1993 and 1997 in all records.

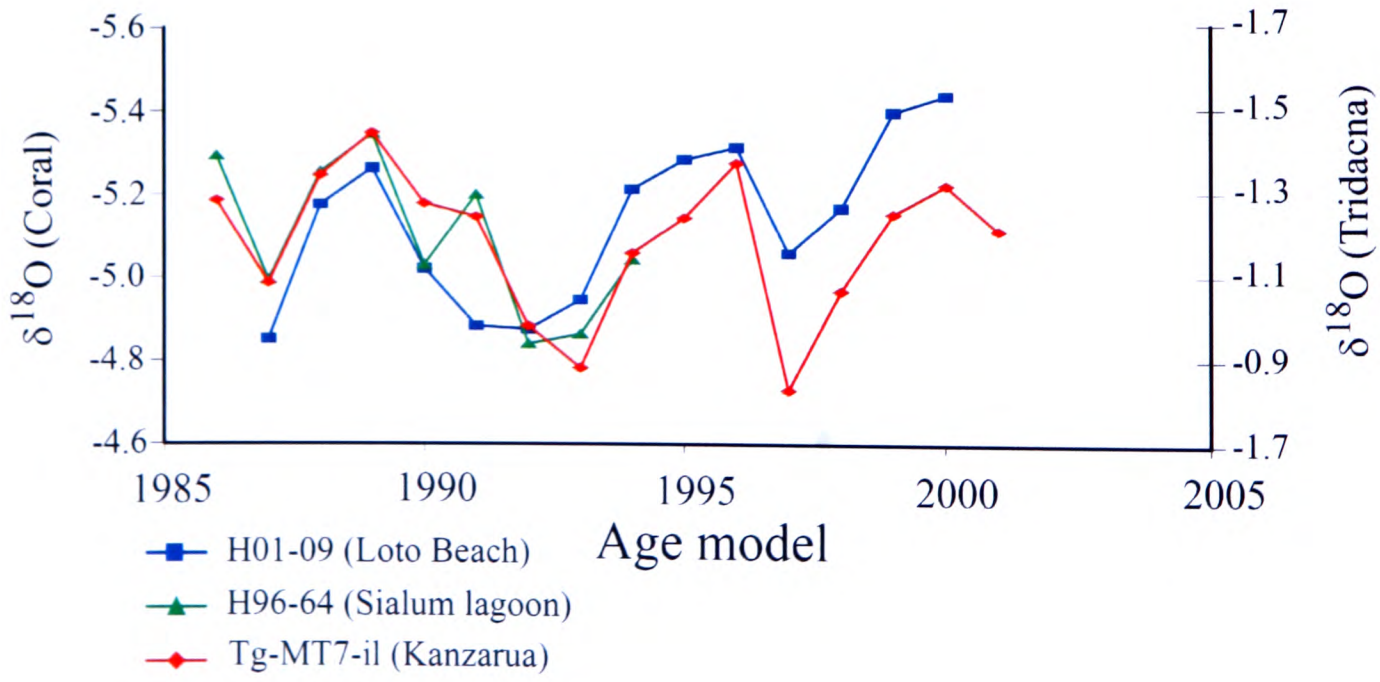

Figure 3-17 Annual average $\delta^{18}O$ in *Porites* H01-9 and H95-64 and *T. gigas* Tg-MT7-il

The mean annual $\delta^{18}O$ is remarkably similar for coral and bivalve with a constant offset of ≈3.9‰. Between 1997 and 2000 there is a small increase in the offset by ≈0.2‰, but trends are similar. This can also be observed in Figure 3-16 where, though the variation in annual amplitudes is similar, Tg-MT7-il results are more positive than the 3.9‰ offset. A similar deviation towards more positive values can be picked up in the predicted $\delta^{18}O$ versus measured $\delta^{18}O$ for Tg-MT7-il. This may be due to microenvironmental factors as Tg-MT7 was collected within a few km to the mouth of the river Tewai which enhanced the effects of reduced precipitation around the 1996/ 97 El Niño event.

Comparison of seasonal amplitudes

To assess any possible attenuation of the *Tridacna gigas* record by diminished growth rates or low sampling resolution the amplitude of the seasonal cycle can be measured and compared with coral $\delta^{18}O$ records as coral growth is assumed to be constant. This was calculated by taking the most positive value in the period Jul/ Aug/Sep of each year and subtracting it from the most negative value in the period Dec/ Jan/ Feb (Figure 3-18). The annual amplitude of Tg-MT7-il is highly variable (from 0.2 to 1‰) and does not diminish with increasing age.

The correspondence between the *Porites* annual $\delta^{18}O$ amplitude is at least as good as the correspondence between the corals. The largest exception to this is during 1992-1994 where Tg-MT7-il actually shows higher annual amplitudes by up to 0.55‰. It is difficult to explain why the amplitudes are so markedly different during these years. This is a period of weak El Niño, when precipitation and temperature variations were suppressed. Again, microenvironmental factors could explain this as its position near the mouth of the river Tewai may amplify the precipitation signal due to reduced runoff, though Tg-MT7-il still records a greater variability in $\delta^{18}O$ than the corals. Nevertheless, these results do show that the *Tridacna gigas* isotopic record is not attenuated with respect to the coral records.

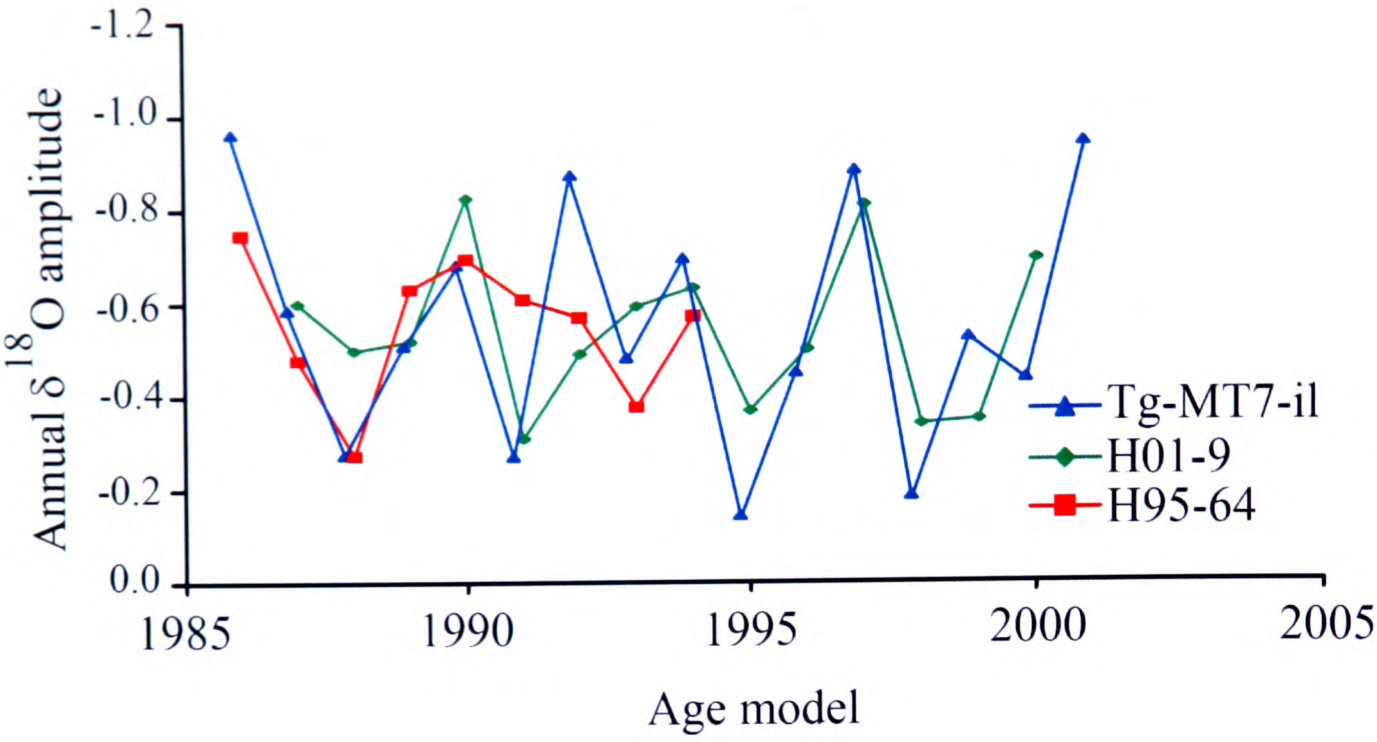

Figure 3-18 Annual amplitude in $\delta^{18}O$ from two *Porites* corals H01-9 and H95-64 and one *Tridacna gigas* from Huon Peninsula.

Comparison of $\delta^{13}C$ between T. gigas *and* Porites

Comparison of $\delta^{13}C$ records from Huon corals H01-9 and H95-64 and the modern *Tridacna gigas* MT7 are shown in Figure 3-19. The offset between the $\delta^{13}C$ values for *Tridacna* and *Porites* is difficult to estimate because of the large differences in variability and the lack of coherence between the *Porites* values, but can be estimated to be in the region of 3 to 4‰. No annual correspondence between $\delta^{13}C$ variation in *Porites* and Tg-MT7-il can be seen. Complex biological factors are likely to dominate $\delta^{13}C$. This is also supported in Elliot *et al.* (submitted).

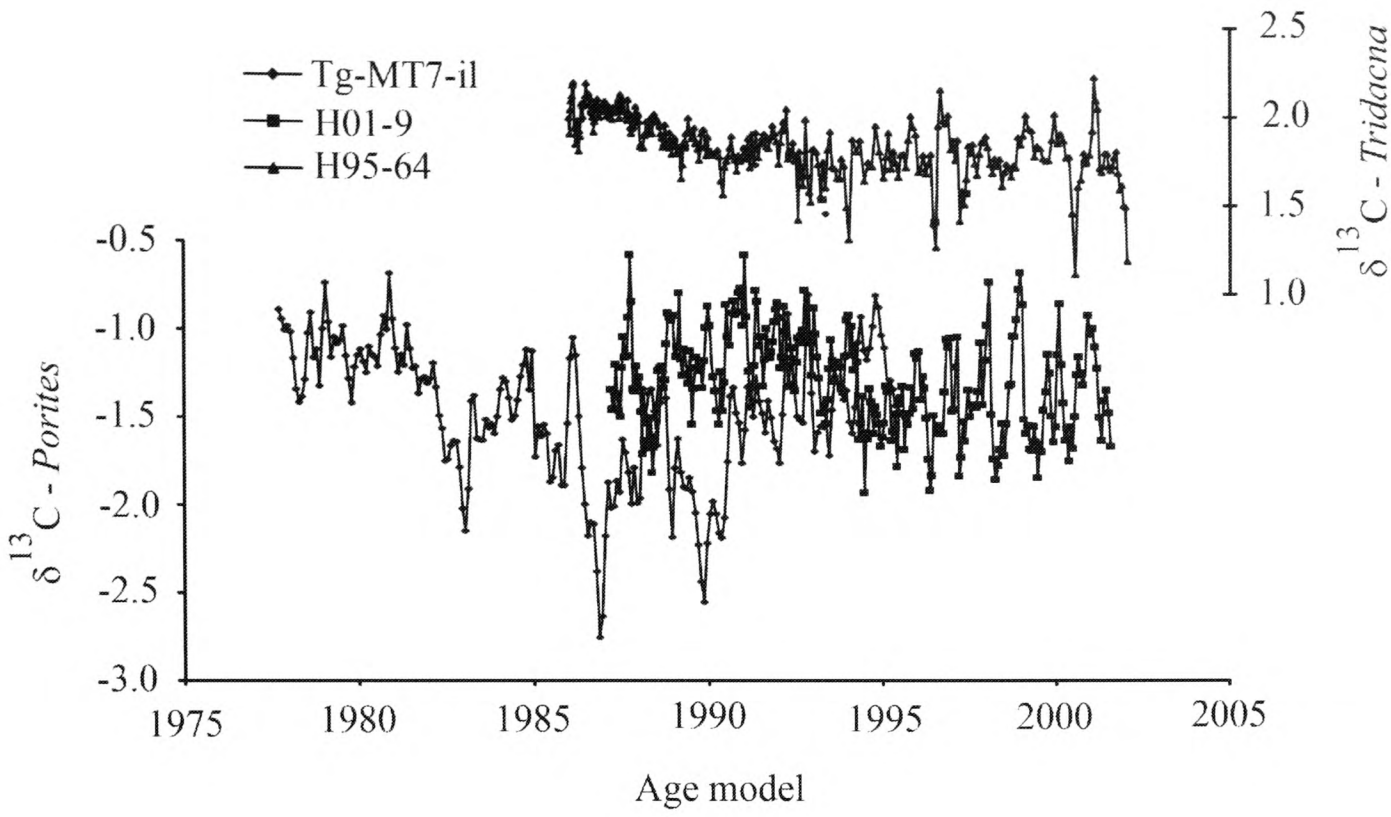

Figure 3-19 Comparing $\delta^{13}C$ profiles of two *Porites* corals (H01-9 from Loto beach and H95-64 from Sialum lagoon) and the modern *Tridacna gigas* Tg-MT7. Chronology was developed based upon $\delta^{18}O$. Note different scales.

Summary

Comparison of $\delta^{18}O$ profiles, annual $\delta^{18}O$ mean and $\delta^{18}O$ annual amplitudes show excellent correspondence between the three records in spite of the fact that 1) these are two completely different organisms, 2) the coral has a strong biological effect on $\delta^{18}O$ and, 3) they were collected from three different reef environments on the Huon Peninsula separated by nearly 30 km. The time series from Tg-MT7-il does not show attenuation of the record due to changes in resolution when compared to coral time series with relatively unchanging resolution. These data show that despite different growth rates, different biological offsets and different locations the $\delta^{18}O$ profiles obtained reflect changes in the regional climate and are accurate climate archives.

3.7 Stable isotopic record and ENSO

The relationship between changes in sea surface temperature and precipitation at the Huon Peninsula and the El Niño Southern Oscillation is well documented (Tudhope

et al., 1995 and see Chapter 2). Comparison of the Tg-MT7-il $\delta^{18}O$ record and the temperature anomaly in the Niño 3.4 box shows a very good correspondence.

El Niño events are associated with the reduction of SST and precipitation in the West Pacific Warm Pool. In general values of $\delta^{18}O$ that are more positive than average (> -1.2‰) correspond with positive anomaly in Niño 3.4, and *vice versa*. Since the annual mean amplitude in Tg-MT7-il $\delta^{18}O$ is 0.53 ‰ the mean expected minimum and maximum $\delta^{18}O$ values on the diagram at –1.47‰ and –0.94‰ can be marked respectively. Where isotopic values exceed these bounds it would be reasonable to expect El Niño and La Niña events. This is especially robust since the mean isotopic amplitude will be increased by the extremes of temperature and precipitation associated with El Niño/ La Niña events.

El Niño events are very well correlated with positive $\delta^{18}O$ events that exceed the mean annual amplitude (Figure 3-20). This illustrates how the $\delta^{18}O$ of *T. gigas* strongly reflects ENSO. The coefficient of correlation between these two records, which gives an indication of how they covary, is 0.53 which is a fairly strong correlation considering the difficulties in establishing a chronology for the stable isotopic record and is slightly higher than the correlation coefficient between temperatures at the Huon Peninsula and the Nino 3.4 temperature anomaly (0.45).

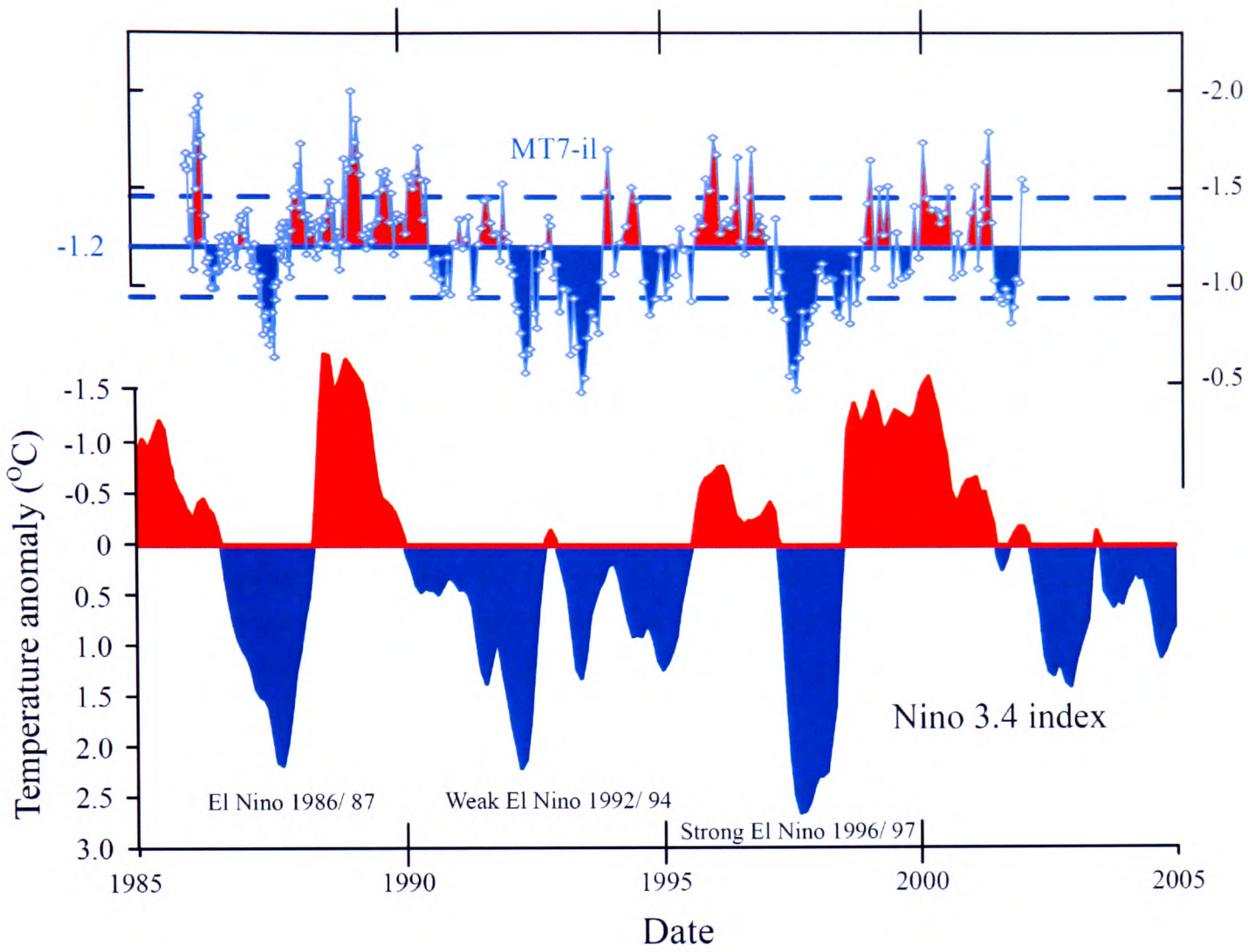

Figure 3-20 $\delta^{18}O$ record from modern *Tridacna gigas* from Huon Peninsula and the temperature anomaly from the Niño 3.4 box. -1.2 line shows average values for MT7-il. Dashed lines show average annual amplitude in $\delta^{18}O$. Both axes are inverted.

3.8 Conclusions

It has been shown here that $\delta^{18}O$ records from *Tridacna gigas* reflect regional climate change in temperature and climate in terms of changing SST and precipitation. *T. gigas* $\delta^{18}O$ is very close to predicted values, supporting the assumption that *Tridacna* sp. calcify their shells in isotopic equilibrium with seawater. Variations of *T. gigas* $\delta^{18}O$ correlate extremely well with variations in $\delta^{18}O$ derived from *Porites* corals from different localities on the Huon Peninsula, despite variations in locality, biology and growth rate of these organisms. This shows that analysis of $\delta^{18}O$ in reef dwelling organisms is a very robust measure of regional climate variation and also indicates that, whilst there is reduction in growth in mature

stages of growth, given sufficient resolution the shell of *Tridacna gigas* still records a full annual cycle in tropical regions. Therefore, it has also been shown that the $\delta^{18}O$ record for *Tridacna gigas* strongly reflects the changing climate not only of the Huon Peninsula, but also the ENSO system and therefore fossil bivalves should be very useful in recording changes to the climate of the WPWP in the past.

References

Aharon, P., Chappell, J. and W. Compston (1980), Stable Isotope and Sea-Level Data from New-Guinea Supports Antarctic Ice-Surge Theory of Ice Ages, *Nature*, **283**, 549-651

Aharon, P., and J. Chappell (1986), Oxygen Isotopes, Sea-Level Changes and the Temperature History of a Coral-Reef Environment in New-Guinea over the Last 105 Years, *Palaeogeography Palaeoclimatology Palaeoecology,* **56**, 337-379

Aharon, P. (1991), Recorders of Reef Environment Histories - Stable Isotopes in Corals, Giant Clams, and Calcareous Algae, *Coral Reefs*, **10**, 71-90

Asami, R., Yamada, T., Iryu, Y., Meyer, C.P., Quinn, T., and Paulay, G. (2004), Carbon and oxygen isotopic composition of a Guam coral and their relationships to environmental variables in the western Pacific, *Palaeogeography Palaeoclimatology Palaeoecology*, **212**, 1-22.

Arthur, M., Williams, D. F., and Jones, D. S (1983), Seasonal temperature-salinity changes and thermocline development in the mid Atlantic Bight as recorded by isotopic composition of bivalves, *Geology*, **11**, 655-659

Bonham, K. (1965), Growth rate of Giant Clam *Tridacna gigas* at Bikini Atoll as revealed by Radioautography, *Science,* **149**, 300-302

Chakroborty, S. and Romesh, R. (1993), Monsoon induced sea surface temperature changes recorded in Indian corals, *Terra Nova*, **5**, 545-551

Dunbar, R. B. and Wellington, G. M. (1981), Stable isotopes in a branching coral monitor seasonal temperature variation, *Nature*, ***293***, 453-455

Elliot, M. Welsh, K. Chilcott, C., MuCulloch, M., Chappell, J and Ayling, B. Profiles of trace elements (Mg/ Ca, Sr/ Ca and Ba/ Ca) derived from giant long lived *Tridacna gigas* bivalves. (Submitted to *Geochimica et Cosmochimica Acta*)

Elliot, M., DeMenocal, P., Linsley, B. and Howe, S.S. (2003), Environmental controls on the stable isotopic composition of *Mercenaria mercenaria*: Potential application to palaeoenvironmental studies, *Geochemistry, Geophysics and Geosystems*, **4**, 1056-1072

Epstein, S.R., Buschaum, H. A., Lowenstam, and H.C. Urey (1953), Revised carbonate-water isotopic temperature scale, *Bulletin of the Geological Society of America*, **64**, *1315-1326*

Evans, M.N., Fairbanks, R. G. and Rubenstone, J.L. (2000), A proxy index of ENSO teleconnections, *Nature,* **394**, 732-733

Fairbanks, R.G., M.N. Evans, J.L. Rubenstone, K. Broad, M.D. Moore, C.D. Charles, (1997), Evaluating climate indices and their geochemical proxies measured in corals. *Coral Reefs*, **16**, 93-100

Grossman, E. L., and T. L. Ku (1986), Oxygen and Carbon Isotope Fractionation in Biogenic Aragonite - Temperature Effects, *Chemical Geology*, **59**, 59-74

Hall, C.R., Dollase, W.A., and Corbato, C.W., (1974), Shell growth in *Tivela stultorum* (Mawe, 1823) and *Callista chione* (Linnaeus, 1758) (Bivalvia): Annual periodicity, latitudinal differences, and diminution with age. *Palaeogeography, Palaeoclimatology, Palaeoecology*, **15**, 33–61

Jones, D.S., Arthur, M.A., and Allard, D.J., (1989), Sclerochronological records of temperature and growth from shells of *Mercenaria mercenaria* from Narragansett Bay, Rhode Island, *Marine Biology,* **102**, 225–234

Kennedy, H., Richardson, C.A., Duarte, C.M. and Kennedy, D.P. (2001), Oxygen and carbon stable isotopic profiles of the fan mussel, *Pinna nobilis*, and reconstruction of sea surface temperatures in the Mediterranean. *Marine Biology*, **139,** 1115-1124

McConnaughey, T.A. (1989), C-13 and O-18 isotopic disequilibria in biological carbonates: I. Patterns, *Geochimica et Cosmochimica Acta*, *53*, 151-162

McCrea, J.M. (1950), On the Isotopic chemistry of the carbonates and paleotemperature scale, *Journal of Chemical Physics*, **18,** 849-857

McGregor, H. V., and M. K. Gagan (2003), Diagenesis and geochemistry of Porites corals from Papua New Guinea: Implications for paleoclimate reconstruction, *Geochimica et Cosmochimica Acta,* **67,** 2147-2156

Patzold, J., Heinrichs, J.P., Wolschendorf, K., and G. Wefer (1991), Correlation of Stable Oxygen Isotope Temperature Record with Light Attenuation Profiles in Reef-Dwelling Tridacna Shells, *Coral Reefs*, **10**, 65-69

Romanek, C. S., Jones, D.S., Williams, D.F., Krantz, D.E. and Radkte, R (1987), Stable Isotopic Investigation of Physiological and Environmental-Changes Recorded in Shell Carbonate from the Giant Clam Tridacna-Maxima, *Marine Biology*, **94**, 385-393

Romanek, S. and Grossman E.L. (1989), Stable Isotope Profiles of *Tridacna maxima* as Environmental Indicators, *Palaios*, **4**, 402-413

Rosewater, J. (1965), The Family Tridacnidae in the Indo-Pacific, *Indo-Pacific Mollusca*, **1**, 347-396

Sato, S., (1995), Spawning periodicity and shell microgrowth patterns of the venerid bivalve *Phacosoma japonicum* (Reeve, 1850): *Veliger*, **38**, 61–72

Schone, B., Duncan, E., Feibig, J., Pfeiffer, M. (2005), Mutvei's solution: an ideal agent for resolving microgrowth structures in biogenic carbonates. *Palaeogeography, Palaeoclimatology, Palaeoecology*, **228**, 149-146

Schmidt, G. (1999), Error analysis in paleosalinity calculations. *Paleoceanography.* **14**, 422-429

Surge, D., K. C. Lohmann, and D. L. Dettman, (2001), Controls on isotopic chemistry of the American oyster, Crassostrea virginica: Implication for growth patterns. *Palaeogeography, Palaeoclimatology and Palaeoecology,* **172**, 283–296.

Thebault, J. Chauvaud, L., Clavier. J., Guarini, J., Dunbar, R., Fichez, R., Mucciarone, D. A., and Morize, E. (2005), Reconstruction of seasonal temperature variability in the tropical Pacific Ocean from the shell of the scallop, *Comptopallium radula. Geochimica et Cosmochimica Acta,* **71**, 918-928

Tudhope. A.W., Shimmield, G.B., Chilcott, C.P., Jebb, M., Fallick, A.E. and Dalgleish, A.N. (1995), Recent changes in climate in the far western equatorial Pacific and their relationship to the Southern Oscillation; oxygen isotope records form massive corals, Papua New Guinea. *Earth and Planetary Science Letters*, **136,** 575-590

Tudhope, A., W., Chilcott, C.P., McCulloch, M.T., Cook, E.R., Chappell, J. Ellam, R.M., Lea, D., Lough, J.M. and Shimmield, G.B. (2001), Variability in the El Niño - Southern oscillation through a glacial-interglacial cycle, *Science*, **291**, *1511-1517*

Watanabe, T. and. T. Ota. (1999), Daily reconstruction of water temperature from oxygen isotopic ratios of a modern Tridacna shell using a freezing microtome sampling technique, *Journal of Geophysical Research*, **104**, 667-674

Watanabe, T., A. Suzuki, H. Kawahata, H. Kan and S. Ogawa. (2004), A 60-year isotopic record from a mid-Holocene fossil giant clam (Tridacna gigas) in the Ryukyu Islands: physiological and paleoclimatic implications, *Palaeogeography Palaeoclimatology Palaeoecology*, **212**, 343-354

Weber, J. N. and Woodhead, P.M.J. (1972), Temperature dependence of oxygen-18 concentration in reef coral carbonates, *Journal of Geophysical Research,* **77**, 463

4 Building a chronology for Holocene and Glacial timescales

Chapter Abstract

This chapter describes the methods that were used in this study to construct a chronological models for fossil *Tridacna* sp. collected from the uplifted and subaerially exposed Holocene and Marine Oxygen Isotope Stage 3 (35-65 Ka) reef terraces at Huon Peninsula.

Several methods are used for dating on glacial timescales: 1) direct radiocarbon dating of the *Tridacna* sp. and 2) indirect age determination by comparison to reef crest ages determined from an age model that incorporates U/ Th dating of corals and terrace morphology. Radiocarbon dates derived from 28 *Tridacna* sp. specimens are presented and compared to previous studies of the reefs. It is shown that these records agree with previous studies, there is a disparity between calibrated radiocarbon ages and U/Th ages from corals. It is possible to explain this by variations in reservoir ages caused by changes in the strength of deep water production.

Eustastic sea level events can be used to constrain the relationship between Northern Hemispheric millennial scale climate change and individual terraces. By developing a detailed temporal relationship of fossil samples to eustatic sea level change inferred from reef terrace morphology, a correlation with global millennial scale climatic change is proposed. The proposed relationship between fossil samples collected from Reef Terraces IIa and IIIc and eustatic sea level is used to correlate with North Atlantic climate is shown in detail.

The directly dated samples and extrapolated ages are then used to reconstruct a sea level curve for Marine Oxygen Isotope Stage 3.

4.1 Introduction

The intention of this thesis is to study the palaeoclimate of the West Pacific Warm Pool using stable isotopes records from fossil samples of *Tridacna* sp. uplifted and sub-aerially exposed in reef terraces at Huon Peninsula, Papua New Guinea over glacial and millennial timescales. To use this proxy data to interpret past climate a reliable chronology must be produced. Fortunately the terraces at Peninsula have been well studied and dated during the last 40 years.

The coast of the Huon Peninsula consists of flights of coral terraces that have been uplifted by the collision of the West Pacific and Australian plates. The terraces and fossil reefs have been well documented and extensively dated (Polach *et al.,* 1969, Veeh and Chappell, 1970; Chappell and Polach, 1972; Bloom *et al.*, 1974; Chappell and Polach, 1976; Aharon *et al.*, 1980; Edwards *et al.*, 1993; Chappell *et al.*, 1996a; Yokoyama *et al.,* 2000; Yokoyama *et al.*, 2001, Cutler *et al.*, 2003, Edinger *et al.*, 2007) using a variety of techniques including U/ Th and radiocarbon dating in corals, and radiocarbon dating of *Tridacna* sp.

Three approaches are used to assign a chronology to the data collected:

1. Direct ^{14}C dating of the fossil *Tridacna* sp. collected in this study
2. Comparison with prior dating of stratigraphic units from which the samples were collected
3. Correlation to North Atlantic and global climatic events using eustatic sea level excursions that are recorded in other proxy records

4.1.1 Direct ^{14}C dating of fossil samples

Direct dating has been used successfully on corals and *Tridacna* sp. from Huon Peninsula. Radiocarbon analysis can be employed on samples that range in age up to approximately 45 ka (Fairbanks *et al.*, 2005; Hughen *et al.*, 2004), but beyond this

radiocarbon activity is too close to background levels to be used. *Tridacna* sp. cannot themselves be dated using U/ Th techniques as insufficient uranium is incorporated into the valve during life (Tatsumoto and Goldberg, 1959 and Broecker, 1963) and they have also been found to be "open systems" for uranium, with much uranium incorporated after death (Swart and Hubbard, 1982).

4.1.2 Stratigraphic position and prior dating

Although reef stratigraphy can be quite complex it can be assumed that since tectonic uplift is continuous and the rate of uplift is sufficiently high, the position of one discrete terrace below another can be used to show that samples taken from that terrace must be younger. This relationship does not hold when sea level rise outstrips uplift for extended periods of time, such as the sea level rise of 130m since the Last Glacial Maximum. Terraces that were emplaced during the LGM are still 30m below present sea level and the Holocene terrace has grown unconformably on the terraces that grew approximately 30 ka ago.

Beyond radiocarbon dating, the age of samples can be estimated by comparison with U/ Th dates derived from fossil corals from the same stratigraphic unit. Several studies have used U/ Th dates to study the fossil reefs (Edwards *et al.*, 1993; Chappell, *et al.,* 1996a; Yokoyama *et al.,* 2000; Yokoyama *et al.*, 2001; Cutler *et al.*, 2003). Chappell *et al.*, (1996a) and Yokoyama *et al.*, (2000 and 2001) in particular studied the Marine Oxygen Isotope Stage 3 reefs at Huon Peninsula using U/ Th and radiocarbon dates obtained from corals.

Based upon this extensive dating Chappell (2002) extrapolated sea level histories on millennial timescales using models of reef growth constrained by U/Th dates, realistic vertical accretion rates, and estimates of variation in uplift rates to produce a range of reef morphologies. By choosing the predicted morphologies that most closely fit observed morphologies, Chappell was able to produce a sea level curve and predicted ages for the sea level highstands and associated reef terrace crests.

4.1.3 Millennial scale sea level variations

Correlation of millennial scale climate variability during MIS3 is problematical due to uncertainties associated with dating techniques. Uncertainties in radiocarbon dating include: changes in the rate of production of ^{14}C in the upper atmosphere due to changes in the strength of the solar magnetic field (de Vries, 1958, 1959; Stuiver, 1961; Stuiver and Quay, 1980), and the Earth's magnetic field (e.g. Ellassar *et al.*, 1956; McElhinny and Senanayake, 1982; Guyodo and Valet, 1999) uncertainties attached to calibration of ^{14}C dates (e.g. Bard *et al.*, 2004; Fairbanks *et al.*, 2005 and Reimer *et al.*, 2006), changes in atmospheric radiocarbon content associated with changes to the thermohaline circulation (e.g. Edwards *et al.*, 1993; Yokoyama *et al.*, 2000 and Waelbroeck *et al.*, 2001). Even tiny amounts of diagenetic alteration, which is likely in subaerially exposed environments, can cause anomalously young radiocarbon dates.

U/ Th dating of corals also have uncertainties associated with subtle diagenetic and open system behaviour in U/ Th in corals (Thompson and Goldstein, 2005, Chui *et al.*, 2005). The uncertainties involved in these dating methods are on the timescale of the events themselves therefore another approach is adopted using evidence for changes in eustatic sea level to correlate proxy records of global climatic events.

Millennial scale global SL change recorded at Huon Peninsula

Rapid, millennial scale changes in eustatic sea level affect reef growth due to sudden changes in accommodation space (Chappell, 1974; Aharon *et al.*, 1983; Chappell and Shackleton, 1986; Chappell *et al.*, 1996a). Timing and height of the sea level peaks were refined by Chappell, (2002) as described above.

Other evidence for millennial scale sea level variations during MIS3 comes from $\delta^{18}O$ in benthic foraminifera in sediment cores through changes in ice volume (Shackleton 2000 and Arz *et al.*, 2007), $\delta^{18}O$ variations in planktonic foraminifera caused by salinity changes in restricted basins such as the Red Sea due to the isolation of this basin with eustatic sea level change (Siddall *et al.*, 2003; 2004), and

changes in the exposure of tidal flats in the Persian Gulf which is reflected in the dolomite concentration in a core from the Somali margin (Ivanochko, 2005 (unpublished thesis University of Edinburgh, 2005)). Yokoyama *et al.*, (2001) and Chappell, 2002 showed a minimum estimate of sea level rise of 10-15m on millennial timescales based upon data obtained from accurate dating and current elevation of corals to produce a sea level curve. Siddall *et al.* (2003) and Arz *et al.*, (2007) observe sea level variations of up to 30m. Eustatic changes in sea level of this magnitude must be globally synchronous and can form the basis for robust millennial scale correlation.

Aims of this chapter:

1. To explain the procedures used for radiocarbon dating *Tridacna* sp.
2. To investigate temporal relationship of radiocarbon dated samples and millennial scale eustatic sea level change as a chronological constraint
3. To explain how a chronology was obtained for samples that are older than 45 ka
4. To use dates and elevation of samples to produce a sea level curve

4.2 Field area and sample collection

See Chapter 2 for a review of the Huon Peninsula field area and sample collection.

4.3 Methods

Samples from the large inner layers of *Tridacna* sp. (except for *Tridacna gigas* samples T14 and T70 where the hinge area was large and well preserved) were used for radiocarbon dating. Samples were mechanically cleaned with a trim saw to remove the outer surface (approximately 2/3 of each sample was removed) and a hand held tungsten carbide drill used to clean away any sign of disturbance by borings, fracture or infiltration of ground water. Only samples that were visually free of borings and diagenetic alteration were sent for analysis.

Samples were then cleaned using distilled water and samples of carbonate drilled using the same drill for analysis by X-ray diffraction to check for undetected diagenetic effects. A Bruker-AXS D8 Advance XRD that uses Cu K-alpha radiation (40kV) as the source and a Sol-X energy dispersive detector was used to determine % calcite in carbonate powders.

Two different laboratories analysed the *Tridacna* sp. samples in this study, the NERC Radiocarbon Laboratory in East Kilbride and the Department of Nuclear Engineering and Management at Tokyo University. The procedures at each laboratory were essentially the same. The outer 20% (50% at DNEM, Tokyo) of samples were dissolved away by controlled hydrolysis using dilute HCl acid. The sample was then crushed and homogenised before being hydrolysed to CO_2 using 85% orthophosphoric acid at 25°C. The CO_2 was then converted to graphite using Fe/ Zn reduction.

4.3.1 Correction for marine reservoir age

Since the carbon incorporated into the shells of marine organisms has been resident in the ocean for some time, these ages are generally several hundred years older than their terrestrial counterparts. Therefore it is necessary to correct radiocarbon ages in order to compare marine and terrestrial samples. Standard marine reservoir ages is modelled to be 400 years, however because of ocean circulation there are regional differences to the global marine reservoir age which is designated ΔR (Stuiver and Braziunas, 1993). For Holocene age samples, radiocarbon ages were corrected by 400 years for the marine radiocarbon reservoir effect plus 373 years ±70 years for local ΔR (based upon the marine reservoir correction database at http://calib.qub.ac.uk/marine/). Changes to circulation in MIS3 mean that ΔR cannot be reliably calculated, therefore a reservoir correction of 400 years is applied, with the caveat that ages may be incorrect by several hundred years.

4.3.2 Calibration

Samples from Holocene Terrace

The corrected radiocarbon ages were calibrated used the Calib Rev 5.0.2 program available at http://calib.qub.ac.uk/calib/ (Stuiver and Reimer, 1993) with Marine 04.14 calibration and ages are reported before present.

MIS3 samples

Few radiocarbon calibration curves exist for samples older than 25 ka due to a lack of reliable independent dating techniques to be used for calibration. This study uses the Fairbanks *et al.,* (2005) calibration program (vs 01.07) (available at http://radiocarbon.ldeo.columbia.edu/research/radcarbcal.htm) for radiocarbon samples between 35 ka and 45 ka. Because of the sparse numbers of independent dates available for the construction of this curve, these dates can be used to determine relative ages only and should not be considered reliable for millennial scale correlation.

4.4 Results

Figure 4-1 shows calibrated radiocarbon age vs elevation. There is a strong correlation between elevation and age, confirming the relatively constant rates of uplift (Chappell *et al.*, 1996a). The Holocene samples are taken from a variety of uplift regimes, and in consequence the scatter is fairly large. Many Holocene samples are not included in this figure since most were *ex situ*. There is an extended hiatus in samples between approximately 10 ka and 30 ka as 130m of sea level rise since the LGM had submerged terraces emplaced at this time and subsequent growth of the Holocene complex has buried this material.

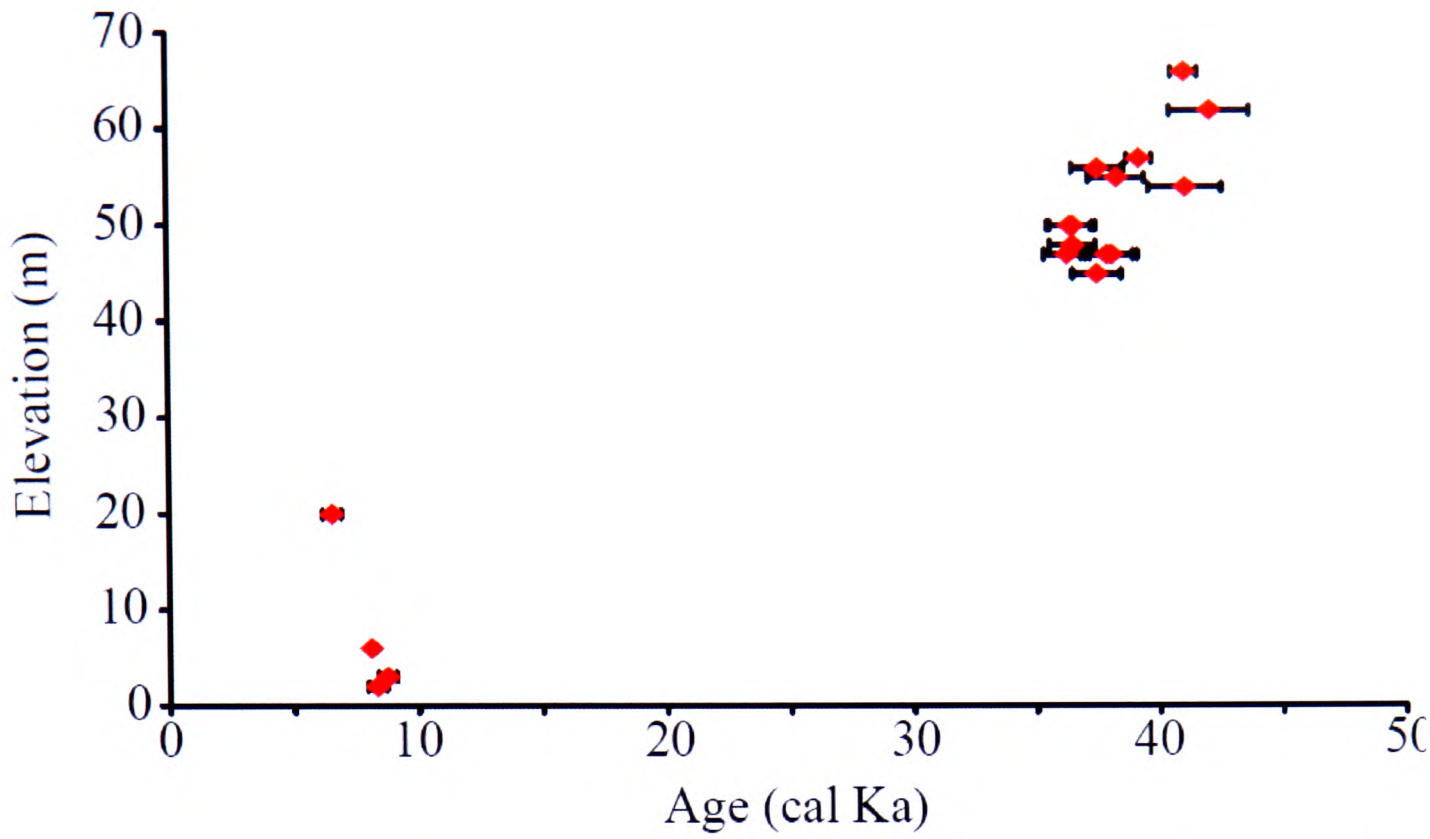

Figure 4-1 Showing in situ samples calibrated radiocarbon age compared to elevation.

Table 4-1 (Page over) Showing the results of radiocarbon analysis and elevation. [N] denotes analysis at NERC Radiocarbon Facility. [T] denotes sample analysed at DNEM, Tokyo Estimated ages are based upon U/ Th dates reported in Chappell *et al.*, 1996a and Yokoyama *et al.*, 2000.

Sample	Species	Reef	Elevation (m)	Distance from terrace crest (m)	Radiocarbon age (uncalibrated)	Age (cal Ka bp)	2 sigma (ka)	% calcite	Predicted age (cal Ka bp)
T72^{T}	*T. maxima*	Holocene	*ex situ*	*ex situ*	4150	3.71	0.42	0.6	6.5-10
T66^{T}	*T. gigas*	Holocene	20	0	6480	6.54	0.38	0.6	6.5-10
T59^{T}	*T. squamosa*	Holocene	*ex situ*	*ex situ*	6890	7.03	0.39	0.6	6.5-10
T60^{T}	*T. gigas*	Holocene	*ex situ*	*ex situ*	7025	7.17	0.42	0.8	6.5-10
T65^{T}	*T. maxima*	Holocene	*ex situ*	*ex situ*	7330	7.45	0.29	0.8	6.5-10
T73^{N}	*T. gigas*	Holocene	*ex situ*	*ex situ*	7129	7.28	0.28	0.1	6.5-10
T58^{N}	*T. gigas*	Holocene	6	6	7257	7.40	0.28	0.1	6.5-10
T49^{T}	*T. gigas*	Holocene	2	4	8230	8.33	0.36	0.5	6.5-10
T51^{N}	*T. maxima*	Holocene	3	3	8548	8.73	0.46	0.2	6.5-10
T75^{N}	*T. gigas*	Holocene	*ex situ*	*ex situ*	8592	8.76	0.46	0.2	6.5-10
T26^{T}	*T. maxima*	IIa	*ex situ*	*ex situ*	29830	35.25	0.40	2.9	38-40
T28I^{T}	*T. maxima*	IIa	*ex situ*	*ex situ*	30823	35.83	0.39	0.4	38-40
T10I^{T}	*T. gigas*	IIa	*ex situ*	*ex situ*	31183	36.17	0.36	0.7	38-40
T13I^{T}	*T. maxima*	IIa	*ex situ*	*ex situ*	32123	37.13	0.40	0.3	38-40
T29I^{T}	*T. gigas*	IIa	*ex situ*	*ex situ*	32153	37.16	0.41	0.4	38-40
T70^{N}	*T. gigas*	IIa	47	3	31590	36.97	0.92	0.6	38-40
T14^{N}	*T. gigas*	IIa	49	1	31694	37.07	0.89	0.5	38-40
T27^{N}	*T. gigas*	IIa	50	0	31820	37.20	0.91	0.0	38-40
T9^{N}	*T. gigas*	IIa	45	5	32794	38.19	1.02	0.5	38-40
T12^{N}	*T. squamosa*	IIa	47	2	33583	38.60	1.05	0.3	38-40
T11^{N}	*T. squamosa*	IIa	47	3	33786	38.80	1.08	0.4	38-40
T31^{N}	*T. crocea*	IIIc(l)	56	1	33181	38.20	1.06	0.3	40-44.5
T34^{N}	*T. maxima*	IIIc(l)	55	2	33985	38.99	1.14	1.0	40-44.5
T32^{T}	*T. maxima*	IIIc(l)	57	0	34893	39.89	0.50	0.3	40-44.5
T33^{N}	*T. crocea*	IIIc(l)	54	3	36986	41.79	1.52	0.0	40-44.5
T39^{T}	*T. maxima*	IIIc(u)	66	0	36923	41.75	0.53	0.8	40-44.5
T30^{T}	*T. crocea*	IIIc(u)	*ex situ*	*ex situ*	37083	41.88	1.62	0.5	40-44.5
T40^{N}	*T. squamosa*	IIIc(u)	62	4	38131	42.79	1.62	0.6	40-44.5

4.5 Discussion

4.5.1 Comparison with other studies

XRD results for T26 show that it has elevated calcite (2.9%) and is therefore excluded from this study. Figure 4-2 shows a comparison of mean ^{14}C age results derived from this study compared with ^{14}C and U/Th dates from derived from corals collected from the same terraces presented in Yokoyama *et al.* (2000). Mean uncalibrated radiocarbon ages for both reefs are consistent with uncalibrated radiocarbon ages obtained from corals from terrace IIa and IIIc. The standard deviation of ^{14}C ages from this study is smaller in both cases than results from Yokoyama *et al.* (2000).

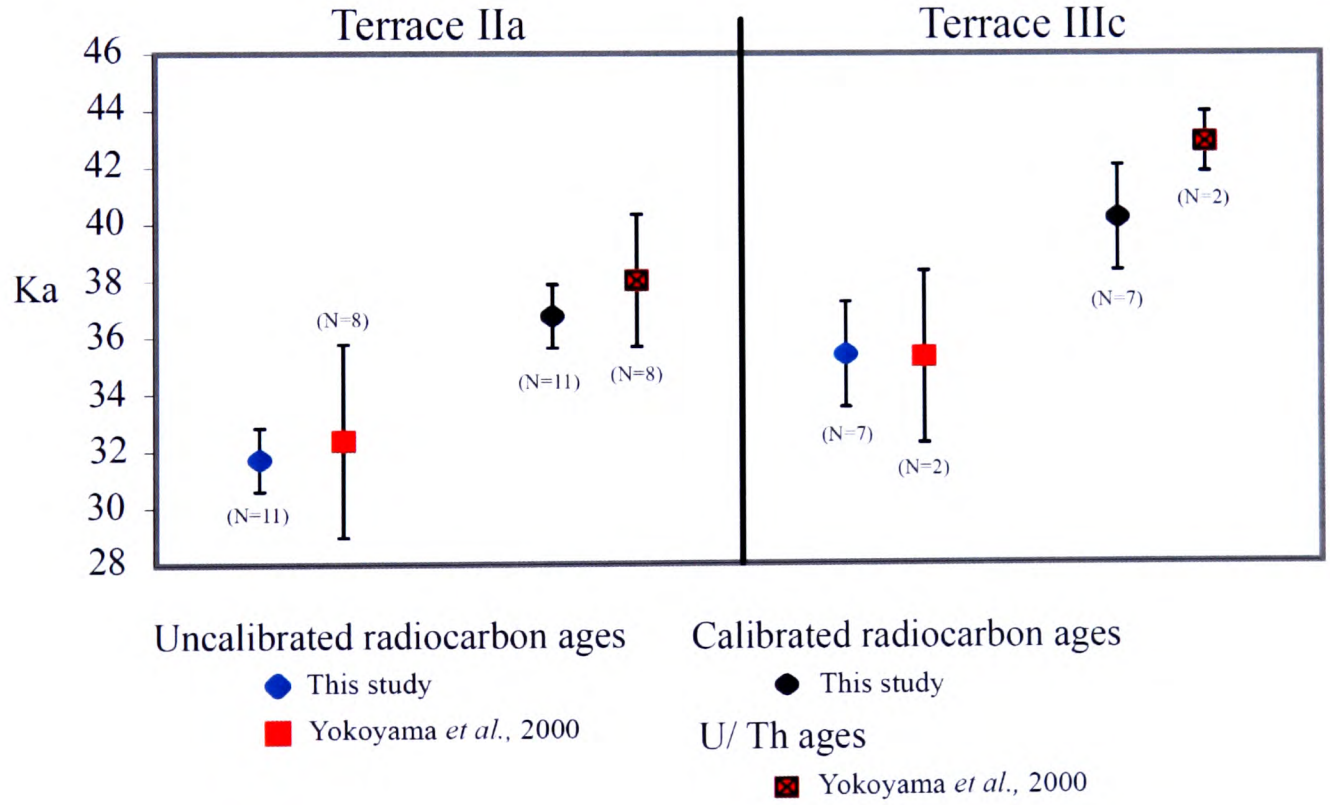

Figure 4-2 Comparing the mean age results from this study with Yokoyama *et al.*, (2000). Bars show the standard deviation in results. The uncalibrated ^{14}C dates from this study are the same as those published by Yokoyama *et al.*, 2000 (no calibrated results published in this paper) and the calibrated ^{14}C dates are similar to the U/ Th dates reported in Yokoyama *et al.* (2000)

Despite cleaning samples Yokoyama *et al.*, (2000) do use some corals with calcite content of up to 2.9% which indicatex slightly higher degree of diagenetic material, which could account for greater variability in ages derived from corals.

Calibrated radiocarbon ages from this study are consistently younger than coral U/Th ages presented in Yokoyama *et al.* (2002) and other studies (see Table 4-2). This is not easy to explain since the calibration curve used here (Fairbanks *et al.*, 2005) is based upon paired measurements of ^{14}C and U/Th in corals, though it does not include samples from Papua New Guinea. Yokoyama *et al.* (2000) suggest that younger radiocarbon ages may be caused by fluctuations in the thermohaline circulation (THC), where the slow down or cessation of the THC during climatic events such as the Heinrich Events causes an excess of atmospheric ^{14}C which would otherwise be delivered to the deep ocean by the THC. This explanation would appear to be account for the younger ages reported from terrace IIa, which is thought to be coeval with Heinrich Event 4 (Chappell, 2002), but does not account for younger than expected radiocarbon ages seen in terrace IIIc which are not associated with any Heinrich Event. Another possibility is that there is contamination by younger carbon, however extremely low calcite values and the small range of ages suggests that this has not occurred.

	Mean age (ka)	
Source	Terrace IIa	Terrace IIIc
Cal. ^{14}C *Tridacna* (this study)	37.9 (*n=11*)	40.3 (*n=7*)
U/Th coral (Yokoyama *et al.*, 2000)	38.0 (*n=8*)	43.0 (*n=2*)
U/Th coral (Tudhope *et al.*, 2001)	38.9 (*n=2*)	n/a
U/ Th coral (Chappell *et al.*, 1996a)	39.6 (*n=3*)	43.9 (*n=1*)

Table 4-2 Showing mean ages of Huon Terraces IIa and IIIc from calibrated ^{14}C ages from *Tridacna* (this study) and published U/Th ages from corals.

In conclusion, the mean ages derived from the *Tridacna* sp. are consistent with previously published coral radiocarbon data, though younger than U/ Th ages for the same terraces. The spread of the radiocarbon ages is smaller than those reported for

corals in Yokoyama *et al.* (2000) for the same terraces. This could be attributed to lower susceptibility of infiltration by younger or older carbon due to the denser shell of *Tridacna* sp. as suggested by previous studies (Chappell and Polach, 1972).

4.5.2 Stratigraphic controls on samples within terraces IIIc and IIa

The stratigraphic relationships between different reef terraces should provide a guide with which to evaluate the accuracy of radiocarbon dates. Figure 4-3 shows a close up for the terraces IIa, IIIc (l) and IIIc(u).

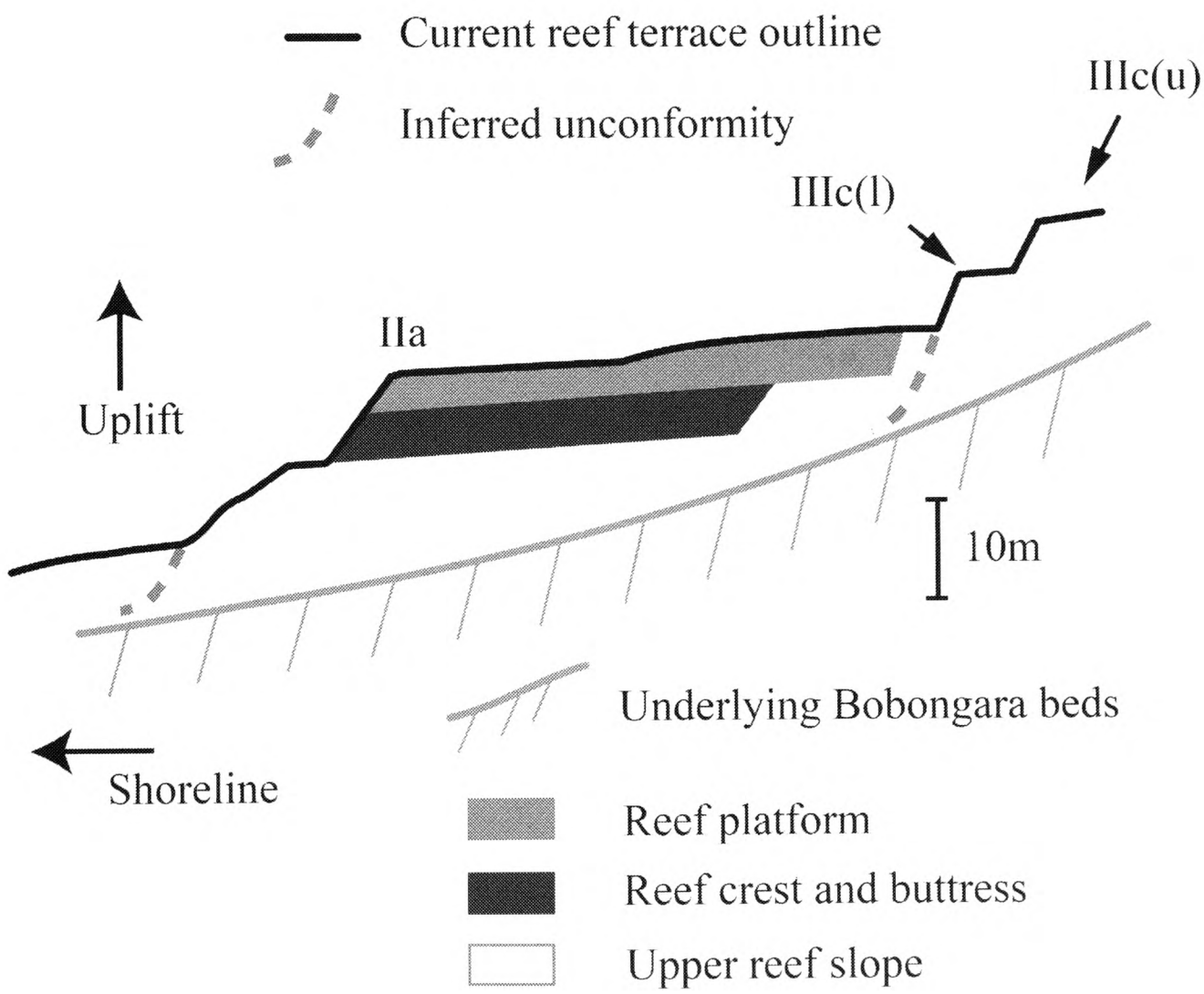

Figure 4-3 Schematic diagram of stratigraphic relationships at Bobongara between terraces IIa and IIIc (l) and (u). Terraces IIIc (u) and (l) are thought to be coseismically generated terraces, formed by metre-scale uplift events preceding terrace IIa. IIa is a large, broad terrace with evidence of reef platform and crest facies formed by accumulation to fill accommodation space created by rapid sea level rise.

Figure 4-4 compares elevation vs. age radiocarbon ages for MIS 3 samples plotted against elevation with each terrace. Dashed lines represent the boundaries of each terrace. Stratigraphic order from oldest to youngest is IIIc(u), IIIc(l) then IIa. There is a small amount of overlap between terraces, however these results show a remarkable degree of consistency of the radiocarbon data and relative dating based upon stratigraphic position with older samples at the base of the reef units and younger samples near the top. Excluding sample T26 for the reasons stated above, calibrated radiocarbon dates obtained from terrace IIa range between 35.8 and 38.8 ka with a total age range for this terrace of 3 ka. The ages of the IIIc terraces range between 38.2 and 42.8 ka. There is a very small degree of overlap between the early samples from terrace IIa and later samples from terrace IIIc(l), though considering the uncertainties affecting radiocarbon ages at this time period the results are remarkably consistent with the reefs stratigraphic position.

The samples that were collected *ex situ* are all consistently younger than the terraces upon which they were found. It is possible, but not likely, that they have been shifted up slope. A more plausible explanation is that they represent the last episode of reef building and have since been eroded by to sub-aerial dissolution of the more porous coral by the high degree of precipitation at Huon Peninsula or due to marine erosion as the terraces were uplifted. It can be hypothesized that the *ex situ* samples represent the last phase of reef growth

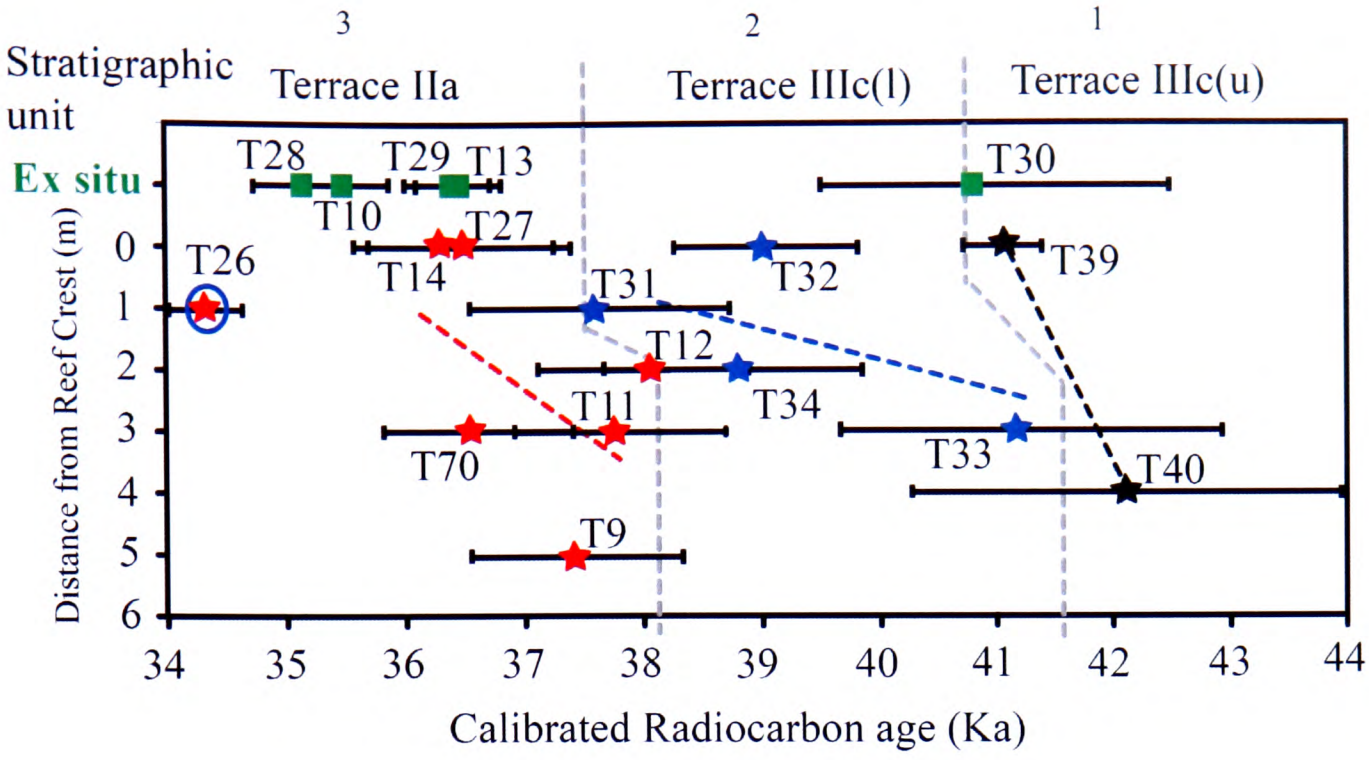

Figure 4-4 The relationship between calibrated radiocarbon age and distance from Reef terrace crest. Terraces are colour coded – IIa is red, IIIc(l) is blue and IIIc(u). *Ex situ* samples are labelled in green. Dashed lines define individual terraces. T26 is shown, though this sample was found to contain elevated levels of calcite in the inner layer (2.9% as opposed to an average of 0.5%).

4.5.3 Models of reef growth and terrace formation

There are several models of how reef terraces are formed under a relative sea level rise that is thought to cause the formation of the terraces. These can be defined as "keep up", "catch up" "give up" and "pack up" (Neumann and Macintyre, 1985 and Esat and Yokoyama, 2006). Reefs are able to respond to a sea level rise by either growing fast enough to keep pace with the sea surface (keep up), or lagging behind the sea surface, but continue growing so that they eventually reach the surface when sea level rise slows or stops (catch up). If sea level rise is sufficiently fast they will stop growing and be drowned (give up).

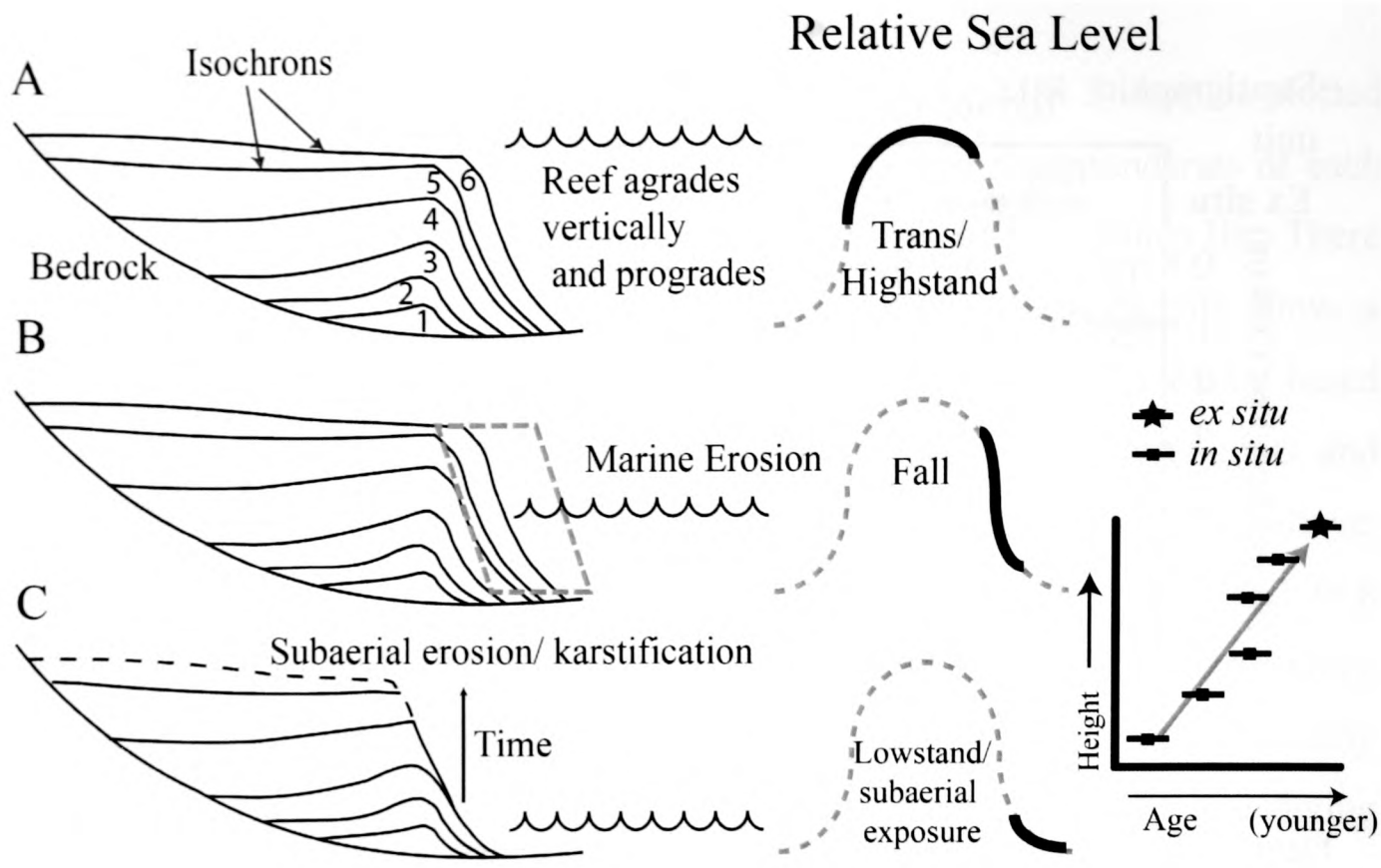

Figure 4-5 Model of reef terrace formation based upon Kennedy and Woodroffe Model A ("Keep up" or "Catch Up" mode) from Kennedy and Woodroffe (2002) and including a marine erosion component from Paulay and McEdwards (1990) to produce the stepped terrace morphology. Black Lines represent lines of equivalent time (Isochrons with arbitrary timescale). A: Reef grows to fills accommodation space during relative sea level transgression. B: Face of reef is removed due to marine erosion during relative sea level fall. C: After sea level fall the face of terrace reveals older reef material. Thus, samples collected from increasing depth in the face of the reef terrace should be relatively older than material above. Note that the oldest part of the reef is likely to be buried.

Keep up and catch up modes of reef growth will result in terraces where older material collected from the face of the terrace will be at a greater distance from the top of the terrace. This is shown in Figure 4-5. The reef progrades when accommodation space becomes restricted due to a relative sea level still stand (Kennedy and Woodroffe, 2002). With the end of the eustatic sea level rise, and subsequent high stand, relative sea level at Bobongara will fall due to high uplift rates and the terraces are raised above sea level. During this regression wave action then erodes the face of the terraces, producing a stepped shape, and finally subaerially erosion removes the top part of the reef surface (Paulay and McEdward, 1990).

Rates of marine and subaerial erosion are not easy to quantify here. Estimates of subaerial erosion of around 0.7 to 0.14 m ky^{-1} for the Great Barrier Reef (Marshall and Davies, 1984) would produce a loss of approximately 5m from the surface of terrace IIa. This amount of erosion is unlikely as the older terraces would be lost completely, however it is assumed that the top surface of the terrace is lost due to some subaerial erosion and the constant exposure of the terraces for +30 ka. The face of the terrace is eroded during relative sea level fall, though again, the rate at which this occurs is difficult to quantify. Paulay and McEdward (1990) suggest rates of between 0 and 4m ky^{-1} depending on whether terraces are on exposed coasts or sheltered ones.

The model described above is supported by two observations: 1) *ex situ* samples that were located on the surface of each terrace were found to be younger than the *Tridacna* sp. found within each terrace. If it is assumed that these samples have not been transported uphill, this implies that they have been eroded from the final stage of terrace growth. 2) The general trend within the terraces is that younger samples were found nearer the reef crest.

The results presented here, whilst not conclusive, tend to support a "keep up" or "catch up" model as there is a general correspondence between distance from reef crest and age (see Figure 4-4). The "keep up" mode of growth for terraces IIa for is assumed for two other reasons. Firstly, investigations of the growth pattern in the Holocene reef confirm this type of keep up or catch up growth. Secondly, the morphology of terrace IIa at Bobongara is consistent with it being a "keep up" type reef (Chappell 2002). This is because the terrace is broad (30-40 m wide) and relatively horizontal with a thick accumulation of shallow water coral facies (Chappell *et al.*, 1996a and Chappell 2002), which implies that it was able to keep pace with sea level such that lack of accommodation space causes it to prograde.

One of the implications of the keep up growth model is that vertical aggradation of terrace IIa can keep pace with sea level change. The maximum estimations for sea

level rise coeval with the growth of terrace IIa is ≈ 30m based upon sea level reconstructions from the Red Sea (Siddall *et al.*, 2003 and Arz *et al.*, 2007). The fastest vertical accretion of reef material seen at Huon Peninsula has been calculated as 10m ka^{-1} based upon U/ Th dating of corals in the post glacial reef (Edwards *et al.*, 1993). If terrace IIa is able to keep pace with sea level rise then it should take 3 ky for 30m of sea level to occur. The actual time will be shorter as the high rate of uplift at Huon will reduce the accommodation space over this time by 3.2 m ka^{-1} due to local uplift. We can estimate a minimum of 2 ka for the sea level rise to occur. This is roughly the duration of the stadial events associated with Heinrich Events.

Temporal relationship of samples to eustatic sea level rise

Based upon the excellent consistency of the radiocarbon dates and assuming a "keep up" type growth pattern for the MIS3 reef terraces, a temporal relationship between samples of *Tridacna* sp. collected from terrace IIa and the large eustatic sea level rise that is associated with terrace IIa can be suggested. Samples from the IIIc reefs are stratigraphically above IIa and can be confidentially placed before the sea level rise. There is likely to be a gap in sampling, though it is not obvious from the radiocarbon results as the lowstand that precedes the initiation of terrace IIa is buried below younger reef material. *In situ* samples grew during or near the end of the sea level rise. Finally it is proposed that the *ex situ* samples represent the final stage of terrace growth which has been subsequentially eroded due to marine or subaerial erosion. Figure 4-6 shows the proposed temporal relationship.

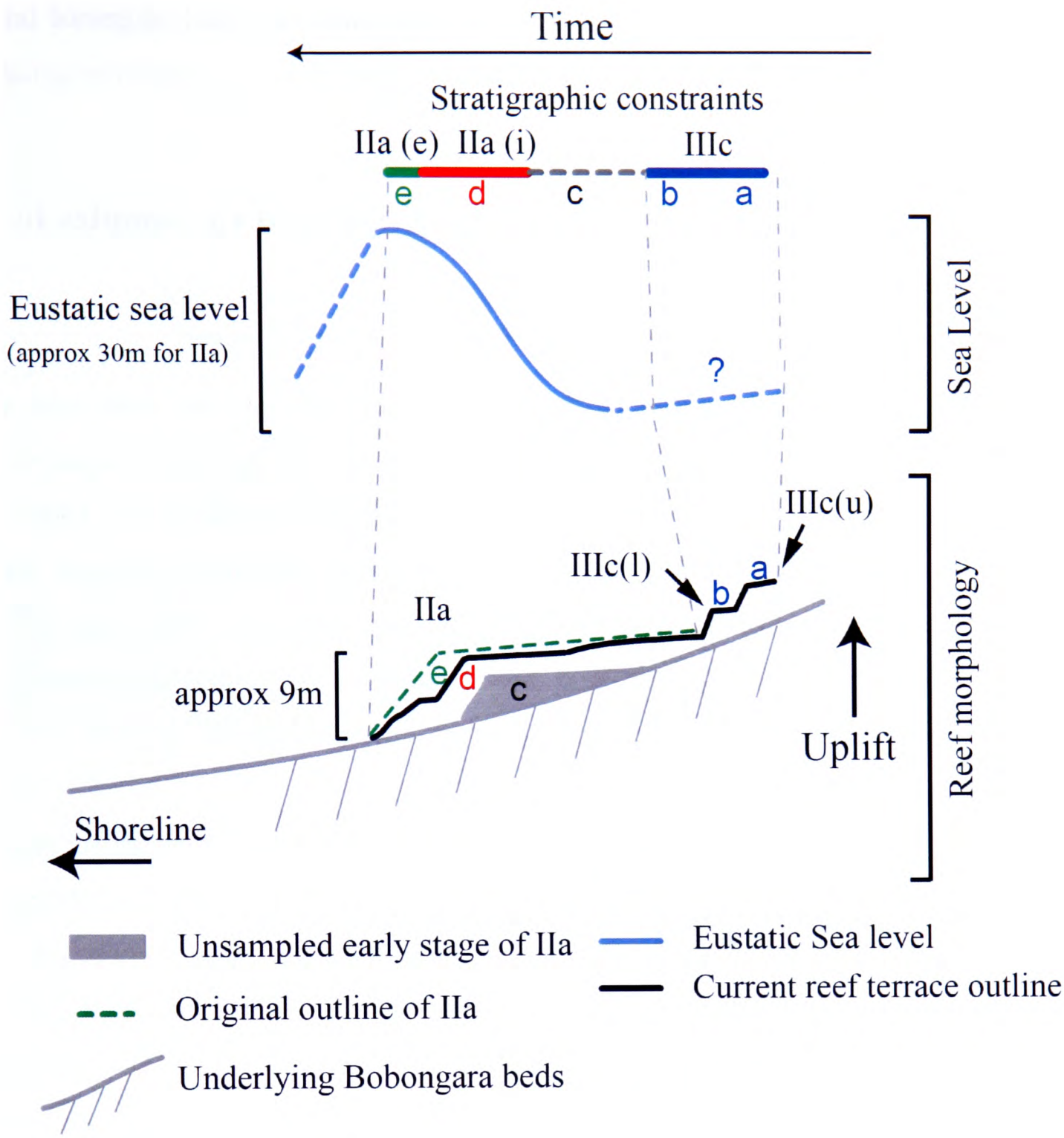

Figure 4-6 Proposed relationship of samples to sea level rise based upon stratigraphic controls. Terraces IIIc(u) and IIIc(l) are minor terraces which are produced either by small rise in eustatic sea level or coseismic events (Chappell *et al.*, 1996a) superimposed on a relative sea level fall at Huon Peninsula. IIIc are emplaced prior to the sea level rise associated with IIa. There is likely to be a hiatus in the record (grey dashed line) as samples at the base of IIa are not accessible. As the top surface of IIa is likely to have been eroded away, it is proposed that the *in situ* samples (marked in red – IIa(i)) were emplaced during the majority if the sea level rise and placing the *ex situ* samples (marked as green line – IIa(e)) toward the end of the sea level rise.

If this hypothesis is correct, it is possible to collect samples that precede the sea level lowstand before the initiation of the sea level excursion responsible for terrace IIa (terraces IIIc) and during the later part of the transgression (*in situ* samples from

terrace IIa). *Ex situ* samples are likely to come from the final stages of terrace growth associated with the sea level highstand.

4.6 Proposed temporal relationship of *Tridacna* sp. samples to sea level excursion c38 to 40 ka

One of the aims of this project is to try and investigate possible millennial scale climate correlatives between the Northern Hemisphere, other millennial scale records and the WPWP. Studies of uplifted reef terraces (Chappell *et al.*, 1996a and Yokoyama *et al.*, 2001), $\delta^{18}O$ of benthic foraminifera off the Portuguese margin (Shackleton *et al.*, 2000) and in the Red Sea (and Arz *et al.*, 2007) and $\delta^{18}O$ of planktonic foraminifera in the Red Sea (Siddall *et al.*, 2003) have uncovered millennial scale oscillations in eustatic sea level during MIS 3.

Despite uncertainties in dating, these eustatic sea level changes must be globally synchronous, therefore it should be possible to use these events for correlation between timeseries. Now that a temporal framework has been proposed for the samples associated with the large rise in sea level which is associated with the production of reef terrace IIa, the evidence for the timing of this sea level excursion in relation to North Atlantic climate will be explored by looking closely at some of the evidence for the timing of this sea level excursion.

Figure 4-7 shows a comparison of the sea level proxies mentioned above in relation to air temperature over Greenland as shown in the GRIP ice core record which is often used as the basis for temporal comparision. It can be seen that whilst all of the records agree on there being a sea level excursion at around this time, there are a range of scenarios regarding the precise relationship between sea level rise and Greenland stadial depending on dating technique. Siddall *et al.*, (2003) based their timescale on AMS radiocarbon dates and correlation with Antarctic $\delta^{18}O$ records. Chappell (2002) established dates for sea level maxima using U/Th dates from corals

and a reef growth model (as outlined above). Arz *et al.*, (2007) used radiocarbon dating of foraminifera and magnetic palaeointensity to apply a chronology.

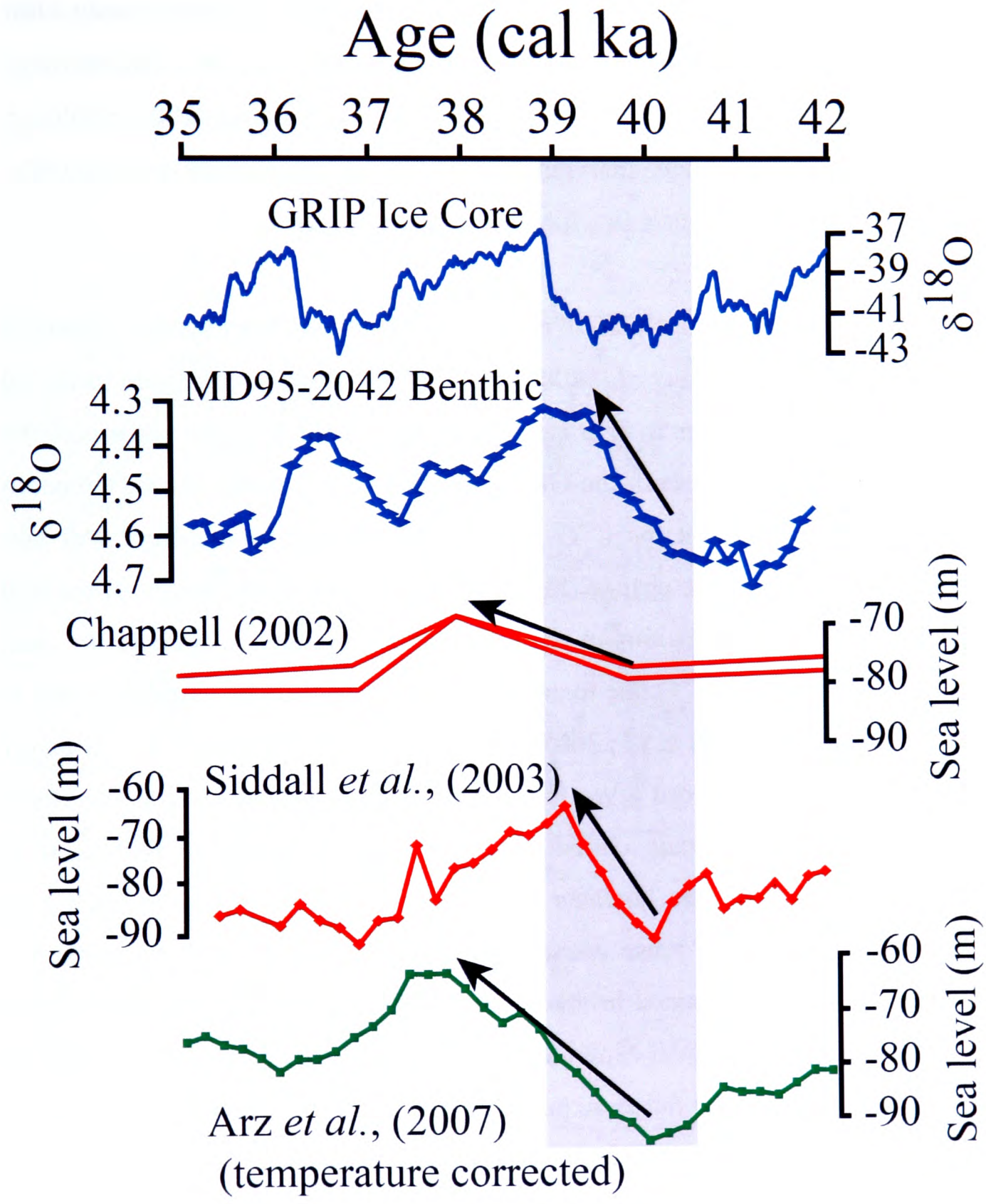

Figure 4-7 Showing the temporal relationships between several proxies for sea level and the GRIP $\delta^{18}O$ ice core record from Greenland. Arrows show inferred positions of sea level excursion that caused the production of terrace IIa. MD95-2042 is the $\delta^{18}O$ record from benthic foraminifera from the Iberian margin published in Shackleton *et al.*, (2000) on timescale shown in Shackleton *et al.*, (2004). Grey box shows the timing of the Greenland stadial associated with Heinrich event 4.

Further supporting evidence for relative timing of sea level minimum and maximum was obtained from dolomite concentration in a sediment core from the Somali margin that reflect changes in the amount of tidal flat that is exposed (Ivanochko, unpublished PhD thesis, 2005). This is correlated with millennial-scale climatic variation in monsoon strength which is strongly related to North Atlantic climate change (Altabet *et al.,* 2002; Burns *et al.*, 2003; Ivanochko *et al.*, 2005; Shultz *et al.*, 1998). This record shows that rapid sea level excursions are coeval with the Northern Hemisphere stadials in which Heinrich events occur.

The best chronological constraint is upon the $\delta^{18}O$ record from benthic foraminifera reported on in Shackleton *et al.*, (2000) and (2004) as this is correlated to the GRIP record by relating changes in $\delta^{18}0$ in a planktonic record from the same core which represents SST and $\delta^{18}O$ from the GRIP core, which is a proxy for air temperature. Whilst it is probable that the $\delta^{18}O$ record from benthic foraminifera will have a component of temperature change (Shackleton *et al.*, 2004), the height of the peak is approximately 0.3 to a maximum of 0.4‰. It is possible to estimate the relative change in global ocean $\delta^{18}O$ due to continental ice reduction by assuming a sea level rise of 30m (from Siddall *et al.*, 2003 and Arz, *et al.*, 2007) as 0.25‰. It therefore seems likely that this record gives the best guide to tying sea level to the Northern Hemisphere millennial scale climate and in consequence, global millennial scale climate variation. It does however raise the issue of why there is such a large discrepancy in dating of these events and the radiocarbon dates. It is likely that many of the samples obtained in this study are from later in the sea level excursion due to the reef growth model explained above; however it has also been noted above that radiocarbon dates for this time period appear to give anomalous dates, and U/Th dating of these terraces give slightly older dates.

In conclusion, much of the evidence for the timing of millennial scale eustatic sea level rise in MIS3 indicates that they occured during the Northern Hemisphere stadials, though the actual highstand may occur at the end of the Bond cycle and be coeval with the subsequent interstadial. Since the larger terraces were produced during the rapid sea level excursions, which created the accommodation space for

them to grow, only the final part of the terrace will have been emplaced during the following interstadial. Based upon the observations above, it is reasonable to propose a model correlation for correlation of *in situ Tridacna* sp. and Northern Hemisphere climate records taking advantage of the proposal that benthic foraminiferal $\delta^{18}O$ is controlled at least partly by sea level and the detailed correlation of Greenland temperature records and sediment cores from the Iberian Margin (Shackleton *et al.*, 2000) shown in Figure 4-8.

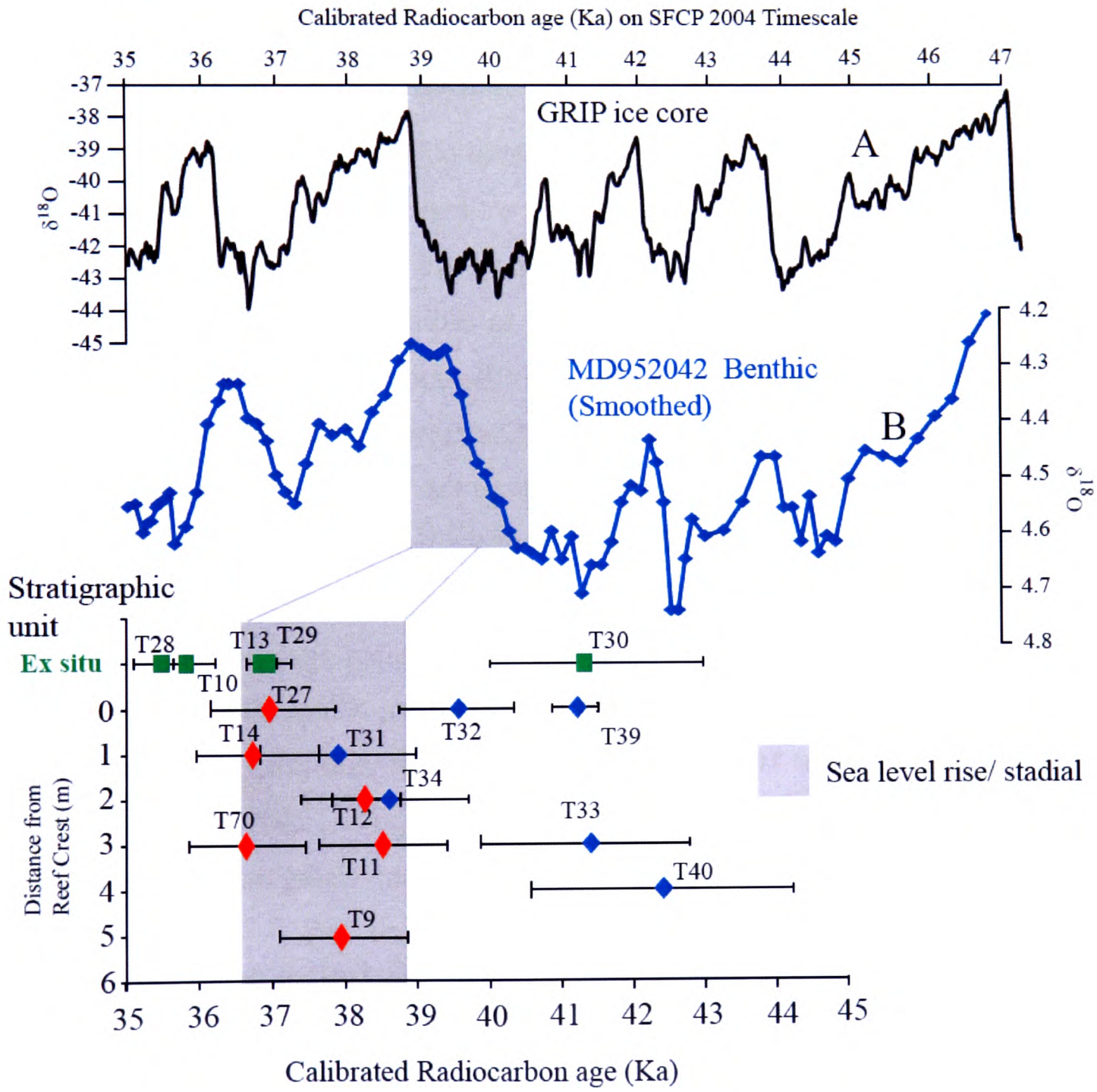

Figure 4-8 Shows chronology for terraces IIa, IIIc(l) and IIIc(u) and proposed correlation with benthic oxygen isotopic record from the Iberian margin. *Ex situ* samples are green squares. *In situ* samples from IIa are red diamonds, and *in situ* samples from IIIc are blue diamonds. Basis of correlation is the assumption that some $\delta^{18}O$ benthic component is related to continental ice volume/ sea level change (Shackleton *et al.*, 2000). Shackleton *et al.* (2004) timescale. Siddall *et al.* (2003) sea level record is placed on the same timescale based upon correlation with Byrd Antarctic record.

The *in situ Tridacna* sp. from IIa are inferred to be from the Northern Hemisphere stadial associated with Heinrich event 4. All other samples are thought to precede this stadial and can be considered to have grown during a "non-stadial" background climate. It is possible that the *ex situ* samples are from the late stage of sea level excursion and therefore may be associated with a Northern Hemisphere interstadial.

4.7 Building a chronology for timescales beyond radiocarbon dating

To derive a chronology for the fossil material collected from reefs that are too old to be dated using radiocarbon methods, estimates of age were based upon the chronology presented in Chappell (2002). If we know a reasonable rate of vertical accumulation for the reefs, and are able to estimate the age of the reef crest from samples within the reef, then it is a relatively simple matter to multiply the depth of the sample in the reef (**d**) by the rate of vertical accumulation of the reef (**r**) and subtract this figure from the estimated age of the highstand associated with the crest (**a**). Chappell (2002) models the growth of the reef terraces under several boundary conditions and is able to present reasonable figures for **r**, **a** and **d** is known from field measurements. Based on this analysis estimated ages (**a**) are: IIIb = 44.5 ka, IIIa(l) = 49 ka, IIIa(m) = 52 ka and IIIa(u) = 60 ka. Chappell (2002) finds the best estimate of **r** of 4m/ 1000 years which agrees well with other measurements of the rate of reef growth in the Holocene reef (Edinger *et al.*, 2007). This approach can only work for samples that are found in life position. Using this data the chronology for the last glacial period is now complete (see Figure 4-9)

Sample	*Species*	Reef	Dist. From crest (m)	Elevation	Extrapolated age
T24	*T. crocea*	IIIb	2	86	44.9
T37	*H. hippopus*	IIIb	7	79	46.0
T23	*T. crocea*	IIIa(l)	0	107	49.0
T41	*T. crocea*	IIIa(l)	8	99	50.7
T42	*T. crocea*	IIIa(m)	1	117	52.2
T15	*T. gigas*	IIIa(u)	0	138	60.0
T22	*T. gigas*	IIIa(u)	0	138	60.0
T44	*T. maxima*	IIIa(u)	0	138	60.0
T6	*T. derasa*	IIIa(u)	3	135	60.7
T38	*T. crocea*	IIIa(u)	4	134	60.9

Table 4-3 Extrapolated ages for *Tridacna* sp. older than 45 Ka

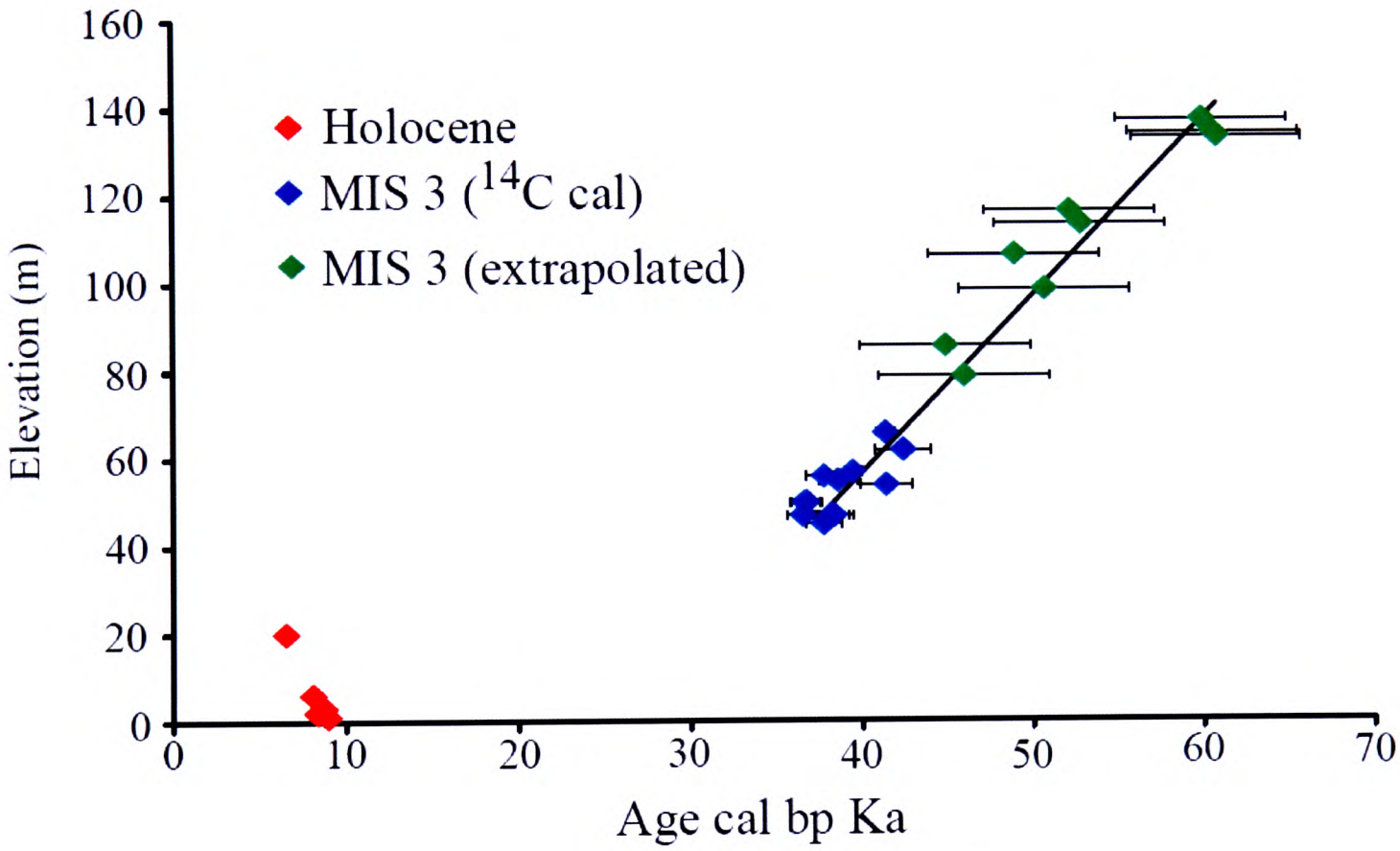

Figure 4-9 Chronology for Holocene and MIS 3 *Tridacna* sp. from Huon Peninsula calibrated radiocarbon ages versus elevation (note that *ex situ* samples are not included as elevation is unknown).

4.8 Producing a sea level curve from fossil *Tridacna* sp. samples

Sea level curves have been produced using isotopic measurements of deep sea cores (e.g. Shackleton, 1987 and Waelbroeck *et al.*, 2002), modelling isotopic changes in

planktonic foraminifera in the Red Sea (Siddall *et al.*, 2003) and using by direct dating of uplifted coral reefs where the current elevation and relative tectonic movement of the area is known (e.g. Chappell, 1974; Chappell *et al.*, 1996a; Chappell 2002; Cutler *et al.*, 2003).

Once a chronology has been established it is reasonable to use this data to estimate a sea level curve. It should be noted that since the method for extrapolating the ages of the samples that predate 43 ka uses the estimates for sea level peaks presented in Chappell (2002) these data points must fit onto the same sea level reconstruction.

To calculate the sea level at which a given sample grew the age of the sample is multiplied by the rate of uplift at the location from which it was collected (3.1-3.3 m ka^{-1} at Bobongara Yokoyama *et al.*, 2001) and this figure subtracted from its current elevation. Finally, an adjustment is made for the water depth at which the sample was thought to have grown. This was taken from estimates of water depth/ reef facies from Chappell *et al.*, (1996a) (0-3m for reef platform, 2-5m for reef crest and 5-15m for reef slope). Uncertainty was calculated using upper and lower bounds of dating uncertainty, uplift rates and depth of the sample within each terrace. However since the age of samples too old to be radiocarbon dated have been effectively extrapolated to fit the Chappell (2002) sea level curve, dating uncertainty was difficult to estimate. Results of this can be seen in Figure 4-10. Uncertainty for the pre-43 ka results is large as a general estimate of 5 ky was applied for sea level reconstruction purposes. This reflects difficulties in estimating errors for this relative chronology.

Figure 4-10 compares the sea level reconstruction derived from this study with the sea level reconstruction from Chappell (2002) and Siddall *et al.*, (2003) data from the Red Sea.

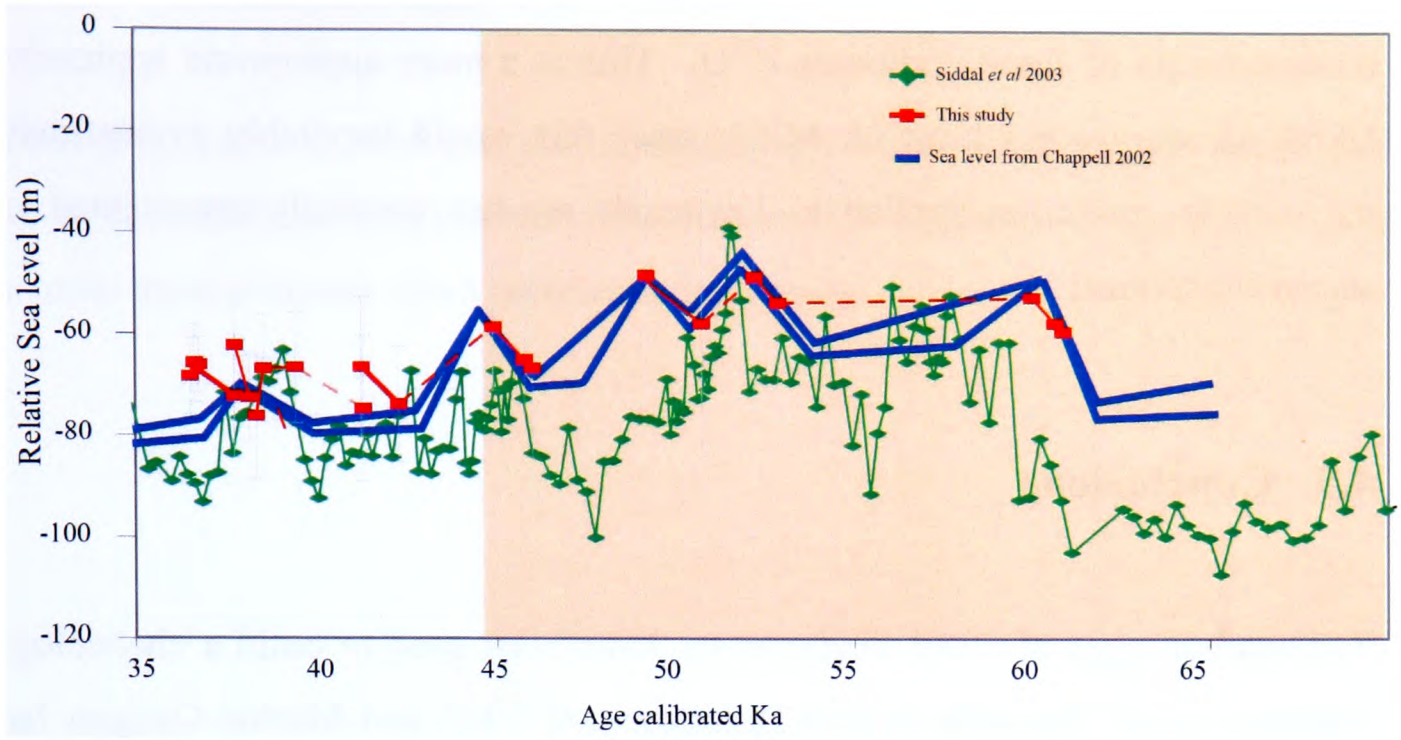

Figure 4-10 A sea level reconstruction calculated from dated *Tridacna* sp. from this study, compared to sea level highstands from Chappell, 2002 and the sea level curve of Siddall *et al.*, (2003). Chronology for pre 43 Ka (shaded area) is based upon estimates of reef age from Chappell (2002), radiocarbon age is used for other samples.

There is generally a very good fit between the two independently derived sea level curves from Chappell (2002) and Siddall *et al.,* (2003) with the height of the sea level peaks within 10-15m of each other, though it is highly likely that Chappell sea level record will underestimate low stands since the lowstand material will be buried under later highstand reefs. It is important to note that the chronologies for each sea level reconstruction are obtained in different ways. Chappell used a model and existing dates from Huon Peninsula to interpolate a sea level that best fits the existing morphology based upon certain rules of reef growth. Siddall *et al.,* (2003) correlated their record to Antarctic temperature records (Byrd and Vostock). An important implication of the fit of these and other sea level curves is that despite differences in dating and the magnitude of the sea level excursions, individual excursions can be correlated with some confidence.

The only sea level peak that is independently dated in this study is the peak associated with terrace IIa at approximately 37-39 ka. The height of the sea level peak that is reconstructed falls within 10m of the other sea level reconstructions.

Producing a sea level curve is extremely useful as it allows an assessment of the isotopic composition of seawater in the past to be calculated and subtracted from measurements of fossil carbonate $\delta^{18}O$. This is a more appropriate approach than taking an average sea level for MIS3, since this would inevitably overestimate the ice volume correction applied as lowstands are not generally represented in the accessible terraces.

4.9 Conclusions

Radiocarbon ages of fossil *Tridacna* sp. have been used to build a chronology for *Tridacna* sp. in the early to mid Holocene (~9-7 ka) and Marine Oxygen Isotope Stage (MIS) 3 (between ≈ 35 and 43 ka) reef terraces from the Huon Peninsula. In MIS3 terraces the radiocarbon ages between discrete reefs barely overlap giving confidence in the radiocarbon ages even though they are measured near to the limit at which radiocarbon dating can be used. This is also confirmed by observations of % calcite, suggesting that there is no significant diagenetic alteration to the *Tridacna* sp. shell material. The MIS 3 data are in good agreement with previous radiocarbon dating performed on corals, but calibrated ages are significantly younger than U/ Th from corals in the same reefs. It has been suggested that this could be an effect of changes in reservoir ages caused by variations in the production of North Atlantic Deep Water.

A detailed study of samples derived from terraces IIa and IIIc was carried out using radiocarbon dates and stratigraphic information. Using proxy records for eustatic sea level, a proposed relationship between these fossil samples and North Atlantic millennial scale climate events is shown. Samples retrieved *in situ* from terrace IIa are shown to be coeval with Northern Hemisphere stadial occurring between Greenland Interstadials 8 and 9.

For reef terraces at a greater than 43 cal ka age, a chronology was built for samples based upon their stratigraphic location. This was achieved using a combination of

age of highstands associated with each reef crest by Chappell (2002) and taking account of the sample's depth in the reef terraces.

A sea level curve is produced that accurately placed the *Tridacna* sp. which can be use to accurately predict the ice volume correction that must be applied to oxygen isotopic measurements when reconstructing climate.

References

Aharon, P., Chappell J. and Compston, W. (1980), Stable Isotope and Sea-Level Data from New-Guinea Supports Antarctic Ice-Surge Theory of Ice Ages, *Nature*, **283**, 549-651

Aharon, P. (1983), 140,000-Yr Isotope Climatic Record from Raised Coral Reefs in New-Guinea., *Nature*, **304**, 720-723

Aharon, P., and J. Chappell (1986), Oxygen Isotopes, Sea-Level Changes and the Temperature History of a Coral-Reef Environment in New-Guinea over the Last 105 Years, *Palaeogeography Palaeoclimatology Palaeoecology,* **56,** 337-379

Altabet, M.A., Higgins, M.J. and D.W. Murray, (2002), The effects of millennial-scale changes in Arabian Sea denitrification on atmospheric CO2, *Nature,* **415** 159–162

Arz, H. W., Lamy, F. Ganopolski, A. Nowaczyk, N. and Patzold, J. (2007), Dominant Northern Hemisphere climate control over millennial scale glacial sea-level variability, *Quaternary Science Reviews*, **26**, 312-321

Bard, E., Rostek, F. and G. Menot-Combes. (2004), A Better Radiocarbon Clock *Science,* **303,** 178-179

Bloom, A. L., Broecker, W.S., Chappell, J. Matthews, R.K and K.J. Mesolla. (1974), Quaternary Sea-Level Fluctuations on a Tectonic Coast - New Th- 230-U-234 Dates from Huon-Peninsula, New-Guinea, *Quaternary Research,* **4**, 185-205

Bond, G.; Heinrich, H., Broecker, W., Labeyrie, L., McManus, J., Andrews, J., Huon, S., Jantschik, R., Clasen, S., Simet, C., Tedesco, K., Klas, M., Bonani, G., and S. Ivy (1992), Evidence for massive discharges of icebergs into the North Atlantic ocean during the last glacial period, *Nature,* **360**, 245–249

Broecker, W.S. (1963), a preliminary evaluation of uranium series inequilibrium as a tool for absolute age measurement on marine carbonates. *Journal of Geophysical Research,* **68**, 1217

Burns, S.J., Fleitmann, D. Matter, A., Kramers, J. and A.A. Al-Subbary, (2003), Indian Ocean climate and an absolute chronology over Dansgaard/Oeschger events 9 to 13, *Science,* **301**, 1365– 1367

Chappell, J. and Polach, H. A. (1972), some of the effects of partial re-crystallisation on ^{14}C on dating Late Pleistocene molluscs and corals. *Quaternary Research*, **2**, 244-252

Chappell, J., and H. A. Polach, (1976), Holocene sea level change and coral reef growth at Huon Peninsula, Papua New Guinea, *Geological Society of America Bulletin,* **87**, 235-240

Chappell, J. (1974), Geology of Coral Terraces, Huon-Peninsula, New-Guinea - Study of Quaternary Tectonic Movements and Sea-Level Changes, *Geological Society of America Bulletin*, **85**, 553-570

Chappell, J., and N. J. Shackleton (1986), Oxygen Isotopes and Sea-Level, *Nature*, **324**, 137-140

Chappell, J., Omura, A., Esat, T., MuCulloch, M., Pandolfi, J., Ota, Y., and B. Pillans. (1996a), Reconciliation of late Quaternary sea levels derived from coral terraces at Huon Peninsula with deep sea oxygen isotope records, *Earth and Planetary Science Letters,* **141**, 227-246

Chappell, J. Ota, Y. and K. Berryman. (1996b), Late quaternary coseismic uplift history of Huon Peninsula, Papua New Guinea, *Quaternary Science Reviews*, **15**, 7-22

Chappell, J. (2002), Sea level changes forced ice breakouts in the Last Glacial cycle: new results from coral terraces, *Quaternary Science Reviews*, **21**, 1229-1240

Chiu, T.-C., Fairbanks, R.G., Mortlock, R.A., Bloom, A.L., (2005), Extending the radiocarbon calibration beyond 26,000 years before present using fossil corals. *Quaternary Science Reviews,* **24**, 1797-1808

Cutler, K.B. Edwards, R.L., Taylor, F.W., Cheng, H., Adkins, J., Gallup, C.D. Cutler, P.M., Burr, G.S. and Bloom, A.L. (2003), Rapid sea-level fall and deep-ocean temperature change since the last interglacial period, *Earth and Planetary Science Letters,* **206**, 253-271

de Vries, H., (1958), Variation in concentration of radiocarbon with time and location on Earth, *Proceedings Koninklijke Nederlandse Akademie van Wetenschappen, Series B* **61**, 94–102

de Vries, H., (1959), Measurement and use of natural radiocarbon. In: Abelson, P.H. (Ed.), *Researches in Geochemistry*. Wiley, New York, pp. 169–189.

Edinger, E. N., Burr.G. S. Pandolfi, J.M., Ortiz, J.C. (2007), Age accuracy and resolution of quaternary corals used as proxies for sea level. *Earth and Planetary Science Letters*, **253**, 37-49

Edwards, R. L., Beck, W., Burr, G.S., Donahue, D.J., Chappell, J., Bloom, A.L., Druffell, E.R.M. and F.W. Taylor (1993), A Large Drop in Atmospheric C-14/C-12 and Reduced Melting in the Younger Dryas, Documented with Th-230 Ages of Corals, *Science*, **260**, 982-986

Elliot, M., Labeyrie, L., Bond, B., Cortijo, E., Turon, J-L., Tisnerat, N. and J-C Duplessy (1998), Millennial-scale iceberg discharges in the Irminger Basin during

the last glacial period: Relationship with the Heinrich events and environmental settings, *Paleoceanography*, **13**, 433-446

Ellassar, W., Ney, E.P., Winkler, J.R., (1956), Cosmic-ray intensity and geomagnetism, *Nature,* **178**, 1226–1227

Esat, T. and Y. Yokoyama (2006), Growth patterns of the last ice age coral terraces at Huon Peninsula. *Global and Planetary Change*, **54**, 216-224

Fairbanks, R. G., Mortlock, R.A. Chiu, T-C., Cao, L., Kaplan, A., Guilderson, T. P., Fairbanks, T.W., Bloom, A.L., Grootes, P.M. and M-J, Nadeau (2005), Radiocarbon calibration curve spanning 0 to 50,000 years BP based on paired Th-230/U-234/U-238 and C-14 dates on pristine corals, *Quaternary Science Reviews*, **24**, 1781-1796

Fairbridge. R.W. (1950), Recent and Pleistocene coral reefs of Australia. *Journal of Geology*, **58**, 330-401

Guyodo, Y., Valet, J.-P., (1999), Global changes in intensity of the earth's magnetic field during the past 800 kyr, *Nature,* **399**, 249–252

Heinrich, H. (1988), Origin and Consequences of Cyclic Ice Rafting in the Northeast Atlantic-Ocean During the Past 130,000 Years, *Quaternary Research Quaternary Research,* **29**, 142-152

Hemming, S. (2004), Heinrich Events: massive late Pleistocene detritus layers of the North Atlantic and their global climatic imprint, *Review of Geophysics*, **42**, RG1005

Hughen, K., Lehman, S., Southon, J., Overpeck, J., Marchal, O., Herring, C., J. Turnbull, (2004), C-14 activity and global carbon cycle changes over the past 50,000 years, *Science*, **303**, 202-207

Ivanochko, T. (2005), Sub-Orbital Scale variations in the Intensity of the Arabian Sea Monsoon. *Thesis. University of Edinburgh. Edinburgh.* pp 230

Ivanochko, T.S., Ganeshram, R.S., Brummer, G.-J.A., Ganssen, G., Jung, S.J.A., Moreton S.G. and D. Kroon, (2005), Variations in tropical convection as an amplifier of global climate change at the millennial scale, *Earth Planetary Science Letters,* **235,** 302–314

Kennedy, D. M. and C.D. Woodroffe (2002), Fringing reef growth and morphology: a review, *Earth-Science Reviews,* **57**, 255-277

Marshal, J.F. and Davies, P.J. (1982), Last interglacial reef growth beneath modern reefs in the Southern Great Barrier Reef, *Nature*, **307**, 44-46

McElhinny, M.W., Senanayake, W.E., (1982), Variations in the geomagnetic dipole 1: The past 50000 years. *Journal of Geomagnetism and Geoelectricity,* **34**, 39–51

Neumann, A.C. Macintyre, I.G. (1985), Reef response to sea level rise: keep-up, catch-up, or give-up, *Proceedings of the 5th International Coral Reef Symposium*, **3** 105–111.

Paulay, G., and L. R. McEdward (1990), A simulation of island reef morphology: the effect of sea level fluctuations, growth, subsidence and erosion, *Coral Reefs*, ***9***, 51-62

Polach, H.A., Chappell, J. Lovering J.F. (1969), ANU Radiocarbon date list III. *Radiocarbon*, **11**, 245-252

Porter, S. C., and Z. S. An (1995), Correlation between Climate Events in the North-Atlantic and China During Last Glaciation, *Nature*, **375**, 305-308

Ota, Y., Chappell, J., Kelley, R., Yonekura, N., Matsumoto, E., Nishimura, T., and J. Head. (1993), Holocene coral reef terraces and coseismic uplift of the Huon Peninsula, Papua New Guinea, *Quaternary Science Research,* **40**, 177-188

Reimer, P. J., Baillie, M.G.L., McCormac, G., Reimer, R.W., Bard, E., Beck, J.W., Blackwell, P.G., Buck, C.E., Burr, G., Edwards, R.L., Friedrich, M., Manning, S., Souton, J.R., Stuiver, M., van der Plicht, J., van der Plicht, J., and C.E. Wenheymer (2006), Comment on "Radiocarbon calibration curve spanning 0 to 50,000 years BP based on paired Th-230/U-234/U-238 and C-14 dates on pristine corals" by R.G. Fairbanks et al. (Quaternary Science Reviews 24 (2005) 1781-1796) and "Extending the radiocarbon calibration beyond 26,000 years before present using fossil corals" by T.-C. Chin et al. (Quaternary Science Reviews 24 (2005) 1797-1808), *Quaternary Science Reviews*, **25**, 855-862

Shackleton, N.J. (1987), Oxygen isotopes, ice volume and sea level, *Quaternary Science Reviews*, **6**, 183-190

Shackleton, N.J., Hall, M.A. & Vincent, E. (2000), Phase relationships between Millennial Scale Events 64,000 to 24,000 Years Ago. *Paleoceanography*, **15**, 565-569

Shackleton, N.J., Fairbanks, R.G., Tzu-chien C. and F. Parrenin, (2004), Absolute calibration of the Greenland time scale: implications for Antarctic time scales and for $\Delta^{14}C$, *Quaternary Science Reviews,* **23,** 1513–1522

Schulz, H., von Rad, U. and H. Erlenkeuser, (1998), Correlation between Arabian Sea and Greenland climate oscillations of the past 110,000 years, *Nature,* **393**, 54–57

Siddall, M., Rohling E.J., Almogi-Labin, A., Hembleben, Ch., Meischner, D., Schmelzer, I., and D.A. Smeed. (2003), Sea-level fluctuations during the last glacial cycle, *Nature*, **423**, 853-858

Siddall, M., Smeed, D.A., Hemleben, C., Rohling, E., Schmelzer, I. and W.R. Peltier. (2004), Understanding the Red Sea response to sea level, *Earth and Planetary Science Letters*. **225,** 421-434

Stuiver, M., Quay, P.D., (1980), Changes in atmospheric carbon-14 attributed to a variable Sun, *Science,* **207**, 11–19

Stuiver, M., (1961), Variations in radiocarbon concentration and sunspot activity. *Journal of Geophysical Research,* **66**, 273–276

Stuiver M. and T.F. Braziunas (1993), 14C Ages of Marine Samples to 10,000 BC *Radiocarbon,* **35**, 137-189

Stuiver M. and P.J. Reimer (1993), Extended 14C data base and revised CALIB 3.0 14C Age calibration program, *Radiocarbon,* **35**, 215-230

Swart, P.K. and J.A.E.B. Hubbard (1982), Uranium in Scleractinian Coral Skeletons, *Coral Reefs,* **1**, 13-19

Tatsumoto, M and E.D. Goldberg (1959), Some aspects of the marine geochemistry of uranium, *Geochimica et Cosmochimica Acta,* **17**, 201

Thompson, W. G. and S. J. Goldstein (2005), open system coral ages reveal persistent sub orbital sea level cycles, *Science,* **308**, 401-404

Tudhope, A., W., Chilcott, C.P., McCulloch, M.T., Cook, E.R., Chappell, J. Ellam, R.M., Lea, D., Lough, J.M. and Shimmield, G.B. (2001), Variability in the El Niño - Southern oscillation through a glacial-interglacial cycle, *Science*, **291**, *1511-1517*

Veeh, H. H. and J., Chappell, (1970), Astronomical Theory of Climate Change: Support from New Guinea. *Science*, **167**, 862-865

Waelbroeck C, Labeyrie L, Michel E, Duplessy JC, McManus JF, Lambeck K, Balbon E, and M. Labracherie (2002), Sea-level and deep water temperature changes derived from benthic foraminifera isotopic records, *Quaternary Science Reviews*, **21**, 295-305

Yokoyama, Y., Esat, T., Lambeck, K. and Fifield, K (2000), Last ice age millennial scale climate changes recorded in Huon Peninsula corals, *Radiocarbon*, **42**, 383-401

Yokoyama, Y., Esat, T. and Lameck, K. (2001), Coupled climate and sea level changes deduced from Huon Peninsula coral terraces of the last ice age, *Earth and Planetary Science Letters*, **193**, 579-587

5 Reconstructing Glacial and Holocene environments in the WPWP

The Western Pacific Warm Pool is an area of immense importance to global climate as it provides significant amounts of heat and water vapour and is also the centre of action for the ENSO system. A paucity of high-resolution palaeo-climate records in this area has meant that there are limited data with which to test global or regional tropical Pacific climate models during periods with very different boundary conditions. Such tests are crucial to improve the robustness of climate models.

This chapter reports on stable isotope results that are both seasonally resolved and averaged across the growth bands of fossil samples of the long lived bivalve *Tridacna* sp. collected from uplifted fossil reefs (aged between 6-10 ka and 35-65 ka) at Huon Peninsula. These records can therefore reconstruct the mean state of the WPWP climate and also elucidate subtle changes to the ENSO system.

Using oxygen isotopes averaged across growth bands of *Tridacna* sp. and correcting for continental ice volume temperatures can be extrapolated for the Early Holocene and MIS3. Taking these values at face value a SST of 26.7±0.5°C is calculated for the Early Holocene and 25.6°C±0.9°C MIS3 reefs respectively. Results for MIS3 are within error of previous estimates of SST's and suggestive of a change to the evaporation/ precipitation balance which indicates a mean state which is more "El Niño-like" agreeing well with previous studies. Results for the Early Holocene show a much greater cooling than expected from previous studies, however these results may be interpreted as showing a much reduced precipitation or increased evaporation. This indicates a long term change to an "El Niño-like" mean state during the Early Holocene and which is inconsistent with some proxy studies, but agrees well with modelling studies of long term change in the hydrology of the WPWP.

Seasonally resolved profiles of $\delta^{18}O$ from *Tridacna* sp. showing that ENSO variability was suppressed in the Early Holocene, and suggesting a lower variability during M1S3 than predicted by orbitally forced modelling studies. These results corroborate other seasonally resolved results from corals.

5.1 Introduction

Two approaches may be taken to investigating or explaining changes to the past climate of the tropical Pacific. The mean state of the climate averaged over decades to millennia or changes to the variability of the ENSO system on interannual timescales can be investigated using either models or proxy data. Palaeoproxy data obtained from sediment cores and peat cores from the WPWP region can only provide information that is averaged over 100's to 1000's of years and evidence of past climate in the tropical Pacific derived from such proxies is often expressed in terms of "El Niño-like" or "La Niña-like" referring to modern interannual state as analogues for past climates (e.g. Stott *et al.*, 2002) which can be useful in as terms of reference, and because it has been suggested that El Niño type conditions could persist on longer timescales (Clement *et al.*, 1999). It is also possible however that sustained change to interannual variability would present itself as changes in mean state if for example the strength or frequency of El Niño events were to change (Clement *et al.*, 2000). Conclusions drawn from records that are averaged over longer periods of time may not reflect subtler changes in the Pacific climate, which require seasonally resolved records to be examined.

Interannually resolved records such as those derived from corals, are becoming more common from the Holocene but are still rare from the last glacial period as their porosity makes them susceptible to diagenesis. Therefore, to disentangle these two forms of climate variability data on subtle changes to the interannual variability of the ENSO system in the past as well as the change in mean state of the tropical Pacific must be collected, preferably from the same proxy. Isotopic records from *Tridacna sp.* can potentially bridge this gap since they preserve well enough to be found in large numbers, can be sampled at a seasonally resolution and finally have been shown to be an equivalent proxy to corals.

Evidence for mean state of the Tropical Pacific during Early to Mid Holocene (10-6.5 ka)

There is conflicting evidence of the mean state of the Pacific climate during the early to mid Holocene. Records from Mg/Ca in planktonic foraminifera indicate that SST's in the Western Warm Pool had reached modern values by the early to middle Holocene (Lea *et al.*, 2000 [ODP Site 806B] and de Garidel-Thoron *et al.*, 2007 [Images core MD97-2140] see Figure 5-1) or slightly warmer at 10 ka (Stott *et al.*, 2004 [Images Site MD76] and Brijker *et al.*, 2006 [G5-2-056P] see Figure 5-1). $\delta^{18}O$ records from sediment cores to the West of Papua New Guinea (Brijker *et al.*, 2006) and pollen and charcoal records from sites in Indonesia and Papua New Guinea (Haberle *et al.*, 2001) indicate a wetter and warmer, or more "La Niña-like" climate during the early Holocene.

Reduction in the number of flooding events in lake sediments from Ecuador, which are interpreted as a reduction in the number of El Niño events has lead Rodbell, *et al.*, (1999) to infer a warm climate in the east Pacific, in other words a more El Niño-like climate. This has some support from the distribution of warm water molluscs in Peruvian archaeological finds (Sandweiss *et al.*, 1996).

Evidence for the frequency of ENSO during the Early Holocene

Several modelling studies predict that during the early Holocene there should be a reduction in El Niño intensity (Lui *et al.*, 2000; Otto-Bliesner *et al.*, 2003 and Brown *et al.*, 2006) between 11-6.5 ka. There is good agreement from annually resolved records. Gagan *et al.*, (1998), Tudhope *et al.*, (2001) and McGregor *et al.*, (2004) used annually resolved coral records, which together span the Holocene and show that ENSO is in a "suppressed" state.

Evidence for the mean state of the Tropical Pacific during the last glacial period

There is currently conflicting evidence as to the state of the ENSO system in the Tropical Pacific during the Last Glacial Cycle. Some studies have suggested that the state of the region is a warm phase "El Niño" like state (Stott *et al.*, 2002 [MD98-

2181] and Koutavas *et al.*, 2002 [V21-30]) whilst other studies have shown a more "La Niña" type state (Andraesen *et al.*, 2001 and Beaufort *et al.*, 2001).

Evidence for the frequency of ENSO during the last glacial period

Modelling studies generally predict an enhanced ENSO variability during the Last Glacial Maximum (Clement *et al.*, 1999; Otto-Bliesner *et al.*, 2003 and An *et al.*, 2004) and during Marine Oxygen Isotope Stage 3 (Clement *et al.*, 1999).

Tudhope *et al.* (2001) analysed multi-decadal records from fossil corals at Huon Peninsula from the reefs that grew during the last glacial period showing that the strength of ENSO does not appear as large as would be predicted by Clement *et al.*, (1999). Tudhope *et al.*, (2001) and Beaufort *et al.*, (2001) suggest that in addition to the precessional forcing of ENSO, there is also a "glacially dampening" which reduces the number and amplitude of ENSO events due to a combination of cooler tropical temperatures producing a weaker coupling between ocean and atmosphere, stronger trade winds reducing the likelihood of El Niño/ La Niña events or changes in the thermocline structure.

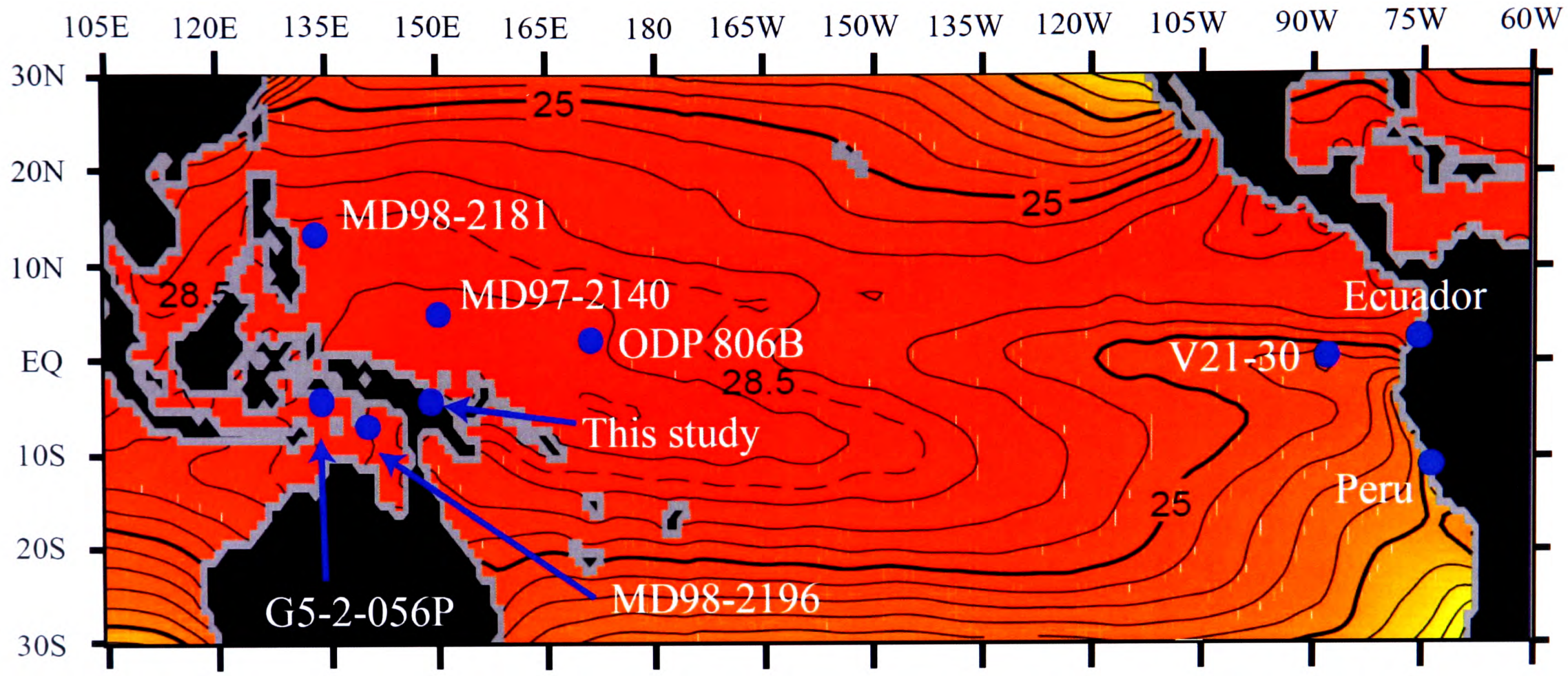

Figure 5-1 Showing some of the records used for Palaeo-ENSO and mean Pacific climate reconstruction referred to in this study compared with annual average temperature (Source: World Ocean Atlas, 2001).

5.1.1 Aim of this chapter

In this chapter 26 fossil samples of the giant clam *Tridacna* sp. were collected from the uplifted reefs at Huon Peninsula, Papua New Guinea (See Chapter 2). These long lived bivalves live in the photic zone on reefs that grew during the last glacial cycle and $\delta^{18}O$ measurements of carbonate extracted from their valves can be used to infer both mean climatic conditions in terms of changes in evaporation/ precipitation balance and sea surface temperatures and give an insight into changes in the frequency and strength of ENSO events (See Chapter 3).

The aims of this chapter are:

1. To investigate the mean state of the climate during the early to mid Holocene using $\delta^{18}O$ measurements from *Tridacna* sp.
2. To investigate the mean state of the climate during Marine Oxygen Isotope Stage 3 (65-30 ka) using $\delta^{18}O$ from *Tridacna* sp.
3. To use high resolution records of $\delta^{18}O$ obtained from selected *Tridacna* sp. to make inferences about interannual variability of climate during the glacial period.

5.2 Field area and sample collection

See Chapter 2 for details.

5.3 Materials and methods

5.3.1 Sampling

As mentioned above, two techniques were used to sample for $\delta^{18}O$ analysis: an "average" technique by sampling across annual growth bands and a "high resolution" technique sampling within annual bands (as described in calibration Chapter 3). In the average technique, the samples were sectioned across their axis of maximum growth and samples

milled using a hand held drill across the annual growth bands of the bivalves. A micromill was used to obtain seasonally resolved profiles from fossil *Tridacna* sp. using the same methods employed on modern *Tridacna gigas* (see Chapter 3 for more details of methods).

5.3.2 Screening for diagenesis

Tridacna sp. valves are composed entirely of aragonite. Aragonite is a metastable form of $CaCO_3$ which does not normally precipitate in modern oceanic water without biological mediation. There are two mechanisms that lead to diagenetic alteration of the original aragonitic skeleton: 1) by precipitation of secondary aragonite in the marine environment 2) alteration in the vadose zone primarily due to dissolution and precipitation of void filling calcite in the vadose zone.

The aragonitic valves of *Tridacna* sp. are denser and considerably less porous than coral skeletons, also due to the high rate of uplift in the area, the samples spend a relatively short period of time in the ocean before being subaerially exposed. Both factors reduce the potential of secondary aragonite precipitation in the marine environment.

Aharon and Chappell (1986) identify three types of alteration to screen for in *Tridacna* sp:

1. Alteration of original aragonite into low Mg calcite by destructive agents such as algal and gastropod boring or at cracks along lines of mechanical weakness and along the margins of the valves where calcite is precipitated into voids.
2. Subtle coarsening of aragonitic fibres (daily banding can still be easily seen/ is not disrupted).
3. Coarsening and gradual replacement of fibres by calcite.

Types two and three do not involve carbon exchange (Chappell and Polach, 1972) and is assumed to be immune from diagenetic alteration of $\delta^{18}O$ (Chappell and Polach, 1972). Inclusion of Type 1 material was avoided by simple visual inspection of the valves when drilling, but may be difficult to identify if dissolution and replacement of original aragonite material is subtle or heterogeneous.

As rainfall $\delta^{18}O$ has an average value of approximately –9.9‰ $\delta^{18}O$ (based upon measurements of Tewai River water in Aharon and Chappell, 1986), it is extremely important to screen for even small amounts of calcite precipitation. If it is assumed that the precipitated calcite has the same isotopic signature as rainfall, then samples containing 1% calcite should shift values of $\delta^{18}O$ of samples with 0.0‰ by 0.1‰. This is likely to be an overestimate as samples of secondary calcite removed from MIS3 *Tridacna* sp. yield values of approximately -5‰ (this study).

Scanning Electron Microscopy and thin section examination was carried out on the samples used in this study. The ratio of aragonite to calcite in each sample was determined using a Bruker-AXS D8 Advance X-Ray Diffractometer that uses Cu K-alpha radiation (40kV/ 40mA) as the source and a Sol-X energy dispersive detector. Carbonate powders were gently crushed using an agate mortar and pestle. Approximately 50mg was transferred to a 2.5 cm diameter glass disk and placed into the instrument for analysis. Calculation of aragonite/ calcite % was made using the TOPAZ programme based upon area under peaks. Analytical precision of this technique is ±0.1% calcite.

The process of drilling is likely to convert aragonite into calcite (Aharon, 1991) and variations in pressure and speed of the drill will affect the amount of calcite produced. This will increase the uncertainty in % calcite and obscure any diagenetic signals. To quantify the amount of calcite produced during drilling, samples of carbonate from the modern *Tridacna gigas* which is composed entirely of aragonite were collected using the sample drill and the percentage of calcite was measured. These were collected on a number different days. A mean value of 0.55% calcite with a standard deviation of 0.4% (n=9). Since this value is higher than the precision of the TOPAZ uncertainty it will be adopted as the overall uncertainty.

5.3.3 Stable isotope analysis

Both high resolution (seasonally resolved) records and average $\delta^{18}O$ were measured for the Holocene and glacial samples. Samples were collected using a micromill and dental drill (see Chapter 3). Oxygen and carbon stable isotope analyses were performed on 0.1 - 0.2 mg

sub-samples. The carbonate samples were reacted with 100% orthophosphoric acid at 75°C in a Kiel Carbonate III preparation device and the resulting CO_2 was then analysed on a Thermo Electron Delta+ Advantage stable isotope ratio mass spectrometer. The standard deviation for a laboratory standard marble powder (MAB2B) run as a sample since the installation of the instrument in July 2005 is ± 0.09‰ for $\delta^{13}C$ and ± 0.08‰ for $\delta^{18}O$. All carbonate isotopic values are quoted relative to PDB.

5.3.4 Building a chronology for bulk $\delta^{18}O$ measurements

The procedure for building a Chronology for these samples is described in detail in Chapter 4.

5.3.5 Estimating the number of years sampled

Tridacna sp. from tropical regions do not always have very well defined growth layers and the counting of growth increments can be problematic. Subtly alternating dark and light bands seen in modern samples are assumed to be annual bands (Bonham, 1965; Aharon and Chappell, 1986, Pätzold *et al.*, 1991 and Elliot *et al.*, [submitted]). The number of years sampled was estimated by making observations of 3-5mm thin sections of each fossil *Tridacna* sp. valve placing the sample on a light table surrounded by black card. A digital photo taken using a digital SLR camera and the contrast in the resulting picture enhanced using Adobe Photoshop. This allows individual years of growth counted by marking dark bands (see Figure 5-2). Since the edge of the valves were most likely to suffer the most from borings, fractures and diagenetic alteration this area was generally not sampled and only the growth bands sampled were recorded.

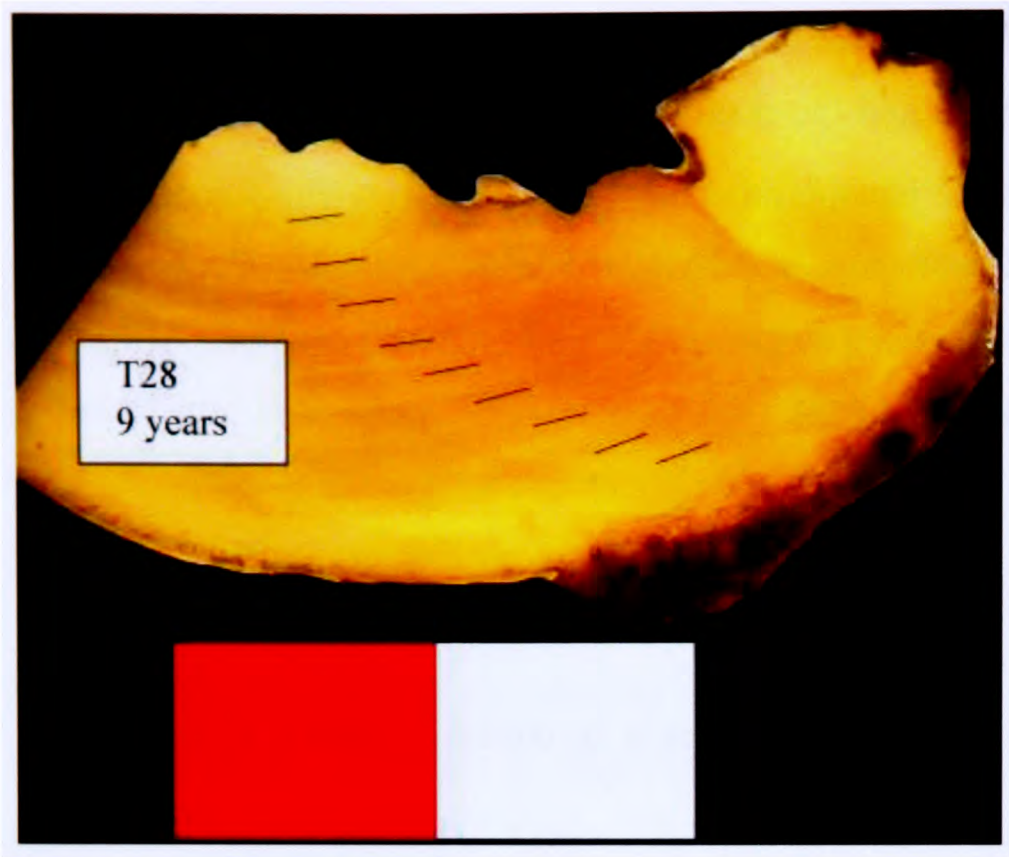

Figure 5-2 Dark and light couplets marked on T28 (*Tridacna maxima*). Specimen was sampled over these growth bands. Scale bar is 2cm.

5.3.6 Building a chronology for seasonally resolved samples

A similar method was used for fossil samples as on the modern *Tridacna gigas* specimen (See Chapter 4). Couplets of dark and light bands in each shell were counted to calculate the number of years of growth. The chronologies were constructed by observation of annual growth and using cycles in $\delta^{18}O$ by assigning the beginning of the year to positive peaks in $\delta^{18}O$ as done in the modern sample described in Chapter 3.

5.4 Results

5.4.1 Screening

Optical thin section

The samples were exceptionally well preserved, with fine banding which is thought to be either tidal or daily banding (according to Watanabe *et al.*, 2004) still visible in most samples. Some patchy calcite replacement was noted especially around sample margins

(Figure 5-3) and associated with borings and fractures, however this can clearly be observed in thin section and also when drilling specimens and was therefore easily avoided when sampling.

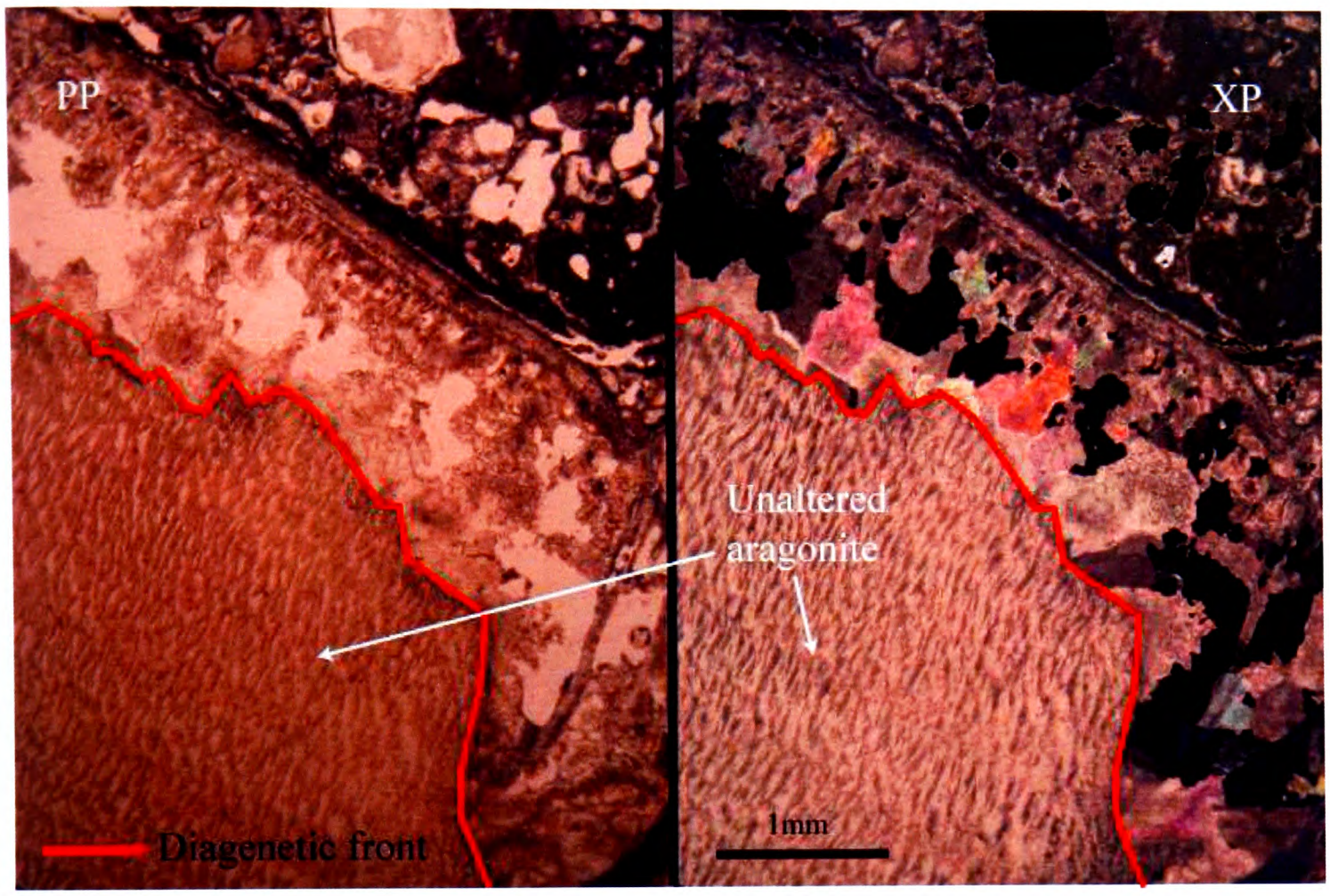

Figure 5-3 Optical thin section of T48 (*Tridacna maxima*) showing diagenetic alteration of third type (as identified by Chappell, 1974). Calcite crystal fills voids left by dissolution of original aragonite. This generally occurs at shell margin. Calcite crystals are seen on the other side of the diagenetic front with high birefringence colours.

Scanning Electron Microscope results

SEM investigations also showed excellent preservation with fine banding still visible in the inner layer of most samples (Figure 5-4).

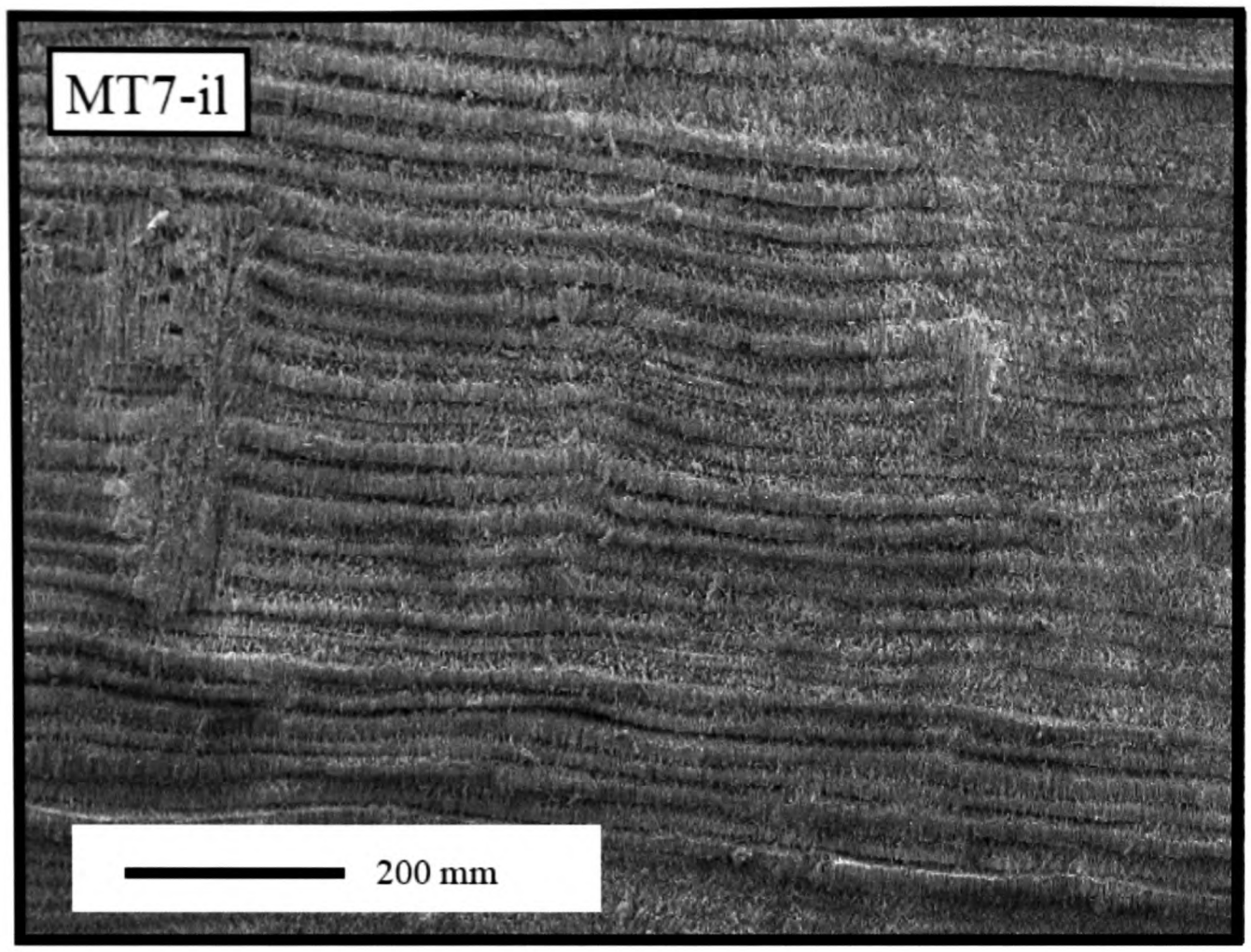

Figure 5-4. Fine banding seen using SEM in modern (Tg-MT7-il) and *Tridacna gigas* inner layer.

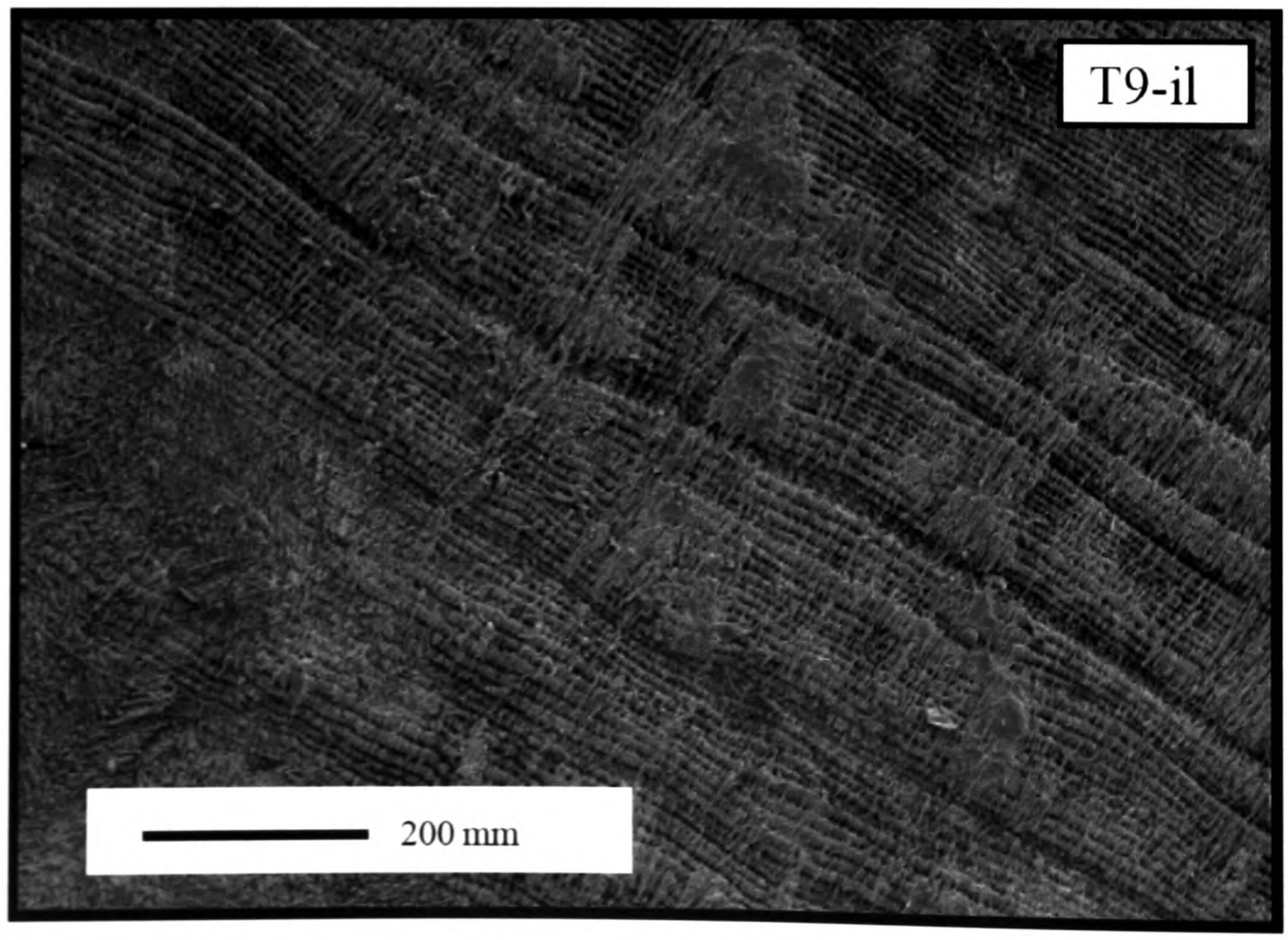

Figure 5-5. Fine banding seen using SEM in fossil (Tg-T9-il) and *Tridacna gigas* inner layer demonstrating the excellent preservation in fossil *Tridacna* sp.

XRD results

The results of SEM and thin section analysis showed that the preservation of the samples was excellent and diagenetic alteration of type 3 was easy to detect visually, however as nature of calcite replacement is potentially heterogeneous, samples were screened based upon their XRD results as this should be the most robust tool for detection of alteration. Results of 4 samples were rejected on the basis that they show higher than 1% calcite. These were T47 with 4.5% calcite, T26 with 2.9% calcite, T17 with 5.1% calcite and T3 with 2% calcite, though it is probably that most of the valve is undamaged.

5.4.2 Oxygen isotopes – averaged over all growth bands

Figure 5-6 shows the results of the $\delta^{18}O$ analysis plotted against elevation, which is equivalent to age to the first approximation. There are two identifiable groups of data – the Holocene data (0-20m) and the MIS3 age data (45-140m). Most of the Holocene data has $\delta^{18}O$ values ranging from -1.8 to -0.5‰ (1.3‰) with two samples between –1.9 and –1.7 ‰, with a mean value of -0.9‰ and a standard deviation of 0.43 (n= 12). The MIS 3 $\delta^{18}O$ ranges between -0.4 to 0.3 ‰ (0.7‰) with mean value of 0.0‰ and a standard deviation of 0.2 (n=26).

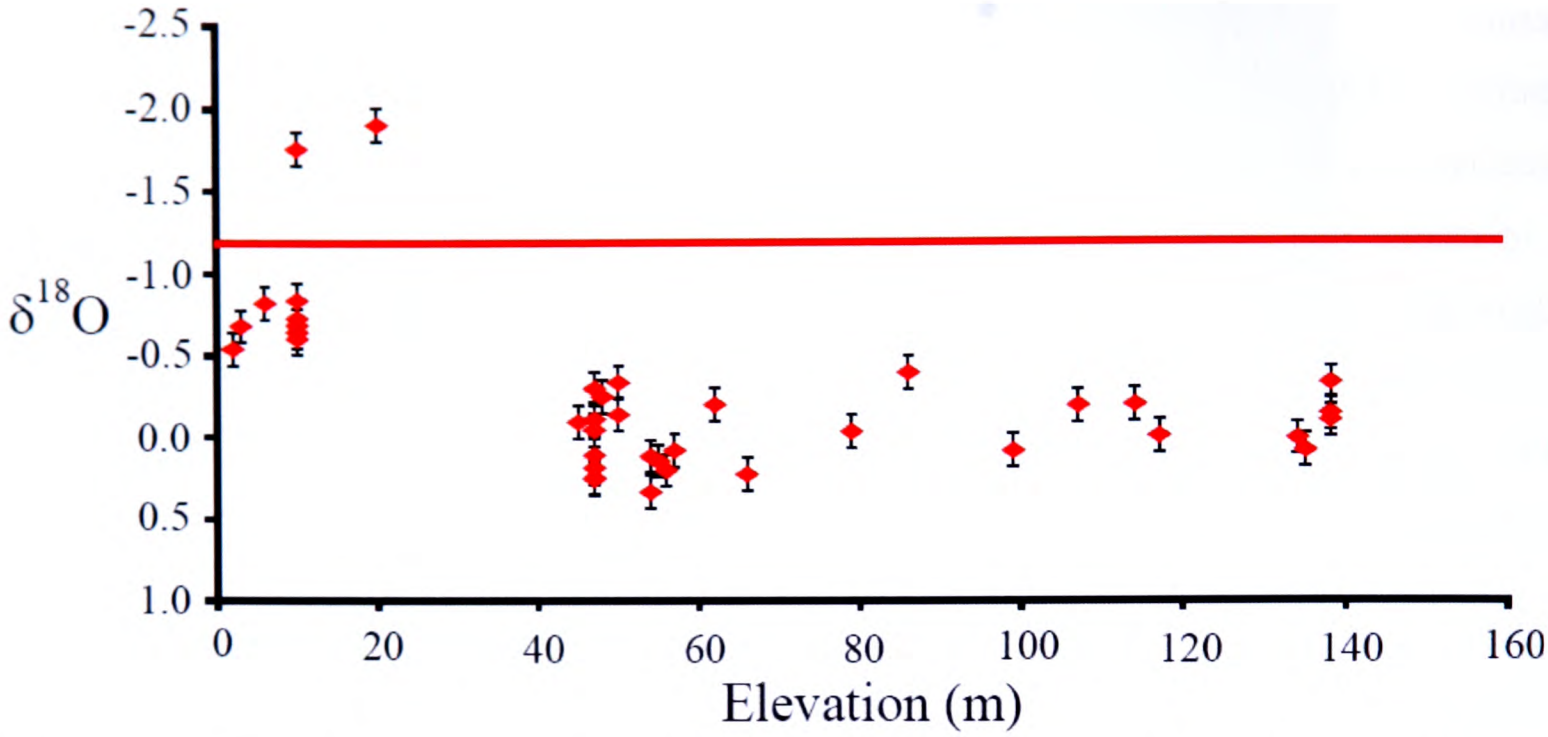

Figure 5-6 $\delta^{18}O$ data collected from *Tridacna* sp. using the bulk sampling technique arranged by elevation. Where sample is *ex situ*, elevation is estimated as the relative height of the crest of each reef at Bobongara or set as 10m as an average height for the Holocene samples. Red line shows average $\delta^{18}O$ value in a modern *Tridacna gigas* of -1.2‰ (see Chapter 4). Error is conservatively estimated as 0.1‰

5.4.3 Carbon isotopes – averaged over all growth bands

Figure 5-7 shows the results of the $\delta^{13}C$ analysis plotted against elevation. The Holocene data shows $\delta^{13}C$ values ranging from 2.46 to 3.14‰ (0.58 ‰), with an average value of 2.77 ‰ and a standard deviation of 0.21 (n= 12). The MIS 3 shows a range of 2.28 to 2.87 ‰ (0.59 ‰) with mean value of 2.57 ‰ and a standard deviation of 0.16 (n=26).

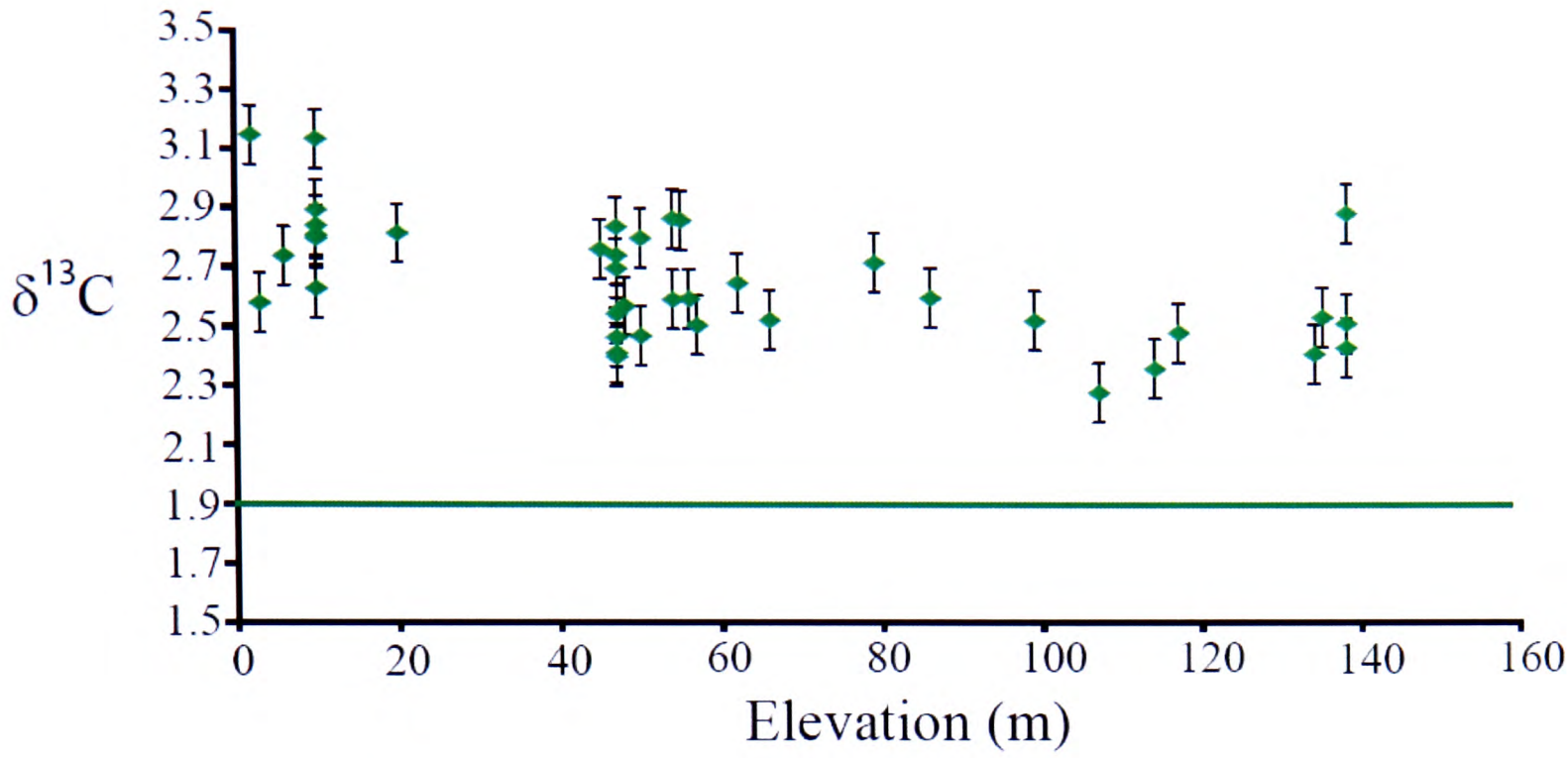

Figure 5-7 $\delta^{13}C$ data collected from *Tridacna* sp. using the averaged sampling technique arranged by elevation. Where sample is *ex situ*, elevation is estimated as the relative height of the crest of each reef at Bobongara or set as 10m as an average height for the Holocene samples. Green line shows average $\delta^{13}C$ value in a modern *Tridacna gigas* of 1.9‰ (see Chapter 4). Error bars are 0.09‰.

(Page opposite) Table 5-1 Samples used for climate reconstruction in MIS 3 reefs at Huon Peninsula. Age and uncertainties are estimated using ^{14} dating up to reef IIIc(u), and from stratigraphic position thereafter (see text).

Sample name	Species	Reef (Terrace)	Depth below crest (m)	Elevation (m)	Average $\delta^{18}O$	No samples	No. years sampled C=counted E=estimated H=high res. record	Radiocarbon age (uncorrected yrs)	Age (calibrated ka)	Age uncertainty 2σ (Ka)	% Calcite
T72	*T. maxima*	Holocene	Ex situ	unknown	-1.8	2	20 (E)	4150	3.71	0.42	0.6
T66	*T. gigas*	Holocene	Ex situ	unknown	-1.9	1	18 (C)	6480	6.54	0.38	0.6
T59	*T. squamosa*	Holocene	Ex situ	unknown	-0.8	1	17 (C)	6890	7.03	0.39	0.6
T60	*T. gigas*	Holocene	Ex situ	unknown	-0.7	1	22 (C)	7025	7.17	0.42	0.8
T65	*T. maxima*	Holocene	Ex situ	unknown	-0.6	1	8(C)	7330	7.45	0.29	0.8
T73	*T. gigas*	Holocene	Ex situ	unknown	-0.6	4	20 (C)	7129	7.28	0.08	0.1
T58	*T. gigas*	Holocene	6	6	-0.8	177	15(H)	7257	7.40	0.15	0.1
T49	*T. gigas*	Holocene	unknown	unknown	-0.5	1	4(C)	8230	8.33	0.36	0.5
T51	*T. gigas*	Holocene	unknown	unknown	-0.7	2	8(C)	8548	8.73	0.06	0.2
T75	*T. gigas*	Holocene	Ex situ	unknown	-0.7	2	20 (C)	8592	8.76	0.08	0.2
T14	*T. gigas*	IIa	1	49	-0.1	213	19 (H)	31694	36.66	0.84	0.5
T29I	*T. gigas*	IIa	Ex situ	unknown	0.2	1	8 (C)	31780	36.75	0.21	0.4
T28I	*T. maxima*	IIa	Ex situ	unknown	0.1	1	9 (C)	30450	35.45	0.26	0.4
T10I	*T. gigas*	IIa	Ex situ	unknown	0.1	2	7 (C)	30810	35.79	0.38	0.7
T13I	*T. maxima*	IIa	Ex situ	unknown	-0.5	1	7 (C)	31750	36.72	0.22	0.3
T27	*T. gigas*	IIa	0	50	-0.3	6	27 (C)	31820	36.79	0.85	0.0
T70	*T. gigas*	IIa	3	47	-0.3	4	24(C)	31590	36.56	0.94	0.6
T11	*T. maxima*	IIa	3	47	-0.1	8	8 (C)	33413	38.41	1.04	0.4
T9	*T. gigas*	IIa	5	45	-0.1	2	12 (C)	32794	37.79	0.95	0.5
T12	*T. squamosa*	IIa	3	47	0.3	2	8 (C)	33210	38.20	1.01	0.3
T32	*T. maxima*	IIIc(l)	0	57	0.1	2	9 (C)	34520	39.49	0.79	0.2
T31	*T. gigas*	IIIc(l)	1	56	0.2	2	3 (C)	32808	37.80	1.47	0.3
T34	*T. maxima*	IIIc(l)	2	55	0.1	2	3 (C)	33162	38.60	1.11	1.0
T33	*T. crocea*	IIIc(l)	3	54	0.1	2	5 (C)	36613	41.44	1.66	0.0
T39	*T. maxima*	IIIc(u)	0	66	0.2	89	10 (H)	36550	41.40	0.31	0.8
T30	*T. crocea*	IIIc(u)	Ex situ	unknown	0.3	2	5 (C)	36710	41.53	1.17	0.5
T40	*T. maxima*	IIIc(u)	4	62	-0.2	56	8 (H)	37758	42.44	1.82	0.6
T24	*T. crocea*	IIIb	2	86	-0.4	2	8 (C)		44.93	4	0.3
T48	*T. maxima*	IIIb	6	80	-0.2	4	11 (C)		45.80	4	1.0
T37	*T. maxima*	IIIb	7	79	-0.0	8	9 (C)		46.02	4	0.9
T23	*T. crocea*	IIIa(l)	0	107	-0.2	2	6 (C)		49.00	4	0.7
T41	*T. crocea*	IIIa(l)	8	99	0.1	59	8 (H)		50.74	4	0.6
T42	*T. crocea*	IIIa(m)	1	117	-0.0	2	7(C)		52.22	4	0.4
T15	*T. gigas*	IIIa(u)	0	138	-0.3	17	60 (E)		60.00	4	0.8
T22	*T. gigas*	IIIa(u)	0	138	-0.1	4	12 (C)		60.00	4	0.5
T44	*T. maxima*	IIIa(u)	0	138	-0.1	2	10(C)		60.00	4	0.5
T6	*T. gigas*	IIIa(u)	3	135	0.1	2	7(C)		60.65	4	0.7
T38	*T. crocea*	IIIa(u)	4	134	0.0	4	5(C)		60.87	4	0.5

5.5 Oxygen isotopes – seasonally resolved records

Six *Tridacna* sp. were selected for high resolution study were T58 (*Tridacna gigas*) from the Holocene reef at Kwambu and from the MIS 3 terraces, T14 (*Tridacna gigas*) from reef terrace IIa (approximately 37-40 ka), T39 (*Tridacna maxima*) and T40 (*Tridacna maxima*) from terrace IIIc(u) approximately 40-44 ka and T41 (*Tridacna crocea*) from IIIa(l) approximately 49 ka. Each shell was then radiocarbon dated as described in the Chapter 4, apart from T41 where the age was estimated based upon the procedure described in Chapter 4.

Holocene – T58 (Tridacna gigas hinge area)

This stable isotope profile is approximately 16 years long with a gap which probably represents a year of missing growth (due to a crack in thin section). $\delta^{18}O$ values range from -1.2 to -0.3‰ with a mean value of -0.8‰ (n=177). Annual amplitude in $\delta^{18}O$ is approximately 0.3‰.

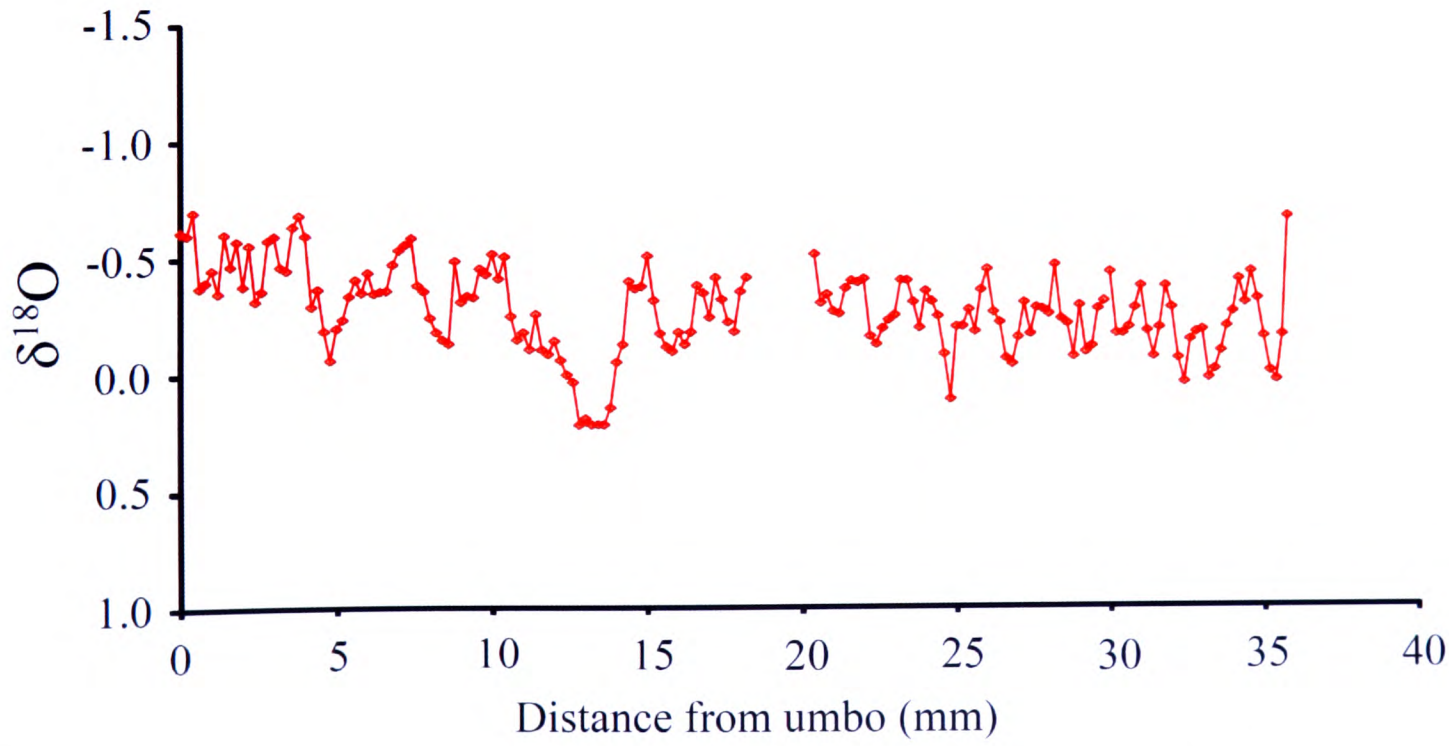

Figure 5-8 Seasonally resolved $\delta^{18}O$ results versus distance from umbo in *Tridacna gigas* T58 8.09±0.08 ka from Holocene reef terrace. Note that y axis is reversed.

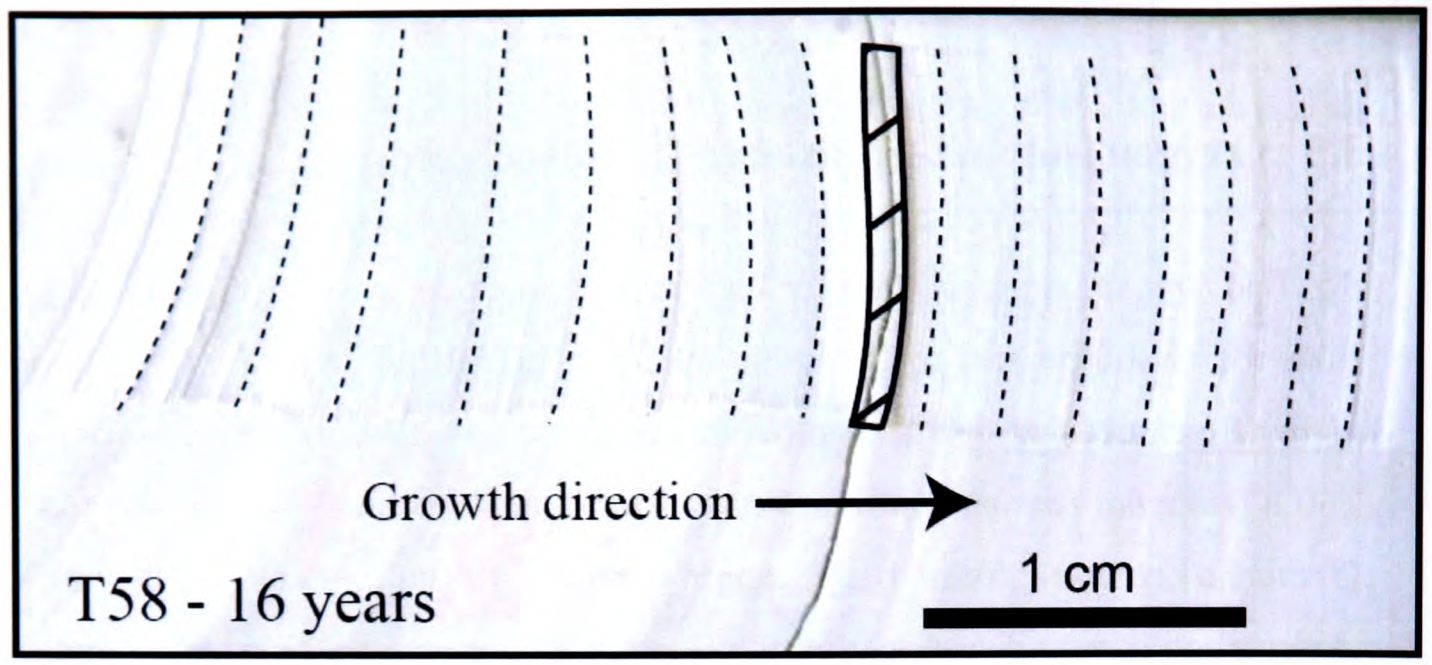

Figure 5-9 T58 showing with annual banding marked (dashed lines). Brown line shows missing year at crack in slide. Scale is 1 cm.

Reef Terrace IIa –T14b (Tridacna gigas hinge area)

This record is approximately 19 years long. $\delta^{18}O$ values range from -0.9 to 0.5‰ with a mean value of -0.1‰ (n=218). Mean annual amplitude in $\delta^{18}O$ is 0.4‰.

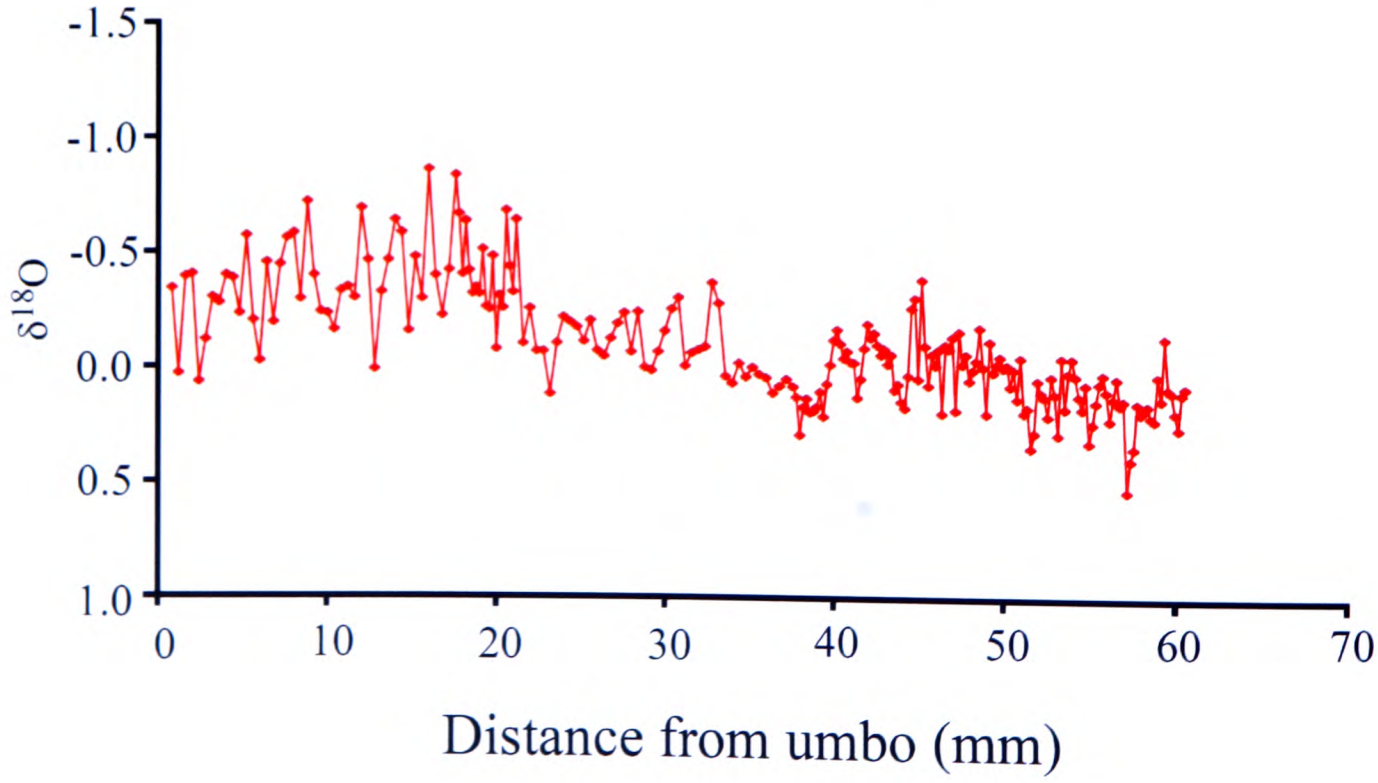

Figure 5-10 Seasonally resolved $\delta^{18}O$ results versus distance from umbo in *Tridacna gigas* T14 (hinge area) 37.45±0.45 ka from reef terrace IIa

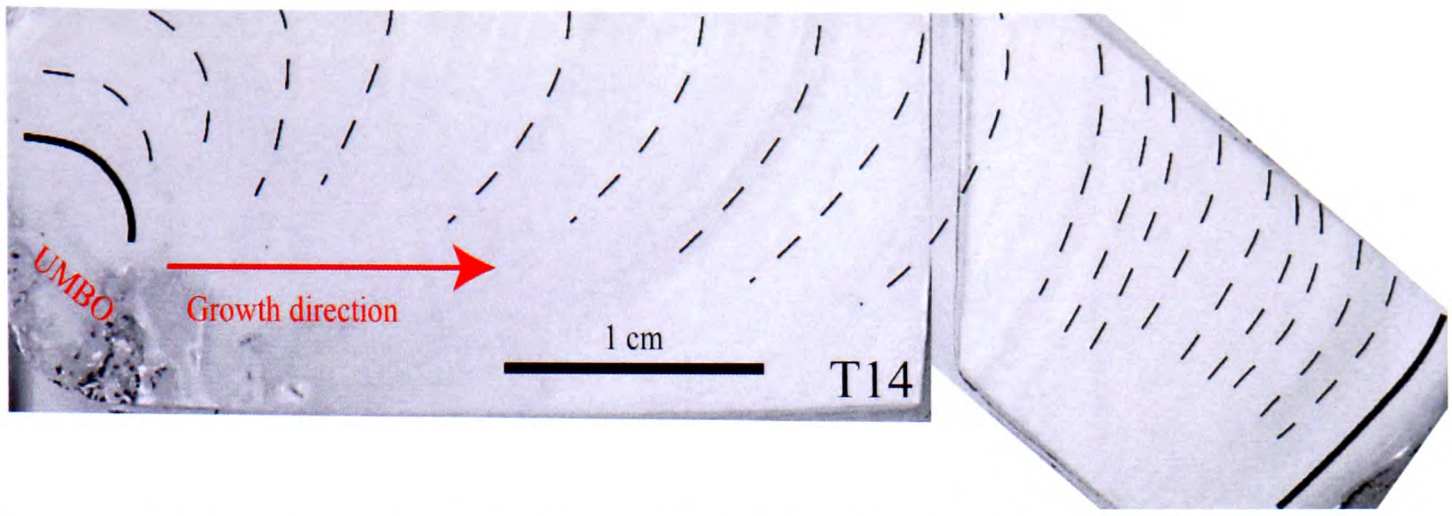

Figure 5-11 T14 hinge area with annual growth increments marked (dashed lines) =. Scale is 1cm. Hinge was cut into two slabs to allow attachment to micromill.

Reef Terrace IIIc(u) – T39 (Tridacna maxima inner layer)

This record is approximately 8 years long. $\delta^{18}O$ values range from -0.8 to 1.0‰, with a mean value of 0.3‰ (n=90). Mean annual amplitude of $\delta^{18}O$ is 0.6‰.

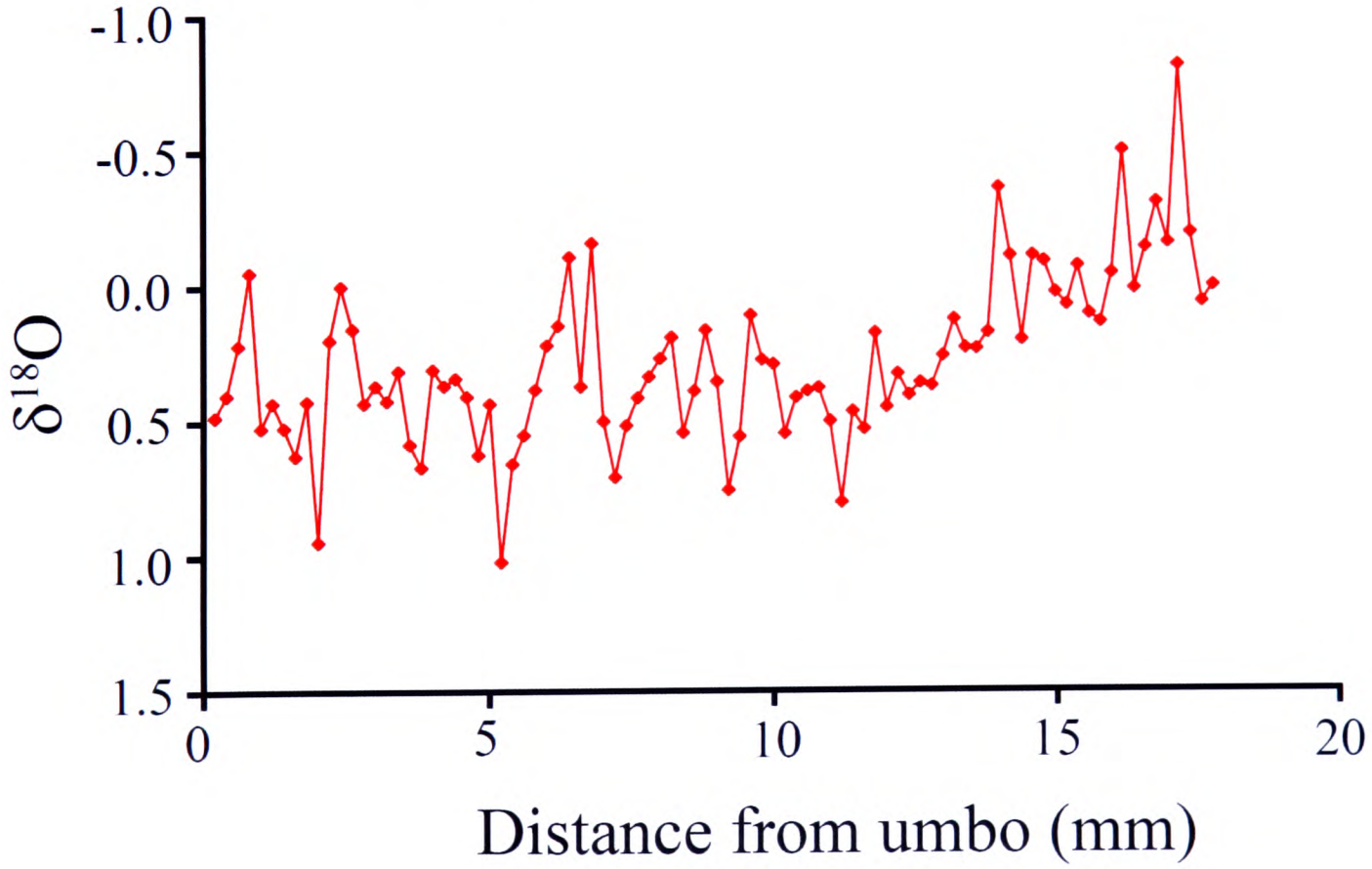

Figure 5-12 Seasonally resolved $\delta^{18}O$ results versus distance from umbo in *Tridacna maxima* T39 (inner layer) 42.07±0.27 ka from reef terrace IIIc(u)

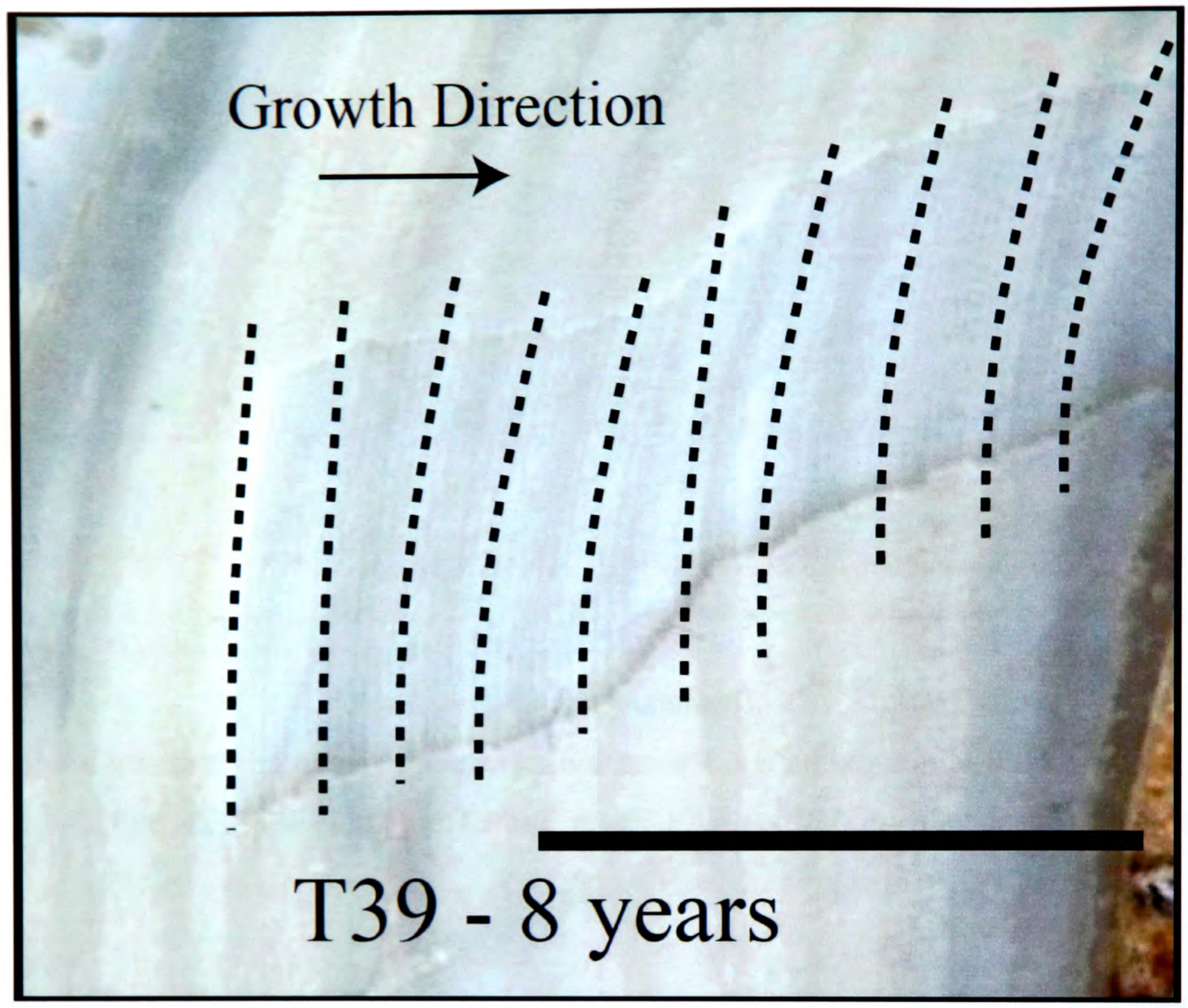

Figure 5-13 Thin section of T39I with annual banding marked on (dashed lines). Scale is 1 cm.

Reef Terrace IIIc(u) – T40 (Tridacna maxima hinge area)

This record is approximately 8 years long. $\delta^{18}O$ values range from –1.0 to 0.2‰, with a mean value of 0.5‰ (n=55). Mean annual amplitude of $\delta^{18}O$ 0.4‰.

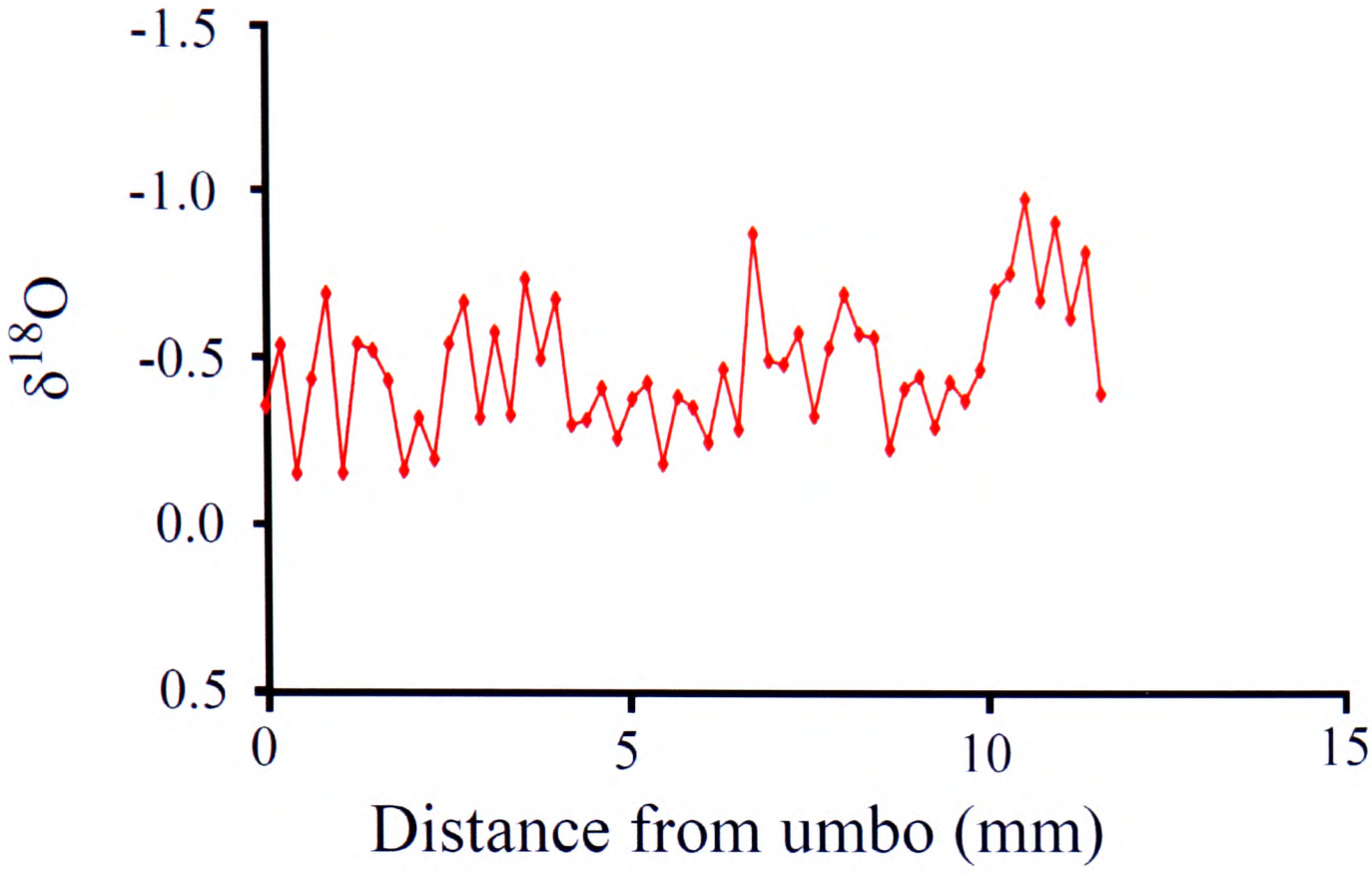

Figure 5-14 Seasonally resolved $\delta^{18}O$ results versus distance from umbo in *Tridacna maxima* T40 (hinge area) 43.02 ±0.8 ka from reef terrace IIIc(u)

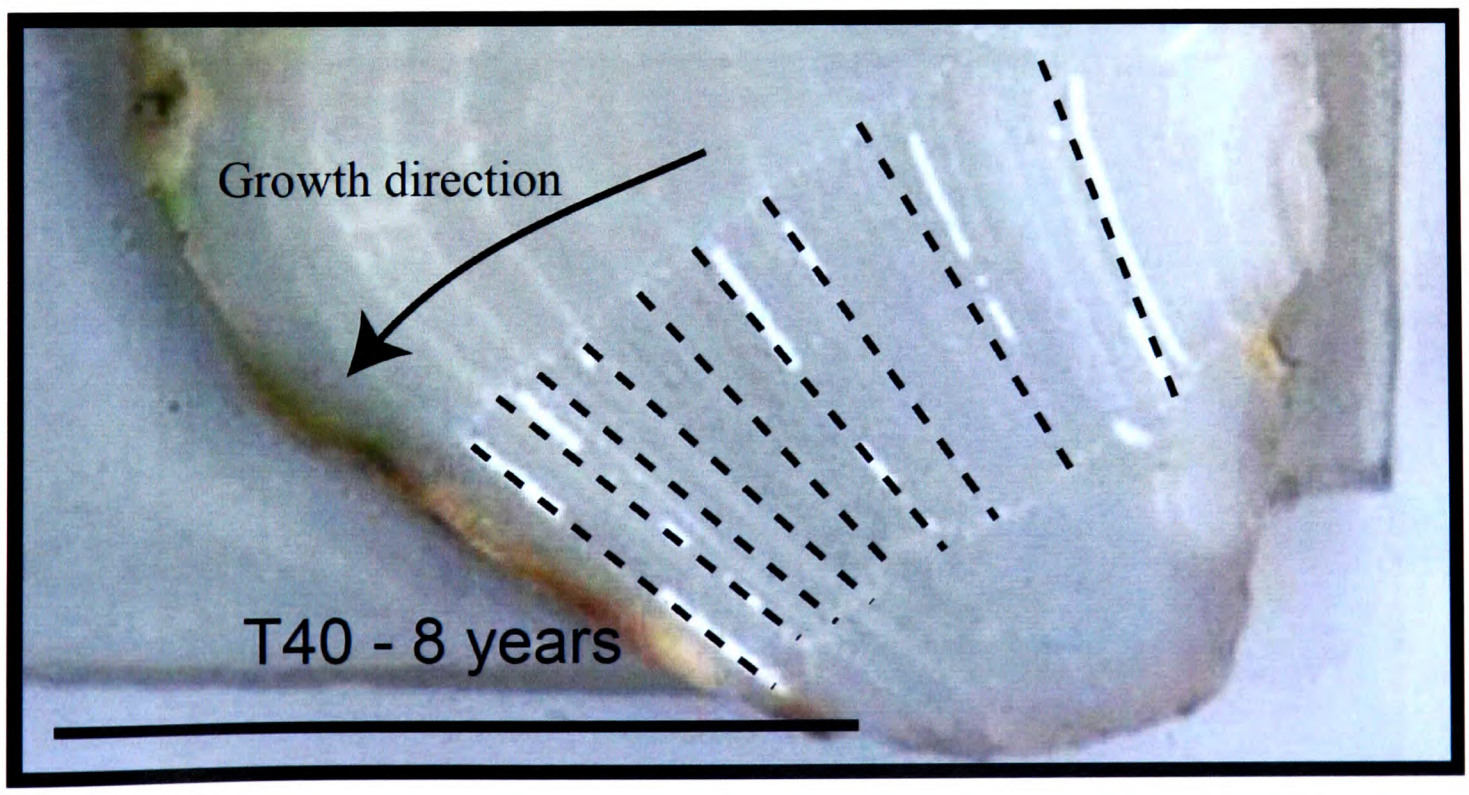

Figure 5-15 Thin section of T40 with annual banding marked (dashed lines). Scale is 1 cm.

Reef Terrace IIIa(l) – T41 (Tridacna crocea hinge area)

This record is approximately 8 years long. $\delta^{18}O$ values range from -0.7 to 0.8‰, with a mean value of 0.1‰ (n=58). Mean annual amplitude of $\delta^{18}O$ 0.8‰.

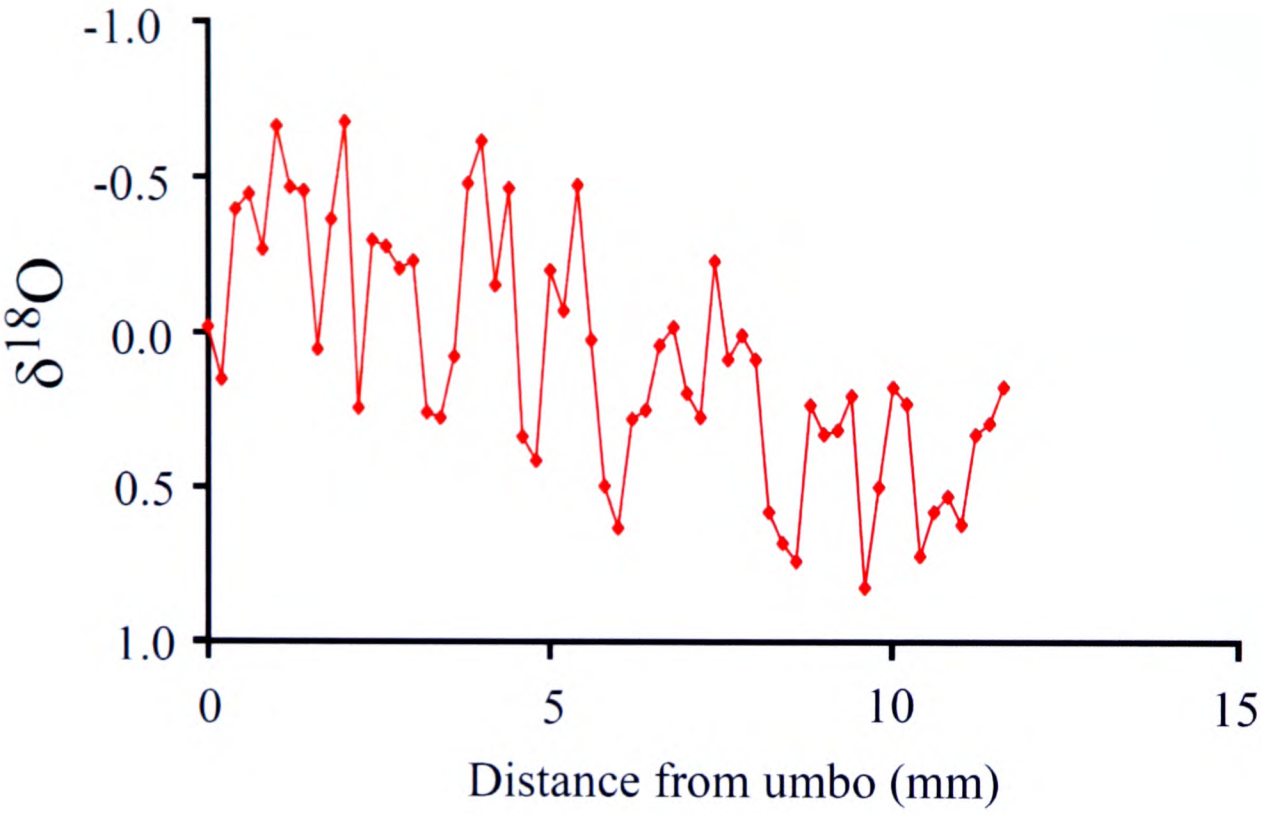

Figure 5-16 Seasonally resolved $\delta^{18}O$ results versus distance from umbo in *Tridacna crocea* T41 (hinge area) estimated to be ≈50.74 ka from reef terrace IIIa(l)

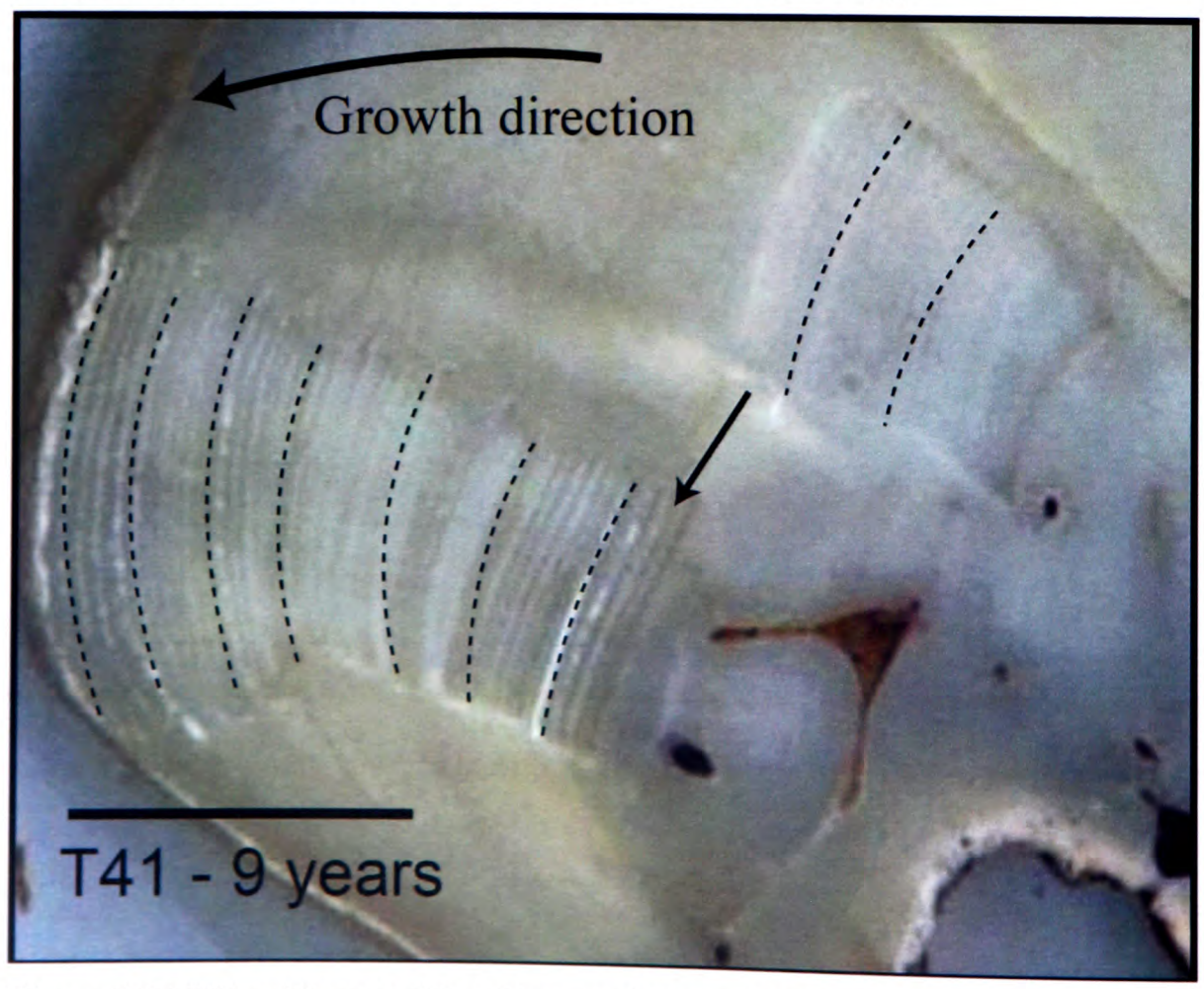

Figure 5-17 T41- with annual banding marked on (Scale is 1 cm).

5.6 Discussion

The $\delta^{18}O$ and $\delta^{13}C$ results from the bulk sampling technique are shown in Figure 5-18 versus age. This figure shows stable isotopes versus time and compares with Aharon *et al.*, (1983) $\delta^{18}O$ data (marked in blue). Modern values are marked with a red line ($\delta^{18}O$) and green line ($\delta^{13}C$). The difference in $\delta^{18}O$ between the Holocene and MIS3 values of $\delta^{18}O$ is 0.9‰. This will be due in part to changes in continental ice volume and also local temperature and sea surface salinity. Sea level for most Holocene samples varies between 0m and -20m (Ota and Chappell, 1999) and for the MIS3 samples varies between -40 and -100m (Siddall *et al.*, 2003) with a mean sea level of -75m.

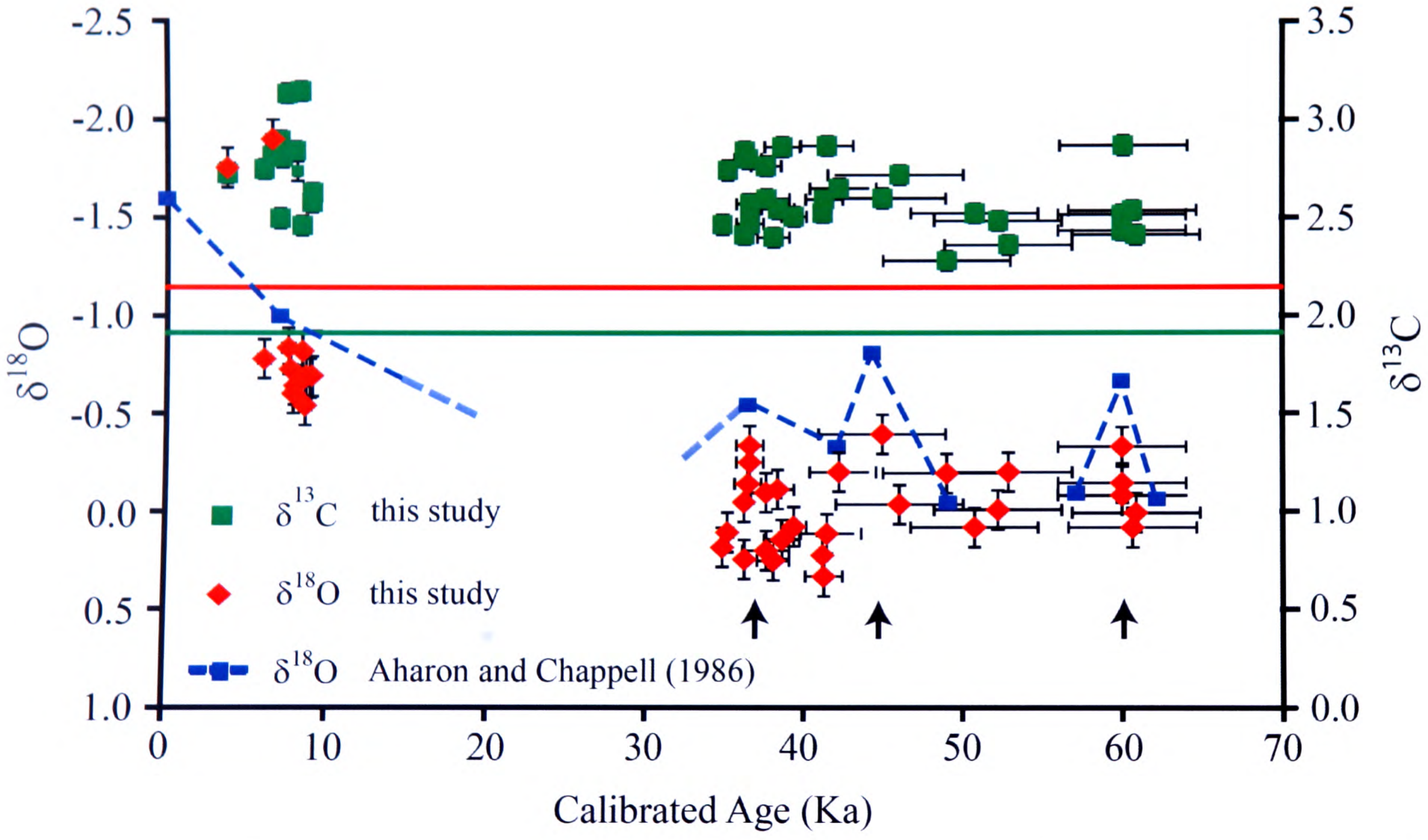

Figure 5-18 Stable isotope results against age model. Red dots are $\delta^{18}O$, and red line shows modern value of -1.2‰. Green squares are $\delta^{13}C$, with green line showing modern value of 1.9‰. Blue dots are $\delta^{18}O$ "bulk" values from *Tridacna* sp. from the terraces at Sialum, Huon Peninsula presented in Aharon *et al.*, (1980), Aharon, (1983) and Aharon and Chappell, (1986). Note that dates have been altered in line with new dating of the reefs presented in this study (see Chapter 5), and are based upon Chappell, 2002. Blue lines joining samples are inferred by Aharon and Chappell (1986). Arrows show major sea level peaks in MIS3 inferred from terrace growth.

5.6.1 Comparison of $\delta^{18}O$ with previous studies

Figure 5-18 shows the relationship between $\delta^{18}O$ results from a previous study carried out using fossil samples of *Tridacna gigas* collected from the reef terraces at Sialum (see Figure 2-2) reported in Aharon *et al.,* (1980) and Aharon and Chappell, (1983). Aharon collected "bulk" samples across the growth bands of *Tridacna gigas* in a similar manner to this study, though instead of using a handheld drill, the outer surface of the *Tridacna gigas* was removed and the hinge area was sliced into slabs and crushed for analysis.

Aharon and Chappell (1983) show a similar pattern of $\delta^{18}O$ where negative peaks in $\delta^{18}O$ results coincident with sea level peaks however Aharon's values are more negative than those shown here, with values of -1.6‰ for a modern *Tridacna gigas*, -1.0‰ for the Holocene reef and -0.3‰ for the MIS 3 reefs. The results from this study are therefore 0.4‰, 0.1‰ and 0.3‰ more positive respectively. There are several possible explanations for the offset here.

Firstly there might be a consistent failure in screening for diagenesis by either study. Both visual inspection and XRD methods were employed in both cases to exclude this possibility, though no estimate of acceptable percentage of calcite was provided (Aharon *et al.,* 1980; Aharon, 1983 and Aharon and Chappell, 1986). The trends are however similar which would be unlikely if the samples presented in Aharon had large amounts of secondary calcite.

Secondly, Aharon collected *Tridacna* sp. samples from a different location on the Huon Peninsula at Sialum. This is approximately 30 km north west of Bobongara where the MIS3 samples where collected and approximately 15 km north west of Kanzarua where the modern sample of *Tridacna gigas* was collected. Restricted lagoonal environments can affect $\delta^{18}O$ of *Tridacna* sp. that grow in them as the evaporation precipitation balance as water is not continuously refreshed from the open ocean and affect the $\delta^{18}O$ water, and there may be a difference in water temperature between lagoons and the open ocean. There is a currently a lagoon at

Sialum, however there is not thought to have been extensive lagoonal development during MIS3 (Chappell, 1974). Furthermore, the lagoon at Sialum is well connected to the open ocean (S. Tudhope pers. comm.) and comparison of $\delta^{18}O$ time series from inside and outside the lagoon show that there is no strong effect upon $\delta^{18}O$ at Sialum (see chapter 3). This may be different in restricted lagoons (see also below).

Finally in Aharon *et al.,* (1980), Aharon (1983) and Aharon and Chappell (1986) carbonate powders were roasted at 400°C to remove organic material, and it is possible that this could have affected the $\delta^{18}O$ by re-equibrilation. Staining with Mutvei's solution that binds to organic matter (Schöne *et al.*, 2005) shows that there is little organic matter present in *Tridacna* sp. valves, therefore this step was not considered necessary in this study. The effects of roasting aragonite powders are not well understood, but may cause conversion to calcite and alter the $\delta^{18}O$ of the carbonate powder by re-equibrilation (Spero, H., pers. comm. 2004) and could explain the observed offset.

5.6.2 Effects of differing reef environments

Figure 5-19 shows the relationship between $\delta^{18}O$ and $\delta^{13}C$. Holocene values are marked in red, MIS3 values are marked in blue. It can be seen that the Holocene and MIS 3 values fall into two distinct groups that are separated largely by $\delta^{18}O$ differences. Two samples display extremely negative $\delta^{18}O$ values (marked by blue circle). The development of lagoons during the Holocene can be seen in some areas such as Bobongara and Sialum, and this may cause the production of micro-environments which will affect the oxygen isotopic ratios incorporated into the valves (as discussed above). As has been shown, the lagoon at Sialum is not thought to be a very restricted environment based upon $\delta^{18}O$ measurements of surface water and regionally reproduced $\delta^{18}O$ in coral (Chapters 2 and 3), however it is not known whether the Holocene lagoon at Bobongara similarly mixed (see below).

Samples T66 and T72 were found on the top of the Holocene Lagoon at Bobongara. T66 was in the centre of the lagoon in life position. T72 was found *ex situ* and its

provenance is unknown, though it is assumed not to have been moved far. The presence of a restricted lagoon at Bobongara would account for the very negative $\delta^{18}O$ -1.7 and -1.9‰ in T72 and T66 respectively due to abnormally high SST's. These values are more negative than modern values (-1.2‰), though both XRD analysis visual observation exclude extensive diagenetic alteration. These samples are therefore separated from the Early Holocene samples, and it is hypothesised that they reflect lagoonal archives, rather than open ocean during the Holocene. The remaining samples have a mean $\delta^{18}O$ of -0.7‰ and a standard deviation of 0.13, and a mean $\delta^{13}C$ of 2.37‰ and a standard deviation of 0.23. There is no such lagoonal development in the MIS 3 terraces at Bobongara.

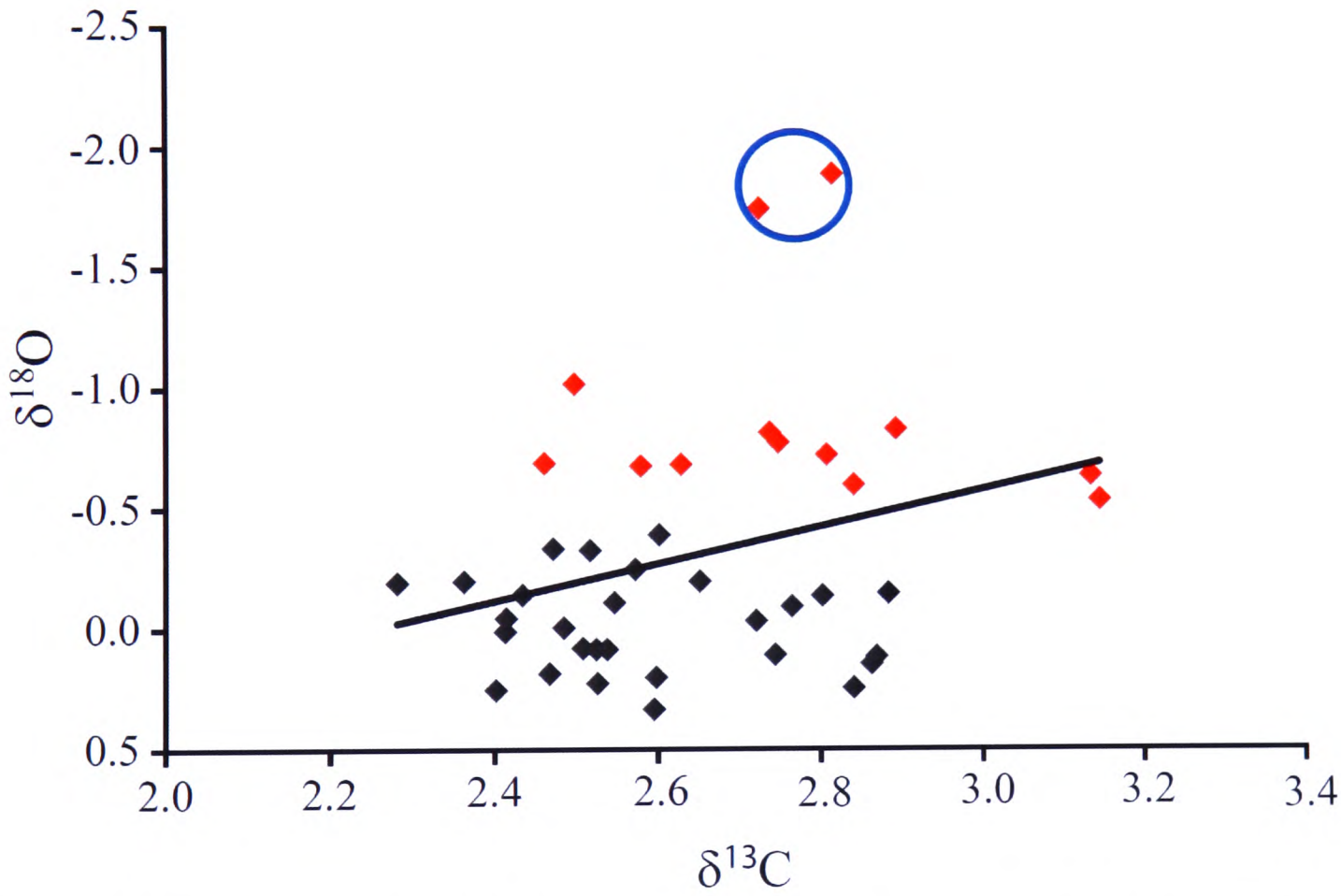

Figure 5-19 Showing the relationship between $\delta^{13}C$ and $\delta^{18}O$ for the Holocene and MIS 3 *Tridacna* sp. Holocene samples are marked in red diamonds and MIS3 samples with black diamonds.

5.6.3 Do *Tridacna* sp. record an accurate average climatic signal?

The reduction or shut down in growth across the shell of a bivalve with ontogeny then later stages of growth may not reproduce the full range of seasonal variability.

There are several causes for this in bivalves: Temperature (Kennish and Olsson, 1975; Jones *et al.,* 1978 and 1989; Romanek and Grossman, 1989; Elliot *et al.,* 2003), salinity and age and reproductive cycle (Hall *et al.,* 1975 and Sato 1995) and tidal cycles and changes in growth patterns through ontogeny. The most important of these is temperature and growth changes through ontogeny. Most bivalves secrete their shells in isotopic equilibrium with sea water over most or all of the year (Arthur *et al.,* 1983; Jones *et al.,* 1989), though bivalves may have growth breaks due to extreme temperature ranges. This is particularly observed in bivalves from high latitudes (e.g. Elliot *et al.*, 2003). Tropical bivalves are more likely to record year round environmental conditions (Aharon, 1991; Elliot *et al.,* 2003; Watanabe and Oba 1999). In many bivalves attenuation of growth occurs in later stages of ontogeny, the seasonal amplitudes thus become reduced due to reduced width of growth bands (Kennedy *et al.,* 2001) and the record may be biased towards the early stages of growth or a particular season of growth. None of the fossil specimens here are thought to be significantly older than 10 years, except in the case of a few *Tridacna gigas* samples. Furthermore, study of the modern *T. gigas* from Huon Peninsula using accurate sampling techniques do not show any significant attenuation of the $\delta^{18}O$ signal with ontogeny (Chapter 3; Aharon, 1991; Watanabe *et al.,* 2004 and Elliot *et al.,* [submitted]).

5.6.4 Growth patterns in *Tridacna maxima*

There are conflicting reports for different species of *Tridacna.* Romanek and Grossman (1989) show that $\delta^{18}O$ in the outer layer of *Tridacna maxima* specimens is able to record the full range of seasonal temperatures variations at Rose Atoll during the juvenile stages of life. Growth is inhibited during the adult phase due to high summer temperatures (up to 34°C). However, in the same study a sample collected from the lagoon channel where temperatures are cooler does not show this attenuation, (though it is only reaching the adult phase of growth when sampled). The growth pattern of the outer layer is complex in *Tridacna maxima*, producing scales on the outer surface, and may account at least in part for this attenuation of growth. Chakroborty and Romesh (1993) also show a $\delta^{18}O$ record from *Tridacna*

maxima which does not attenuate with time, however they do not indicate which part of the shell they sampled. It seems that the outer layer may not be a suitable area to sample and I obtained the $\delta^{18}O$ profiles from the inner layer and hinge area.

The *Tridacna maxima* samples T39 and T40 were seasonally sampled. There is a potential attenuation of $\delta^{18}O$ amplitude in sample T39, though only 8 years of growth is shown (Figure 5-12). T40 does not show reduced $\delta^{18}O$ however, the attenuation observed by Romanek may have occurred in later stages of life. Both records are short however (10 years or less).

Growth patterns in other Tridacna sp.

Unfortunately, modern $\delta^{18}O$ records are not available for other species of *Tridacna* used in this study. One fossil sample of *Tridacna crocea* (T 41) was examined in this study, and does not appear to show attenuation of seasonal amplitude, though it does also have a strong positive trend in $\delta^{18}O$ that is similar to trends observed in a sample of *Tridacna derasa* analysed by Elliot *et al.,* [in prep] shows a shift in average values after 10 years of growth in other samples and coral records (Tudhope *et al.*, 2001).

Given that there are apparent differences in growth patterns between species of *Tridacna* sp. I decided to check for a species bias by comparing the $\delta^{18}O$ results from the four species from similar time horizons: Holocene and MIS3 age terraces. (Figure 5-20 and Figure 5-21 and Table 5-2 and Table 5-3). There is only one *T. squamosa,* in each group, so it is no conclusions can be drawn about this species. There is no substantial offset observed between average $\delta^{18}O$ in Holocene and MIS 3 *Tridacna gigas, Tridacna maxima* and *Tridacna crocea.*

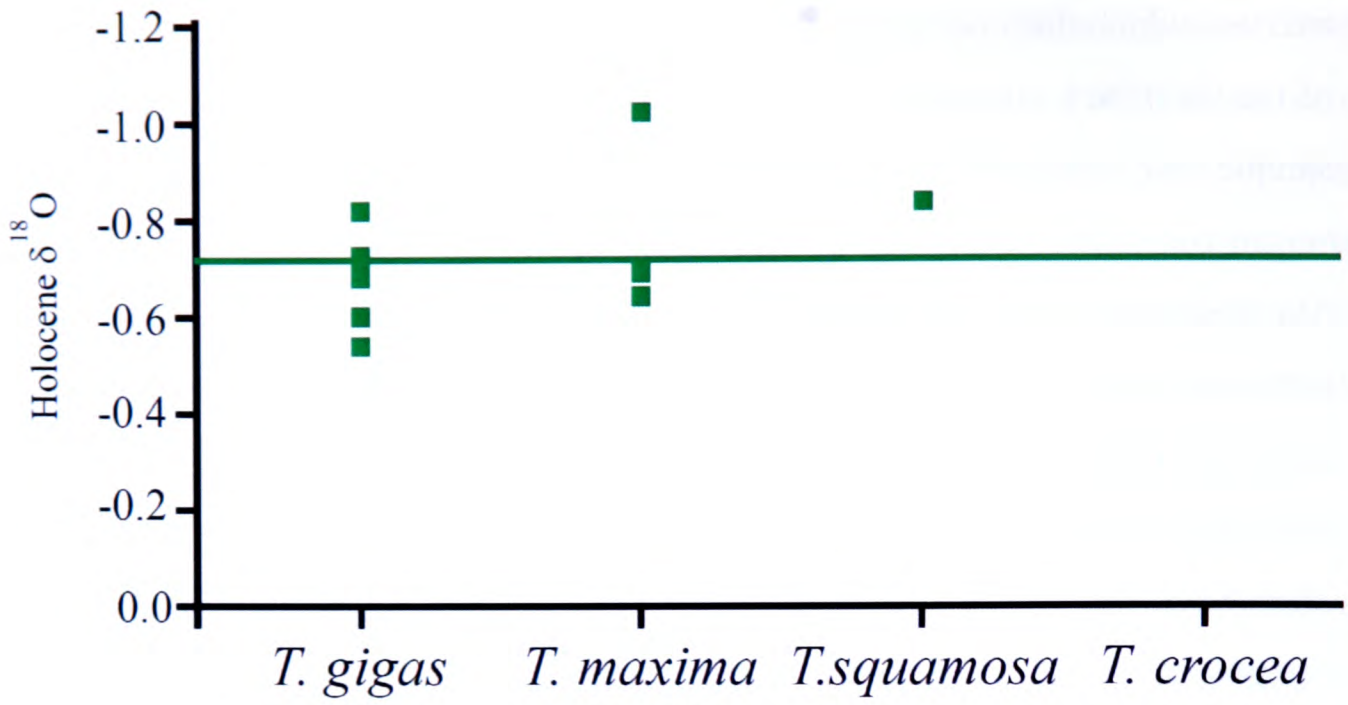

Figure 5-20 Bulk $\delta^{18}O$ results sorted by species for Holocene (minus T66 and T72 samples from lagoonal environments). Green line shows average values for the Holocene.

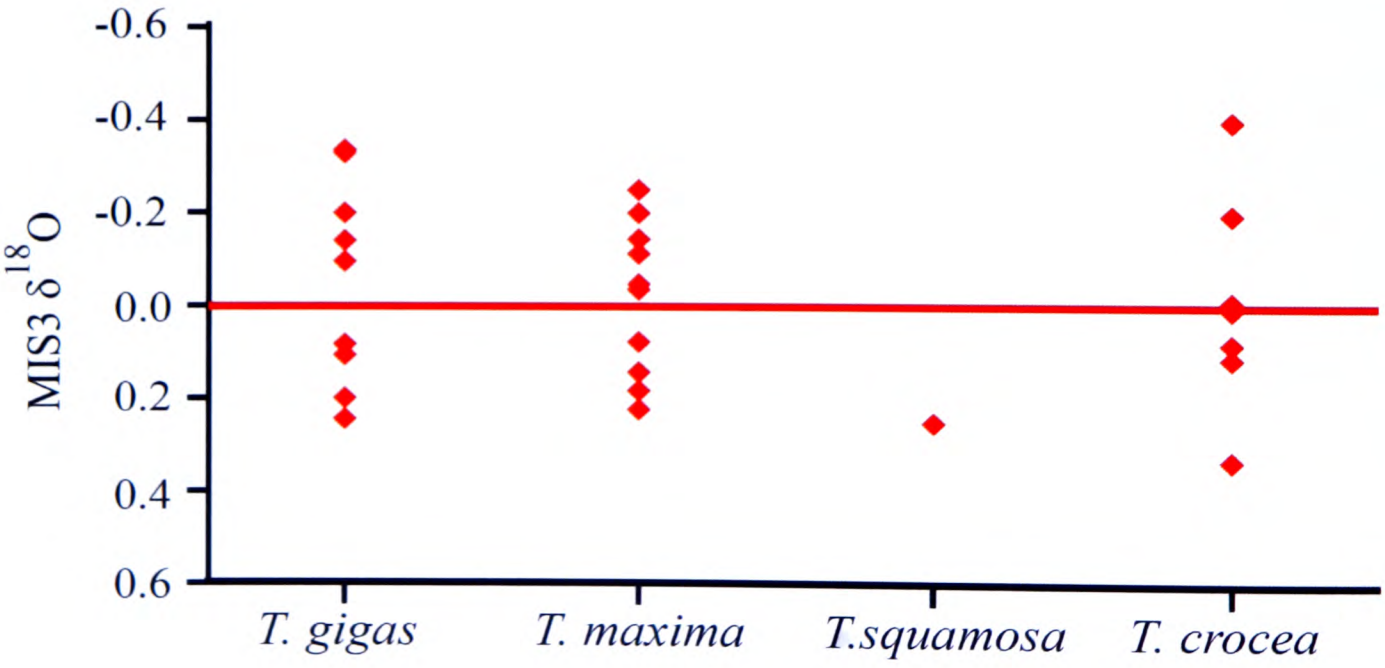

Figure 5-21 Bulk $\delta^{18}O$ sorted results by species for MIS 3 reefs. Red line shows average values for MIS3 samples.

Holocene	$\delta^{18}O = -0.7$	
Species	*T. gigas (n=6)*	*T. maxima (n=3)*
Mean $\delta^{18}O$ by Species	-0.7	-0.8
Holocene mean value – species mean value	-0.1	0.1

Table 5-2 Holocene mean $\delta^{18}O$ for each species compared to reef mean

MIS 3	$\delta^{18}O = 0.0$		
Species	*T. gigas (n=9)*	*T. maxima (n=11)*	*T. crocea (n=7)*
Mean $\delta^{18}O$ by Species	-0.1	0.0	0.0
MIS 3 mean value –species mean value	0.1	0.0	0.0

Table 5-3 MIS 3 mean $\delta^{18}O$ for each species compared to reef mean

5.6.5 Correcting for continental ice volume change

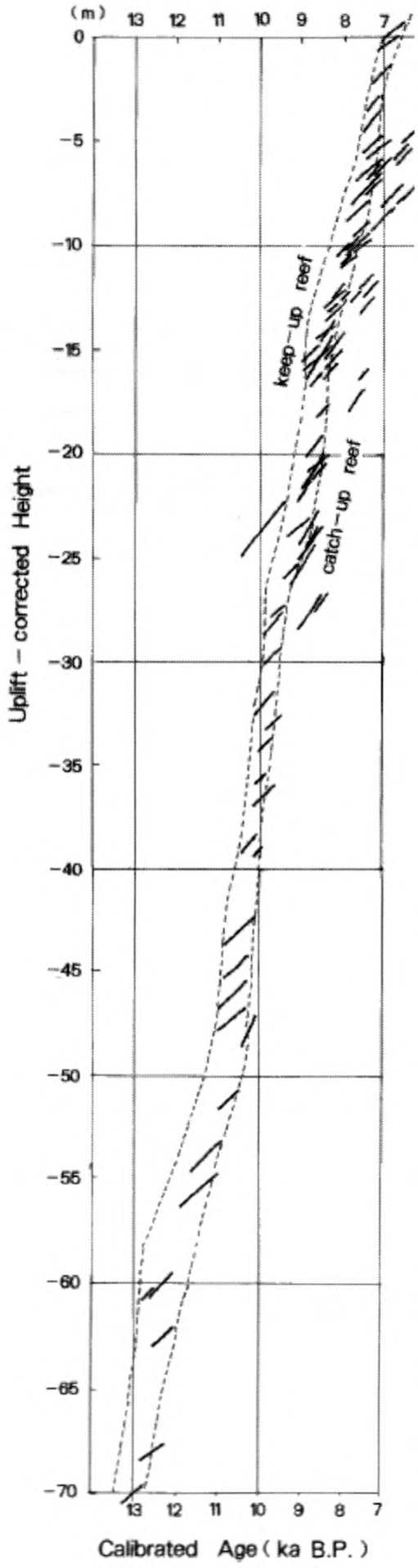

The sea level rose during the early Holocene, as continental ice sheets retreated and several studies have shown that global sea level varied on millennial timescales during MIS3 (Chappell *et al.*, 1996a; Yokoyama *et al.*, 2000; Siddall *et al.*, 2003; Arz *et al.*, 2007). As lighter isotopes tend to be transported to the poles, increases in continental ice volume increases the relative proportion of ^{18}O in the global oceans (Shackleton, 1967) and affects the global $\delta^{18}O$ of water from which *Tridacna* sp. precipitate their shells. Therefore, to extrapolate changes in temperature from *Tridacna* sp. $\delta^{18}O$ records we must account for changes to the global ocean $\delta^{18}O_w$.

Figure 5-22 Composite sea level curve from Ota and Chappell, 1999 based upon age-height-elevation relationships from the transgressive Holocene reef terraces at Huon Peninsula.

Changes in $\delta^{18}O$ in the global ocean can be calculated based upon estimates of sea level at the time of *Tridacna* sp. growth and the likely change in $\delta^{18}O$ of sea water per metre change in sea level ($\delta^{18}O_w$ m^{-1}). To calculate this we must use a reference period of known eustatic sea level change and known global $\delta^{18}O$ seawater composition.

Several authors have used the Last Glacial Maximum for this exercise (e.g. Waelbroeck *et al.*, 2002). Yokoyama *et al.*, (2000) assessment of sea level at the LGM of -130m and estimates of global sea water change at LGM of based upon Schrag *et al.*, (1996) measurement of + 1.1 ±0.2‰ in the pore waters of an Atlantic deep sea core. The relationship between continental ice volume and $\delta^{18}O$ of the oceans is not likely to be linear since the $\delta^{18}O$ of continental ice is subject to temporal variations (Mix and Ruddimann, 1984), however this non-linearity is thought to be very small (Waelbroeck *et al.*, 2002) a linear relationship between sea level and $\delta^{18}O$ at the LGM is therefore assumed. This provides an estimate of the relationship between sea level and $\delta^{18}O_w$ of 0.0085‰ ±0.0015 m^{-1}. Predicted $\delta^{18}O_w$ for sea water at Huon Peninsula during the last glacial cycle can be obtained by estimating the sea level at the time that each *Tridacna* sp. grew.

5.6.5.1 Correcting for ice volume effects in the Holocene

The early Holocene sea level change at Huon Peninsula has been extensively studied (Chappell and Polach, 1976, Chappell and Polach, 1991, Edwards *et al.*, 1993, and Ota and Chappell, 1999) using radiometrically dated coral and molluscs and several sea level curves have been established. Therefore it is possible to use a published sea level curve to accurately predict the $\delta^{18}O_w$ of sea water when the *Tridacna* sp. grew and remove this component from measured $\delta^{18}O$ (see above). The curve selected is reported in Ota and Chappell, (1999) (Figure 5-22).

Calculated $\delta^{18}O$ residual, corrected for the effect of sea level are presented in Table 5-4 and Figure 5-23. All corrected $\delta^{18}O$ values are consistently more positive relative to modern values of –1.2‰, indicating a cooler or drier climate than modern climate.

Sample	Original $\delta^{18}O$	Age ka (cal bp)	Age (ka error 2 sig)	Predicted sea level	Predicted $\delta^{18}O_w$	Residual Tridacna $\delta^{18}O$
T59	-0.84	7.03	0.16	0	0	-0.84
T60	-0.73	7.17	0.21	0	0	-0.73
T73	-0.60	7.28	0.12	-5	0.043	-0.64
T65	-0.64	7.45	0.21	-5	0.043	-0.69
T58	-0.82	8.09	0.15	-10	0.085	-0.90
T49	-0.54	8.33	0.35	-15	0.085	-0.63
T51	-0.68	8.73	0.24	-20	0.128	-0.81
T75	-0.69	8.76	0.24	-20	0.128	-0.81

Table 5-4 Results of removing the ice volume component from $\delta^{18}O_w$

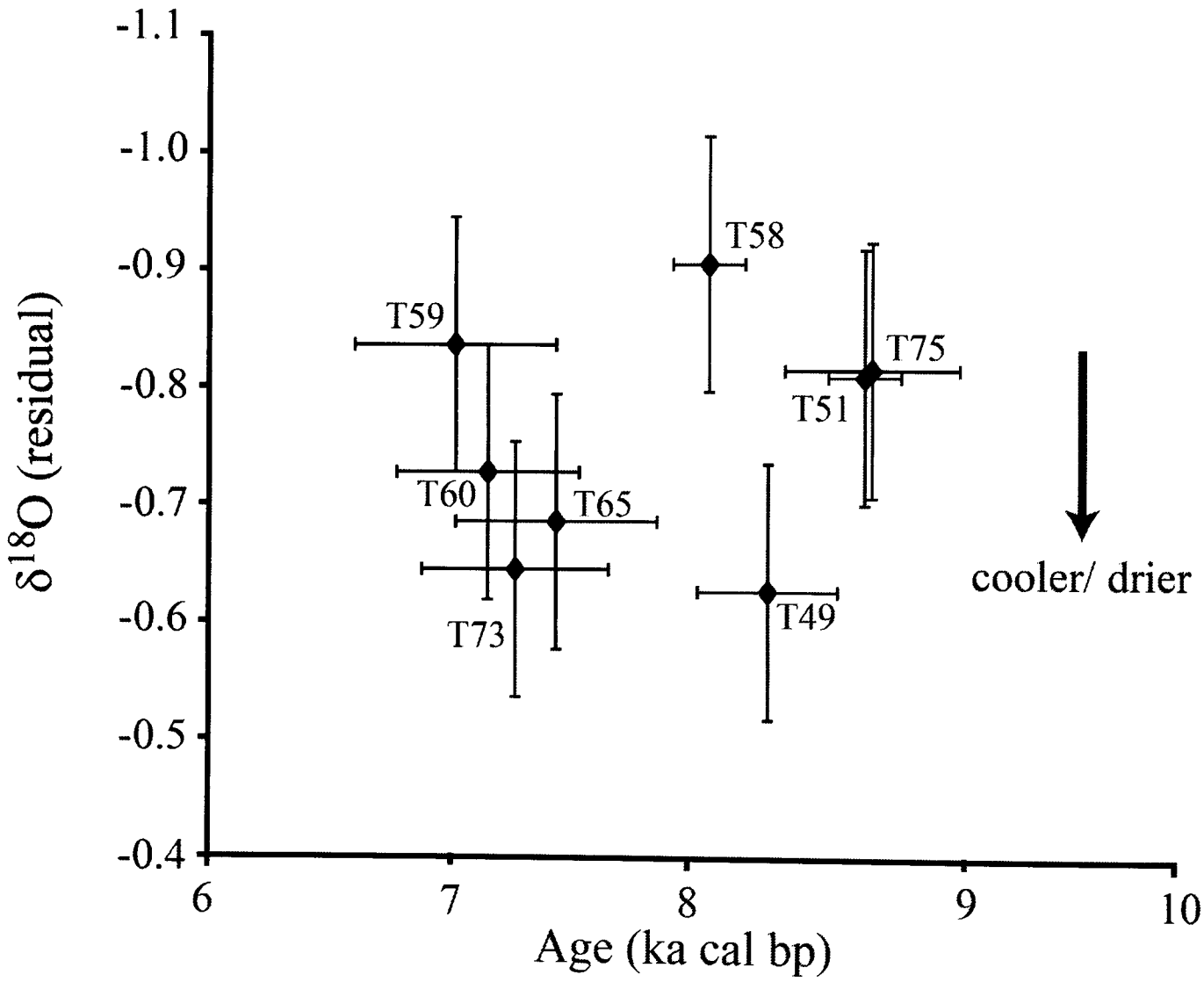

Figure 5-23 Residual $\delta^{18}O$ results of removing the ice volume component from $\delta^{18}O_w$ from Holocene *Tridacna* sp. Modern value is –1.2‰ Note that $\delta^{18}O$ axis is reversed.

5.6.5.2 Correcting for ice volume effects in MIS3

The same approach to removing the ice volume component was used as for the Holocene samples, though the error is higher due to uncertainties with age estimation. In Chapter 4 it was shown that sea level can be calculated if the current elevation and age and relative uplift at Bobongara are known accurately. The samples discussed here were collected from the same reefs that were used to calculate MIS3 change in sea level at Huon Peninsula (Chappell *et al.*, 1996a and Chappell, 2002). As shown in Chapter 4, the sea level reconstruction that is produced by Chappell (2002) and Siddall *et al.*, (2003) are very similar in terms of sea level peaks, and differ primarily in terms of low stands as reef material associated with lowstands are buried. Since the dating of these samples is based largely on age estimates from Chappell (2002) this sea level reconstruction is almost identical to the one produced from the MIS3 terraces. Results are presented in Table 5-5 and Figure 5-24.

Sample	Reef Terrace	Elevation (m)	Original $\delta^{18}O$	Age (ka cal bp)	Age uncertainty 2 σ (ka)	Predicated Sea Level	Predicted $\delta^{18}O_w$	Residual $\delta^{18}O$
T70	IIa	47	-0.30	36.56	0.91	-72	0.61	-0.91
T14	IIa	49	-0.14	36.66	0.89	-69	0.59	-0.73
T27	IIa	50	-0.34	36.80	0.91	-69	0.59	-0.92
T9	IIa	45	-0.11	37.79	1.02	-75	0.64	-0.39
T12	IIa	48	0.25	38.20	1.05	-76	0.64	-0.76
T11	IIa	47	-0.10	38.41	1.08	-79	0.67	-0.77
T31	IIIc	53	0.08	37.80	1.06	-65	0.56	-0.48
T33	IIIc(l)	51	0.17	41.39	1.52	-70	0.59	-0.42
T32	IIIc(l)	54	0.14	39.49	0.50	-70	0.59	-0.45
T34	IIIc(l)	52	0.22	38.06	1.14	-78	0.66	-0.44
T39	IIIc(u)	60	0.11	42.40	0.53	-70	0.59	-0.48
T40	IIIc(u)	56	-0.20	42.44	1.62	-77	0.65	-0.85
T24	IIIb	84	-0.39	44.93	-	-59	0.50	-0.89
T48	IIIb	80	-0.17	45.80	-	-66	0.56	-0.73
T37	IIIb	79	-0.03	46.02	-	-67	0.57	-0.61
T23	IIIa(l)	107	-0.19	49.00	-	-49	0.41	-0.61
T41	IIIa(l)	99	0.13	50.74	-	-58	0.50	-0.37
T42	IIIa(m)	117	-0.01	52.22	-	-49	0.42	-0.42
T15	IIIa(u)	138	-0.33	60.00	-	-53	0.45	-0.78
T22	IIIa(u)	138	-0.20	60.00	-	-53	0.45	-0.65
T44	IIIa(u)	138	-0.14	60.00	-	-53	0.45	-0.59
T6	IIIa(u)	135	0.08	60.65	-	-58	0.49	-0.41
T38	IIIa(u)	134	0.01	60.87	-	-60	0.51	-0.50

Table 5-5 Results of removing ice volume component from *Tridacna* sp. $\delta^{18}O$ from MIS 3 reefs. Note that uncertainty in age is not given for samples where age has been extrapolated from stratigraphic position (See text for explanation).

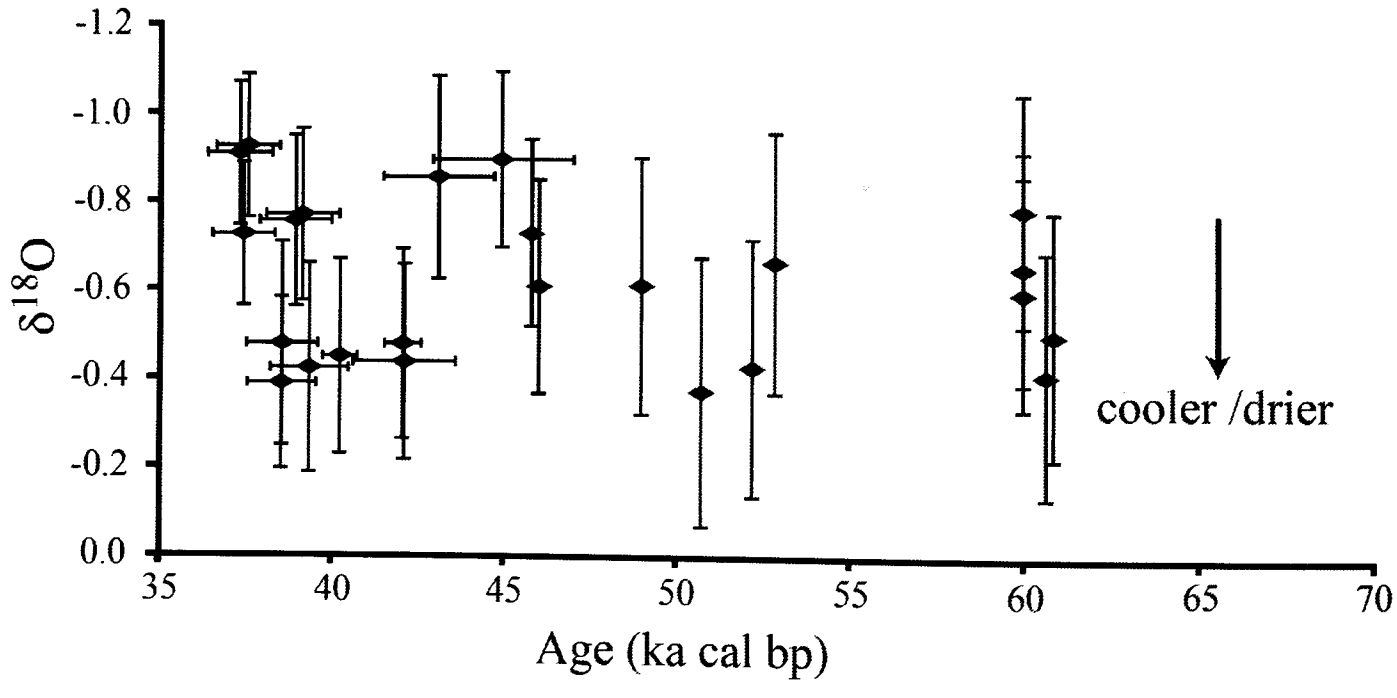

Figure 5-24 Bulk $\delta^{18}O$ results corrected for ice volume component from *Tridacna* sp. $\delta^{18}O$ from MIS3 reefs Modern values are –1.2‰. Note that $\delta^{18}O$ axis is reversed.

Determine the mean state of Glacial and Holocene WPWP climate

Having removed the component of $\delta^{18}O$ that is related to continental ice volume it is necessary to convert this residual into a meaningful proxy for climate. For the purposes of comparison it is first assumed that the $\delta^{18}O$ residual is due solely to temperature change, though it may be that there are significant changes in $\delta^{18}O_w$ due to evaporation/ precipitation changes. The reconstructed temperatures can then be compared with regional SST records. Temperatures were calculated from the temperature equation of Grossman and Ku (1986) for aragonitic species of bivalves and foraminifera:

Equation 4 $$T(^{o}C) = 21.8 - 4.69\,(\delta^{18}O_c - \delta^{18}O_w)$$

with a 0.2‰ correction for conversion between SMOW and PDB scales (see Bemis, 1998 for detailed explanation) we can extrapolate temperatures shown in Table 5-6.

Sample age	Holocene	MIS3 35-60 ka
$\delta^{18}O_c$ (measured)	-0.7‰	-0.1‰
$\delta^{18}O_w$ (predicted)	0.15‰	0.54‰
Temperature	26.2±0.5°C	25.6±0.9°C
Difference from modern values (29.1°C)	2.9±0.5°C	3.5±0.9°C

Table 5-6 showing mean measured $\delta^{18}O$ values, mean predicted $\delta^{18}O$ of sea water (assuming no change in evaporation/ precipitation balance) and mean predicted temperatures.

Combining an analytical error of 0.1‰ $\delta^{18}O$ and assuming a general sea level error of 20m for MIS 3 and 5m for the Holocene, this gives us an overall error in terms of temperature of 0.5°C and 0.9°C for the Holocene and MIS 3 respectively.

SST records have been obtained by analysing Mg/ Ca in planktonic foraminifera in sedimentary cores MD97 2140 (De Garidel-Thoron *et al.*, 2005) and ODP 806 (Lea *et al.*, 2000) (shown in Figure 5-1). Figure 5-25 shows that SST's are consistently warmer than estimates from *Tridacna* sp. During MIS3 temperatures predicted by *Tridacna* sp. are slightly lower than those from Mg/ Ca records in deep-sea cores

(3.5°C as opposed to 2-3°C shown by other studies). If SST's recorded at both core sites reflect SSTs at Huon Peninsula (i.e. there is no strong local temperature gradient) then the results presented here could suggest a shift evaporation/ precipitation balance that produces more positive $\delta^{18}O_w$, or more saline conditions, similar to El Niño events in the WPWP.

5.6.5.3 Reconstructed temperatures during the early to mid Holocene

The early to mid Holocene (≈9-7 ka) record shows average values that indicate a cooling of 2.9°C ±0.5, which is considerably more than indicated by other sources of SST for the early Holocene WPWP (Figure 5-25). SST's inferred from Mg/ Ca measurements on *G. ruber* in deep sea cores indicate approximately modern temperatures of 29°C in the Western Warm Pool. Other studies of the WPWP climate at this time also indicate warm and wet climate (Stott *et al.*, 2004; Brijker *et al.*, 2006 and Haberle *et al.*, 2001). It is unlikely that there is such a regional difference in temperature the Western Pacific Warm Pool, though in the modern climate salinity gradients dominate the surface hydrology of the WPWP (De Garidel Thoron *et al.*, 2007), therefore it is possible that some of the difference in reconstructed temperatures is related to changes in local $\delta^{18}O_w$, which is controlled by evaporation/ precipitation balance. One possibility is that there is reduced precipitation at Huon Peninsula. Brijker *et al.*, (2006) suggest that the low amplitude variability in $\delta^{18}O$ in cores from the Indo Pacific Warm Pool combined with a low peat charcoal records from Papua New Guinea (Haberle *et al.*, 2001) indicate a La Niña like mean climate during the Early Holocene, which is characterised by warmer/ wetter conditions. The data does not support this conclusion, and indicates a more El Niño-like mean climate.

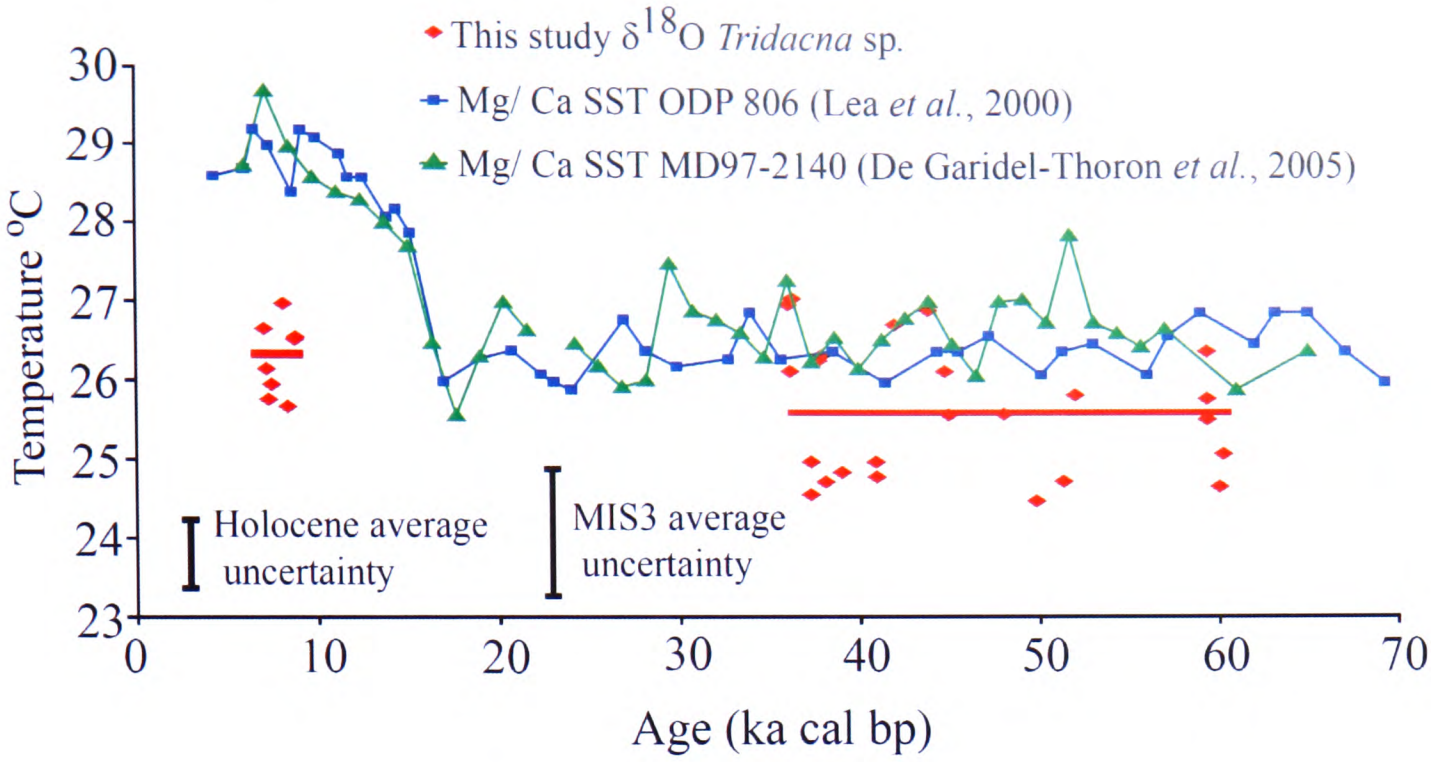

Figure 5-25 Reconstructed temperature from *Tridacna* sp. $\delta^{18}O$ corrected for ice volume. Also shown are SST records from the Mg/Ca *G. ruber* in Western Warm Pool from ODP 806 (Lea *et al.*, 2000) and MD97-2140 (De Garidel-Thoron *et al.*, 2005) (see Figure 2-2 for locations).

Offset between modern values (-1.2‰) and mean residual early to mid Holocene values (-0.8‰) is 0.4‰. Tudhope *et al.,* (2001) also show SST's of -0.9 to -1.3°C based upon $\delta^{18}O$ in corals (a relative change of +0.32‰) at 6.5 Ka. Assuming that temperatures are similar to modern, this implies an increase in salinity of approximately 1.5‰ p.s.u. (according to relationship for the Tropical Pacific calculated by Fairbanks *et al.*, 1997 of 1‰ p.s.u. = 0.273‰ $\delta^{18}O$). Using modelled $\delta^{18}O$ results from a coupled ocean-atmosphere GCM, Oppo *et al.*, (2007) show an increase in salinity of 0.5-0.7 p.s.u., which is considerably lower than that implied by these results. However, Oppo *et al.,* (2007) also predict a change in the $\delta^{18}O$ of WPWP precipitation during the mid Holocene which may account for some of the difference between predicted and measured $\delta^{18}O$.

5.6.5.4 Reconstructed temperatures during MIS3

The mean reconstructed temperature for MIS3 (37.5 to 61 ka) from $\delta^{18}O$ *Tridacna* sp. is an average of 25.6°C ±0.9, with a range of 27.1 to 24.5°C (assuming constant $\delta^{18}O_w$ due to changes in evaporation/ precipitation). Average reconstructed temperatures from Mg/ Ca in the cores MD97-2140 and ODP 806 are 26.8°C ±0.6

and 26.4°C±0.6 respectively (Figure 5-25). Whilst the uncertainty in these results is relatively high, this implies cooler SST in the WPWP than indicated by the Mg/ Ca records, if we assume that the difference is caused entirely by temperature.

Assuming an average temperature of 26.6°C in the WPWP, based upon Mg/Ca reconstructions in these cores, and using the temperature equation from Grossman and Ku (1986) a mean residual $\delta^{18}O$ of –0.8‰ for MIS3 *Tridacna* sp. would be predicted. Residual mean $\delta^{18}O$ from *Tridacna* sp. is -0.6‰ (0.2‰ difference). Making the assumption that the difference between the temperature reconstructions is from changes in evaporation/ precipitation balance, then using the same relationship of $\delta^{18}O_w$ to salinity I predicted an increase in salinity of approximately 0.7 p.s.u.

This is consistent with estimates for WPWP salinity change during the last glacial cycle from the west of WPWP (Stott *et al.*, 2002), but not the east of the WPWP (Lea *et al.,* 2000) where combined $\delta^{18}O$ and Mg/ Ca measurements indicate a freshening during glacial periods. De-Garidel Thoron *et al.*, (2007) point out that the core site analysed in Lea *et al.,* (2000) (ODP 806) on the Ontong-Java Plateau has decreased salinity during El Niño events, as the main zone of high precipitation moves towards the centre of the tropical Pacific due to the relaxation o trade winds. These results are therefore consistent with an overall "El Niño-like" mean state during MIS3, if the difference between temperature reconstructions from Mg/ Ca in foraminifera and *Tridacna* sp. is entirely due to changes in $\delta^{18}O_w$.

Summary of bulk $\delta^{18}O$ results

Early to mid Holocene *Tridacna* sp. $\delta^{18}O$ indicate a significantly cooler or drier climate in the Western Pacific Warm Pool than indicated by Mg/ Ca ratios from planktonic foraminifera. If we assume that there are no strong regional temperature gradients at this time, then it must be concluded that a drier climate/ more saline surface waters existed, as predicted by model results (Brown *et al.,* 2006; Oppo *et al.*, 2006).

In the glacial period the results indicate a similar or slightly greater degree of cooling than temperature reconstructions derived from Mg/Ca in sediment cores. This may be accounted for by a reduction in precipitation and infers a mean climate that is more El Niño-like.

5.7 Change in interannual variability during the Holocene and Glacial periods

The seasonally resolved $\delta^{18}O$ records collected from *Tridacna* sp. were interpolated to seasonal records (4 samples per year) to allow them to be compared with published *Porites* coral $\delta^{18}O$ records from Huon Peninsula. These seasonally resolved records were then filtered to removed all variability outside of the 2.5-7 year (ENSO) band using a Gaussian filter in Analyseries 1.1 (Paillard and Labeyrie, 1996). The results of both of these steps can be seen in Figure 5-26.

Figure 5-26 (This page and over) *Tridacna* sp. $\delta^{18}O$ seasonally resolved and resampled data (4 samples per year) (thin red line) and band pass filter at the 2.5 to 7 year (ENSO) band (thick black line).

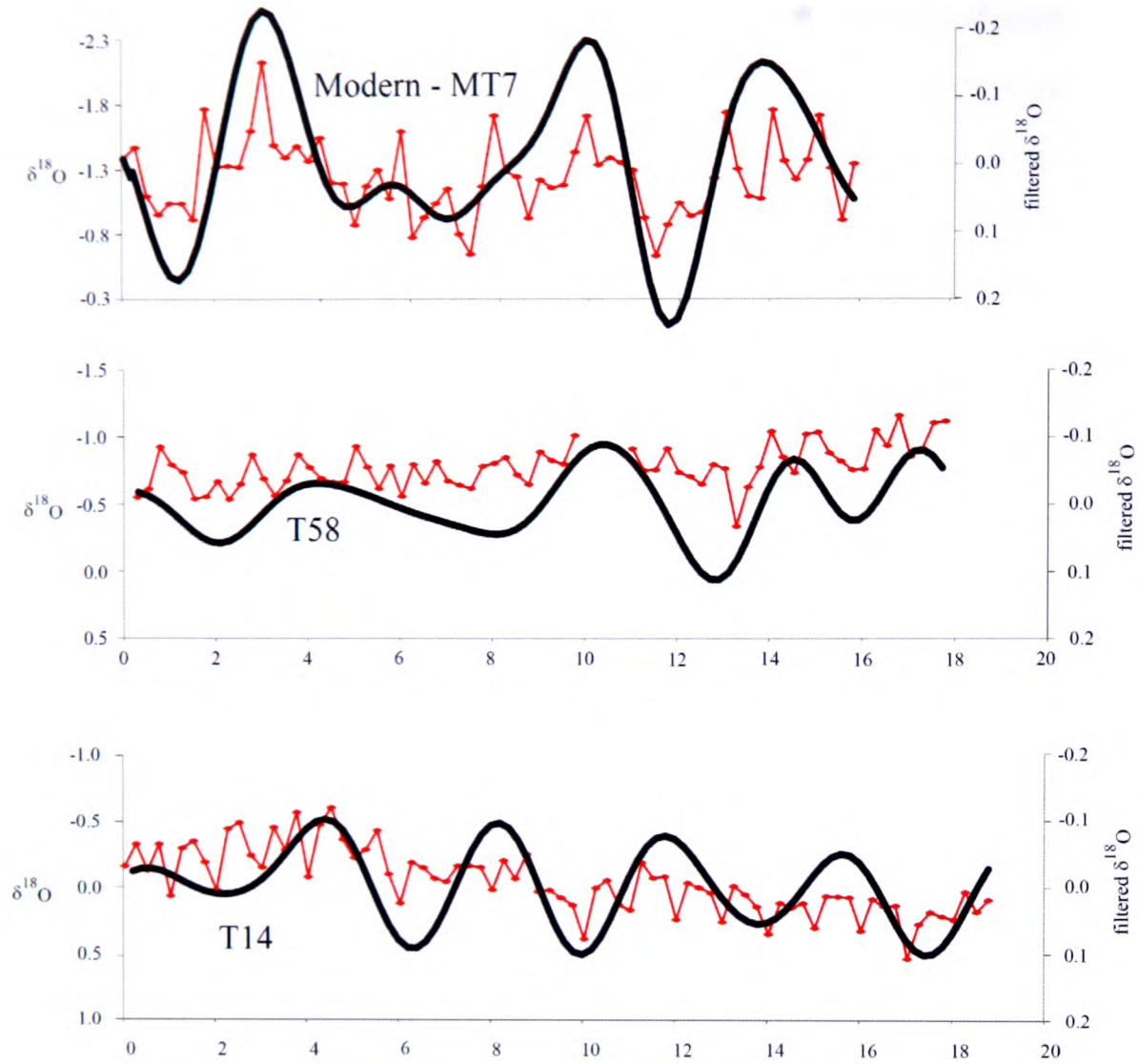
Modern - MT7
T58
T14
δ18O
filtered δ18O

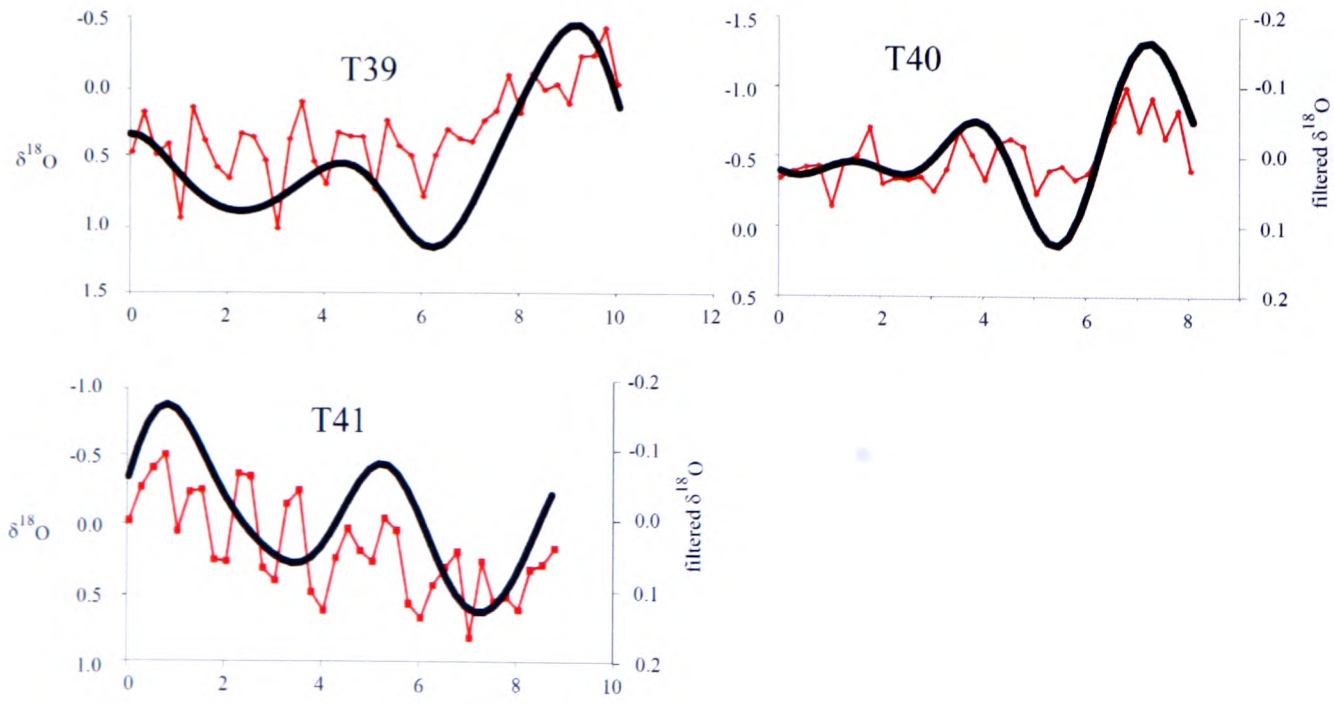
T39
T40
T41
δ18O
filtered δ18O

The band pass filtering removes variability at intra-annual (seasonal) and decadal timescales. To compare relative amounts of ENSO "strength" the standard deviation of the bandpass filtered records was obtained. As this is the same procedure used by Tudhope *et al.*, (2001) and we have shown in Chapter 4 that $\delta^{18}O$ time series from modern *Tridacna gigas* from the Huon Peninsula reflect ENSO similarly to corals it is reasonable to compare these records, with the caveat that shown here are too short to be statistically significant and also multiple species are used.

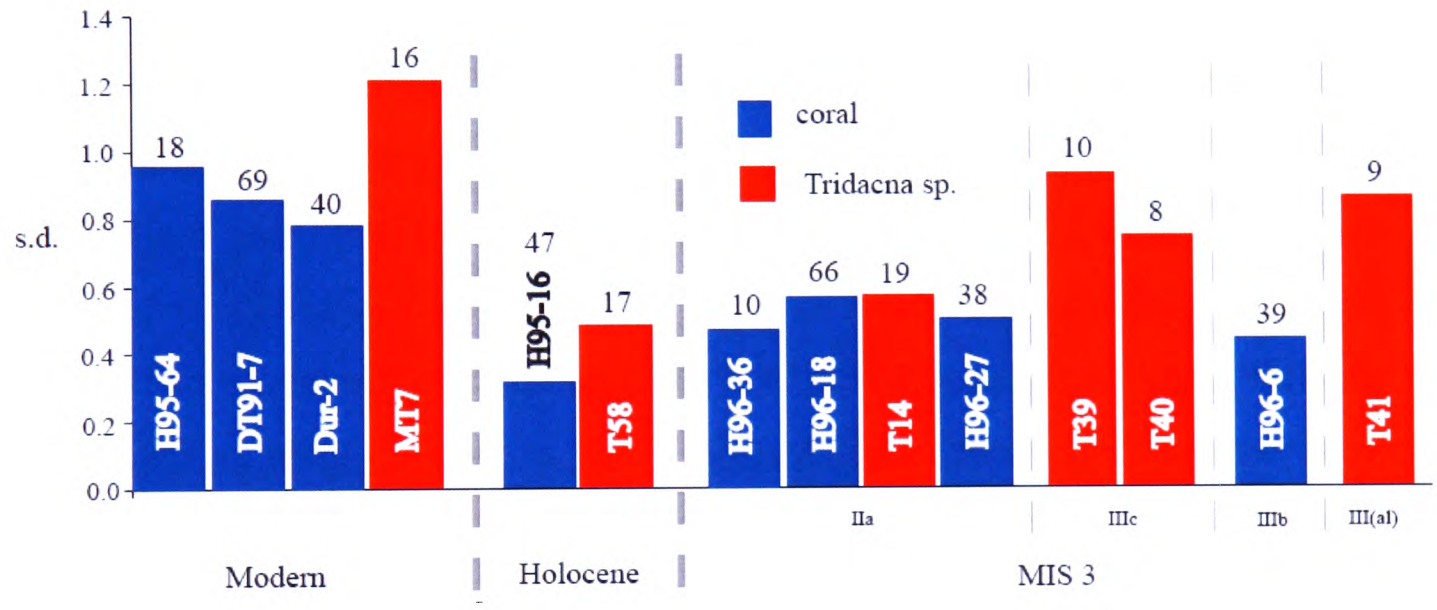

Figure 5-27 Showing the standard deviation of bandpass filtered $\delta^{18}O$ from published coral records (Tudhope *et al*, 2001) and *Tridacna* sp. collected from Huon Peninsula (this study). The results are presented by reef terrace. Black numbers indicate the length of the record that was bandpassed in years. Other numerals refer to the name of each sample.

The results shown in Figure 5-27 give an estimation of the variability of ENSO as it shows the variability represented in each *Porites* or *Tridacna* sp. time series at the ENSO bandwidth. The results presented here are relatively consistent with those from *Porites*. The standard deviation (s.d.) derived from the modern sample is higher than those seen in modern *Porites*. This is probably because Tg-MT7 grew during two of the strongest El Niño events in the last century (1986/87 and 1996/97). None of the modern corals grew during the 1996/97 El Niño event. From this we can

conclude that using short records for band pass studies may give anomalous results; again this is likely due to the fact that the records are too short to be of statistical significance.

Tridacna gigas, T58 from the Holocene shows a suppressed ENSO variability shown also by other coral records from the early Holocene of the WPWP (McGregor *et al.*, 2004) though not as great as that implied by the coral H95-16. A potential explanation for this is that there is a one year gap in the record, which may have affected the band pass analysis. The 19 year long *Tridacna gigas* T14 from terrace IIa shows a suppressed variability in the ENSO band that is seen in *Porites* from the same terrace.

The results of this exercise can be compared to a modelled prediction of ENSO variability in the same way as Tudhope *et al.*, (2001). ENSO variability has been modelled for the last glacial cycle by Clement *et al.*, (1999) using the Zebiak-Cane simple coupled ocean-atmosphere model which is forced by Milankovitch variations in solar insolation. Clement *et al.*, (1999) found that the frequency of ENSO events was dominated by precessional forcing. This is can be shown as ENSO "power" which is estimated by x100 times the variance of the 2.5 to 7 year band output of SST anomalies in the Niño 3.4 box from the model which gives an output which represents a prediction of ENSO variability (Clement *et al.*, 1999 and Tudhope *et al.*, 2001).

Figure 5-28 is a composite diagram showing variations in ENSO "power" predicted from the model over the last 70 ka (bottom), compared with s.d. of band pass filtered *Porites* and *Tridacna* $\delta^{18}O$ time series (middle) and temperature reconstructions from Mg/ Ca sediment core records and *Tridacna* $\delta^{18}O$. Higher s.d. reflects increased variability in the ENSO band, and therefore an increase in the number of El Niño events.

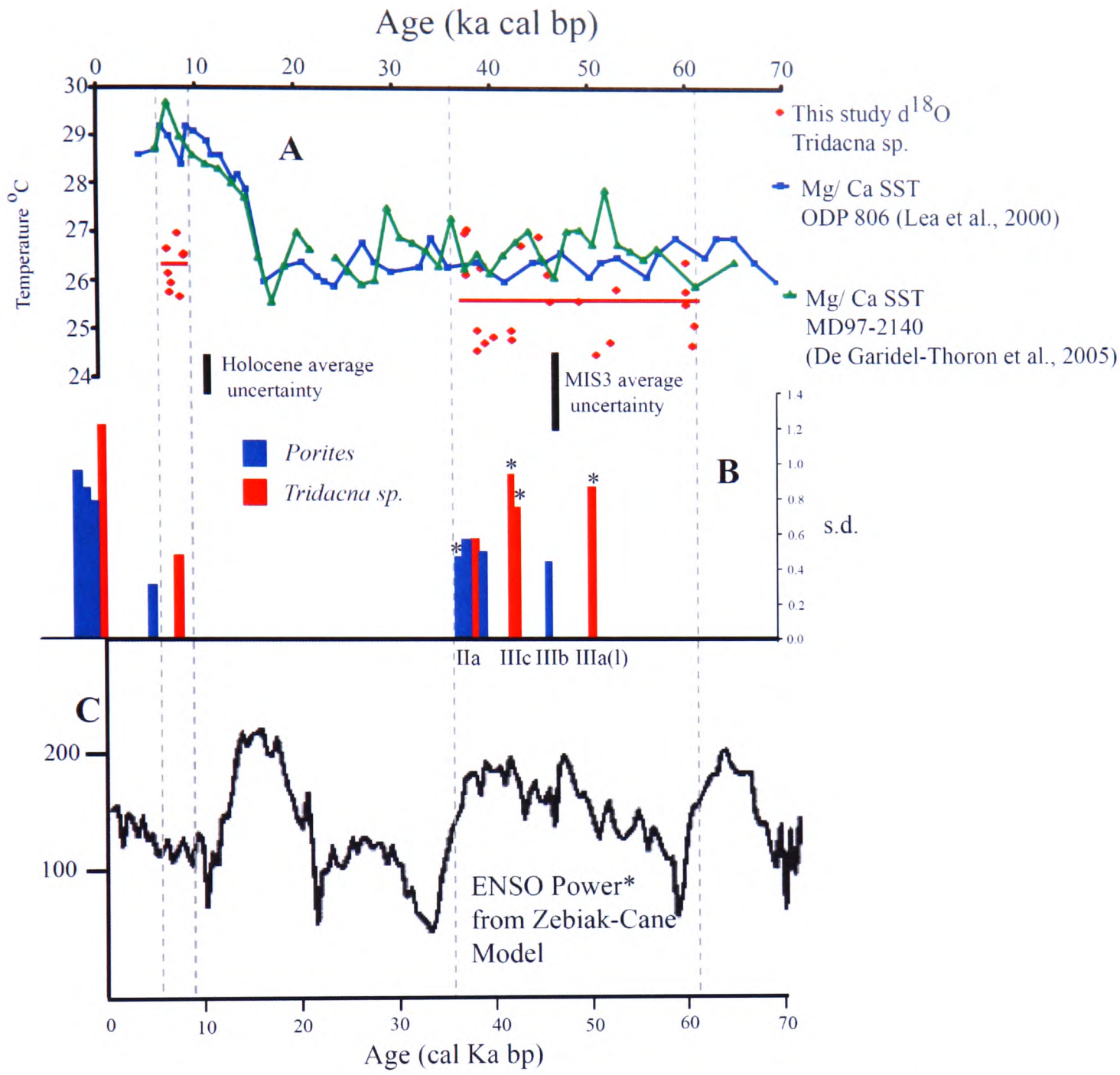

Figure 5-28 A: Temperature reconstruction from $\delta^{18}O$ *Tridacna* sp. (This study) and Mg/ Ca from deep sea cores in the Western Warm Pool. B. Standard deviation of (2.5 to 7 year Gaussian bandpassed) $\delta^{18}O$ time series from *Porites* coral (from Tudhope *et al.*, 2001) and *Tridacna* sp., (this study) (*indicates records of 10 years of less). C: ENSO "power" from Zebiak-Cane Model forced with orbital parameters (Clement *et al.*, 1999). Power is approximately the x100 variance in the 2.5-7 year band of (multitaper spectral analysis of non-overlapping 512 segments) model Niño 3.4 SST index.

Figure 5-28 shows that the results of band bass filtering of *Tridacna* sp. records are consistent with results already obtained from *Porites*. The highest ENSO variability is indicated during the present day and the lowest during the mid Holocene. ENSO variability during MIS3 is generally not as high as expected from the model (which predicts higher than modern variability). Combined with low variability during the Holocene, bulk values indicate cooler or drier climate than indicated by Mg/ Ca

sediment core records, whilst during MIS 3 only slightly drier or cooler values are indicated.

Brown *et al.*, (2006) compare a coral record of ENSO from Huon Peninsula from 6.5 ka and model predictions from the coupled ocean-atmosphere HADCM3 model for the early Holocene. This model predicts a 10% reduction in ENSO activity caused by orbital variation, which is much lower reduction than those shown by the coral (60%) reduction. The $\delta^{18}O$ record from *Tridacna gigas* T58 (8.09 ±0.08 cal ka), shows very similar variability as the coral record from Brown *et al.* (2006) (H95-16 and T58 in Figure 5-28) in terms of interannual variability and low number of extreme events (0 in H95-16 and 1 in T58). Brown *et al.* (2006) suggest that the reason for this difference between predicted and measured amplitude of ENSO strength may be due to shifts in local precipitation during the mid Holocene. A shift the position of region of highest precipitation away from the Huon Peninsula means that any observed ENSO variation appears dampened as a significant proportion of the variability seen in proxy records from this region is due to interannual variations in $\delta^{18}O_w$, which is controlled by evaporation/ precipitation balance. This assumption is supported by the bulk $\delta^{18}O$ which implies a drier climate at Huon Peninsula for the early to mid Holocene (8.76 ka to 7.03 ka).

The amount of charcoal in peat is thought to be linked to ENSO variability as during El Niño event extreme drying causes greater incidence of fire in Indonesia and Papua New Guinea and an increase in charcoal deposited in bogs. Haberle *et al.* (2001) show low peat charcoal during the period 9-6 ka, which they infer as warmer wetter and more stable climate associated with reduced ENSO activity. A possible way of explaining the low charcoal records in Papua New Guinea in terms longer term drying is that they are responding to a dry, but relatively stable climate where there are few extreme events. We can see therefore that the mean state of the climate and the frequency or strength of ENSO is related in the Early Holocene.

The variability in temperatures produced from $\delta^{18}O$ *Tridacna* sp. in MIS3 appears greater than during the Holocene and the Mg/ Ca produced MIS3 SST record. The

Tridacna sp. records shown here average 10 years in length and incorporate changes in $\delta^{18}O_w$. The combination of these factors means that they more likely to be sensitive to interannual variations in climate than the SST records derived from foraminiferal Mg/ Ca. Clement *et al.*, (1999, 2000) predict an increase in ENSO (compared with modern) activity during parts of MIS3. This may provide an explanation for the greater variation in reconstructed temperatures.

The results in MIS 3 show much greater variability between reefs when *Tridacna* sp. results are included. IIa and IIIb reef terraces have been previously shown to be coeval with perturbations on the thermohaline circulation during the Heinrich events (Chappell 2002). The s.d. for two of the *Tridacna* sp. found in the terraces IIIc and IIIa(l) is almost as great as that found in the modern *T. gigas* from Huon Peninsula, and greater than the modern coral s.d. suggesting that there may be more variability in the strength of ENSO during MIS3 than previously reported by Tudhope *et al.* (2001) in response to factors other than insolation. However, these two records are eight and nine years long. Since this is approaching the bandwidth that has been filtered these results cannot be considered statistically significant and would have to be confirmed by future studies using longer records.

5.8 Conclusions

Stable isotopes analysis of *Tridacna* sp. from uplifted coral terraces on the Huon Peninsula, Papua New Guinea have been used to reconstruct past climates during the early to mid Holocene and Marine Oxygen Isotope Stage 3. Comparison of different species do not appear to show consistent species bias in $\delta^{18}O$, suggesting that there are no strong offsets related to different species.

Using an estimation of sea level, *Tridacna* sp. $\delta^{18}O$ values were corrected for variations in ice volume and converted to temperature estimates, assuming local $\delta^{18}O_w$ (i.e. evaporation/ precipitation balance) to be constant. Comparing these results with other SST reconstructions from the Western Pacific Warm Pool show slightly cooler temperatures during MIS3 and significantly cooler temperatures

during the early to mid Holocene. As changing $\delta^{18}O_w$ in surface waters also controls $\delta^{18}O$ in marine carbonate, this suggests that the WPWP was slightly more saline due to reduced precipitation/ enhanced evaporation during MIS 3. These results also indicate a more "El Niño-like" mean state, and significantly more saline surface waters during the early Holocene, suggesting a large change in precipitation patterns in the WPWP. This corresponds well to the conclusions of Oppo *et al.,* (2007) who suggest that during the mid Holocene: a) there is a change in the relationship between $\delta^{18}O_w$ and surface salinity and b) a stronger Asian Monsoon will cause more moisture to be transported to the Indian Ocean, with an increase in continental precipitation at the expense of maritime precipitation.

Comparison of bandpass filtered $\delta^{18}O$ time series with a previous study for Huon show very similar results in terms of ENSO variability. The early to mid Holocene shows a suppressed ENSO, as predicted by modelling studies forced by changes in insolation.

Results from Marine Oxygen Isotope Stage 3 support the previous findings of Tudhope *et al.* (2001) that contrary to modelled predictions, ENSO activity is more suppressed than expected based upon changes in insolation alone and that increased trade winds during the glacial period dampen ENSO activity.

The variability of ENSO observed in T40 and T41 is slightly higher than that seen in MIS3 *Porites*. It is worth noting that Terraces IIa and IIIb, which display lower ENSO variability, have been shown to be coeval with Heinrich Events 4 and 5 respectively by Chappell (2002). Various modelling studies have suggested that ENSO should be reduced in strength or frequency during stadials in the North Atlantic region (e.g. Ivanochko, *et al.*, 2005 or Timmermann *et al.*, 2005a, 2005b and 2007).

References

Aharon, P., Chappell J. and Compston, W. (1980), Stable Isotope and Sea-Level Data from New-Guinea Supports Antarctic Ice-Surge Theory of Ice Ages, *Nature*, **283**, 549-651

Aharon, P. (1983), 140,000-Yr Isotope Climatic Record from Raised Coral Reefs in New-Guinea., *Nature*, **304**, 720-723

Aharon, P., and J. Chappell (1986), Oxygen Isotopes, Sea-Level Changes and the Temperature History of a Coral-Reef Environment in New-Guinea over the Last 105 Years, *Palaeogeography Palaeoclimatology Palaeoecology,* **56**, 337-379

Aharon, P. (1991) Recorders of reef environmental histories: stable isotopes in corals, giant clams and calcareous algae. *Coral Reefs*, **10**, 71-90

An, S.-I., Timmermann, A., Bejarano, L. Jin, F.-F. Justino, F. Liu, Z. and Tudhope, A. W. (2004), Modelling evidence for enhanced El Niño–Southern Oscillation amplitude during the Last Glacial Maximum, *Paleoceanography,* **19**, PA4009

Andreasen, D.J., Ravelo, A.C. and A.J. Broccoli (2001), Remote forcing at the Last Glacial Maximum in the tropical Pacific Ocean. *Journal of Geophysical Research.* **106**, 879-898

Arthur, M.A., Williams, D.F. and D.S. Jones, (1983) Seasonal temperature-salinity changes and thermocline development in the Mid-Atlantic Bight as recorded by the isotopic composition of bivalves, *Geology,* **11**, 655-659

Beaufort, L., Garidel-Thoron, T.d., Mix, A.C. and N. G. Pisias (2001), ENSO-like forcing on oceanic primary production during the late Pleistocene, *Science,* **293**, 2440–2444

Bonham, K. (1965), Growth rate of Giant Clam *Tridacna gigas* at Bikini Atoll as revealed by Radioautography, *Science.* **149**, 300-302

Brijker, J.M., Jung, S.J.A., Ganssen, G.M., Bickert, T and Kroon, D. (2006) ENSO related decadal scale climate variability from the Indo-Pacific Warm Pool. *Earth and Planetary Science Letter,* **253** 67-82

Brown, J., Collins, M and A. Tudhope (2006), Coupled model simulations of mi-Holocene and comparisons with coral oxygen isotope records, *Advances in Geosciences*, **6**, 29-33

Chakroborty, S. and R. Romesh (1993), Monsoon induced sea surface temperature changes recorded in Indian corals, *Terra Nova*, **5**, 545-551

Chappell, J. (1974), Geology of Coral Terraces, Huon-Peninsula, New-Guinea - Study of Quaternary Tectonic Movements and Sea-Level Changes, *Geological Society of America Bulletin*, **85**, 553-570

Chappell, J. and H. A. Polach, (1972), Some effects of partial recrystallisation on C^{14} dating late Pleistocene corals and molluscs, *Quaternary Research*, **2,** 244-252

Chappell, J., and H. A. Polach, (1976), Holocene sea level change and coral reef growth at Huon Peninsula, Papua New Guinea. *Geological Society of America Bulletin,* **87**, 235-240

Chappell, J., and H. Polach, (1991), Post-glacial sea level rise from a coral record at Huon Peninsula, Papua New Guinea, *Nature,* **349**,147-149

Chappell, J., Omura, A., Esat, T. M., McCulloch, M. T., Pandolfi, J., Ota Y., and B. Pillans, (1996a), Reconciliation of late Quaternary sea levels derived from coral terraces at Huon Peninsula with deep sea oxygen records. *Earth and Planetary Science Letters,* **141**, 227-236.

Chappell, J. (2002), Sea level changes forced ice breakouts in the Last Glacial cycle: new results from coral terraces, *Quaternary Science Reviews*, **21**, 1229-1240

Clement, A. C., Cane, M. A., and A. Seager (2001), An orbitally driven tropical source for abrupt climate change, *Journal of Climate*, **14**, 2369-2375

Clement, A. C., Seager, A and M.A. Cane (1999), Orbital controls on the El Niño/Southern Oscillation and the tropical climate, *Paleoceanography*, **14**, 441-457

Clement, A. C., Seager, A and M.A. Cane (2000), Suppression of El Niño during the mid-Holocene by changes in the Earth's orbit, *Paleoceanography*, **15**, 731-737
CLIMAP Project Members (1981), The surface of the ice-age earth. *Science*, **191**, 1131-1137.

de Garidel-Thoron, T., Rosenthal, Y., Bassinot, F., and L. Beaufort (2005), Stable sea surface temperatures in the western Pacific warm pool over the past 1.75 million years, *Nature*, **433**, 294-298

de Garidel-Thoron, T., Y. Rosenthal, L. Beaufort, E. Bard, C. Sonzogni, and A. C. Mix (2007), A multiproxy assessment of the western equatorial Pacific hydrography during the last 30 kyr, *Paleoceanography*, **22**, 3204-322

Edwards, R. L., Beck, J.W., Burr, G.S., Donahue, D.J., Chappell, J.M.A., Bloom, A.L., Druffell, E.R.M., and F.W. Taylor. (1993), A Large Drop in Atmospheric C-14/C-12 and reduced melting in the Younger Dryas, documented with Th-230 Ages of Corals, *Science*, **260**, 982-986

Elliot, M. Welsh, K. Chilcott, C., MuCulloch, M., Chappell, J and Ayling, B. Profiles of trace elements (Mg/ Ca, Sr/ Ca and Ba/ Ca) derived from giant long lived *Tridacna gigas* bivalves. (Submitted to *Geochimica et Cosmochimica Acta*)

Elliot, M., de Menocal, P.B., Linsley, B.K. and Howe, S.S. (2003) Environmental controls on the stable isotope composition of *Mercenaria mercenaria*: Potential application to palaeoenvironmental studies. *Geochemistry, Geophysics, Geosystems*, **4**, 1056

Fairbanks, R.G., M.N. Evans, J.L. Rubenstone, K. Broad, M.D. Moore, C.D. Charles, (1997), Evaluating climate indices and their geochemical proxies measured in corals. *Coral Reefs*, **16**, 93-100

Gagan, M.K., Ayliffe, L.K., Hopley, D., Cali, J.A., Mortimer, G.E., Chappell, J., McCulloch, M. T. and M.J. Head (1998), Temperature and Surface-Ocean Water Balance of the Mid-Holocene Tropical Western Pacific, *Science*, **279**, 1014-1017

Grossman E.L. and T.L. Ku (1986) Oxygen and carbon fractionation in biogenic aragonite: temperature effect, *Chemical Geology*, **59**, 59–74

Haberle, S.G., Hope, G.S. and W.A. van der Kaars, (2001), Biomass burning in Indonesia and Papua New Guinea: natural and human induced fire events in the fossil record. *Palaeogeography, Palaeoclimatology, Palaeoecology*, **171**, 259–268

Hall, J.R., Dollase, C.R. and Corbato, C.W. (1974) Shell growth in *Tivela stultorum* (Mawe, 1823) and *Callista chione* (Linnaeus, 1758) (Bivalvia): Annual periodicity, latitudinal differences and diminuation with age: *Palaeogeography, Palaeoclimatology and Palaeoecology*, **15**, 33-61

Ivanochko, T.S., Ganeshram, R.S., Brummer, G.-J.A., Ganssen, G., Jung, S.J.A., Moreton S.G. and D. Kroon, (2005), Variations in tropical convection as an amplifier of global climate change at the millennial scale, *Earth Planetary Science Letters*, **235**, 302–314

Jones, D.S., Thompson, I and Ambrose, W. (1978), Age and growth rate determinations for the Atlantic surf bivalve *Spisula solidissima* (Bivalvia: Mactracea) based on internal growth lines in the shell cross-section, *Marine Biology*, **47**, 63-70

Jones, D.S., Arthur, M.A. and Allards, D.J. (1989), Sclerochronology of records of temperature and growth from shells of *Mercenaria mercenaria*. Narragansett Bay, Rhode Island. *Marine Biology*, **102**, 225-234

Kennedy, H., Richardson, C.A., Duarte, C.M. and Kennedy, D.P. (2001), Oxygen and carbon stable isotope profiles of the fan mussel, *Pinna nobilis* and reconstruction of sea surface temperatures in the Mediterranean, *Marine Biology*, **139**, 1115-1124

Kennish, J.M. and Olsson, R.K., (1975), Effects of the thermal discharge on the microstructural growth of *Mercenaria mercenaria*: *Environmental Geology*, **1**, 42-64

Koutavas, A., and J.P. Sachs (2002b), El Niño-like pattern in ice age tropical Pacific sea surface temperature, *Science*, **297**, 226-230

Lea, D. W., Pak, D. K., and H. J. Spero (2000), Climate impact of late quaternary equatorial Pacific sea surface temperature variations, *Science*, **289**, 1719-1724

Liu, Z., J. Kutzbach, L. Wu (2000), Modelling Climate Shift of El Niño Variability in the Holocene, *Geophysical Research Letters,* **27**, 2265-2268

Martinez, J.I., De Deckker, P., and A. Chivas (1997), New estimates for salinity changes in the Western Pacific Warm Pool during the Last Glacial Maximum: oxygen-isotope evidence, *Marine Micropaleontology*, **32**, 311-340

Martínez, J.I., Keigwin, L., Barrows, T., Yokoyama, Y., and J. Southon (2003), La Niña-like conditions in the eastern equatorial Pacific and a stronger Choco jet in the northern Andes during the last glaciation, *Paleoceanography*, **18**, 1033-1035

McGregor, H.V. and M.K. Gagan (2004) Western Pacific coral δ 18O records of anomalous Holocene variability in the El Ni Ô o-Southern Oscillation, *Geophysical Research Letters.* **31**, L11204

Mix, A.C. and W.F. Ruddimann (1984), Oxygen-isotope analyses and Pleistocene ice volumes, *Quaternary Research,* **21**, 1–20

Oppo, D, Schmidt, D. and A. LeGrande (2007), Sea water isotope constraints on tropical hydrology during the Holocene, *Geophysical Research Letters,* **34**, L13701
Ota, Y., and J. Chappell (1999), Holocene sea-level rise and coral reef growth on a tectonically rising coast, Huon Peninsula, Papua New Guinea, *Quaternary International*, **55**, 51-59

Ota, Y. and Chappell, J. (1999), Holocene sea level rise and coral reef growth on a tectonically rising coast, Huon peninsula, Papua New Guinea. *Quaternary International,* **55,** 51-59

Otto-Bliesner, B., Brady, E., Shin, S., Liu, Z., and C. Shields (2003), Modeling El Niño and its tropical teleconnections during the last glacial-interglacial cycle, *Geophysical Research Letters*, **30**, 2198-2202

Pandolfi, J. and J. Chappell (1994), Stratigraphy and relative sea level changes at the Kanzarua and Bobongara sections, Huon Peninsula, Papua New Guinea, In *Study on coral reef terraces of the Huon Peninsula, Papua New Guinea: Establishment of Quaternary Sea Level and Tectonic History* Y. Ota. Ed., pp. 119-139

Paillard, D., and L. Labeyrie (1996), Macintosh program performs time-series analysis, *EOS*, **77**, 379

Pätzold, J., Heinrichs, J.P., Wolschendorf, K. and G. Wefer. (1991), Correlation of Stable Oxygen Isotope Temperature Record with Light Attenuation Profiles in Reef-Dwelling Tridacna Shells, *Coral Reefs*, **10**, 65-69.

Rodbell, D. T., Seltzer, G.O., Anderson, D.M., Abbott, M.B., Enfeld, D.B. and J.H. Newman (1999), A ~15,000 year long record of El Niño driven alleviation in South Western Ecuador, *Science,* **283**, 516-519

Romanek, C and E. Grossman (1989) Stable isotopic profiles in *Tridacna maxima* as environmental indicators, *Palaios*, **4**, 402-413

Sandweiss, D., Maasch, K., Chai, F., Andrus, C., Reitz, E (2004), Geoarchaeological evidence for multidecadal natural climate variability and ancient Peruvian fisheries, *Quaternary Research*, **61**, 1531-1533

Sato, S. (1995) Spawning periodicity and shell growth microgrowth patterns of the venerid bivalve *Phacosoma japonicum* (Reeve, 1850): *Veliger*, **38**, 61-72

Schrag, D. P., Hampt, G. and D. W. Murray (1996), Pore fluid constraints on the temperature and oxygen isotopic composition of the glacial ocean, *Science*, **272,** 1930-1932

Schöne, B., Duncan, E., Feibig, J., and M. Pfeiffer (2005), Mutvei's solution: an ideal agent for resolving microgrowth structures in biogenic carbonates. *Palaeogeography, Palaeoclimatology, Palaeoecology*, **228**, 149-146

Shackleton, N.J. (1967). Oxygen isotope analyses and Pleistocene temperatures re-assessed, *Nature,* **215,** 15-17

Siddall, M., Rohling E.J., Almogi-Labin, A., Hembleben, Ch., Meischner, D., Schmelzer, I., and D.A. Smeed. (2003), Sea-level fluctuations during the last glacial cycle, *Nature*, **423**, 853-858

Stott, L. Cannariato, K., Thunell, R. Haug, G.G., Koutavas, A. and S. Lund (2004), Decline in the surface temperature and salinity in the western tropical Pacific Ocean in the Holocene Epoch. *Nature*, **431**, 56-59

Stott, L., Poulsen, C., Lund, S. and R. Thunell. (2002), Super ENSO and global climate oscillations at Millennium timescales, *Science*, **297**, 222-226

Timmermann, A., An S-I., Krebs, U., and H. Goosse (2005a), ENSO suppression due to weakening of the North Atlantic thermohaline circulation, *Journal of Climate*, **18**, 3122-3139

Timmermann, A., Krebs, U. Justino, F. Goosse, H. and T. Ivanochko (2005b) Mechanisms for millennial-scale global synchronization during the last glacial period, *Paleoceanography*, **20**, PA4008

Timmerman, A. Okumara, Y., An, S-I., Clement, A., Dong, B., Guilyardi, E., Hu, A., Jungclaus, J., Krebs, U., Renold, M., Stocker, T.F., Stouffer, R.J., Sutton, R., Xie, S.-P. and J. Yin (2007) The influence of shutdown of the Atlantic Meridonal overturning circulation on ENSO, *Journal of Climate*, **20**, 4899-4919

Tudhope, A., W., Chilcott, C.P., McCulloch, M.T., Cook, E.R., Chappell, J. Ellam, R.M., Lea, D., Lough, J.M. and Shimmield, G.B. (2001), Variability in the El Niño - Southern oscillation through a glacial-interglacial cycle, *Science*, **291**, *1511-1517*

Watanabe, T. and T. Oba, (1999) Daily reconstruction of water temperatures from oxygen isotopic ratios of a modern *Tridacna* shell using a freezing microtome sampling technique. *Journal of Geophysical Research,* **40**, 20,677-20,674

Watanabe, T., A. Suzuki, H. Kawahata, H. Kan and S. Ogawa. (2004), A 60-year isotopic record from a mid-Holocene fossil giant clam (Tridacna gigas) in the Ryukyu Islands: physiological and paleoclimatic implications, *Palaeogeography Palaeoclimatology Palaeoecology*, **212**, 343-354

Waelbroeck, C., Labeyrie, L., Michel, E., Duplessy, J.C., McManus, J.F., Lambeck, K., Balbon, E. and M. Labracherie (2002): Sea-level and deep water temperature changes derived from benthonic foraminifera isotopic records, *Quaternary Science Reviews*, **21**, 295-305

Yokoyama, Y., Lambeck, K., De Deckker, P., Johnston, P. and L. K. Fifield (2000), Timing of the Last Glacial Maximum from observed sea-level minima, *Nature*, **406**, 713-716

6 Probing millennial scale variability of the WPWP during MIS 3

This chapter describes $\delta^{18}O$ results from *Tridacna* sp. that were collected prior to and during the sea level excursion which has been associated with Heinrich Event 4 in the North Atlantic.

The relative change in $\delta^{18}O$ over this period is compared with a predicted $\delta^{18}O_w$ signal from reduction in continental ice volume. This allows the investigation of the mean climatic state of the Western Pacific Warm Pool during a Northern Hemisphere stadial by taking advantage of the fact that eustatic sea level variation can be correlated globally in several proxy records.

Over this time period there is a greater apparent variation in the $\delta^{18}O$ measured at Huon Peninsula than can be accounted for by eustatic sea level/ continental ice volume reduction alone, which implies a warmer or wetter mean state at this time. This contradicts evidence that the Tropical Pacific possesses a more El-Niño like mean climate state during Northern Hemisphere stadials. Rather than applying a mean state analogue based upon the modern ENSO system, this evidence may support an inferred southward deflection of the ITCZ which has been suggested by other studies. Caveats remain however over the timing of events and the fact that variations in sea surface temperature and surface water $\delta^{18}O_w$ cannot be separated.

6.1 Introduction

Millennial scale climate variability was first observed in North Atlantic climate records in ice cores where sharp temperature rise occurs in decades and cooling over thousands of years (Dansgaard *et al.*, 1993). These temperature oscillations became known as Dansgaard-Oeschger (DO) cycles and thereafter observed in proxies for sea surface temperatures recovered from deep sea cores in the North Atlantic region (e.g. Bond *et al.*, 1992, 1993). Series of DO cycles are bundled together into longer Bond cycles which cumulate in massive ice rafting events as observed in layers of ice rafted debris in North Atlantic sediment deposits (Heinrich, 1988). These

deposits have been extensively studied and have been related to major ice sheet collapses from the Laurentide ice sheet and other Northern Hemisphere ice sheets.

In the North Atlantic Heinrich Events are associated with periods of extreme cold (Greenland stadials) and a weakened thermohaline circulation (THC). Reduction in the strength of the THC is inferred from the reduction of North Atlantic Deep Water (NADW) production shown by variation in source of deep water using $\delta^{13}C$ from benthic foraminifera in deep sea cores (Sarnthein *et al.*, 1994; Vidal *et al.*, 1997 and Elliot *et al.*, 2002) and recent studies of Pa/ Th in Atlantic cores, a tracer for Atlantic Meridonal Overturning (McManus *et al.*, 2004; Gerhardi *et al.*, 2005 and Hall *et al.*, 2006). Several modelling studies also indicate that NADW production should be reduced and THC slow down during the Heinrich Events (Rahmstorf, 1995; Manabe and Stouffer, 1995; Ganopolski and Rahmstorf, 2001 and Knutti *et al.*, 2004).

Millennial scale climate variability can be seen in other climate records from regions outside the North Atlantic. A large number of palaeoclimate records show millennial scale variation in the strength of the Asian Monsoon during the last glacial cycle (Altabet *et al.*, 2002; Burns *et al.*, 2003; Ivanochko *et al.*, 2005; Shultz *et al.*, 1998; Wang *et al.*, 2001), as do proxy records which imply changes in rates of precipitation in Central America (Peterson *et al.*, 2000) and bottom water anoxia in the Santa Barbara Basin (Behl and Kennett, 1996 and Kennett *et al.*, 2000). In some records climatic correlatives of Heinrich events are inferred to be prominent as there are the same number of rapid climate events as the Heinrich events, and other rapid climate shifts are not seen: Lake Tullane pollen record (Grimm *et al.*, 1993), Brazilian margin terrigenous runoff (Arz *et al.*, 1998) and precipitation (Wang *et al.*, 2004), Lake Baikal (Selenga delta) runoff, (Prokopenko *et al.*, 2001), and Chinese loess average grain size (Porter and An, 1995) and in records of precipitation derived from peat bogs in Northern Queensland (Turney *et al.*, 2004 and Muller *et al.*, 2008).

Evidence for millennial scale climate change in the WPWP

Some authors have suggested that the sources for abrupt climate global climate change should lie in the Tropics as the are the sources of heat and moisture for the

global climate system (Pierrehumbert, 2000). It is relatively easy to suggest how variations in the climate of the North Atlantic could be affected by variations in the production of NADW (e.g. Ganopolski and Rahmstorf, 2001) it is not so straight forward to understand how the hydrological system in the tropics can maintain a different configuration on millennial timescales. Cane (1998) suggested that that the ENSO system is capable of operating on much longer than interannual timescales if there were a long term change in teleconnections in the Pacific that are similar to those that operate during an El Niño event. Clement *et al.*, (2001) explored the idea that the Tropical Pacific could be the source of some global millennial scale climate variability by modelling interruptions to the ENSO system, reducing the number of extreme events by effectively locking into the seasonal cycle and causing La Niña-like mean climate. It was suggested that this could occur during certain parts of the precessional cycle when the perihelion is in the boreal and then austral summers.

Marine records of sea surface temperature and hydrology with sufficiently high resolution to examine millennial scale variations in the WPWP are rare because it is a region of low productivity with a deep carbonate compensation depth. A study from the South China Sea by Stott *et al.,* (2002) shows variation in sea surface salinity which is strikingly similar to the Northern hemispheric (NH) temperature record seen in the GRIP and GISP2 ice cores in Greenland. Stott *et al.*, (2002) suggest using the term "Super-ENSO", or in other words a long term changes in mean climate of the Tropical Pacific on millennial timescales that is analogous to ENSO on interannual timescales, to account for their observed changes in sea surface salinity. They go further and suggest that the mean state of the Tropical Pacific is that of an El Niño state, (i.e. saline conditions in the WPWP) during stadial conditions in the Northern Hemisphere and a more "normal" or La Niña-like state during Northern Hemisphere interstadials and that ENSO is capable of driving millennial scale climate variations. There are, however, two problems with this study. Firstly, questions remain regarding whether dating methods employed in this study are sufficiently accurate to differentiate between millennial scale events such as stadials/ interstadials during this time period. Secondly, the South China Sea climate is tied strongly to the Asian Monsoonal system (Dannemann *et al.*, 2003 and

Rosenthal and Broccoli, 2004) and climate change here may not entirely reflect the ENSO system. Chen *et al.* (2005) present a record is from the Western Pacific Warm Pool close to Papua New Guinea. This record also seems to show higher salinity during Heinrich events, however, dating of MIS3 events on this record is based upon the assuming that the low $\delta^{18}O$ represents Heinrich events. Levi *et al.*, (2007) show increase in salinity in the Indo-Pacific Warm Pool during periods of weakened THC (i.e. the Younger Dryas and Heinrich Event 1), which they link to the southward deflection of the Intertropical Convergence Zone (ITCZ). A study of peat humification from Northern Queensland has suggested an increase in precipitation reflecting a more La Niña-like mean state for the Tropical Pacific during Northern Hemisphere stadials, especially those associated with Heinrich events (Turney *et al.*, 2004). Turney *et al.*, (2004) suggest that this occurs during Northern Hemisphere stadials and suggest that modifications to the ENSO system are driving these transitions.

Increasingly studies link changes in the mean position of the Intertropical Convergence Zone (ITCZ) and global millennial scale climate change (e.g. Ivanochko *et al.*, 2005; Levi *et al.*, 2005 and Timmermann *et al.*, 2005). Muller *et al.*, (2008) present both evidence for a southerly depressed ITCZ in the WPWP region and a model showing that this is a response to freshwater injection to the North Atlantic during Heinrich events. Generally these studies indicate that the trigger for millennial scale climatic variation is in the North Atlantic region and the tropics are merely responding (Timmermann *et al.*, 2005) or amplifying (Ivanochko *et al.*, 2005) to temperature changes in the Northern Hemisphere that alter the mean position of the ITCZ. Broccoli *et al.*, (2006) show that the mean position of the ITCZ can be depressed to the south during a Northern Hemisphere stadial due to changes in trade wind strength and an asymmetric response of the Hadley circulation.

Therefore whilst there is some evidence for changes in the mean state of ENSO on millennial timescales, which some studies imply are the cause of global millennial climate variations, there is significant evidence that a change in the position of the ITCZ responding to North Atlantic climate variations may account for the same

evidence. This study will attempt to address the mean state of the WPWP during the Northern Hemisphere stadial associated with Heinrich event 4 by taking advantage of two observations outlined in Chapters 3 and 4:

1. As shown in Chapter 3, $\delta^{18}O$ profiles derived from *Tridacna* sp. reflect changes in interannual SST and precipitation that are highly correlated with ENSO. Long term changes in the mean state of the ocean will be reflected in $\delta^{18}O$ records from fossil *Tridacna* sp.
2. As shown in Chapter 4, samples collected from terrace IIa are likely to have grown during sea level excursion that has been associated with a Northern Hemisphere stadial.

It should be possible to test a hypothesis based upon a model of a more El Niño-like climate during a Northern Hemisphere stadial which is shown in Figure 6-1. This schematic diagram shows the proposed temporal relationship between temperatures over Greenland and a predicted relative change in $\delta^{18}O$ of *Tridacna* sp. based upon the increase in WPWP salinity proposed for this time period by Stott *et al.*, (2002). As seen in previous Chapters, reduced SST's and precipitation are expected during El Niño events (Chapter 2) therefore, bulk *Tridacna* sp. $\delta^{18}O$ values should be relatively more positive (Chapter 3) whilst an El Niño like state persists.

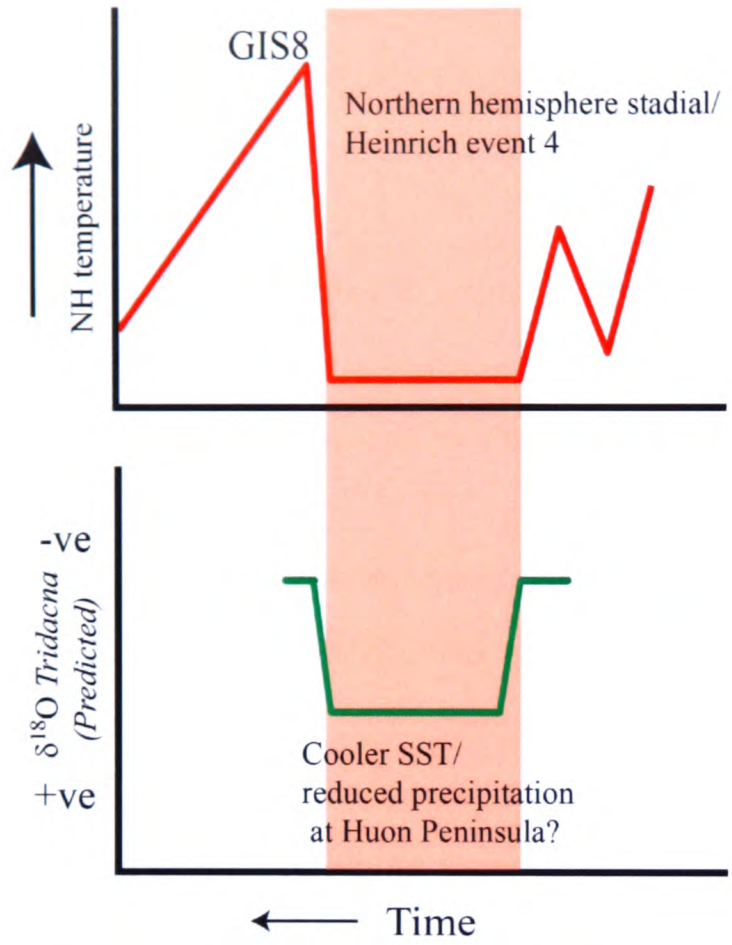

Figure 6-1 Schematic diagram showing proposed effect on $\delta^{18}O$ at Huon Peninsula showing Northern Hemisphere temperature and $\delta^{18}O$ in *Tridacna* sp. from the Huon Peninsula.

By measuring average $\delta^{18}O$ in *Tridacna* sp. collected from during the stadial and immediately preceding it and accounting for $\delta^{18}O_w$ caused by continental ice volume reduction it should be possible to determine if there is a residual change in $\delta^{18}O$ and therefore infer the mean state of the Tropical Pacific.

6.2 Field area

Samples collected for this survey were collected from Bobongara, on the Huon Peninsula from reef terraces IIa, IIIc (l) and IIIc(u) as described in detail in Chapter 2 and Chapter 4.

6.3 Materials and methods

Selected *Tridacna* sp. were sectioned and prepared using the techniques described in Chapter 5 and carbonate samples were collected across all of their annual growth bands using a hand held dental drill at low speed (<400 revolutions per second) and a

tungsten carbide drill bit. The resulting powder was spit for X-Ray Diffraction analysis of % calcite and stable isotope testing as described in Chapter 5

Stable Isotope Analysis

Chapter 5 gives details of the procedures used to determine the oxygen isotopic composition of carbonate samples extracted from *Tridacna* sp.

Chronology

Chapter 4 gives details of the procedures used to date *Tridacna* sp. samples used in this study.

6.4 Results

Results from 17 fossil *Tridacna* sp. were used for this study. The percentage of calcite in each sample was 1% or lower indicating that the samples were very well preserved. The number of years sampled in each specimen varied between ~3 and ~27 years with a mean of 10 years.

The age of samples ranges from 35.5 to 42.4 ka. Bulk $\delta^{18}O$ values vary between 0.3 and –0.4‰ with a range of 0.7‰. There is a cluster of data with the most negative $\delta^{18}O$ values at approximately 37 ka (see Figure 6-2). There is a high degree of variability in the $\delta^{18}O$ data associated with terrace IIa (0.6‰ within this terrace alone).

Sample	Species	Terrace	Distance from top (m)	Elevation (m)	$\delta^{18}O$	Number of samples	Age (cal ka bp)	2 sigma error	% calcite	Number of years sampled
T28I	*T. maxima*	IIa	unknown	ex	0.18	1	35.45	0.79	0.4	9
T10I	*T. gigas*	IIa	unknown	ex	0.11	2	35.79	0.73	0.7	7
T13I	*T. maxima*	IIa	unknown	ex	-0.05	1	36.72	0.80	0.8	7
T29I	T. gigas	IIa	unknown	ex	0.25	1	36.75	0.81	0.4	8
T70	*T. gigas*	IIa	3	47	-0.30	4	36.56	1.83	0.9	18
BT14	*T. gigas*	IIa	1	49	-0.14	213	36.66	1.78	0.7	19
BT27	*T. gigas*	IIa	0	50	-0.34	6	36.79	1.82	0.6	27
BT9	*T. gigas*	IIa	5	45	-0.10	2	37.79	2.04	1.0	12
BT12	*T. squamosa*	IIa	2	48	0.25	2	38.20	2.11	0.5	8
BT11	*T. squamosa*	IIa	3	47	-0.11	8	38.41	2.15	0.6	8
BT31	*T. crocea*	IIIc(l)	1	56	0.20	2	37.8	2.13	0.5	9
BT34	*T. maxima*	IIIc(l)	2	55	0.14	2	38.6	2.28	0.8	3
BT32	*T. maxima*	IIIc(l)	0	57	0.08	2	39.49	1.00	0.5	8
BT33	*T. crocea*	IIIc(l)	3	54	0.11	2	41.44	3.04	0.2	5
BT39	*T. maxima*	IIIc(u)	0	66	0.22	89	41.40	1.06	0.9	10
BT30	*T. crocea*	IIIc(u)	unknown	ex	0.33	2	41.52	3.23	0.5	5
BT40	*T. squamosa*	IIIc(u)	4	62	-0.40	1	42.44	3.24	0.9	8

Table 6-1 Results of dating and $\delta^{18}O$, % calcite and number of years sampled in each *Tridacna* sp.

Most *Tridacna* sp. were collected *in situ*, still in life position with both valves together facing upwards though some were collected *ex situ*, lying unattached on the surface or the face of the terrace. These samples could have been transported from terraces above or moved from terraces below by human activity. Radiocarbon ages of these samples indicate that they were deposited immediately after or at the same time as the terrace on which they were found. These samples most probably originate from the top of terrace IIa and relate to the end of the relative highstand or possibly regression and have been eroded and detached from the terrace. A more detailed discussion of this is given in Chapter 4.

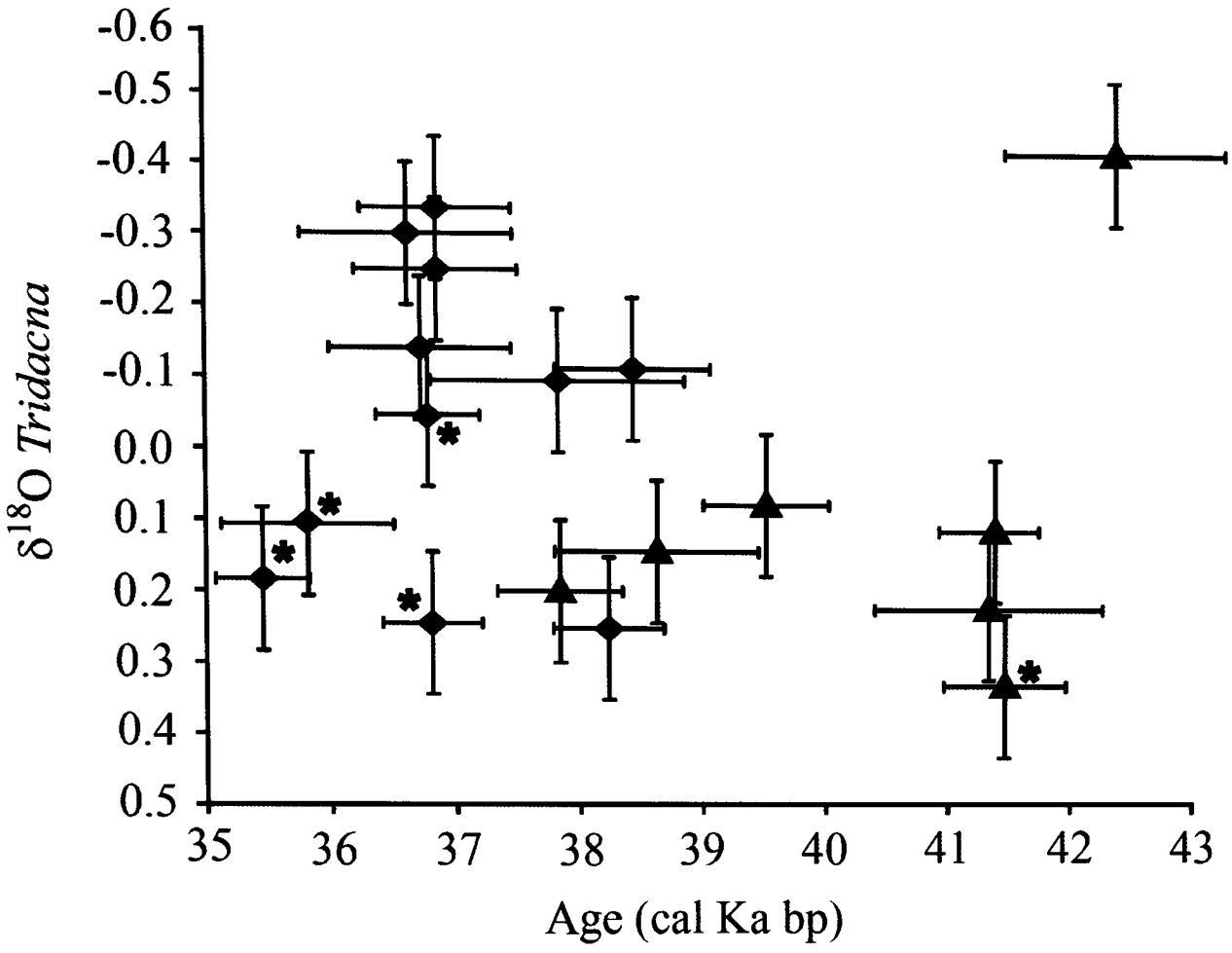

Figure 6-2 Showing the $\delta^{18}O$ results from terraces IIa. Calibrated radiocarbon uncertainty is 2 σ and $\delta^{18}O$ uncertainty is 0.16 ‰ (2 σ). *Ex situ* samples are marked with an *.

6.5 Interpretation

Relation of results to sea level excursion

The rational for the chronology is set out in detail in Chapter 4, however a summary is provided here. Chronologically, the *Tridacna* sp. from IIIc precedes the sea level lowstand. It is highly likely that the *in situ Tridacna* sp. collected from terrace IIa are coeval with the sea level rise preceding the highstand, most of which took place during the Greenland cold stadial associated with Heinrich 4 and the Northern Hemisphere stadial, *ex situ* samples from IIa are likely to come from the sea level highstand or possibly an early regressive phase. Samples from IIIc predate the sea level low stand.

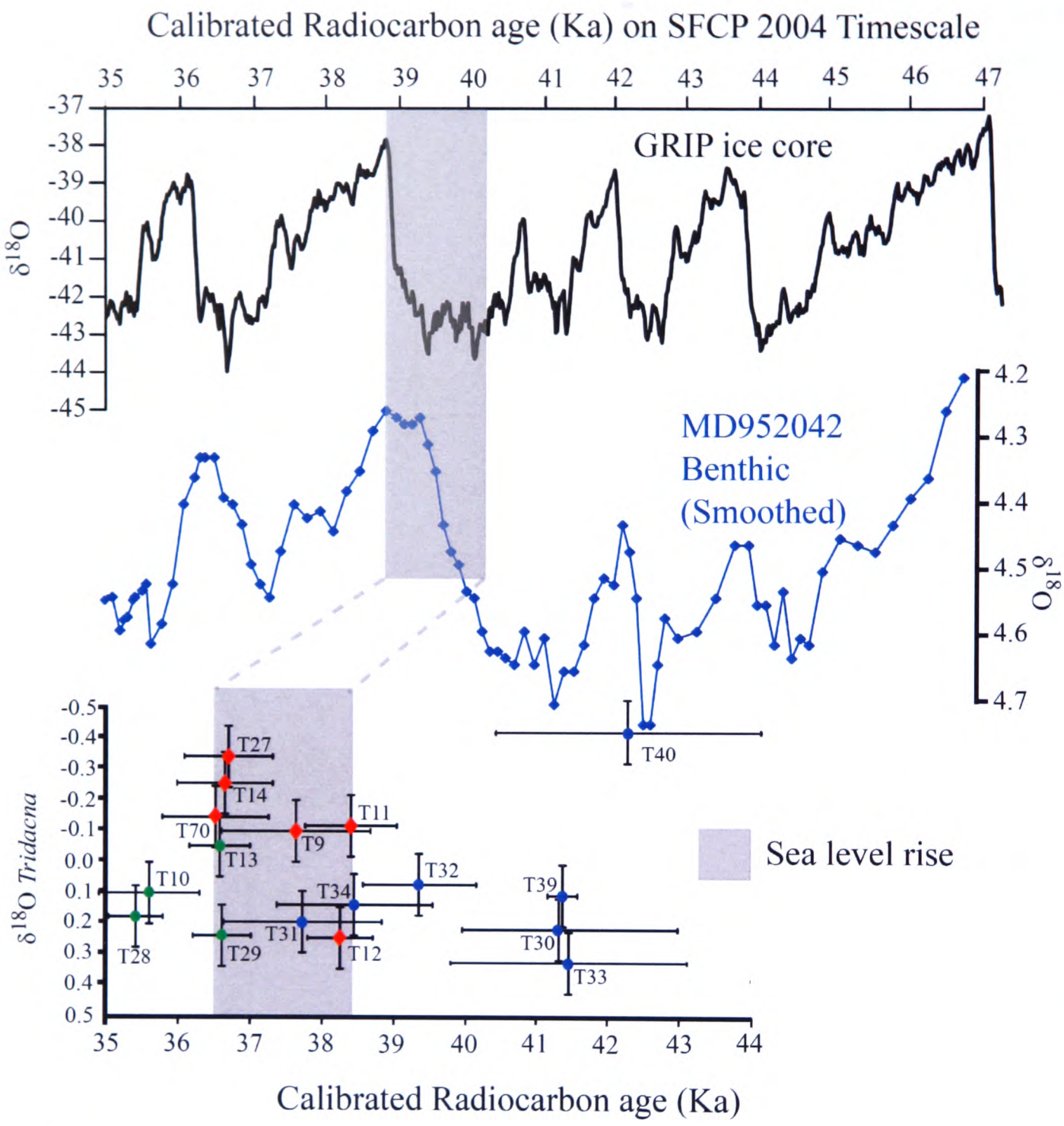

Figure 6-3 Shows the proposed temporal relation of samples collected from terrace IIa and IIIc to North Atlantic climate (GRIP ice core record) based upon the assumption that the peak in sea level occurs at just before GIS8. MD952042 benthic is a treated here as proxy for sea level (as suggested in Shackleton, 2000) however it is possible that changes in $\delta^{18}O_w$ or temperature can also affect this signal (Shackleton *et al.*, 2004).

Figure 6-3 shows the proposed temporal relationship between averaged $\delta^{18}O$ from this study reflecting local temperature, salinity and global ice volume change and the changes in atmospheric temperature over Greenland and change in sea level based upon $\delta^{18}O$ in benthic foraminifera record from a North Atlantic core (see Chapter 4).

It is clear that there is a significant amount of variation in $\delta^{18}O$ throughout this time period. It is possible that this is the combined effects of reduced continental ice and

changes in mean climate state. Therefore it is proposed to calculate a mean $\delta^{18}O$ for each identified stratigraphic unit to try and constrain the overall variation in $\delta^{18}O$ with respect to ice volume change. Because the climatic signature that is being investigated is a relative one and because of some of the uncertainty in the dating of these samples, it is not proposed to extract an ice volume component from these values, but simply to compare them to an estimate of the relative change in $\delta^{18}O_w$ caused by reduction in continental ice volume.

Since the number of years sampled in each *Tridacna* sp. varies between ~3 and 27 years in length some of the averaged $\delta^{18}O$ data will have more significance in reconstructing mean climate state than others. The significance of a 3 year long record is clearly much less than a 27 year long record, therefore to constrain the variation within each stratigraphic unit a weighted average is calculated based upon the number of years of growth represented by each $\delta^{18}O$ measurement using the following equation:

$$\text{Weighted mean del}^{18}\text{O}_{\text{for stratigraphic group}} = \frac{[T_{x1}\ \text{del}^{18}\text{O}.T_{x1y}]+[T_{x2}\ \text{del}^{18}\text{O}.T_{x2y}].....[T_{xn}\ \text{del}^{18}\text{O}.T_{xny}]}{T_{x1y}+T_{x2y}+.....T_{xny}}$$

Where individual samples are T_{xn}, and number of years sampled are T_{xny} for each identified stratigraphic section. The results of this averaging are shown in Table 6-2 and Figure 6-4.

Stratigraphic unit	Total number of years sampled	Weighted mean $\delta^{18}O$
IIa(e)	31	0.13
IIa(i)	92	-0.19
IIIc	48	0.09

Table 6-2 Results of weighted mean $\delta^{18}O$ of each stratigraphic unit analysed in this study

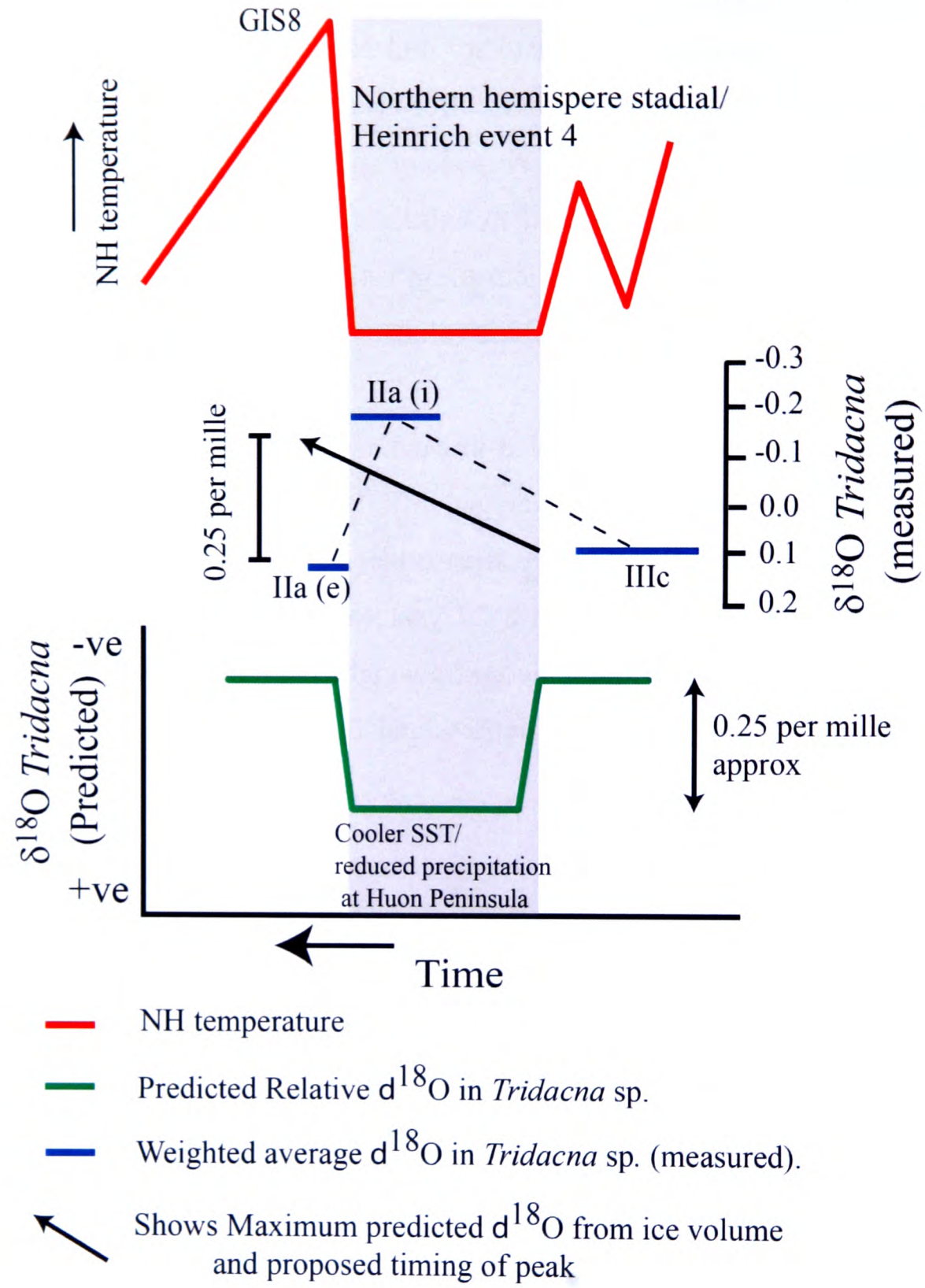

Figure 6-4 Schematic diagram showing proposed temporal relationship between predicted $\delta^{18}O_w$ at Huon Peninsula and $\delta^{18}O$ measured in fossil *Tridacna* sp. Weighted mean $\delta^{18}O$ for each stratigraphic grouping is shown by blue lines. The maximum isotopic change in oceanic $\delta^{18}O$ from ice volume changes is shown as a black arrow (based upon a 30m sea level rise (Siddall *et al*, 2003 and Arz *et al.*, 2007)). The green line shows a predicted change in $\delta^{18}O_w$ for mean El Niño-like state (after correcting for sea level variation).

The black arrow shows the maximum change in global ocean $\delta^{18}O$ based upon a change of 0.0085 ‰ m^{-1} (see Chapter 5 for explanation) associated with the sea level

rise thought to have caused the building of terrace IIa (approx 30m according to Siddall *et al.*, 2003 and Arz *et al.*, 2007).

A predicted change in the $\delta^{18}O_w$ of sea water for a long term change in mean state of the WPWP to an El Niño state (as a suggested by Stott *et al.*, [2002]) is shown. This does not include a prediction of $\delta^{18}O_w$ due to continental ice volume reduction. A prediction of 0.25‰ for an El Niño-like state is made based upon the amplitude of deviation seen in during an El Niño event at the Huon Peninsula observed in a modern *Tridacna gigas* from the Huon Peninsula (see Chapter 3). Since the increase in $\delta^{18}O$ caused by a long term El Niño-like state is similar to the variation caused by sea level increase/ ice volume decrease, an El Niño-like state would appear as no variation in $\delta^{18}O$ if both events are coeval.

6.6 Discussion

The difference in weighted average values for the reefs preceding the lowstand and the *in situ* samples from IIa are approximately the same as those expected from 30m sea level rise, which would imply that only variation in sea level is being recorded in *Tridacna* sp. $\delta^{18}O$ and there is no shift toward El Niño-like mean climate conditions as inferred by Stott *et al.*, (2002) or might be expected by some models (e.g. Cane, 1998).

However, as has been demonstrated lowstands are not likely to be sampled here and therefore the estimated of reduction of 0.25‰ $\delta^{18}O$ between terraces IIIc and IIa due to sea level rise is likely to be an overestimate as the terraces will not "see" this full range. In addition there is a greater variability within the *Tridacna* sp. which is masked by taking weighted means of each stratigraphic grouping. The full variation over the terrace is 0.6‰.

Taking this result at face value it implies that the hydrology of the sea surface in the WPWP becomes wetter/ warmer during a Northern Hemisphere stadial. This would directly contradict suggestions of an El Niño-like mean climate state.

This result might appear to support the conclusion that the Tropical Pacific has become locked into the La Niña state as predicted by Clement *et al.*, (2001) locking onto the seasonal cycle. This should lead to an increase in the amplitude of the seasonal cycle. As we have seen in Chapter 5, corals (from Tudhope *et al.*, 2001) and *Tridacna* sp. (this study) from terrace IIa show a suppressed ENSO signal. By observation it does not appear that there is an increase in the annual amplitude of the $\delta^{18}O$ signal in these corals and *Tridacna* sp., however longer records would be required to test this.

Ivanochko *et al*, (2005) link the ITCZ, Asian Monsoon and ENSO systems as amplifiers of climate on millennial scales. They cite Charles *et al.*, (1997) noting the linkage between a weakened Asian Monsoon and El Niño that has been observed during the last few centuries. Therefore a southward deflection of the ITCZ on millennial timescales would be linked to a "super ENSO" type El Niño-like climate and more saline Western Pacific Warm Pool. This relationship may not hold during the glacial period due to enhanced trade wind strength which would prevent the onset of a full El Niño conditions (the glacial dampening effect referred to by Tudhope *et al.*, [2001]). Instead a simple model of a southerly deflected ITCZ during Northern Hemisphere stadials (Broccoli *et al.*, [2006]), without the need to invoke "super-ENSO" would be sufficient to explain the observations in this and other studies shown here. Furthermore the balance of evidence would therefore indicate that the North Atlantic region is the source for millennial scale climate change.

Figure 6-5 shows the mean position of the ITCZ in the Boreal and Austral summers is shown in relation to this study area, and those of Peterson *et al.*, (2000) and Stott *et al.*, (2002) which show reduced precipitation during Northern Hemisphere stadials and Arz *et al.*, (1998) and Turney *et al.*, (2004) and Muller *et al.*, (2008) whose records show increased precipitation during Northern Hemisphere stadials and lie near the southern position of the ITCZ during the Austral summer. Since the highest rainfall occurs at the Huon Peninsula during the Austral summer (see Chapter 2) it is

likely that a southerly depressed ITCZ would result in increased precipitation at Huon Peninsula.

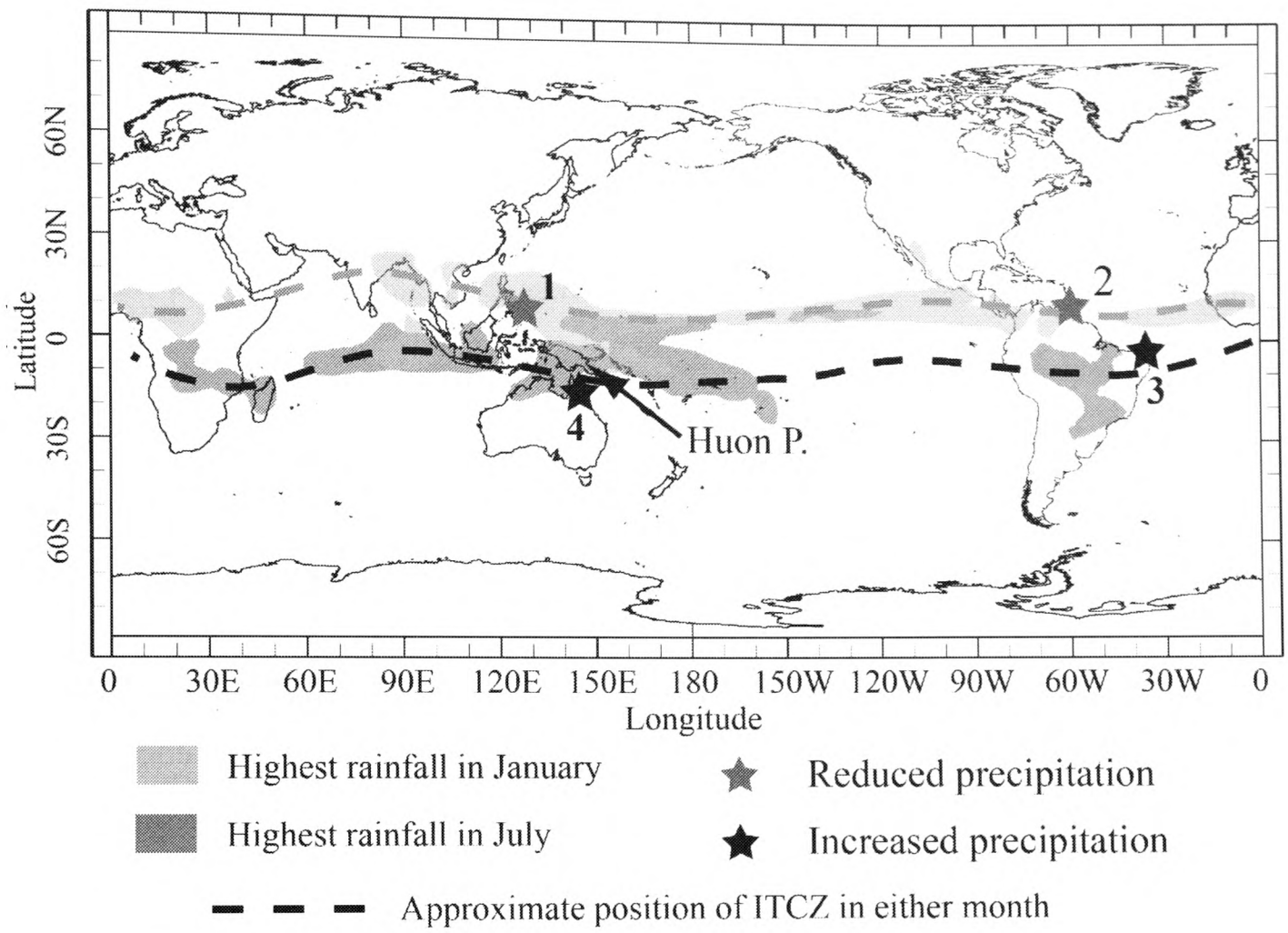

Figure 6-5 Shaded areas show areas of 7mm precipitation per day or above in the Boreal summer (green) and the Austral summer (blue) (NASA GPCP V2). Stars show studies mentioned in this work: 1 = Stott *et al.*, (2002); 2 = Peterson *et al.*, (2000); 3 = Arz *et al.*, (1998); 4 = Turney *et al.*, (2004) and Muller *et al.*, (2008)

In modeling studies presented in Timmermann *et al.,* (2005) and Muller *et al.*, (2008) in which global millennial scale climate change was induced by density anomalies in the North Atlantic region which cause pan-oceanic meridonal changes in the position and strength of the ITCZ there is an increase in precipitation south of the equator which accounts for the increased precipitation in north eastern Australia and also shows a slight increase in precipitation over Papua New Guinea, whilst maintaining an increased salinity in the northern part of the pacific warm pool.

There are however several caveats for the observed values which must be acknowledged. Differences in $\delta^{18}O$ may be caused if there are significant variations in depth if reef facies vary between terraces sampled. There are also caveats

associated with the correlation of terrace IIa to a Northern Hemisphere stadial, especially as the earliest part of the terrace is likely to be missing.

The full range of reef environments that samples were taken from have been identified by Pandolfi and Chappell (1994). These water depth of these environments range from the reef platform (0-2m) reef crest (2-5m) and upper reef slope (5-15m). The sampled area of Terrace IIa is composed of reef crest and reef platform (Pandolfi and Chappell, 1994) whereas the small IIIc terraces are thought to be upper reef slope facies (Pandolfi and Chappell, 1994) and possibly some reef crest material (Chappell, J. pers. comm.). It is possible that the changes in $\delta^{18}O$ reflect environmental temperature changes between these three environments. According to the World Ocean Atlas (2005) temperature profile with depth at Huon Peninsula is in the order of 0.2°C temperature variation between 0 and 20m, though this is based upon open water measurements. Temperature loggers from Sialum Lagoon on the Huon Coast are shown in Chapter 2. There is no detectable difference between a temperature logger placed at 2m depth in the lagoon and one left near the entrance at 8m depth (see Chapter 2). It may be possible in the past that a much shallower thermocline may cause greater differences in temperature gradients.

There still remain issues associated with the precise timing of the sea level highstand that caused the production of terrace IIa. Though, as explained in Chapter 4, the best guide for this record is the Shackleton *et al.,* (2000) reconstruction, the benthic foraminiferal $\delta^{18}O$ may not only represent changes in ice volume but also be influenced by changes in deep water temperature. Additionally, it is possible that a disproportionate number of the samples collected form this study may come from the later stages of terrace growth as it is difficult to discern the extent to which the earliest portion of the terrace exists and was therefore accessed. Further investigation of this stage of terrace growth through drilling or by investigating new field areas where this is exposed due to erosion or faulting are necessary to extract the climate history. Finally, there is no way of independently of assessing temperature in these records and thus extracting sea surface salinity. As has been demonstrated in Chapter 3, variations in evaporation/ precipitation balance play near

as significant a role as temperature in determining the measured $\delta^{18}O$ and in consequence this story could be more complex than indicated here.

6.7 Conclusions

Carbonate powders averaged over 3 to 19 years of growth were extracted from *Tridacna* sp. and analysed for their $\delta^{18}O$ composition. These appear to vary in concert with sea level changes. However, the variation in $\delta^{18}O$ probably exceeds that expected from sea level/ continental ice volume variation, indicating that there is a climatic component to this $\delta^{18}O$ signal and further suggesting that hydrological change is occurring in the West Pacific Warm Pool during this period. Taken at face value, this indicates either wetter or warmer conditions at Huon Peninsula, which taking other measures of changes in precipitation at other sites into account, suggests that the mean position of the ITCZ is displaced southward by increases in trade wind strength during Northern Hemisphere stadials.

There are however important caveats with this interpretation. Firstly there is no independent measure of temperature. Secondly there is some disagreement about the precise timing of the sea level excursion, and finally it is also not known how much of the earliest part of the terrace is missing which may skew the results. In light of these caveats any conclusions presented here should be treated with caution.

Further investigation of the timing of the sea level rise c. 39ka is needed along with a need to gather samples from the earlier parts of terrace IIa and also to collect longer records so that subtle changes in the state of ENSO can be recorded.

References

Altabet M., Higginson M. J. and D.W. Murray (2002), The effect of millennial-scale changes in Arabian Sea denitrification on atmospheric CO2, *Nature,* **415,** 159-62

Arz, H. W., Patzold, J. and G. Wefer (1998), Correlated millennial-scale changes in surface hydrography and terrigenous sediment yield inferred from last-glacial marine deposits off northeastern Brazil, *Quaternary Research,* **50,** 157-166

Arz, H. W., Lamy, F. Ganopolski, A. Nowaczyk, N. and Patzold, J. (2007) Dominant Northern Hemisphere climate control over millennial scale glacial sea-level variability, *Quaternary Science Reviews*, **26**, 312-321

Behl, R.J., and J.P. Kennett, (1996), Brief Interstadials Events in Santa Barbara Basin, Northeast Pacific, During the Past 60 kyr, *Nature*, **379**, 243-246

Bond G.C., Heinrich, H., Broecker, W., Labeyrie, L., McManus, J., Andrews, J., Huon, S., Jantschik, R., Clasen, S., Simet, C., Tedesco, K., Klas, M., Bonani, G. and S. Ivy, (1992) Evidence for massive discharges of icebergs into the North Atlantic ocean during the last glacial, *Nature,* **360**, 245-249

Bond, G., Broecker, W., Johnsen, S., MacManus, J., Labeyrie, L., Jouzel, J. and G. Bonani, (1993), Correlations between Climate Records from North-Atlantic Sediments and Greenland Ice, *Nature*, ***365***, 143-147

Burns, S.J., Fleitmann, D., Matter, A., Kramers, J., and Al-Subbary, A.A. (2003) Indian Ocean climate and an absolute chronology over Dansgaard/ Oeschger events 9 to 13. *Science*, **301**, 1365-167

Broccoli, A.J., Dahl, K.A., R.J. Stouffer (2006), response of the ITCZ to Northern Hemisphere cooling, *Geophysical Research Letters*, **33**, 1-4

Cane, M.A. (1998), A role for the Tropical Pacific, *Science*, **282**, 59-61

Chappell, J., Omura, A., Esat, T. M., McCulloch, M. T., Pandolfi, J., Ota Y., and B. Pillans, (1996a), Reconciliation of late Quaternary sea levels derived from coral terraces at Huon Peninsula with deep sea oxygen records. *Earth and Planetary Science Letters,* **141**, 227-236.

Chappell, J. Ota, Y. and K. Berryman. (1996b), Late quaternary coseismic uplift history of Huon Peninsula, Papua New Guinea, *Quaternary Science Reviews*, **15**, 7-22

Chappell, J. (2002), Sea level changes forced ice breakouts in the Last Glacial cycle: new results from coral terraces, *Quaternary Science Reviews*, **21**, 1229-1240

Charles, C.D., Hunter, D.E. and R.G. Fairbanks, (1997), Interaction between the ENSO and the Asian monsoon in a coral record of tropical climate, *Science,* **1997,** 925– 928

Chen, M. H., Li, Q., Zheng, F., Tan, X., Xiang, R. and Z. Jian (2005), Variations of the Last Glacial Warm Pool: Sea surface temperature contrasts between the open western Pacific and South China Sea, *Paleoceanography*, **20**, PA001057

Clement, A. C., Cane, M. A. and R. Seager, (2001), An orbitally driven tropical source for abrupt climate change, *Journal of Climate,* **14**, 2369-2375

Dannenmann, S., Linsley, B. K., Oppo, D., Rosenthal, Y. and L. Beaufort, (2003), East Asian monsoon forcing of suborbital variability in the Sulu Sea during Marine Isotope Stage 3: Link to Northern Hemisphere climate, *Geochemistry Geophysics Geosystems*, **4**, GC000390

Dansgaard, W., Johnsen' S.J., Clausen, H.B., Dahl-Jensen, D., Gundestrup, N.S., Hammer, C.U., Hvidberg, C.S., Steffensen, J.P., Sveinbjörnsdottir, A.E., Jouzel, J. & G. Bond (1993), Evidence for General Instability of Past Climate from a 250-Kyr Ice-Core Record, *Nature, **364**,* 218-220

Elliot, M., DeMenocal, P., Linsley, B. and Howe, S.S. (2003), Environmental controls on the stable isotopic composition of *Mercenaria mercenaria*: Potential application to palaeoenvironmental studies, *Geochemistry, Geophysics and Geosystems*, **4**, 1056-1072

Ganopolski, A. and S. Rahmstorf, (2001) Rapid changes of glacial climate simulated in a coupled climate model, *Nature,* **409**, 153-158

Gerhardi, J.-M., Labeyrie, L., McManus, J.F., Francois, R., Skinner, L.C. and E. Cortijo (2005). Evidence from the northeastern Atlantic basin for variability in the rate of meridonal overturning circulation through the deglaciation. *Earth and Planetary Science Letters*, **240**, 710-723

Grimm, E. C., Jacobson, G. L. Jr., Watts, W.A, Hansen, B.A.C.S. and K. A. Maasch (1993), A 50,000-year record of climate oscillations from Florida and its temporal correlation with the Heinrich events, *Science*, **261**, 198–200

Hall, I.R. Moran, S. B., Zahn, R., Knutz, P.C., Shen, C.-C. and R.L. Edwards, (2006), Accelerated drawdown of meridonal overturning in the late-glacial Atlantic triggered by transient pre-H event freshwater perturbation, *Geophysical Research Letters,* **33**, GL026239

Heinrich, H. (1988), Origin and Consequences of Cyclic Ice Rafting in the Northeast Atlantic-Ocean During the Past 130,000 Years, *Quaternary Research,* **29**, 143-152

Ivanochko, T. S., Ganeshram, R.S, Brummer, G.A., Ganssen, G., Jung, S.G.A., Moreton, S.G. and D. Kroon (2005), Variations in tropical convection as an amplifier of global climate change at the millennial scale, *Earth and Planetary Science Letters*, **235**, 302-314

Kennett, J. P., Cannariato, K. G., Hendy, I. L. and R. J. Behl (2000), Carbon isotopic evidence for methane hydrate instability during quaternary interstadials, *Science*, **288**, 128–133.

Knutti, R., Fluckiger, J., Stocker T.F. and Timmermann, A., (2004), Strong hemispheric coupling of glacial climate through freshwater discharge and ocean circulation, *Nature,* **430,** 851–856

Levi, C., L. Labeyrie, F. Bassinot, F. Guichard, E. Cortijo, C. Waelbroeck, N. Caillon, J. Duprat, T. de Garidel-Thoron, and H. Elderfield (2007), Low-latitude hydrological cycle and rapid climate changes during the last deglaciation, *Geochemistry Geophysics Geosystems*, **8,** 2006GC001514

Manabe, S. and R.J. Stouffer, (1995), Simulation of abrupt climate change induced by freshwater input in to the North Atlantic Ocean, *Nature*, **378**, 165-167

McManus, J.F., Francois. F.R., Gerhardi, J-M., Keigwin, L.D. and Brown-Leger, S. (2004), Collapse and rapid resumption of Atlantic meridonal circulation linked to deglacial climate changes, *Nature*, **428**, 834-837

Muller, J. Kylander, M., Wüst, R.A.J., Weiss, D., Martinez-Cortinzas, A., LeGrande, A.N., Jennerjahn, T., Behling, H., Anderson, W.T. and G. Jacobson, (2008), Possible Evidence for wet Heinrich phases in tropical NE Australia: the Lynch's Crater deposit, *Quaternary Science Reviews*, **27**, 468-475

Pandolfi, J. and Chappell, J. (1994), Stratigraphy and relative sea level changes at the Kanzarua and Bobongara sections, Huon Peninsula, Papua New Guinea, In *Study on coral reef terraces of the Huon Peninsula, Papua New Guinea: Establishment of Quaternary Sea Level and Tectonic History* Y. Ota. Ed., pp. 119-139

Peterson, L.C., Haug, G.H., Hughen, K.A. and U. Rohl, (2000), Rapid changes in the hydrologic cycle of the tropical Atlantic during the last glacial, *Science*, **290,** 1947–1951

Pierrehumbert, R. T. (2000) Climate change and the tropical Pacific: the sleeping dragon awakes. *Proceedings of the National Academy of Science*, **97**, 1355-1358

Porter, S. C., and C. S. An (1995), Correlation between Climate Events in the North-Atlantic and China during Last Glaciation, *Nature*, **375**, 305–308

Prokopenko, A. A., Williams, D.F., Karabanov, W.B. and G. K. Khursevich (2001), Continental response to Heinrich events and Bond cycles in sedimentary record of Lake Baikal, Siberia, *Global Planetary Change*, **28**, 217–226

Rahmstorf, S. (1995), Bifurcations of the Atlantic thermohaline circulation in response to changes in the hydrological cycle, *Nature*, ***378***, 145-149

Rosenthal, Y., and A. J. Broccoli (2004), In search of paleo-ENSO, *Science*, **304**, 219-221

Sarnthein, M, K. Winn, S. J. A. Jung, J. C. Duplessy, L. D. Labeyrie, H. Erlenkeuser, and G. Ganssen (1994), Changes in east Atlantic deepwater circulation over the last 30,000 years: Eight time slice reconstructions, *Paleoceanography*, **9**, 209-267

Schulz, H., von Rad, U. and Erlenkeuser, H. (1998) Correlation between Arabian Sea and Greenland climate oscillations for the past 110,000 years, *Nature*, **393**, 54-57

Shackleton. N. J and Hall, M. A. (2000), Phase relationships between millennial scale events 64,000-24,000 years ago, *Paleoceanography,* **15**, 565-569

Shackleton, N.J., Fairbanks, R.G., Chiub, T., and F. Parrenin, (2004), Absolute calibration of the Greenland timescale: implications for Antarctic time scales and $\Delta^{14}C$, *Quaternary Science Reviews*, **23**, 1513-1522

Siddall, M., Rohling, E. J., Almogi-Labin, A., Hemleben, C., Meischner, D., Schmelzer, I. and D. A. Smeed (2003), Sea-level fluctuations during the last glacial cycle, *Nature*, **423**, 853-858

Stott, L., Poulsen, C., Lund, S. and Thunell, R. (2002), Super ENSO and global climate oscillations at Millennium timescales, *Science*, **297**, 222-226

Timmermann, A., Krebs, U. Justino, F. Goosse, H. and Ivanochko, T. (2005) Mechanisms for millennial-scale global synchronization during the last glacial period, *Paleoceanography*, **20**, PA4008

Tudhope, A., W., Chilcott, C.P., McCulloch, M.T., Cook, E.R., Chappell, J. Ellam, R.M., Lea, D., Lough, J.M. and G.B. Shimmield (2001), Variability in the El Niño - Southern oscillation through a glacial-interglacial cycle, *Science*, **291**, 1511-1517

Turney, C.S.M., Kershaw, A.P., Clemens, S.C., Branch, N., Moss, P.T. and Fifield L.K. (2004), Millennial and orbital variations of El Niño/Southern Oscillation and high-latitude climate in the last glacial period, *Nature,* **428**, 306-310

Vidal. L, Labeyrie, L., Cortijo, E. Arnold, M. Duplessy, J.C. Michel, E., Becque, S., and van Weering, T.C.E. (1997), Evidence for changes in the North Atlantic Deep Water linked to meltwater surges during Heinrich events, *Earth and Planetary Science Letters,* **146**, 13-27

Wang, Y. J., Cheng, H., Edwards, R.L., An, Z.S., Wu, J. Y., Shen, C.-C., Dorale J. A. (2001), A high-resolution absolute-dated Late Pleistocene monsoon record from Hulu Cave, China, *Science*, **294**, 2345 – 2348

Wang, X., Auler, A., Edwards, L., Cheng, H., Cristall, P., Smart, P.L., Richards, D.A. and C.-C. Shen, (2004), Wet periods in northeastern Brazil over the past 210 ka linked to distant climate anomalies. *Nature*, **432**, 740-743

7 Conclusions and future work

The aim of this project was to use a relatively novel palaeoclimate archive to study both the mean state of the Western Pacific Warm Pool (WPWP) and the state of ENSO during the early to mid Holocene, the last glacial period and to attempt to correlate proxy evidence for the state of the WPWP with Northern Hemisphere climate. The focus for this work was on testing the results of climate modelling experiments on the state of the tropical Pacific and ENSO and comparing with other proxy records available. The locality for this study and the climate archive used were specifically picked to provide information on the WPWP on these timescales.

7.1 General conclusions

As temperature and precipitation vary in concert on annual and interannual timescales at Huon Peninsula, and both of these climatic variables affect the oxygen isotopic ratio in the skeletons of carbonate producing organisms it was expected that this would influence timeseries of $\delta^{18}O$ extracted from *Tridacna* sp. collected here as they do with corals (Tudhope *et al.*, 1995). However bivalves have more complex life histories compared to corals and early studies suggested that this might cause attenuation of annual amplitude in $\delta^{18}O$ in later stages of life or that sampling techniques were not sufficiently high resolution enough to capture the full signal throughout the life of the bivalve (Aharon, 1991).

Using new micromilling techniques it has been shown that variations in $\delta^{18}O$ that match very closely what is predicted from environmental data available for the region confirming that a) *Tridacna gigas* precipitates its shell in isotopic equilibrium with sea water, b) these timeseries can be used successfully for detecting interannual variations in WPWP climate, and so can be used to reconstruct the mean state of the WPWP and also the state of ENSO. The comparison of this record with corals shows very consistent patterns of $\delta^{18}O$ that further support the use of these climate archives in palaeoenvironmental studies. Similar patterns in $\delta^{18}O$ are observed even

though corals generally do not display a reduction in growth as observed in bivalves over ontogeny. This study also shows that *Tridacna gigas* do not exhibit any obvious seasonal or ontogenic growth breaks nor any significant isotopic trends. Within the uncertainty of the environmental data available, the measured annual isotopic cycle shown the full amplitude predicted. Multi-taxon approaches to climate reconstruction using corals and molluscs are therefore feasible given sufficiently high sampling resolution.

Radiocarbon dating of *Tridacna* sp. from between approximately 35 and 44 cal. ka show similar radiocarbon ages for corals collected from the same terraces, but consistently younger ages than U/Th age of the same corals. Good agreement between radiocarbon ages and stratigraphic control and very low amounts of calcite, implies that the *Tridacna* sp. is unaffected by diagenesis to a significant degree. These anomalously young ages may be related to changes in global reservoir ages brought about by variations in the volume of deep water production shown in other studies from this area.

Results from *Tridacna* sp. of early to mid Holocene age agree with models of Pacific climate in terms of changes to the frequency of ENSO (Clement *et al.*, 1999; 2000 and Brown *et al.*, 2006) and the hydrological cycle (Oppo *et al.*, 2007), but disagreements with other records (Brijker *et al.*, 2006) may also indicate that the larger Indo-Pacific Warm Pool may be spatially quite heterogeneous at this time.

Averaged $\delta^{18}O$ results from Marine Oxygen Isotope Stage 3 aged *Tridacna* sp. are broadly in agreement with other studies suggesting a more "El Niño-like" mean state during the last glacial period (Martinez *et al.*, 1999; Stott *et al.*, 2002). Seasonally resolved $\delta^{18}O$ timeseries were unfortunately short, however they appear to confirm coral results indicating the ENSO is dampened in terms of strength and number of extreme events during the last glacial cycle (Tudhope *et al.*, 2001). Some of the shorter records from terraces where corals have not been analysed do appear to hint at an increased variability, but were too short to be of any statistical significance.

Finally an attempt to correlate proxy information for the mean state of the WPWP with Northern Hemisphere temperature during the last glacial period was made based upon using eustatic sea level as a tool for correlation. This approach is necessary to link records on millennial timescales given the uncertainties in methods used for absolute dating of events this far back into the past. The conclusions drawn here are tentative because whilst proxy records from around the globe tend to agree on the timing of the initiation of the sea level excursion that appears to be related to Heinrich Event 4, there is less agreement about the timing of the resulting highstand (Chapter 4) and it is probable that samples collected from the terrace faces at Huon Peninsula are likely to be skewed towards the age of the highstand. This can be tackled be accessing earlier stages of terrace growth.

7.2 Future prospects

Tridacna sp. present a very good prospect for investigating these variations in ENSO variability, and though the longest record measured here was 18 years long, *Tridacna gigas* has been shown to live for up to 60 years (Watanabe *et al.*, 2004). There are however limited studies on species of *Tridacna* other than *Tridacna gigas*, and therefore a fuller investigation of the life histories of these species must be carried out.

With future study, eustatic sea level as reflected by the uplifted reef terraces at Huon Peninsula should prove an invaluable aid to accurate correlation of palaeoproxy information on millennial timescales, especially if lowstands and earlier phases of terrace growth can be accessed to give a more complete and continuous record. This may be achieved by either drilling terraces or by careful investigation of faulted blocks and landslips to access these earlier periods of terrace growth.

Climatic change on suborbital timescales is observed in both the tropics and the high latitudes. Two schools of thought appear to exist presently on whether this originates in the tropics through suborbital variations to ENSO (e.g. Cane 1998; Clement *et al.*, 2001, Stott *et al.*, 2002 or Turney *et al.*, 2004) or the high latitudes causing the

average position of the ITCZ to be altered (e.g. Ivanochko *et al.*, 2005; Timmermann *et al.*, 2005 or Muller *et al.*, 2008). It may be possible to provide an answer to this puzzle by using both corals and *Tridacna* sp. to provide records that are compatible, sufficiently long enough to elucidate subtle changes in ENSO variability and mean state climate state.

Finally, an independent measure of temperature is required to separate variation in evaporation/ precipitation and sea surface temperature to truly understand variations in mean climate of the WPWP and their implications for global climate. This may be achieved by further study of trace element profiles in modern *Tridacna* sp.

References

Aharon, P. (1991), Recorders of Reef Environment Histories - Stable Isotopes in Corals, Giant Clams, and Calcareous Algae, *Coral Reefs*, **10**, 71-90

Brijker, J.M., Jung, S.J.A., Ganssen, G.M., Bickert, T and Kroon, D. (2006) ENSO related decadal scale climate variability from the Indo-Pacific Warm Pool. *Earth and Planetary Science Letter,* **253** 67-82

Brown, J., Collins, M and A. Tudhope (2006), Coupled model simulations of mi-Holocene and comparisons with coral oxygen isotope records, *Advances in Geosciences*, **6**, 29-33

Cane, M.A. (1998), A role for the Tropical Pacific, *Science*, **282**, 59-61

Clement, A. C., Seager, A and M.A. Cane (1999), Orbital controls on the El Niño/Southern Oscillation and the tropical climate, *Paleoceanography*, **14**, 441-457

Clement, A. C., Cane, M. A. and R. Seager, (2001), An orbitally driven tropical source for abrupt climate change, *Journal of Climate,* **14**, 2369-2375

Ivanochko, T.S., Ganeshram, R.S., Brummer, G.-J.A., Ganssen, G., Jung, S.J.A., Moreton S.G. and D. Kroon, (2005), Variations in tropical convection as an amplifier of global climate change at the millennial scale, *Earth Planetary Science Letters,* **235,** 302–314

Martinez, J.I., De Deckker, P., and A. Chivas (1997), New estimates for salinity changes in the Western Pacific Warm Pool during the Last Glacial Maximum: oxygen-isotope evidence, *Marine Micropaleontology*, **32**, 311-340

Muller, J. Kylander, M., Wüst, R.A.J., Weiss, D., Martinez-Cortinzas, A., LeGrande, A.N., Jennerjahn, T., Behling, H., Anderson, W.T. and G. Jacobson, (2008), Possible Evidence for wet Heinrich phases in tropical NE Australia: the Lynch's Crater deposit, *Quaternary Science Reviews*, **27**, 468-475

Oppo, D, Schmidt, D. and A. LeGrande (2007), Sea water isotope constraints on tropical hydrology during the Holocene, *Geophysical Research Letters,* **34**, L13701

Ota, Y., and J. Chappell (1999), Holocene sea-level rise and coral reef growth on a tectonically rising coast, Huon Peninsula, Papua New Guinea, *Quaternary International*, **55**, 51-59

Stott, L., Poulsen, C., Lund, S. and Thunell, R. (2002), Super ENSO and global climate oscillations at Millennium timescales, *Science*, **297**, 222-226

Timmermann, A., Krebs, U. Justino, F. Goosse, H. and T. Ivanochko (2005) Mechanisms for millennial-scale global synchronization during the last glacial period, *Paleoceanography*, **20**, PA4008

Tudhope., A.W., Shimmield, G.B., Chilcott, C.P., Jebb, M., Fallick, A.E. and Dalgleish, A.N. (1995), Recent changes in climate in the far western equatorial Pacific and their relationship to the Southern Oscillation; oxygen isotope records form massive corals, Papua New Guinea. *Earth and Planetary Science Letters*, **136**, 575-590

Tudhope, A., W., Chilcott, C.P., McCulloch, M.T., Cook, E.R., Chappell, J. Ellam, R.M., Lea, D., Lough, J.M. and Shimmield, G.B. (2001), Variability in the El Niño - Southern oscillation through a glacial-interglacial cycle, *Science*, **291**, *1511-1517*

Turney, C.S.M., Kershaw, A.P., Clemens, S.C., Branch, N., Moss, P.T. and Fifield L.K. (2004), Millennial and orbital variations of El Niño/Southern Oscillation and high-latitude climate in the last glacial period, *Nature,* **428**, 306-310

Watanabe, T., A. Suzuki, H. Kawahata, H. Kan and S. Ogawa. (2004), A 60-year isotopic record from a mid-Holocene fossil giant clam (Tridacna gigas) in the Ryukyu Islands: physiological and paleoclimatic implications, *Palaeogeography Palaeoclimatology Palaeoecology*, **212**, 343-354